Functional deficits after stroke:

The key underlying mechanisms and the therapeutic potential of growth hormone

Sonia Sanchez Bezanilla

MSc Biomedicine

A thesis submitted in fulfilment of the requirements for the degree of Doctor of Philosophy in Medical Biochemistry

School of Biomedical Sciences and Pharmacy

Faculty of Health and Medicine

University of Newcastle

July 2020

DECLARATIONS

Originality

I hereby certify that the work embodied in the thesis is my own work, conducted under normal supervision. The thesis contains no material which has been accepted, or is being examined, for the award of any other degree or diploma in any university or other tertiary institution and, to the best of my knowledge and belief, contains no material previously published or written by another person, except where due reference has been made. I give consent to the final version of my thesis being made available worldwide when deposited in the University's Digital Repository, subject to the provisions of the Copyright Act 1968 and any approved embargo.

Statement of authorship

I hereby certify that the work embodied in this thesis contains published papers of which I am joint author. I have included as part of the thesis a written statement, endorsed by my supervisor, attesting to my contribution to the joint publication work.

Thesis by Publication

I hereby certify that this thesis is in the form of a series of papers. I have included as part of the thesis a written declaration from each co-author, endorsed in writing by the Faculty Assistant Dean (Research Training), attesting to my contribution to any jointly authored papers.

ACKNOWLEDGEMENTS

First, I would like to thank my primary supervisor Dr. Lin Kooi Ong for all the help and invaluable support he has offered me during the last three years. Thank you for always encouraging me to be the best scientist possible. Everything that I have achieved during my PhD is mainly thanks to you. I could have not asked for a better supervisor. I would also like to thank my co-supervisors Prof. Rohan Walker and Prof. Michael Nilsson for their support, encouragement and helpful input.

Next, I would like to thank the past and present members of the Walker/Nilsson lab. You all kept me sane during the crazy moments of my PhD. In particular thank you to Kasia, Giovanni and Murielle for the endless laughs, for teaching me everything I need to know to survive my PhD and to show me that there is life beyond the PhD. I would also like to thank one of the latest additions in the lab, Bec, for all the good moments in and out of the lab, your helpful advice and encouragement. Lastly, I would like to thank Prajwal for making my days in the lab better.

Special thanks to all my friends in Australia and back home in Spain and all the people I have met along the way for all the support during this crazy journey. Most of all, thank you Paola for hearing me complain every single day about my PhD but still push me to the end. You are the person that has kept me mentally sane. Lastly but not least, I want to thank my wonderful family. To my parents and my sister for supporting me both emotionally and financially during all these years. You have always encouraged me to be the best version of myself. I could not have made it without you. MUCHAS GRACIAS!

PUBLICATIONS

1. **Sanchez-Bezanilla S.**, TeBay C., Nilsson M., Walker F.R., Ong L.K. Visual Discrimination Impairment After Experimental Stroke Is Associated With Disturbances in the Polarization of the Astrocytic aquaporin-4 and Increased Accumulation of Neurotoxic Proteins. Experimental neurology. 2019 Aug 1;318:232-43. doi:10.1016/j.expneurol.2019.05.001
2. **Sanchez-Bezanilla S.**, Hood R.J., Nilsson M., Walker F.R., Ong L.K. Longitudinal analysis of the functional outcomes after photothrombotic cortical stroke and its association with neuronal loss, gliosis and accumulation of amyloid-beta. To be submitted to the Journal of Cerebral Blood Flow & Metabolism.
3. **Sanchez-Bezanilla S.**, Åberg N.D., Crock P., Walker F.R., Nilsson M., Isgaard J., Ong L.K. Growth hormone promotes motor function after experimental stroke and enhances recovery-promoting mechanisms within the peri-infarct area. International Journal of Molecular Sciences. 2020 Jan 17; 21(2):E606. doi:10.3390/ijms21020606
4. **Sanchez-Bezanilla S.**, Åberg N.D., Crock P., Walker F.R., Nilsson M., Isgaard J., Ong L.K. Growth Hormone Treatment Promotes Remote Hippocampal Plasticity after Experimental Cortical Stroke. International Journal of Molecular Sciences. 2020. 21(12), 4563; https://doi.org/10.3390/ijms21124563

ADDITIONAL PUBLICATIONS

1. **Sanchez-Bezanilla S.**, Nilsson M., Walker F.R., Ong L.K. Can we use 2, 3, 5-triphenyltetrazolium chloride stained brain slices for other purposes? The application of western blotting. Frontiers in molecular neuroscience. 2019 Jul 30;12:181. doi:10.3389/fnmol.2019.00181
2. Zhao Z, Ong LK, Pietrogrande G, **Sanchez-Bezanilla S**, Warren K, Ilicic M et al. Low oxygen post conditioning improves stroke-induced cognitive impairment. bioRxiv. 2018. doi:10.1101/483453.
3. Pietrogrande G., Zalewska K., Zhao Z., Abdolhoseini M., Chow W.Z., **Sanchez-Bezanilla S.**, et al. Low Oxygen Post Conditioning prevents thalamic secondary neuronal loss caused by excitotoxicity after cortical stroke. Scientific reports. 2019 Mar 19;9(1):4841. doi:10.1038/s41598-019-39493-8
4. Hardy S.A, Mabotuwana N.S., Murtha L.A., Coulter B., **Sanchez-Bezanilla S.**, Al-Omary M.S., Senanayake T., Starkey M., Lee R.J., Rainer P.P., Hansbro P.M., Boyle A.J. Novel Role of Extracellular Matrix Protein 1 (ECM1) in Cardiac Aging- and Myocardial Infarction. PloS one. 2019 Feb 21;14(2):e0212230. doi:10.1371/journal.pone.0212230

CONFERENCE PROCEEDINGS

1. **Sonia Sanchez-Bezanilla**, Clifford Tebay, Michael Nilsson, Frederick R. Walker, Lin Kooi Ong. The role of glymphatic system in post-stroke cognitive impairment. 2018 ASMR Newcastle Satellite Scientific Meeting. Newcastle, Australia, 1st June 2018.
2. **Sonia Sanchez-Bezanilla**, Clifford Tebay, Michael Nilsson, Frederick R. Walker, Lin Kooi Ong. The link between cognitive impairment and neurotoxic protein aggregation after experimental stroke. 2018 Australasian Neuroscience Society. Brisbane. Australia. 3rd-6th December 2018
3. **Sonia Sanchez-Bezanilla**, Michael Nilsson, Frederick R. Walker, Lin Kooi Ong. Impaired associative memory and behavioral flexibility after experimental stroke. 2018 Australasian Neuroscience Society. Brisbane. Australia. 3rd-6th December 2018
4. **Sonia Sanchez-Bezanilla**, Michael Nilsson, Frederick R. Walker, Lin Kooi Ong. Impaired associative memory, visual discrimination and behavioural flexibility after experimental stroke. 2019 European Stroke Organisation Conference. Milan. Italy. 22nd-24th May 2019
5. **Sanchez-Bezanilla S.**, Nilsson M., Walker F.R, Ong L.K. Impaired behavioral flexibility and associative memory after experimental stroke. 2019 International Brain Research Organisation Conference. Daegu. Korea. 21st-25th September 2019
6. **Sanchez-Bezanilla S.**, Hood R.J., Nilsson M., Walker F.R., Ong L.K. Assessment of cognitive impairment after experimental stroke using a rodent touchscreen platform. 2019 Australasian Neuroscience Society. Adelaide. Australia. 2nd-5th December 2019
7. Zhao Z., Ong L.K., Hood R., Pietrogrande G., **Sanchez Bezanilla S.**, Warren K., Ilicic M., Kluge M., TeBay C., Ottersen O., Johnson S., Nilsson M. and Walker F.R. Low oxygen post conditioning improves cognition and reduces amyloid beta accumulation post-stroke in mice. 2019 Australasian Neuroscience Society. Adelaide. Australia. 2nd-5th December 2019

8. **Sanchez-Bezanilla S.**, Åberg N.D., Crock P., Walker F.R., Nilsson M., Isgaard J., Ong L.K.. Growth hormone in experimental stroke: From motor improvement to neurogenesis and beyond. 2019 Australasian Neuroscience Society. Adelaide. Australia. 2nd-5th December 2019.

Table of Contents

TABLE OF FIGURES

ABBREVIATIONS

Aβ: amyloid β

α-Syn: α-Synuclein

Ang-1/2: angiopoietin-1/2

AQP4: aquaporin-4

ATP: adenosine triphosphate

BBB: blood brain barrier

BDNF: brain-derived neutrotrophic factor

CANTAB: Cambridge neuropsychological test automated battery

CD: cluster of differentiation molecule

CNS: central nervous system

CSF: cerebrospinal fluid

CSPG: chondroitin sulphate proteoglycans

CT: computer tomography

DCX: doublecortin

DG: dentate gyrus

DTI: diffusion tensor imaging

GFAP: glial fibrillary acidic protein

GH: growth hormone

GHR: growth hormone receptor

Iba-1: ionized calcium binding adapter molecule-1

IGF-1: insulin-like growth factor 1

IGF-1R: IGF-1 receptor

IL: interleukin

MCA: middle cerebral artery

MCAO: middle cerebral artery occlusion

MMP: matrix metallopeptidase

MRI: magnetic resonance imaging

NO: nitric oxide

NVU: neurovascular unit

PAL: paired associative learning

PET: positron-emission tomography

rhGH: recombinant human growth hormone

ROS: reactive oxygen species

SGZ: subgranular zone

SN: substantia nigra

SND: secondary neurodegeneration

SVZ: subventricular zone

TBI: traumatic brain injury

TGA: Therapeutic Goods Administration

TNF-α: tumour necrosis factor-α.

tPA: tissue plasminogen activator

TTC : 2,3,5-Triphenyltetrazoliumchloride

VD: visual discrimination

VDR: visual discrimination reversal

VEGF: vascular endothelial growth factor

VIM: vimentin

WD: Wallerian degeneration

ABSTRACT

***Background and aims**:* Stroke is currently the leading cause of long-term disability worldwide. Despite the efforts to minimise these negative outcomes, few treatments have been approved and have been mainly focused on the acute phase. This has led to a challenging situation where more than 90% of stroke survivors will experience long-lasting impairments in motor function and/or cognition. Therefore, clinical and pre-clinical research should focus on improving the understanding of underlying mechanisms contributing to neurological damage and functional impairment in later stages after stroke. One of the possible mechanisms that could explain these impairments is the development of secondary neurodegeneration (SND) in remote brain areas synaptically connected to the primary infarct site, such as the thalamus and hippocampus. This process is especially interesting because it occurs over a timescale of weeks to years after the primary infarct, providing a very interesting therapeutic target for chronic stroke treatment. This thesis focused on investigating the evolution of the functional outcomes after stroke and the mechanisms associated with these deficits (Chapter 3 and 4). Additionally, I was interested in studying a potential therapeutic intervention such as growth hormone (GH) to promote brain plasticity and alleviate motor and cognitive impairment (Chapter 5 and 6).

Methods: The photothrombotic stroke model targeting the motor and sensory cortex was used to induce ischemia in mice. A touchscreen platform was used to analyse cognitive performance, and the grid walk and cylinder test were used to assess motor function. I also analysed the changes occurring after stroke in different brain areas (peri-infarct, thalamus and hippocampus) combining various molecular biology techniques such as Western Blot, immunohistochemistry, immunofluorescence and various histological stainings. In chapters 5 and 6, I used recombinant human GH (rhGH) delivered subcutaneously *via* a mini-osmotic pump for 28 days.

Results: Stroke significantly impairs multiple cognitive domains and these deficits last for months after the primary infarction. Motor impairments were also long-lasting but a modest spontaneous recovery was observed over time. These deficits were associated with SND processes such as neuronal death, neuroinflammation (astrogliosis and microglia activation) and accumulation of neurotoxic proteins (amyloid-β and α-synuclein) in the thalamus and hippocampus (Chapters 3 and 4). Additionally, motor and cognitive impairment could be reversed by using GH as a therapeutic intervention. GH enhanced functional outcomes through a series of neurorestorative mechanisms including neurogenesis, synaptic plasticity and cerebrovascular remodelling (Chapters 5 and 6).

Conclusion: Overall, in this thesis, I have deepened our understanding regarding cognitive and motor impairment after stroke and the mechanisms associated with these impairments. These important findings provide potential targets for translational medical research in the future. Finally, I have demonstrated that GH is an effective treatment following experimental stroke to promote brain plasticity and functional performance in the recovery phase after stroke. My results are encouraging and support the idea that GH represents a promising therapeutic intervention, which should be considered for clinical studies.

CHAPTER 1: INTRODUCTION

1.1. Stroke burden

Stroke is the second leading cause of death and the leading cause of long-term disability worldwide (1). Each year stroke affects up to 15 million people globally, of whom almost 5 million die and another 5 million are permanently disabled (2). Stroke incidence increases greatly with age, the risk double every decade after the age of 55 years in both men and women (3). In Australia alone almost 56,000 people suffer from a stroke each year, and those who survive require daily care. This presents a major financial burden estimated to be $5 billion per year (4). The biggest cost coming from loss of productivity, driven by the fact that around 30% of stroke survivors are of working age, and followed by costs to the healthcare system (4, 5). Therefore, it is crucial to better understand stroke pathophysiology and develop new treatments for this complex disease.

In the past years, stroke research has been heavily focused on the development of acute therapies, resulting in highly successful interventions and reduction in mortality rates, and therefore increasing the numbers of stroke survivors living with the health impairments of stroke. It is estimated that by 2050, stroke incidence will more than double and one million people will require post-stroke care, treatment and rehabilitation in Australia (6, 7). It is well known that stroke survivors mainly suffer from life-long impairment in motor and cognitive function. Accordingly, future studies should focus on long-term treatments during the subacute and chronic phases of stroke targeting both the motor functional recovery and the cognitive impairment.

Therefore, in this thesis, I will investigate the trajectory of the motor and cognitive deficits during the subacute and chronic phases post-stroke, and the cellular and molecular mechanism occurring in the brain within this period. Moreover, I will focus on a new therapeutic intervention to enhance recovery after stroke in a pre-clinical stroke model.

1.2. Ischemic stroke

Stroke is a neurological event caused by a disruption in the blood supply to the brain. There are two main types of stroke. The first is known as haemorrhagic stroke, which is caused by the rupture of a blood vessel followed by bleeding into the brain tissue. The second is ischemic stroke, caused by an occlusion of a blood vessel (typically caused by an embolic or thrombotic clot) leading to a reduction of blood flow to the innervated brain regions (8-10). Ischemic stroke is the most common, as it accounts for approximately 80% of all strokes, and therefore will be the focus of this thesis. Stroke results in damage of the affected brain area and this can manifest itself in a wide range of symptoms such as muscle weakness, paralysis, impaired speech, fatigue and cognitive deficits (11, 12) depending on the region in which it occurs.

Deprivation from oxygen and nutrients results in an ischemic cascade ultimately leading to cell death and necrosis (13). Within minutes following a vessel occlusion, the reduced blood flow leads to damage and death of the surrounding tissue. The tissue damaged after an ischemic stroke can be divided into two regions: the core and the penumbra (Figure 1) (14, 15). The ischemic core is the area suffering the greatest reduction in blood flow (<20% of normal) and contains tissue therapeutically unsalvageable from cell death. The penumbra is the area immediately surrounding the core, which contains tissue potentially salvageable. This area displays only a moderate reduction in blood flow, which is sufficient to not cause immediate neuronal death (14, 15). However, it is strongly affected by the neurotoxic factors released from the core and therefore, immediate reperfusion is necessary to maintain tissue integrity. If not salvaged, this tissue will die and become part of the infarct core, which will enlarge the stroke lesion (13). Therefore, the aim of acute stroke therapies is to target the ischemic penumbra and restore the blood flow as fast as possible. Despite decades of research, very few treatments for acute stroke have been developed and approved.

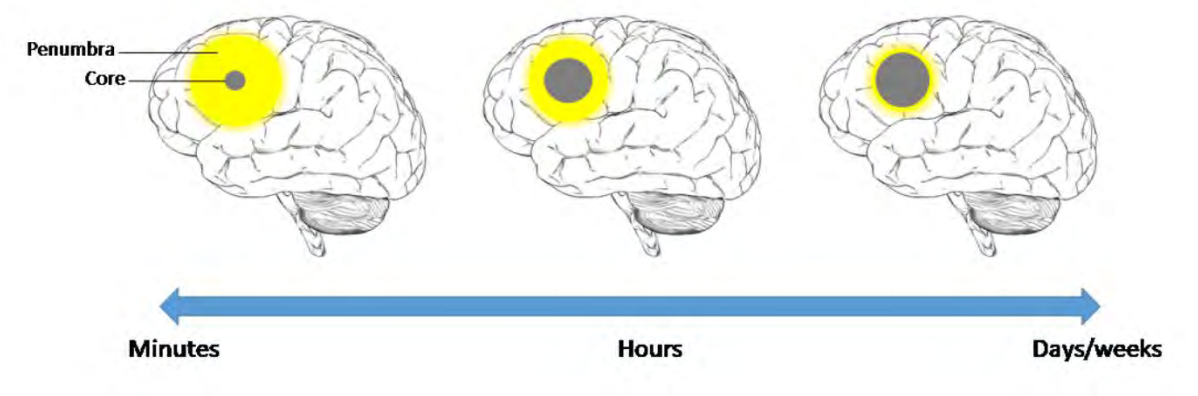

Figure 1. Representation of the development of the infarct core and penumbra overtime after the ischemic stroke. After stroke, the core undergoes irreversible cell death (grey). This core is surrounded by tissue that it is still salvageable, the penumbra (yellow). If not salvaged this tissue will die and become part of the infarct core.

1.3. Current therapies

Timing is a crucial factor in acute stroke treatment: the quicker the treatment, the more brain tissue can be salvaged. Saver *et al*. (2006) in a systematic review estimated that patients experiencing large vessel occlusion lose 120 million neurons, 830 billion synapses and 714 km of myelinated fibres each hour (16). Comparing those numbers to the normal aging process, the stroke brain ages approximately 3.6 years every hour before any treatment is administered.

Despite the hundreds of experimental papers that have investigated promising neuroprotective strategies to salvage penumbral tissue and limit irreversible damage in animals, there are just a few acute interventions currently available for ischemic stroke in humans.

Thrombolysis: The current standard therapy for restoring blood flow in the occluded vessel is intravenous administration of recombinant tissue plasminogen activator (tPA). tPA is recognised to be capable of breaking down occluding clots by converting plasminogen to plasmin (a clot degrading enzyme) which results in the cleavage of the fibrin mesh and disruption of the integrity of the clot. After the clot is dissolved, the normal blood flow is

restored. Currently tPA is the gold standard and most efficient pharmacological intervention. However, a clear disadvantage is that for tPA to be effective it has to be administered within 4.5 hours of the ischemic onset (17, 18). If administered after 4.5 hours, the risk of suffering from complications such as intracranial hemorrhage, major systemic hemorrhage, and angioedema increase significantly (19). Promisingly, a recent study by Ma *et al*. (20) has suggested that the time window may be extended to 9 hours in patients with favourable perfusion-imaging profile; however, further trials of thrombolysis within this time window are required to confirm these findings. The limited time window of administration together with the significant risk of complications associated with bleeding makes this treatment only administrable in 5-10% of patients (21). This number can reach 20% in well-organised systems of pre-hospital care (22).

Thrombectomy: Endovascular mechanical thrombectomy has recently been added as an effective acute treatment for ischemic stroke. This therapy is based on using a stent retriever to remove the clot (23). The therapeutic window for mechanical thrombectomy is around 6 hours; however, results from the DAWN (24) and DEFUSE 3 (25) trials suggest that the therapeutic window for thrombectomy could be extended to up to 24 hours in carefully selected patients who have a mismatch between the volume of brain tissue that may be salvaged and the volume of infarcted tissue. A meta-analysis of five positive randomised control trials for this approach (MR-CLEAN, EXTEND-IA, ESCAPE, SWIFT PRIME, and REVASCAT) (26-30) demonstrated that clot retrieval greatly improves functional outcomes after stroke (31, 32). Phan *et al.* (32) showed that a combination of thrombolysis and thrombectomy reduced the relative risk ratio of disability in daily functioning by 30%, based on the modified Rankin Scale. Despite these encouraging results, only a small percentage of hospitals provide 24/7 endovascular services (33).

Stroke care units: The routine management of patients in dedicated stroke care units has been proven to significantly reduce death and disability. Patients in these units also present with improved stroke clinical outcomes compared to those treated in general wards (34, 35).

The improved outcomes are influenced by the comprehensive care, rehabilitation and specialised resources that stroke patients receive in these stroke care units.

Secondary prevention: Apart from these acute therapies, secondary prevention is also an important component of stroke treatment to avoid a recurrent stroke. The most beneficial secondary stroke prevention (as well as primary) involves risk factor modification. Risk factors for ischemic stroke can be divided into non-modifiable (age, gender, race and ethnicity) and modifiable. Modifiable risk factors include hypertension, diabetes, smoking, alcohol consumption, high cholesterol, atrial fibrillation, diet, physical inactivity and obesity (36). Although each risk factor can occur individually, they commonly occur in combination. Modifiable risk factors can be controlled and limited with medication or a change in lifestyle habits and are therefore the main targets of secondary prevention. Hypertension is the most important risk factor for ischemic stroke and it has been demonstrated that the use of anti-hypertensive medication can reduce stroke recurrence by up to 40% (37). Administration of antithrombotics such as aspirin after stroke are also aimed towards the secondary prevention of a recurrent stroke. These drugs prevent platelet aggregation, further thrombosis and thus recurrent stroke. However, benefits from these treatments are modest (21, 38). In addition to drugs, lifestyle intervention is vital to secondary stroke prevention. Studies have shown that combination of multiple approaches can reduce the risk of recurrent stroke by an estimated 80-90% (39).

Restoring the blood circulation in the affected brain area using any of the acute treatments available is essential to minimise the negative outcomes after stroke. However, the majority of stroke patients cannot receive either tPA or thrombectomy. This leaves a high percentage of stroke survivors experiencing significant functional impairments and extended recovery process (40). An additional therapeutic approach in acute ischemic stroke is to induce neuroprotection to preserve the penumbra. Huge efforts have been invested into the evaluation of these new acute therapeutic interventions using preclinical models of stroke. Many animal studies have successfully demonstrated the efficacy of therapeutic interventions

targeted at blocking cell death in the penumbra. However, translation of promising therapies fail during clinical trials (out of 100 trials, none provided enough evidence to support benefits to stroke patients) (41, 42). These results suggest that new approaches should be adopted and emphasis should be placed in fully understanding the mechanisms occurring during the recovery phase of stroke. As such, *in this thesis I will focus on examining how the brain responds after stroke especially during the subacute and chronic phase, with the aim of developing new interventions to enhance optimal brain repair and functional outcomes.*

1.4. Functional disturbances after stroke

Stroke survivors are likely to experience a certain level of physical and cognitive impairment. Additionally, studies have found that it was common that stroke patients who presented significant disability 3 months after stroke did not achieve significant improvements at 12 months (40) and one-third of stroke survivors only attained poor functional outcome at 5 years post-stroke. The severity of disability depends on numerous factors such as pre-comorbidities, age, location and size of the stroke and response to treatment (43).

During an ischemic stroke, any blood vessel is susceptible to being blocked. However, the middle cerebral artery (MCA) is the vessel most commonly occluded in patients (44). The MCA supplies blood to a portion of the frontal, temporal and parietal lobes, which includes primary motor and somatosensory cortical areas of the face, trunk and upper limbs, and in the dominant hemisphere, the areas for speech (45, 46). Therefore, the most common neurological consequence of stroke is impairment of motor skills, which manifests as weakness in the muscles, paralysis, loss of sensation, hemiparesis and speech impairment. Impairments in these areas greatly affect a patient's quality of life, as they are unable to perform tasks of daily living unassisted (47). Physical consequences of stroke also include the development of chronic pain, incontinence, sight disturbances, changes in consciousness and alertness, sleep disturbances, and inability to lift or hold objects (43).

In addition to the physical disability, a high number of stroke survivors also suffer from cognitive impairment. The prevalence of cognitive impairment varies from 20% to 80%, depending on the country, race, and diagnostic criteria (48). Cognitive impairment may emerge from a disruption in the complex network interactions between cortical and subcortical sites, through secondary mechanisms of injury. Therefore, this impairment does not necessarily manifest immediately after stroke but often slowly develops overtime and several studies have suggested that 15% to 38% of stroke patients meet the criteria of cognitive impairment at 3 months post-stroke with the domains of learning, memory and attention mostly affected (48-50). Longitudinal studies have further provided some understanding of the long-term impact of stroke on cognitive functioning, with studies showing that approximately 20-30% of stroke patient exhibit deterioration in cognition at 2 years post-stroke (51, 52). A recent study by Delavaran *et al*. (53) showed that 46-61% of stroke survivors suffer from cognitive impairment at 10 years post-stroke compared with age-matched healthy participants. Post-stroke cognitive impairment is associated with increases in mortality rates, disability, dependency and institutionalisation (54). Additionally, cognitively impaired stroke survivors are at significant risk of experiencing further deterioration of their cognitive abilities and of developing dementia one year post-stroke (55, 56). Indeed, it is estimated that the risk of developing dementia following stroke is between 4 and 12 times higher than age matched healthy controls (57, 58). In summary, it is evident that post-stroke cognitive impairment significantly influences an individual's quality of life and functional performance. Thus, stroke survivors with cognitive impairment are less independent and need more care and assistance, increasing the healthcare cost (54). This warrants a dedicated effort to develop therapeutic strategies aimed at improving outcomes in this population.

1.4.1. Treatments for functional outcomes

The ultimate goal of all therapies is to improve patient outcome, and in the settings of stroke, this involves reducing impairment and disability, and restoring functional and cognitive ability. However, a very few advancements have been made regarding treatments to enhance

neurological and functional recovery. Some promising research directions have emerged but the efficacy of these new therapies still need to be proven (Figure 2).

As previously mentioned, motor deficits are the most widely recognised impairments after stroke, which restricts muscle movement or mobility. Recovery of the motor function is a complex process that may occur through a combination of spontaneous and learning-dependent processes (43). Currently, clinical practice in stroke rehabilitation focuses heavily on exercise, physical therapy and occupational therapy aimed to provide stroke patients with the greatest possible level of functional independence (59, 60). Although there are no clear guidelines regarding the best practice, it is clear that rehabilitation should begin as soon as possible after stroke (61) and could continue for months or years after the initial stroke event (43). Recovery of the loss motor function through different rehabilitation techniques is a long and slow process and just a few number of the therapies used routinely in the clinical setting have been proven to be effective from systematic reviews (62). Therefore, efforts should be placed in designing new therapeutic interventions to enhance recovery.

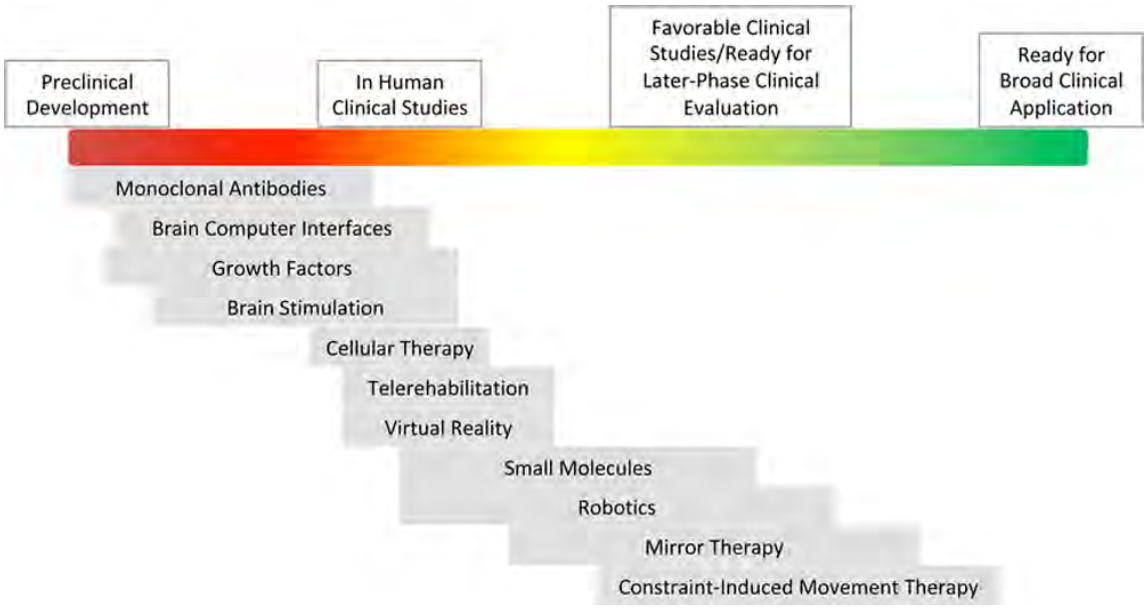

Figure 2. Summary of current experimental treatments for stroke recovery and how far they are from being implemented in clinical practice. Image adapted with permission from (63).

Cognitive impairment is also a widely known and problematic outcome for stroke patients. Despite the fact that cognitive impairment has been identified as a targeted outcome of stroke treatment, there is a higher emphasis on physical rehabilitation (64-66). Health professionals tend to focus on physical measures and outcomes rather than cognitive deficits and executive function likely due to the lack of effective evidence-based treatment options (48, 67). Some studies have demonstrated that physical activity, as well as improving motor function after stroke, may also improve cognitive performance (68). The emerging evidence in stroke survivors is supported by animal models where exercise has been shown to induces an increase in different trophic factors, which leads to improvement in cognitive function (69). Cognitive rehabilitation, cognitive training, and psychological interventions have also been used to alleviate cognitive deficits in humans (70). However, the efficacy of these interventions is unclear and inconclusive due to the small numbers of research trials performed and the contradictory results (71). Cognitive rehabilitation techniques have some important limitations. Firstly, the treatments are generally just focused on singles domains, rather than multiple domains. Given that stroke leads to deficits in multiple cognitive domains, it would be unrealistic for a patient to undertake separate interventions for each cognitive domain, due to the amount of time and effort that would be required. Additionally, cognitive rehabilitation involves considerable time and resources.

These limitations of cognitive rehabilitation emphasise the need for alternate interventions to improve the cognitive functioning of stroke patients. One alternative is the use of pharmacological interventions. Some studies have examined the effects of cytidinediphosphocholine, a widely used neuroprotective drug (72), in stroke survivors with cognitive impairments. These studies showed improved orientation, attention and executive function compared to the placebo group (73-75). Some pharmacological treatments used in the clinical practice for Alzheimer's disease have also shown to be promising for the treatment of post-stroke cognitive impairment. For instance, different clinical trials using a cholinesterase inhibitor such as donepezil, have suggested that donepezil has some benefits in the cognition

of patients with post-stroke cognitive impairment (76-79). Despite the positive results presented by some of the studies, further investigations are warranted to determine the efficacy of the different therapies.

The lack of therapies to treat cognitive deficits may be due to the lack of understanding of basic mechanisms of neurological damage occurring in the brain during the recovery phase after stroke. Therefore, in this *thesis I will focus on understanding the processes occurring in the subacute and chronic phases of stroke contributing to functional deficits, including cognitive impairment.*

1.5. Molecular mechanisms of ischemic stroke

1.5.1. The ischemic cascade

Immediately after the vessel occlusion, ischemia causes brain injury at a cellular level by initiating a series of events, termed the ischemic cascade. Initially, the occlusion leads to a loss of oxygen supply and ATP reduction in affected cells. This lack of ATP causes the failure of ion pumps, which in turn leads to an excess glutamate release. These high levels of glutamate cause a persistent activation of N-methyl-d-aspartate acid (NMDA) and α-amino-3-hydroxy-5-methylisoxazole propionic acid (AMPA) receptors, resulting in excitotoxicity. As the cell's membrane start to progressively degrade, they become more permeable and eventually cause mitochondria failure and programmed cell death (41, 80, 81).

In later stages, the ischemic cascade causes an activation of microglia and astrocytes. Microglia plays an important role in responding to the initial and later phases of the repair process after stroke (82, 83). Astrocytes play a critical role in creating a tight structural barrier crucial for sealing the core and preventing damage from further spreading into the surrounding tissue (84). This is known as the glial scar.

1.5.2. The neurovascular unit

It has been proposed that the failure of pre-clinical studies to translate into human stroke therapies may be due to the fact that previous treatments have focused exclusively on preventing neuronal death after stroke (85, 86). However, other cell types such as glial cells are highly involved in the ischemic process and in fact account for the majority of the brain's cells. Neurons exist in the brain as part of a complex, intimately connected network with other cell populations as part of what is known as the neurovascular unit (NVU) (87, 88).

The NVU, first defined by Harder *et al.* (89), is considered to be a functionally and structurally interdependent multicellular complex, comprising neurons, inter-neurons, astrocytes, microglia, oligodendrocytes, basal lamina, endothelial cells, pericytes and perivascular macrophages (Figure 3). Each component is closely related to each other, forming an anatomical and functional whole, which allow them to work in a synchronized and reciprocal way. These connections between components are established through gap junctions and adhesion molecules. This system of highly connected elements regulate blood flow and cellular permeability to meet metabolic demands (90, 91). Each element of the NVU has its own role during the stroke, and it has been proposed that successful recovery is achieved by restoring the NVU (92-94). It appears that remodelling of the NVU continues for many weeks and potentially months following stroke. However, it is not clear the role that each element of the NVU plays during stroke recovery. Elucidating these endogenous neurorestorative mechanisms might help in finding new therapeutic interventions aiming at further enhancing recovery. Therefore, here I will focus on some of these key components.

Neurons: In the context of stroke, neurons in the core die within minutes after the ischemic insult. These neurons can die through different pathways such as necrosis, apoptosis, ferroptosis and autophagy (95-98). Considerable effort has been made to investigate these cell death pathways, and some neuroprotective agents have been suggested to prevent neuronal cell death and rescue penumbra tissue in animal models of stroke. However, in the clinical trials these compounds have not showed any benefit (99).

While ischemic stroke causes neuronal death and extensive brain damage, it also triggers neurogenesis. This neurogenesis occurs in areas called neurogenic niches, which are the subgranular zone (SGZ) and the subventricular zone (SVZ). Experimental studies have shown an increased neuronal proliferation in the rodent SVZ after stroke. Newly proliferated neural stem cells migrate to the infarct area, differentiate into mature neurons and integrate into the lesion (100-102). Biopsies from ischemic human brains have also demonstrated stroke-induced neurogenesis in the penumbra (103). However, this self-repair mechanism operates only acutely after stroke and is insufficient to promote long-term recovery. Additionally, for the newly proliferating neurons to be fully functional, they need to mature and integrate into the existing neuronal circuits (104). These findings have been considered very promising as a potential therapeutic target to enhance brain repair.

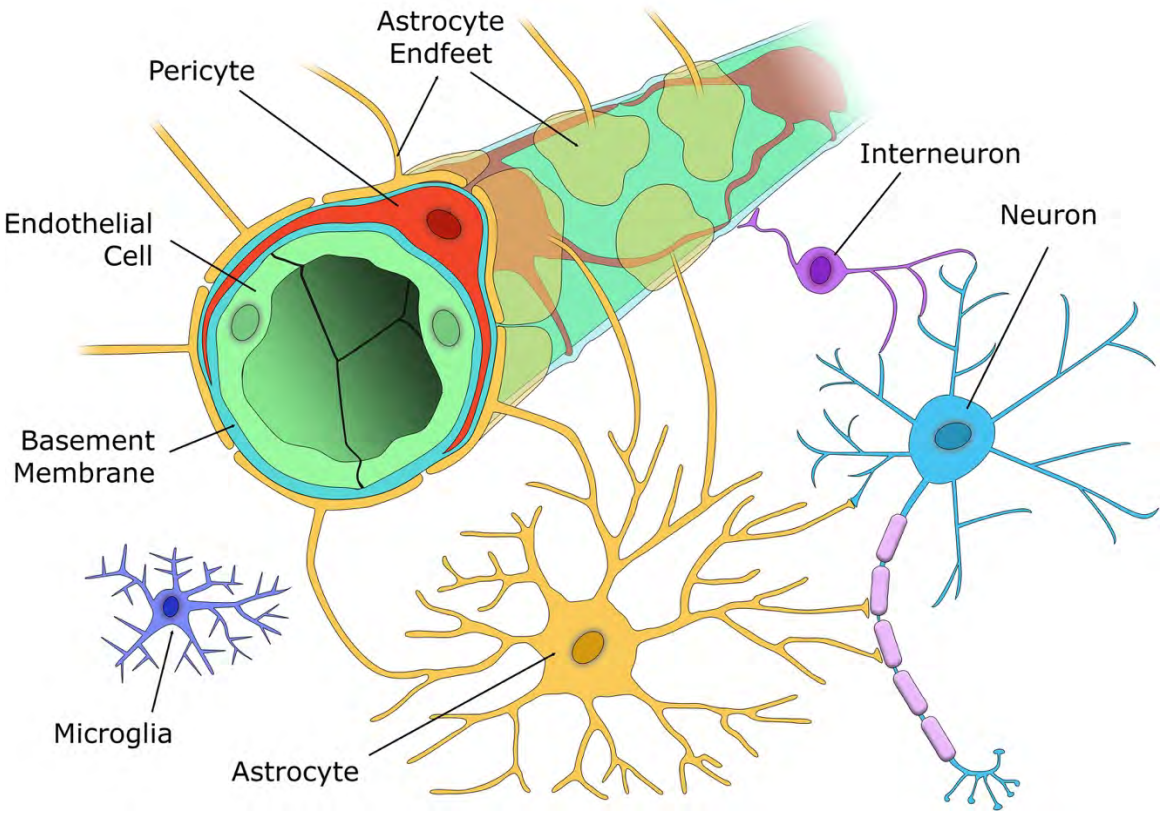

Figure 3. Schematic representation of the neurovascular unit (NVU) and its components. The endothelial cells are connected with each other through tight junctions and adherens junctions to form the brain blood barrier together with pericytes. This first protective layer is then surrounded by the basement membrane and astrocytes endfeet. Astrocytes also communicate with neurons, which in turn

send signals to alter the blood flow according to metabolic demand. Microglia are the immune cells of the brain and respond to disturbances to protect the brain. Image adapted from (105).

Blood vessels: The cerebral vasculature is responsible for delivering oxygenated blood and nutrients to the brain. After stroke, the cells around the occluded vessel die within minutes and therefore restoration of the blood flow as quickly as possible is one of the main priorities (106). In response to ischemia, the brain undergoes a series of self-repair mechanisms such as increased cerebral blood flow, collateral circulation, angiogenesis and arteriogenesis. Collateral vessels provide an alternate blood flow route to vital areas where the main supplying vessel fails, increasing perfusion to tissue at risk of death (107, 108). Arteriogenesis is the remodelling of pre-existing arterial anastomoses to fully developed and functional arteries. This process is induced by physical forces (109, 110) and is a main mediator in increased cerebral blood volume in the early stages. Good collateral supply together with arteriogenesis are main contributors to good cerebral blood flow in the acute phase of stroke and this has been strongly associated with better clinical outcomes (111-113).

Angiogenesis occurs in the later stages and consists in the formation of new blood vessels from proliferating endothelial cells. Both experimental and clinical studies have shown that angiogenesis in the penumbra is associated with higher rate of survival and enhanced recovery after stroke (114, 115). The cellular mechanisms involved in angiogenesis are not fully understood. It is clear that numerous growth factors, such insulin-like growth factor 1 (IGF1), brain derived neurotrophic factor (BDNF), vascular endothelial growth factor (VEGF), and Angiopoietin-1/2 (Ang-1/2) released after the ischemic event play a crucial role in angiogenesis (116). While several experimental studies have demonstrated that these factors promote angiogenesis after stroke (117), the use of these factors in clinical trials have so far failed (118-120). The failure of angiogenesis therapies may be due to the fact that those therapies consisted of one single angiogenic factor and the timing of administration. Future therapeutic intervention targeting angiogenesis should instead include multiple angiogenic factors.

Astrocytes: In a healthy brain, astrocytes have several important roles in controlling blood–brain barrier (BBB) permeability, brain homeostasis, regulating synaptic transmission, secretion or absorption of neurotransmitters and metabolic support amongst others (121-125). After stroke, the actions of astrocytes are extremely important and well characterised. Within minutes after occlusion, the astrocytes respond by formatting a glial scar. This process involves the change of astrocyte morphology by exhibiting a hypertrophy in their processes and an increase in the expression of key cytoskeletal proteins, glial fibrillary acid protein (GFAP) and vimentin (VIM) (82). These reactive astrocytes create a dense matrix of extracellular matrix proteins that rapidly initiate the formation of the glial scar around the infarct core. This glial scar is highly important as it seals off the site of injury and limits the spread of toxic substances from dying cells into the surrounding undamaged tissue (126, 127). Li *et al.* (82) demonstrated the importance of this scar in neuroprotection and brain repair by creating GFAP and VIM knockout mice. These mice presented significantly larger infarct volumes than wild type mice. A subsequent study by Liu *et al.* (128) also demonstrated that these knockout mice exhibit persistently impaired motor function relative to the wild type. Additionally, Hayakawa *et al.* (129) demonstrated that astrocytes can release and transfer functional mitochondria to injured neurons after stroke to support cell viability. Although the formation of the glial scar clearly has some beneficial effects after stroke, it also has a negative impact in the brain. Different studies have demonstrated that reactive astrocytes secret inhibitory molecules, such as chondroitin sulphate proteoglycan (CSPG), which impede axonal regeneration and re-innervation, leading to slower recovery within the central nervous system (CNS) (130-132). Understanding the evolution of the reactive astrocytes and the glial scar overtime is critical for the development of future interventions. Furthermore, astrocytes play an important role in waste brain clearance. It has been demonstrated that the astrocytic endfeet wrap around the brain vasculature forming a perivascular space, which allows the clearance of interstitial solutes and waste products from the brain. This clearance is mediated by aquaporin 4 (AQP4) water channels highly expressed in the endfeet of astrocytes (133).

However, this clearance is disturbed after stroke (134), suggesting that this pathway might represent a promising target.

Microglia: microglia are recognised as the resident immune cells of the CNS. Microglia carry out many functions including scavenging, phagocytosis of cellular debris, antigen presentation, synaptic pruning, secretion of neuroprotective cytokines and initiation and regulation of pro-inflammatory and anti-inflammatory molecules (135-137). In the healthy brain, microglia adopt a classical 'resting' phenotype characterised by a small soma with multiple branching processes. In this state, microglia are continuously extending and retracting their processes to monitor the microenvironment and rapidly respond to injury (138-140). After ischemic stroke, microglia transition into an 'activated' phenotype in the area closest to the infarction. Microglia retract their processes and adopt an amoeboid morphology with enlarged cell somas and shorter processes, they can phagocytose debris and release high levels of pro-inflammatory cytokines and free radicals (141). Activation and recruitment is triggered within hours of stroke and their involvement in the processes occurring at the peri-infarct site persist for a few weeks (142). In rodents, microglial activation has been reported as early as one hour after stroke, while in the humans activated microglia have been detected within 24 – 48 hours (143-145). A substantial amount of research has been focussing on whether activated microglia is ultimately harmful or beneficial for stroke recovery, with data supporting both possibilities. The general consensus seems to be that microglia activation has both a neuroprotective and neurotoxic effect after injury, depending on the specific neurotrophic factors and cytokines released at different time points after stroke. Pro-inflammatory cytokines, ROS, nitric oxide (NO) and proteolytic enzymes released in the early phases of stroke are involved in the exacerbation of inflammatory process, BBB breakdown cytotoxicity, the recruitment of peripheral immune cells and ultimately contribute to further neuronal damage. However, in later stages microglia switch from a pro-inflammatory phenotype to an anti-inflammatory phenotype (146).

Different *in vivo* studies have recently outlined the importance of microglia in response to ischemic stroke. Lalancette-Hébert *et al.* (147) demonstrated that suppression of microglia activation and proliferation after stroke caused bigger infarcts and increased neuronal loss on 1 day and 3 days after stroke. These findings were also supported by Szalay *et al.* (148) and Jin *et al.* (149). Contrary to this, a number of articles have supported the negative impact of microglia in the stroke brain. Neher and his group (150) reduced microglia phagocytosis by knocking out two phagocytic proteins. They observed that the knockout stroke rats presented less neuronal loss and better functional recovery. Similarly, another study by Liu *et al.* (151) has shown that the use of minocycline (a drug that inhibits microglia activation) for 4 weeks resulted in a reduction in microglia activation, increased neurogenesis and improved functional outcomes after stroke. Additionally, clinical studies have shown that administration of minocycline to stroke patients promoted better functional recovery than the control group (152-154). It needs to be highlighted that minocycline has also been shown to inhibit many other peripheral immune processes such as expression of matrix metallopeptidase (MMP), T cell infiltration, inflammatory cytokine production, apoptosis of oligodendrocytes as well as reduced neuronal death (155-160). Therefore, minocycline may provide neuroprotection in the ischemic brain via mechanisms that are independent of microglia.

The presented evidence suggests that microglial activation plays a critical role in stroke recovery, although further research is required to determine whether this role is beneficial or deleterious. Of special importance is to understand the temporal dynamic of microglia activation weeks after stroke to develop interventions accordingly.

1.5.3. Secondary neurodegeneration

While most stroke research focuses on changes occurring within the surrounding areas of the infarct, they are not the only regions affected. It has been documented that the brain exhibits changes in regions remote from, but synaptically connected to, the primary site of ischemic insult in the weeks and months following stroke (161, 162). This phenomenon is known as secondary neurodegeneration (SND), and can be observed as atrophic brain regions by

histopathological and neuroimaging techniques. SND was first described in 1914 by Constantin von Monakow who originally termed this phenomenon as ‘diaschisis’ (163). Since then, SND has been identified in humans following stroke and confirmed using a variety of different neuroimaging approaches such as computerized tomography (CT) (164-167), magnetic resonance imaging (MRI) (168-171) and diffusion tensor imaging (DTI) (172, 173). In experimental stroke models, SND has also been consistently shown (161, 162, 174-177). SND occurs over a longer period of time than the primary infarction process, and has recently been associated with the development of a number of late phase functional recovery disturbances, including neurological deficits, dementia, depression, cognitive impairment and fatigue.

One brain region particularly susceptible to SND after cortical stroke is the thalamus. Specific thalamic nuclei (ventral posteromedial nucleus, ventral posterolateral nucleus and posterior complex of the thalamus) are highly connected with the ischemic cortex via thalamocortical and corticothalamic projections (178-180). Degeneration within this area has been attributed to retrograde degeneration of the thalamocortical fibers. Additionally, other brain regions have been documented to be susceptible to SND, including the substantia nigra and the distal pyramidal tract (Figure 4) (181-183). More recently, numerous studies have started focusing their attention on the SND processes happening in the hippocampus. The hippocampus is one of the main adult brain regions implicated in higher cognitive function, most notably learning and memory processes. Interestingly, many stroke patients suffer from cognitive impairment despite the fact that the hippocampus is not usually directly damaged by stroke. Experimental studies have demonstrated an association between ischemic injury and secondary hippocampal degeneration in mice (184-186). Clinical studies have also demonstrated a link between hippocampal atrophy and cognitive dysfunction (187-189).

The development of SND occurs after neuronal damage at the infarct site and appears over an extended period. The earliest signs of SND in remote areas have been observed in humans after around one week post stroke and it can persist for years (161, 166). This prolonged time

course has encouraged researchers to start considering SND as a potential therapeutic target to prevent further neuronal death, enhance brain plasticity and improve functional outcomes during the recovery phase after stroke.

SND has a clear negative effect on the quality of life in stroke survivors, however still relatively little is known about this process and its link with the development of cognitive deficits. Advancing our fundamental knowledge of how SND develops is a promising avenue to increase our understanding in stroke pathophysiology, and a first step towards the development of potential therapeutic interventions. *Accordingly, I have directed much of my investigative effort to model and understand SND using an experimental stroke models. Specifically, I will focus on thalamic SND, as the literature suggests that this site is routinely disturbed, and hippocampal SND due to its importance in cognitive function.*

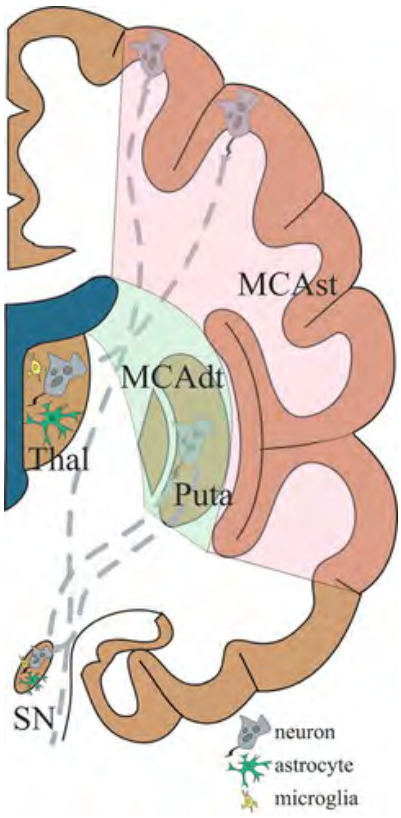

Figure 4. Schematic representation of secondary degeneration after MCAO. Occlusion of the MCA causes neuronal death, axonal degeneration and gliosis in distant areas such as thalamus (Thal) and

substantia nigra (SN). MCAdt, middle cerebral artery deep territory; MCAst, middle cerebral artery superficial territory; Puta, putamen. Image adapted with permission from (161).

1.5.3.1. Mechanisms of SND

Neuronal death

SND represents an incredibly complex biological phenomenon. SND is a form of progressive neuronal death accompanied by glial activation and neuro-inflammation in brain regions remote to but synaptically connected to the infarct site. However, the mechanisms that lead to neuronal degeneration in these areas are not fully understood. It is widely believed that part of this degeneration is due to a process known as Wallerian degeneration (WD). WD develops when a nerve fibre connection is cut or axonal transport is significantly disrupted (190, 191). This anterograde and retrograde degeneration of fibres may cause excitotoxicity and oxidative stress in remote regions, leading to neuronal death. Necrosis represents an important mechanism for neuronal death in SND sites (192, 193). Additionally, morphological features indicative of apoptosis, such as DNA fragmentation, nuclear condensation, apoptotic bodies and increased caspase-3 activity, have also been observed in SND sites after stroke (194, 195). These findings support the possible involvement of necrosis and apoptosis in SND. Together with neuronal death, SND is characterised by intense neuroinflammation (microglia and astrocyte activation) as well as the accumulation of protein aggregates such as amyloid β (Aβ) (Figure 5).

Neuroinflammation

Some evidence support the idea that neuroinflammatory processes driven by microglia and astrocytes may contribute to the neuronal damage at sites of SND; however, their exact roles are yet to be fully described. In both humans and animals, cytokine upregulation and microglial/astrocytic activation have been frequently detected before or concurrently with neuronal damage in areas of SND, suggesting a detrimental role of neuroinflammation in the development of SND (161). In support to this, the expression of pro-inflammatory cytokines

(TNF-α and IL-6) released by astrocytes and changes in microglial activation have been shown to precede neuronal death in the thalamus (196-198). Clinical studies have shown an increased neuroinflammation in SND sites after stroke. Using MRI, Ogawa *et al.* (199) demonstrated a persistent neuron loss and gliosis in the ipsilateral thalamus of stroke patients at 1-12 months post middle cerebral artery occlusion (MCAo). Further clinical studies showed enhanced microglia activation in the ipsilateral thalamus which persisted for up to 2 years post-stroke (200, 201). Similar results have been observed in other regions such as the hippocampus. These clinical findings align well results obtained in animal studies. Several rodent studies have shown an increased astrogliosis and microglial activation consistently in areas of SND after stroke (185, 202-206). For instance, Dihne *et al.* (198) showed delayed glial activation and neuronal loss in thalamic nuclei 14 days after MCAo. Most recently, Patience *et al.* (203) observed an increased gliosis in different areas including the thalamus and hippocampus at 4 weeks post-stroke. Neuroinflammation at sites of post stroke SND can be observed 3 days after stroke and persist for weeks (143, 144, 162).

Several studies have used interventions to modulate the outcomes of SND. Schroeter *et al.* (207) found significantly increased neurodegeneration and microglia activation in the ipsilateral thalamus of osteopotin knockout mice. However, no effect was detected in the infarct area. In another study, Zuo *et al.* (208) demonstrated that suppression of Cathepsin B (protease involved in regulation of cell death and protein catabolism) after stroke has a neuroprotective effect and reduces the activation of both microglial and astrocytic in the ipsilateral thalamic nuclei. However, it had no effect on infarct volume. These findings support the idea that neuroinflammatory mechanisms independent to those at the infarct site occur at sites of SND. This is an important observation as it highlights the need to target the specific mechanisms at sites of SND. However, in order to develop SND focused interventions a better understanding of the underlying mechanisms and neuroinflammatory processes is required.

Neurotoxic protein accumulation

Another key hallmark of post-stroke SND is the accumulation of neurotoxic proteins, such as Aβ and α-synuclein (α-syn) (161, 209-211). The accumulation of these proteins may provide an obvious explanation for a number of pathological disturbances known to emerge in the months following stroke, such as cognitive impairment and dementia. For instance, it is well know that the risk of developing dementia after stroke is substantially higher than age matched controls (57). This disease is characterised by a progressive neurodegeneration and accumulation of neurotoxic proteins, clinical features that are consistent with the SND processes seen after stroke. While the link between stroke and the risk of developing dementia and other cognitive deficits has not been proven yet, a lot of effort has been placed on these outcomes in the context of SND.

Aβ is the most widely known neurotoxic protein and extensively implicated in neurodegeneration (212-214). Aβ is produced as a monomer (Aβ40 and Aβ42) (215). These monomers have the propensity to self-assemble into different soluble low molecular weight oligomers, then form soluble high molecular weight oligomers, and eventually continue to accumulate and aggregate to form insoluble Aβ fibrils and plaques (213, 216). Classically, the plaques have been linked to cognitive dysfunction; however, emerging literature has indicated that soluble Aβ oligomers may be responsible for the disruption of cellular functions, including calcium dysregulation, membrane depolarization, impairment of mitochondrial functions and synaptic dysfunction (213, 214, 217, 218). More recently, it has also been demonstrated that Aβ oligomers constrict capillaries and can deposit in cerebral vasculature (219). In rodent studies, the accumulation of Aβ is particularly common and robust finding in SND sites. Studies have shown that Aβ appears as a diffuse aggregate in thalamic SND sites 1–6 weeks after stroke and over time transforms into plaque-like deposits at 9 months (211, 220). Our group has also reported an increased accumulation of soluble Aβ oligomers within the thalamus 6 weeks after stroke (221). Furthermore, pharmacological interventions to reduce

Aβ accumulation in thalamic SND sites are associated with an improvement of functional outcomes (209, 210, 222).

A second protein extensively implicated in neurodegeneration is α-syn. α-syn is involved in synaptic activity and in normal condition is presented as a natively unfolded cytosolic protein. In pathological conditions, such as Parkinson's disease α-syn undergoes oligomerisation and abnormal aggregation under different environmental conditions (223, 224). Similarly to Aβ, recent evidence suggests that the oligomeric form of α-syn is responsible for the neuronal toxicity and cognitive decline in neurodegenerative diseases through multiple mechanisms such as inflammation, oxidative stress and autophagy (225-229). Interestingly, all these pathophysiological mechanisms are similar to those present after stroke, however, the specific role of α-syn in stroke is unclear. Some pre-clinical studies have previously demonstrated that an ischemic insult can promote an increased α-syn expression, phosphorylation, and aggregation in the brain (225, 230). Although there has been certain advancements in the last couple of years, the involvement of α-syn in stroke is still largely unknown.

There are numerous possible mechanisms that could explain the increase in neurotoxic protein accumulation: overproduction, a decrease in degradation and/or impaired brain waste clearance. To this date, it is unclear which of these mechanisms is predominantly involved in the increased deposition of these proteins and it is most likely a combination of all of them. A deeper understanding of the mechanisms underpinning protein build-up may help identify an appropriate therapeutic target in clinical trials. *Therefore, in the chapter 3 of this thesis I will investigate the link between an increased accumulation of neurotoxic proteins and the failure of the clearance mechanisms. Additionally, in chapter 4 I aim to investigate the progression of the neurotoxic protein accumulation overtime.*

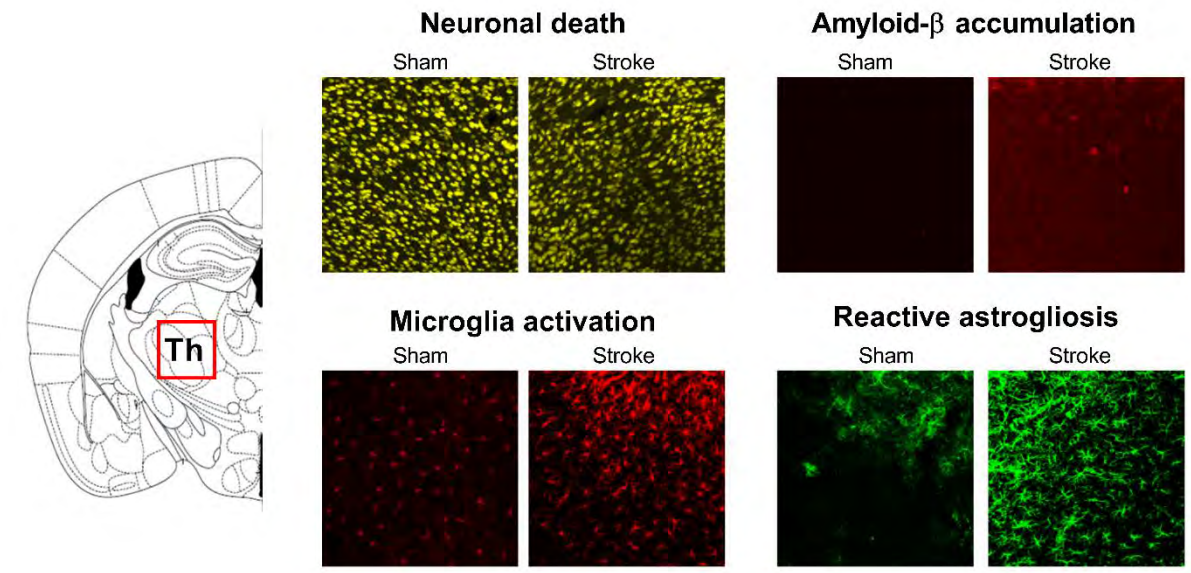

Figure 5. Secondary neurodegeneration (SND) hallmarks. Stroke results in significant neuronal loss, increase Aβ accumulation, activated microglia and reactive astrogliosis in the SND sites. Th = thalamus.

1.6. Animal models of stroke

Focal ischemia

The use of animal models of stroke has contributed to our understanding of the cellular and molecular mechanisms occurring in the brain after ischemic stroke. Rodents are widely used in stroke research due to low mortality, ease of use, cost-effectiveness and similarities in cerebrovascular anatomy to that of humans. Currently, there are several well established models of experimental stroke. Each of them with their own set of advantages and disadvantages that need to be carefully considered when selecting the most appropriate model to answer a specific experimental question. These include: (i) mechanical occlusion of the MCA (MCAo); (ii) thrombotic occlusion via injection of preformed clots or micro-emboli into the MCA; (iii) injection of endothelin-1 (a potent vasoconstrictor) and (iv) photothrombosis by injection of Rose Bengal (231).

The MCAo model is one of the most commonly used experimental stroke models. In this model, an intraluminal filament is introduced *via* the common carotid artery until it reaches the origin of the MCA, resulting in the hypoperfusion of the MCA vascular territory (232, 233). The

time of occlusion is variable but the filament is normally placed for between 60-120 minutes, or permanently. This procedure does not required craniotomy. Alternatively, MCAo can be induced using a clip, ligature or electrocoagulation which requires a craniotomy to directly access the blood vessel, and therefore is not recommended as exposure of the brain can significantly influence intracranial pressure and BBB function. One of the main advantages of the MCAo model is that it strongly mimics human ischemic stroke because around 70% of human strokes occur due to occlusion of the MCA (234). However, this model has certain limitations. Firstly, it is characterised by significant variability in lesion size even within the same mouse strain and has a significant risk of mechanically induced subarachnoid haemorrhage (235). Secondly, MCAo produces large to very large infarctions and can damage multiple areas of the brain such as thalamus and substantia nigra (236). Thirdly, it is a technically complex procedure and time consuming, which reduces the number of animals that can be used in experimental groups and affects the sample size (231). Finally, this model can also cause serious complications, such as retinal injury and consequent visual dysfunction (affecting behavioural assessments) (237), and impaired mastication and swallowing functions due to damage to the external carotid artery (238).

The thromboembolic stroke model also closely mimics the pathophysiology of human stroke. This involves the preparation of artificial or autologous clots *ex vivo* that then are injected into the carotid artery (239). The major disadvantage is the large variations in lesion size and location. Therefore, this model is not commonly used except to test thrombolytic agents.

Another model of focal ischemic stroke is local application of a potent vasoconstrictor, such as endothelin-1, via stereotaxic intracerebral injection (240). This method is characterised by being less invasive than MCAo, highly reproducible, causing minimal oedema and the ability to precisely target specific brain circuits (241, 242). The main disadvantage is that endothelin-1 receptors are also present in astrocytes and neurons (243), and therefore it has been reported to promote astrocytosis and facilitate axonal sprouting (242). This model is not suitable to investigate glial and neuronal responses.

Finally, the photothrombotic stroke is a model of occlusion of small cerebral vessels (approximately 25% of human ischemic stroke is caused by small vessel injury) (244, 245). The infarct size generated by the photothrombotic stroke is relatively smaller compared to the MCAo model, and it is usually located at the cortical area. This model induces ischemia by intraperitoneal injection of photosensitising dye (e.g. Rose Bengal). This dye is allowed to circulate in the bloodstream for a short period to ensure adequate dispersal to the cerebral vasculature (Figure 6). Then, the dye is photoactivated using an external cold light source. Once the dye is activated, it produces oxygen radicals that cause damage to the endothelium, and activation and aggregation of platelets. This coagulation process subsequently induces occlusion in the cortical vessels within the entire field of light exposure (246, 247). The photothrombotic model allows for precise targeting of specific cortical areas and is highly reproducible. The size and location of the infarct induced is consistent and reduces the variability among lesions. These characteristics make this method ideal for the study of basic cellular and molecular mechanisms and pathways, particularly in recovery studies (248). Additionally, it is minimally invasive, relatively fast and easy to perform than other models, which allows for an increased sample size. Multiples studies have also demonstrated that photothrombotic strokes consistently produce SND in areas synaptically connected to the cortex, making it ideal to study stroke-induced retrograde degeneration (205, 206, 221, 249). The main disadvantage of this model is that it produces an infarct that is predominantly core, with minimal penumbral tissue, which is quite different to human stroke (250). Another limitation is that the rapid ischemic damage is associated with marked early cytotoxic and vasogenic oedema, which is different from human stroke. *Taking into account that the focus of this thesis is to study long-term functional outcomes as well as the cellular and molecular mechanisms involved, the photothrombotic stroke model was considered the most suitable model and it was used in the studies of this thesis.*

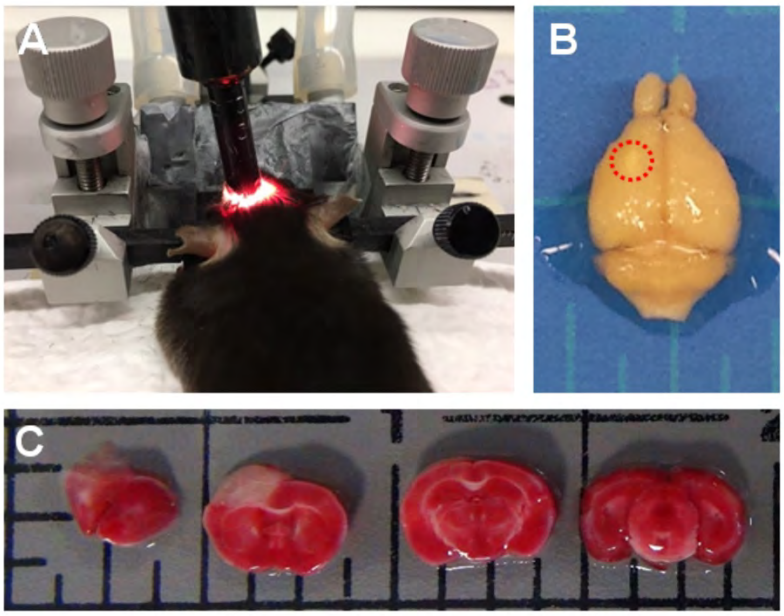

Figure 6. Photothrombotic stroke model targeting the left somatosensory and motor cortices. (A) Photothrombotic stroke set-up. (B) Visible cortical infarct caused by the stroke (dotted red circle). (C) 2,3,5-Triphenyltetrazoliumchloride (TTC) staining of damaged brain areas after photothrombotic stroke. Red areas represent healthy/normal tissue, while white areas represents damaged/dead tissue.

1.7. Functional assessments in animal models of stroke

As mentioned before, rodents have served as an excellent model to develop a deeper understanding of human stroke. Apart from assessing the histopathological, cellular and molecular characteristics of stroke, it is also important to assess the functional outcomes after experimental stroke and how these develop overtime. The evaluation of these functional outcomes allows for the assessment of the degree of damage caused longitudinally. The primary goal of stroke treatment is to improve the behavioural function in stroke survivors. Therefore, using experimental models to identify the behavioural deficits is essential to develop potential therapeutic treatments. The selection of adequate behavioural tests, according to the area of the brain damage and the interventions tested, is essential for the success of translational research.

1.7.1. Sensorimotor assessment

Impairments in the upper and lower limb are commonly seen in humans, and therefore it is necessary to use tests that measure homologous impairments in rodents (248). There are many sensorimotor tests available for rodents, but none of them have been demonstrated to be superior to others in fully characterising the different deficits that occur after stroke. Additionally, in long-term studies, sensorimotor tests that are sensitive enough to chronic impairments should be used. Therefore, it is recommended that a battery of different sensorimotor test should be performed in order to obtain a better understanding of the array of impairments and to prevent false-positive results. Although many different tests have been developed, here I will just focus on discussing those most commonly used sensorimotor tests in mice.

Cylinder test: One of the most commonly used test in rodents is the cylinder test, which is used to evaluate spontaneous forelimb use (251). In this test, mice are placed in a transparent glass cylinder and forelimb use during vertical exploration is evaluated by recording which forelimb is used to touch the wall of the cylinder. The first forelimb to touch the cylinder during a full rear is scored as a placement for that limb. Healthy animals will touch the wall equally with both left and right forelimbs. While ischemic mice will tend to use more frequently the non-impaired forelimb during vertical exploration (251). The cylinder task has been demonstrated to be objective, easy to undertake and grade, no pre-training needed and it is sensitive to long lasting deficits that other tests cannot detect (252). These characteristics make this test useful test for long-term recovery studies.

Grid walk: The grid walking task, also known as the foot fault task, has been used to assess motor impairments of limb functioning and placing deficits during locomotion in mice. Animals are placed on an elevated grid with squares sized approximately 2x2 cm and recorded while exploring the surroundings. The number of foot faults (paw slips through an open grid) made by the right and left limbs are counted (251). Healthy mice will walk placing their paws precisely on the grid. Stroke mice typically make significantly more foot faults with the impaired limb

than non-stroke mice. It is a simple test, requires minimal equipment, no pre-training and it is a sensitive test for detecting motor function impairments long-term after ischemia (253).

Staircase test: The staircase test is used to assess skilled reaching in mice. This test measures the ability of mice to extend their forelimbs and grasp food pellets (254). Mice are positioned in a chamber that contains an elevated platform with two staircases located on each side. The design of the chamber allows the mice to only use the right forelimb to retrieve the pellets from the right side and the left forelimb to retrieve the pellets from the left side. The staircases have six steps with food pellets. Latency to grasp the pellet, number of pellets obtained from each side and location in the staircase are measured to detect impairments (255). A healthy mouse will collect the pellets rapidly while stroke mice take longer times and show a tendency to grasp pellets with the non-impaired forelimb. It has been shown to be sensitive for detecting long-term deficits. However, this test requires food deprivation and a complex and long training periods.

Adhesive removal test: The adhesive removal test is typically used to evaluate sensory and motor impairments after injuries to the sensorimotor cortex. During the test, a small piece of adhesive tape is attached on each forepaw. The non-stroke mice rapidly sense the tape and remove it quickly. Tactile responses are measured by recording the latency to contact (sensory deficit) and remove (motor deficit) the adhesive tape. Mice with unilateral brain damage typically take longer to contact and remove the adhesive tape from the impaired limb (252, 256). Detection of long-term deficits have been reported in some stroke model but not others (257, 258).

Rotarod: Rotarod is one of the most commonly used tests to assess motor coordination and balance after stroke. Mice are placed on a rotating cylinder where they will try to remain to avoid falling onto a platform (259). The riding time is typically used as a parameter to evaluate motor function. Animals with ischemia stay on the rotating cylinder significantly shorter times (260). This test is easy to perform; however, it is not sensitive enough to distinguish spontaneous recovery from therapy-induced recovery.

Pellet Retrieval Task: This test is useful to examine an animal's ability to reach and retrieve a single food pellet (261). Mice are placed in a chamber with an opening in the middle of the front wall. The food pellets are placed in a tray located outside of the front wall. Mice must reach through the small opening, grasp and collect the pellet. The pellet is placed in the indentation opposite to their unaffected paw in order to assess unilateral brain damage. Attempts, successes, failures and drops are scored as parameters to evaluate impairments. Ischemic damage to the motor cortex results in impairments of skilled reaching (262). One main disadvantages of this test is that mice are food restricted and require a long period of pre-training to reach for food pellets.

Taking into account the advantages and limitations of the previously mentioned sensorimotor assessments, I considered that the most appropriate and relevant tests to measure long-term deficits and/or improvements in motor function after stroke are the cylinder test and grid walk. Therefore, they will be the sensorimotor assessments used in this thesis.

1.7.2. Cognitive assessment

Apart from sensorimotor deficits, cognitive deficits often occur after stoke as a results of damage to different brain areas. Since impairment in different cognitive domains are really common after stroke, cognitive testing is a necessary component to understand the full scope of the functional deficits. Preclinical tests should utilize models that reproduce common, clinically relevant cognitive deficits, using a battery of test sensitive to multiple cognitive domains. Additional effort should be made to monitor long-term behavioural changes to reflect chronicity and evaluate progression of cognitive function. Some cognitive domains impaired after stroke have been demonstrated in animal models (working memory, associative memory), while others are lesser known due to lack of assessment methods available (executive function, attention).

Classically, the Morris water-maze has been one of the most widely used behavioural tasks to assess spatial learning and working memory in mice (263). Different variants of the initial

method have been developed but they are all based in the same concept. Mice are placed in a circular pool and they are trained to swim to locate a platform hidden underwater. Time to reach the platform, time spent in each quadrant of the pool and swim path can be analysed to study swimming behaviours and determine memory impairments. In ischemic animals, the impairments observed when performing this task are long lasting (264-266). One advantage of using the water maze over other mazes is that mice cannot use olfactory trails to find the submerged platform and food deprivation is not required. However, this task presents multiple disadvantages such as results might be confounded by motor impairments, ceiling effects and hypothermia. Additionally, this task also relies on stressful circumstances to encourage performance, a factor that it is known to negatively affect cognition.

The radial arm maze is another test used to study spatial working memory. The device consists of a central platform with eight or twelve radial arms projecting from the centre with food pellet placed at the end of these arms (267). Mice are placed in the centre and allowed to explore the radial arms. Healthy mice will remember which arms they have previously visited to collect the reward. Ischemic animals make more errors when searching for food, showing impairment in working memory (268, 269). Similar to the water-maze, this task may be confounded by sensorimotor deficits. Additionally, being a one-trial task mice do not have sufficient time for habituation, making this task sensitive to other factors such as experimenter handling, anxiety and environmental factors.

While all the previously mentioned classical behavioural tasks could still be useful, greater emphasis should be placed on designing cognitive tasks that directly translate across species and are clinically relevant. This can be achieved using automated rodent touchscreen platforms that use testing paradigms analogous to those routinely used in humans (270). These touchscreen platforms for rodents are computer-automated behavioural testing methods based in visual stimuli and mice respond to a computer screen *via* a nose-poke directly to the stimulus (Figure 7). This method is non-aversive and low-stress and instead it relies on reward to motivate animals' performance. Rodents are previously trained until they

acquire a basic level of performance. Once they have reached a basic level, more complex tasks can be introduced to mimic human cognitive tests. Cognitive performance is assessed over numerous trials, conferring much higher sensitivity and enabling detection of cognitive enhancements as well as decline. Mice are habituated into the touchscreen over a couple of days, which reduces the potential of external factors to impact on the performance. Further, these platforms contain a battery of numerous cognitive tests, including tasks to study certain cognitive domains that cannot be tested with classical method such as attention and executive function. Additionally, it offers the potential for a high degree of standardization, minimal human involvement and is translationally relevant, as some of the tasks are direct analogues of clinical tests (e.g., similar to human CANTAB (Cambridge neuropsychological test automated battery) tests). Another advantage of using computer-generated visual stimuli is that the stimuli can be easily adapted and manipulated depending on requirements (270, 271). One potential limitation is that these tasks are time-consuming as they need to be completed over numerous days. Another potential limitation is that touchscreen tasks require a good motor function so that animals are able to cross the testing chamber, respond to the stimuli presented in the screen and collect a reward. However, the motoric demand is much lower than the one required in water-maze and arm maze (270, 271). These limitations should be taken into account when performing these tasks; however, the advantages clearly outweigh the few disadvantages. Most importantly, given the analogy between the rodent touchscreen and the tests used in clinical populations, these tasks can be extremely useful to improve the direct translation of specific findings into human populations as well as facilitate the development of new therapeutic interventions. *Therefore, a mouse touchscreen platform was used for the experiments that form part of this thesis.*

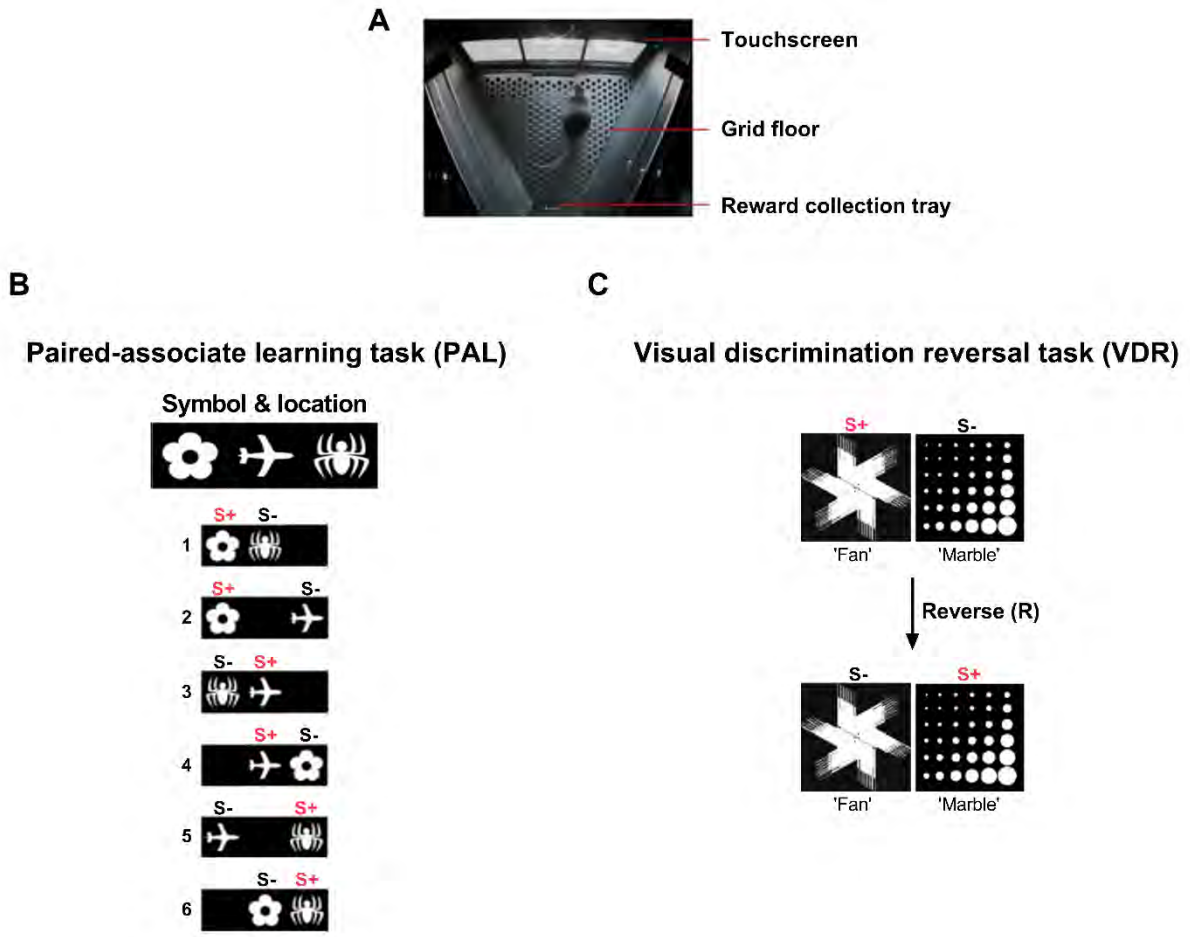

Figure 7. Touchscreen platform for cognitive assessment in mice. (A) A visual stimulus is presented in the touchscreen and the mouse must respond to the stimulus by nose poking the screen. If the mouse select the correct image, a liquid reward will be delivered in the rewards collection tray. (B) In the paired-associate learning task (PAL) mice must select the symbol that appears in the correct location (S+) to obtain a reward. This task measures associate memory and learning. (C) In the visual discrimination reversal task (VDR) mice must select the correct image (S+) to obtain a reward. Once the performance of the mice have reached ~70% correct responses, the images are reversed. The image that was correct (S+) is now incorrect (S-) and vice versa. The first part of this task measures ability to discriminate between two stimuli and the reversal measures behavioural flexibility.

1.8. Spontaneous recovery

It is well known that most stroke survivors achieve a certain level of recovery even without direct rehabilitation, during the weeks and months following the infarct. This spontaneous recovery is considered to be possible due to a variety of repair mechanisms coordinated by glia, neurons and vasculature (87, 88, 93, 94, 272). Historically, it was long believed that the

adult or injured brain was unable to remodel. However, in the last decades, this has been disproven and in fact, strong scientific evidence have demonstrated that the adult brain has a remarkable capability to respond to internal or external stimuli by reorganizing its structure, function, and connections (273-275). This mechanism is referred to as brain plasticity and can lead to a certain degree of spontaneous recovery after brain injury (Figure 8) (276). Plasticity mechanisms mainly observed in animal models include: cortical remapping, change in the trajectory of axons, modulation of certain neurotransmitters, synaptic plasticity, angiogenesis and neurogenesis (275). *Specifically, in this thesis I will focus in synaptic plasticity, angiogenesis and neurogenesis.*

Neurogenesis is one of the brains plasticity mechanisms that has been more commonly studied. Evidence of neurogenesis has been well documented in primary ischemic sites in both animal models and the human brain (104, 277-281). However, this process in SND sites has not been fully explored yet. Sites of ischemia have been shown to start repopulating with new neurons from 14 days and up to 12 months after stroke in animal models (280-285). Ling *et al.* (286) and Chen *et al.* (287) showed that neurogenesis can also occur in the thalamic SND sites at 14 days after stroke in rats.

Similarly to neurogenesis, the brain experiences complicated angiogenesis processes post-stroke. The effect of angiogenesis in stroke recovery is widely considered to be beneficial. Both pre-clinical and clinical studies have shown that increased angiogenesis in the penumbra is associated with enhanced recovery and longer survival times (114, 115, 288). The increased angiogenesis helps in the spontaneous recovery by “cleaning up” the necrotic tissue after stroke (289, 290) and by creating a “vascular niche” to support the generation and migration of new neurons (291, 292).

Synaptic plasticity is also known to play an important role in recovery after stroke. Synaptic plasticity is necessary for maintaining neuronal networks and it is achieved through improvements of communication in synaptic connections between existing neurons. Previous

studies have demonstrated that an enhancement in synaptic plasticity promotes functional outcomes after stroke (293).

Numerous studies have considered the impact of the above-mentioned mechanism in the evolution of functional outcomes after stroke. Specifically, an area in which brain plasticity has been extensively studied is motor recovery after stroke. As previously highlighted, motor impairments are highly common in stroke patients and the quality of life of these patients are dependent on the degree of motor recovery achieved. The first voluntary movements start to manifest from 6 to 33 days after stroke and the biggest improvements happen in the first month after stroke (294). Evidence of motor recovery after stroke has demonstrated that many forms of brain plasticity occur at the same time. Injury to a region of the motor cortex can result in spontaneous intra-hemispheric changes or shift to the uninjured hemisphere. On the other hand, cognitive recovery after stroke has been less studied due to its complexity and the variety of cognitive domains affected. Additionally, cognitive recovery might be more influenced by SND processes (294, 295).

These advances in understanding the spontaneous brain repair after stroke have been complemented by numerous therapeutic approaches with the goal of promoting brain plasticity, and thus re-establishing function and reducing disability after stroke. Some studies have concentrated on the days or weeks after a stroke, aiming to accelerate self-repair, while others have targeted the chronic phase months or years after stroke. However, to date, no therapeutic interventions have been approved clinically to enhance brain plasticity and spontaneous recovery (294). *Therefore, as part of my thesis I will study a new potential therapeutic intervention to enhance brain plasticity and functional recovery after stroke.*

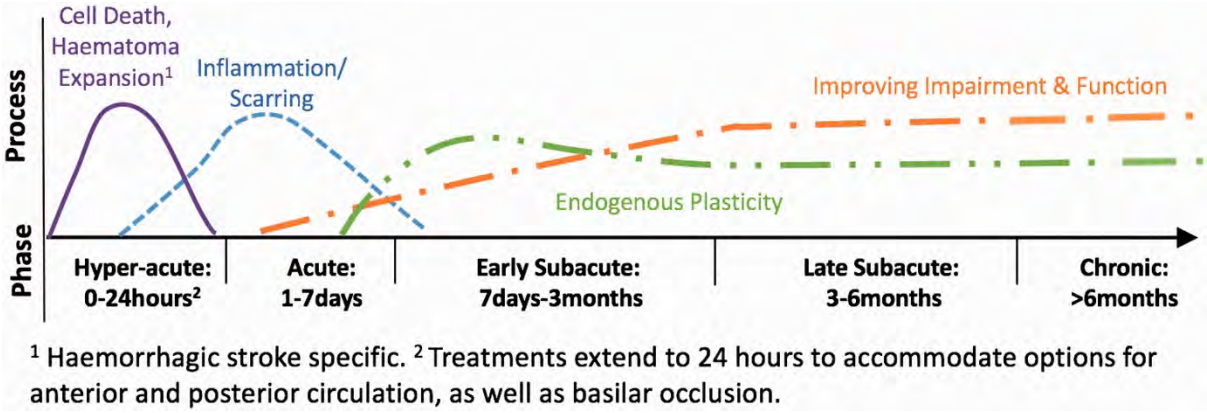

Figure 8. Schematic representation of the changes happening after stroke. During the first 24 hours (hyper-acute phase) the main process occurring is neuronal death. This is followed by an acute phase (1-7 days) driven mainly by inflammation and formation of the glia scar. In the following weeks and months (subacute and chronic phases), the brain suffers a spontaneous endogenous plasticity which in turn leads to improvements in functional outcomes. Adapted with permission from (296).

1.9. Growth hormone as a therapeutic intervention

1.9.1. Growth hormone

Growth hormone (GH) is an endogenous peptide hormone that is predominantly released into the circulatory blood stream from the anterior pituitary gland. GH production and secretion is controlled by the GH releasing hormone at the hypothalamus and inhibited by somatostatin (297). This pleiotropic hormone controls several complex physiological processes, including postnatal longitudinal growth in target tissues (liver, muscle, adipose and bone) and cellular metabolism (Figure 9). It can act by directly binding to GH receptors (GHR) on target cells or indirectly by generating insulin-like growth factor 1 (IGF-1) in the liver, which regulates the paracrine production of IGF-1 in many other tissues (297, 298).

Most importantly, different studies suggest that the GH/IGF-I axis may also play an important role in CNS functions, including neuronal growth, development and protection, myelin formation and glial cell differentiation (299, 300). GHR have been identified in several areas of the brain such as the choroid plexus, hippocampus, thalamus and hypothalamus in both rodents (301) and humans (302, 303). IGF-1 receptor (IGF-1R) is expressed in neuronal stem

cells, neurons and glial cells throughout the brain (304-306). Furthermore, whilst the pituitary is considered to be the exclusive source for GH, studies have observed an endogenous expression of GH in the hippocampus (307, 308). Additionally, growing evidence has demonstrated that peripheral GH uptake from the blood to the brain may occur through different routes.

Apart from stimulating brain plasticity, GH has also been shown to potentially improve cognitive function in both animal and human studies (309, 310). For instance, GH administration improves short-term and long-term memory in GH-deficient young adults (311) and in rats (312, 313). In contrast, lack of GH in adult humans with hypopituitary is associated with the impairment of most cognitive domains compared with matched controls, and these symptoms can be reserved with GH replacement therapy (310).

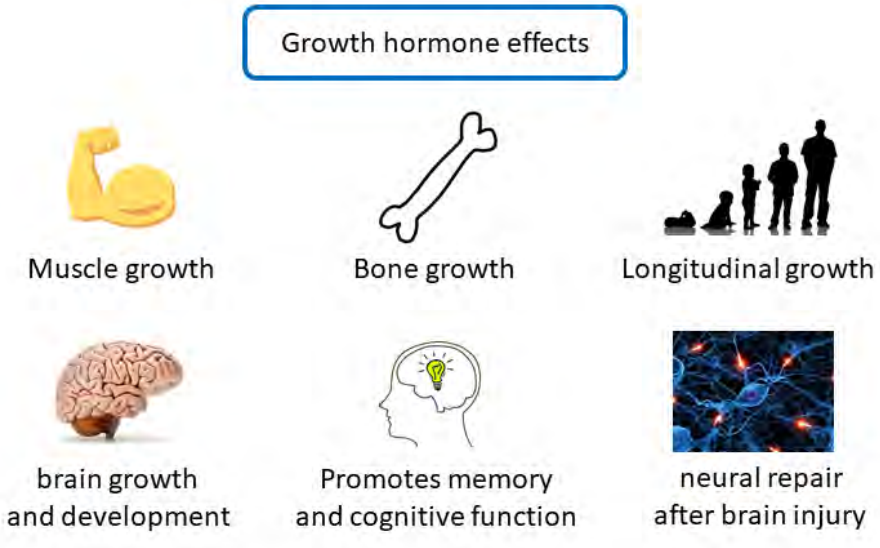

Figure 9. Schematic representation of the beneficial effects of GH. GH is widely known for promoting muscle, bone and longitudinal growth. Additionally, GH plays an important role in CNS functions, including brain growth, neuronal repair as well as improving cognitive function.

1.9.2. Current clinical use

Currently, recombinant human GH (rhGH) is clinically approved by TGA/FDA for indications in both the adult and paediatric population. In Australia, it is indicated as replacement therapy

in adults with GH deficiency, short stature due to decreased or failed secretion of pituitary GH, Turner syndrome, Prader-Willi syndrome and for treatment of growth disturbance in children with chronic renal insufficiency. Its safety and efficacy are well-documented (314) and therefore GH treatment is particularly attractive and ideally suited for clinical translation.

1.9.3. Growth hormone in brain injury and stroke

GH deficiency is a common feature of different neurological disorders. For instance, around one quarter of patient with traumatic brain injury (TBI) and subarachnoid haemorrhage suffer from GH deficiency shortly after injury (315). This deficiency has been linked with a variety of cognitive issues including poor verbal learning, verbal short-term memory and attention. Clinical studies have demonstrated that GH administration significantly improved cognitive rehabilitation and quality of life in TBI patients (316-319). This positive effect in cognition has been confirmed in experimental models of TBI together with increased expression of BDNF and synaptophysin (320). The positive effect of GH on brain repair and cognitive function have been also demonstrated in other neurological conditions such as severe frontal cortex lesion, cortical ablation (321, 322), hypoxic-ischemic injury (323, 324), kainate-induced injury (325) and after hypophysectomy (326, 327).

Recent clinical findings have also demonstrated the presence of GH deficiency after ischemic occlusion starting from 7 days to years after stroke (328-331). Some of the potential mechanisms that could explain the GH deficiency after stroke include direct occlusion/damage to the pituitary gland, occlusion/damage to the hypothalamus (or brain regions responsible of secreting GH regulatory hormones), inflammatory processes, secondary injury insults or a combination of these mechanisms (328). Taking all this together, it is reasonable to think that GH could be used as a therapeutic intervention to enhance neuroprotection and improve functional outcomes after stroke. To date, a very limited amount of clinical studies have investigated the therapeutic potential of GH. A pilot study by Song *et al.* (332) identified that the long-term administration of rhGH (once a week for 24 weeks) resulted in significant functional improvement and less fatigue. In another small clinical trial, Jin *et al.* (333) showed

that administration of rhGH for 6 months on top of citicoline treatment resulted in further functional improvement in stroke patients. Despite the promising results, further clinical studies are still needed to confirm this restorative effect.

Additionally, some pre-clinical studies have demonstrated the beneficial effects of GH in the stroke brain. Administration of GH has been proven to be successful in reducing the damage in the penumbra by enhancing survival of neurons when administered acutely after stroke in both *in vivo* (323, 324) and *in vitro* models (334). However, these previous pre-clinical studies have only focused on the neuroprotective effect of GH during the acute phase post-stroke and they did not analyse functional outcomes. This neuroprotective effect is different from the much longer neuroregenerative plasticity that takes place during the recovery phase after stroke. Surprisingly few studies have investigated the effect of a delayed administration of GH after stroke in neuroregeneration and functional outcomes. In one of the only such studies to date, Pathipati *et al.* (335) found that GH delivered directly into the lateral ventricle had the ability to enhance spatial memory, as measured by the Morris water maze. A study performed in our group (336) later confirmed these results by using a more sophisticated approach. They demonstrated that GH significantly improved associative memory and learning in stroke mice, as measured by a more translationally relevant platform such as touchscreen testing. Additionally, the authors found a reduction in neuronal tissue loss, higher levels of neurotrophic factors, increased angiogenesis, synaptogenesis and myelination within the peri-infarct region. These two studies are the first evidence to show that delayed administration of GH after stroke can positively influence cognition and brain plasticity. Given the fact that GHR are expressed in many regions of the brain including the hippocampus, this may explain the cognitive enhancement promoted by GH therapy and may represent a promising intervention in the future. *However, further evidence regarding the effect of GH in the hippocampus is necessary to provide compelling evidence for the usage of GH after stroke. In addition, there is still a large gap in our understanding of whether GH treatment could also enhance motor function after stroke. Therefore, in the chapters 5 and 6 of this thesis, I will address this matter.*

CHAPTER 2: RESEARCH AIMS AND HYPOTHESES

2.1. Rationale

Stroke is the biggest cause of long-term disability in the world. Currently, intravenous administration of tPA (thrombolysis) and endovascular clot retrieval (thrombectomy) are the only treatments clinically approved for stroke treatment. These treatments are focused on minimising brain damage and limiting complications acutely after stroke. However, despite the advancements over recent decades, most stroke patients cannot benefit from these acute therapies due to the short time window of action offered by tPA and the need of specialised stroke centres to perform a thrombectomy. Therefore, most stroke survivors suffer significant and often life-long motor and cognitive impairment. Motor impairment is usually addressed using physiotherapy and specific rehabilitation, which is often a long and slow process. On the other hand, cognitive impairment lacks of a specific treatment. New therapeutic interventions to promote functional recovery and brain plasticity after a stroke would be highly desirable.

Currently, it is not clear why cognitive deficits appear post-stroke and several mechanisms are likely to be contributing factors. Understanding the pathophysiological mechanisms occurring after stroke, with special emphasis in the subacute and chronic phases, would be key to broaden our knowledge regarding post-stroke cognitive impairment and to develop therapeutic interventions. Post-stroke secondary neurodegeneration (SND) has come into focus as a promising mechanism for cognitive impairment. This phenomenon is particularly interesting because it occurs over a timescale of months to years following stroke, which would greatly expand the time window for intervention. SND causes a progressive loss of tissues at sites connected to the area damaged. Amongst the areas affected by SND, include the thalamus and substantia nigra. More recently, some studies have started to focus their attention on the hippocampus. The hippocampus is involved in higher cognitive function and indirect damage to this region would explain cognitive impairment. It is well known that SND has a negative effect on the quality of life of stroke survivors; however, there is still a large gap in our

understanding about this process and its link with the development of cognitive deficits. Therefore, it is necessary to further elucidate the exact mechanisms underpinning the deleterious events of SND and its progression to different brain regions.

Neuronal death, neuroinflammation and accumulation of neurotoxic proteins are the main hallmarks of SND. Recently, studies have focused on understanding the relative contribution of the accumulation of neurotoxic proteins (such as Aβ and α-syn) to the development and progression of post-stroke SND. Since these proteins have been linked with neurodegenerative diseases, it is reasonable to consider they may play a crucial role in the development of cognitive impairment post-stroke. The underlying mechanisms of the accumulation of neurotoxic proteins over time after stroke and their link with cognitive deficits post-stroke is at this stage unknown.

After stroke, the adult brain has the ability to generate an adaptive response to promote recovery, which includes the proliferation of new cells and differentiation into different populations. However, this endogenous self-repair mechanism is limited and operates only acutely after stroke. Therefore, an intervention that could potentiate this effect would be highly desirable. GH has been postulated as a promising therapeutic intervention post-stroke. It has been shown that GH has the ability to improve cognition in health and disease *via* stimulation of brain plasticity processes in both rodents and humans. An important advantage of GH is its approval profile, safety and efficacy, which makes GH treatment particularly attractive and ideally suited for clinical translation. In the context of stroke, GH has already proved its ability to enhance the survival of neurons and reduce damage in the penumbra when administered acutely after stroke in rodents. Recently, delayed GH administration has been examined for its ability to stimulate cognition after stroke. However, further questions remain unanswered. Evidence regarding the neurorestorative effect of GH in the hippocampus are necessary to provide compelling evidence for the usage of GH after stroke. In addition, there is still a large gap in our understanding of whether GH treatment could also enhance motor function and improve multiple cognitive domains after stroke.

2.2. Aims and Hypotheses

The overall aim of this thesis is to investigate the link between the functional deficits after stroke and the pathophysiological mechanisms with a specific focus on the subacute and chronic phases. Additionally, I explored whether GH is suitable as a potential therapeutic intervention to alleviate the functional deficits.

More specifically the aims are:

- Investigate the link between cognitive impairment and SND processes, with a particular focus on thalamic and hippocampal regions (publication 1)
- Investigate cognitive and motor deficits long-term after stroke and whether they are associated with SND processes (publication 2)
- Determine the effect of delayed administration of rhGH on motor function and brain plasticity in the peri-infarct region (publication 3).
- Determine the effect of delayed administration of rhGH on cognition and brain plasticity in the hippocampus region (publication 4)

The hypotheses associated with the work arising from this thesis are:

- Stroke induce cognitive impairment is due to an increased accumulation of Aβ and α-Syn in the brain and a reduced waste clearance (publication 1).
- Stroke induce long-term motor and cognitive deficits is due to an increased neuronal loss, Aβ accumulation, astrogliosis and microglia activation in the peri-infarct and hippocampus (publication 2).
- Delayed administration of rhGH, starting at 48 hours post-stroke, improves performance in motor tasks and this is due to an enhancement in neurorestorative processes within the peri-infarct (publication 3).
- Delayed administration of rhGH, starting at 48 hours post-stroke, improves cognitive performance and this is due to an enhancement in neurorestorative processes within the hippocampus (publication 4).

CHAPTER 3: PUBLICATION 1

Visual discrimination impairment after experimental stroke is associated with disturbances in the polarization of the astrocytic aquaporin-4 and increased accumulation of neurotoxic proteins

As per the peer-review paper accepted and published in: Experimental Neurology

CONTRIBUTIONS

We, the co-authors, attest the Research Higher Degree candidate, Sonia Sanchez Bezanilla, contributed to the paper entitled **"Visual discrimination impairment after experimental stroke is associated with disturbances in the polarization of the astrocytic aquaporin-4 and increased accumulation of neurotoxic proteins"** as outlined below:

- 70% Conception and design of research;
- 80% Experimental procedures;
- 75% Analysis and interpretation of the findings;
- 75% Writing and critical appraisal of the content

Clifford TeBay		*18/02/2020*
Name of Co-author	*Signature*	*Date*
Michael Nilsson		*19/02/2020*
Name of Co-author	*Signature*	*Date*
Frederick R. Walker		*19/02/2020*
Name of Co-author	*Signature*	*Date*
Lin Kooi Ong		*19/02/2020*
Name of Co-author	*Signature*	*Date*

Lesley MacDonald-Wicks

Assistant Dean Research Training

10/3/2020

Visual discrimination impairment after experimental stroke is associated with disturbances in the polarisation of the astrocytic aquaporin-4 and increased accumulation of neurotoxic proteins.

Sonia Sanchez-Bezanilla[a, b], Clifford TeBay[a], Michael Nilsson[a, b, c, d], Frederick R Walker[a, b, c, d] Lin Kooi Ong[a, b, c]

a - School of Biomedical Sciences and Pharmacy and Priority Research Centre for Stroke and Brain Injury, University of Newcastle, Callaghan, NSW, Australia.

b - Hunter Medical Research Institute, New Lambton, Heights, NSW, Australia.

c - NHMRC Centre of Research Excellence Stroke Rehabilitation and Brain Recovery, Heidelberg, VIC, Australia.

d - Centre for Rehab Innovations, University of Newcastle, Callaghan, NSW, Australia.

Correspondence:
Lin Kooi Ong
School of Biomedical Sciences and Pharmacy and the Priority Research Centre for Stroke and Brain Injury, University of Newcastle, Callaghan, NSW, Australia. Hunter Medical Research Institute, Newcastle, NSW, Australia.
Phone: +61 492 15736
E-mail: lin.ong@uon.edu.au

Abstract

Numerous clinical studies have documented the high incidence of cognitive impairment after stroke. However, there is only limited knowledge about the underlying mechanisms. Interestingly, there is emerging evidence suggesting that cognitive function after stroke may be affected due to reduced waste clearance and subsequent accumulation of neurotoxic proteins. To further explore this potential association, we utilised a model of experimental stroke in mice. Specifically, a photothrombotic vascular occlusion targeting motor and sensory parts of the cerebral cortex was induced in young adult mice, and changes in cognition were assessed using a touchscreen platform for pairwise visual discrimination. The results showed that the execution of the visual discrimination task was impaired in mice 10 to 14 days post-stroke compared to sham. Stroke also induced significant neuronal loss within the peri-infarct, thalamus and the CA1 sub-region of the hippocampus. Further, immunohistochemical and protein analyses of the selected brain regions revealed an increased accumulation and aggregation of both amyloid-β and α-synuclein. These alterations were associated with significant disturbances in the aquaporin-4 protein expression and polarisation at the astrocytic end-feet. The results suggest a link between the increased accumulation of neurotoxic proteins and the stroke-induced cognitive impairment. Given that the neurotoxic protein accumulation appeared alongside changes in astrocytic aquaporin-4 distribution, we suggest that the function of the waste clearance pathways in the brain post-stroke may represent a therapeutic target to improve brain recovery.

Keywords: α-synuclein, amyloid-β, aquaporin-4, cognitive impairment, stroke

Abbreviations: SND, secondary neurodegeneration; CSF, cerebrospinal fluid; ISF, recirculation and interstitial fluid; AQP4, aquaporin 4; PAL, paired associate learning; Aβ, amyloid-β; VD, visual discrimination; α-Syn, α-synuclein; DG, dentate gyrus

Introduction

Stroke is associated with an elevated risk of cognitive impairment and dementia (Kuzma et al., 2018). Clinically, several studies have documented that up to 80% of stroke survivors experience some level of cognitive deficit (Levine et al., 2015). The cognitive domains which are commonly affected in stroke survivors include memory, learning and executive functions (Sun et al., 2014). However, the cellular mechanisms behind these deficits are yet to be determined. Although larger lesions are associated with greater cognitive impairment after stroke, the size and location of the primary infarct do not reliably predict the extent of these deficits (Gottesman and Hillis, 2010; Saczynski et al., 2009). One explanation for the modest association between cognitive impairment and tissue loss is that prior work has not taken into consideration loss of tissue at secondary sites. There is now mounting evidence demonstrating that stroke initiates delayed tissue and neuronal loss in remote regions that are functionally connected to the primary infarction site, a phenomenon increasingly referred to as secondary neurodegeneration (SND) (Baumgartner et al., 2018; Ong et al., 2017a; Wang et al., 2004; Xie et al., 2011).

SND has been consistently observed in clinical neuroimaging studies and in pre-clinical studies (Ong et al., 2017a; Zhang et al., 2012b), develops within days and can last for weeks, months and even years after the primary infarction. The key hallmarks of SND include neuronal death, neuroinflammation and increased accumulation of neurotoxic proteins (such as amyloid-β (Aβ)) (Iizuka et al., 1990; Kluge et al., 2018; Makinen et al., 2008; Patience et al., 2015; van Groen et al., 2005). Recently, our research team has reported that the accumulation of Aβ observed within the thalamus (a major site of SND) after stroke is associated with enhancement of soluble Aβ oligomers (Ong et al., 2017b). Previous studies have also shown that these neurotoxic proteins and in particular soluble oligomers are linked to cellular pathology and cognitive decline within the context of neurodegenerative diseases (Lesne et al., 2006; Lesne et al., 2013). Critically, these neurotoxic proteins continue to build up overtime after stroke (Aho et al., 2006; Liu et al., 2015a; Sahathevan et al., 2016) and several studies suggest that this might be due to a failure in their clearance (Arbel-Ornath et al., 2013; Garcia-Alloza et al., 2011). It is well documented that paravascular cerebrospinal fluid (CSF) recirculation and interstitial fluid (ISF) solute clearance is dependent upon the astroglial aquaporin-4 (AQP4) water channel (Iliff et al., 2012; Peng et al., 2016; Wang et al., 2017), and disturbances in this water channel has been previously linked with impaired clearance in different neurological conditions (Iliff et al., 2014; Ren et al., 2013; Wang et al., 2012).

Our group has recently identified that stroke, induced through photothrombotic vascular occlusion of the somatosensory and motor cortex, produces significant impairment of learning and memory using a touchscreen based assessment of paired associate learning (PAL) (Ong et al., 2018; Zhao et al., 2018). We further identified that the impaired performance was associated with significant accumulation of amyloid-β (Aβ) within the peri-infarct territories (Zhao et al., 2018). In this study, we aimed to determine whether the impairments that we previously observed in PAL task performance after a cortical stroke are generalizable to other cognitive domains. Specifically, we examined whether cognitive impairment are also generalised to other forms of visual-spatial memory, such as that assessed using the visual discrimination (VD) task (Horner et al., 2013). Further, we also intended to explore the molecular and cellular mechanisms behind these deficits. We investigated the accumulation and aggregation of not only Aβ but also α-synuclein (α-Syn), a second protein extensively linked to neurodegeneration (Kim et al., 2016; Stoica et al., 2012). We considered the accumulation of these proteins not only in the peri-infarct territory but also in SND sites, such

as the thalamus and hippocampus. Finally, we investigated the changes in the polarization of AQP4 in each of these regions.

Our primary hypothesis was that stroke would reduce the ability of mice to discriminate between two different stimuli. Secondly, we hypothesised that these deficits might be due to increased accumulation of Aβ and α-Syn in the brain. Finally, we proposed that disturbances in the polarization of AQP4 might play an important role in the accumulation of neurotoxic proteins and loss of neuronal cells, leading to cognitive impairment.

Materials and Methods

The data that supports the findings for this study are available from the corresponding author on reasonable request. An extended methods section is provided in the Supplementary Material.

Experimental design

Animal research was undertaken in accordance with the ARRIVE guidelines (Animal Research: Reporting of In Vivo Experiments). All the experimental groups were randomized, and all outcome analyses were performed in a blinded manner. A total of 62 mice (C57BL/6 male, 10 weeks old) were used in this study. Details on animal numbers for each experiment and inclusion/exclusion criteria are included in the supplementary material (Supplementary Fig. 1). The first cohort (sham n=10, stroke n=11) were subjected to a mouse touchscreen platform for VD task using images with a low similarity index (default images; fan and marble). The second cohort (sham n=10, stroke n=11) were subjected to VD task using images with a high similarity index and the brain tissue was used for histology analyses. The third cohort of mice (sham n=7, stroke n=7) were allocated for western blotting. At day 0, mice were subjected to photothrombotic occlusion or sham surgery. At day 3 post-stroke, mice were subjected to a mouse touchscreen platform for VD task during 10 consecutive days (days 3 to 13). Motor tests were performed one day before stroke/sham surgery and at day 14 before the mice were euthanized. Brains and blood samples were collected at 14 days post-stroke.

Sample Size Calculation

Sample size was estimated using G*Power 3.1 software. To determine the sample size required for the first and second cohort, we used preliminary data from the VD task (% correct rate at final session; sham versus stroke), and we obtained an effect size of Cohen's d=1.5. Allowing a type 1 error of 5%, α=0.05 with the power of 80%, β=0.2 we calculated a sample size of 9 mice per group. More than 9 mice per group would ensure that a stroke effect will be detected. For the third cohort (western blot analyses), we obtained an effect size of d=2 and we calculated a sample size of 6 mice per group.

Photothrombotic occlusion

Photothrombotic occlusion was performed as previously described (Zhao et al., 2017). This model is recognised to possess a number of advantages, including that is highly reproducible, has low experiment to experiment variance, controllable vascular occlusion size and location, and is widely used and extensively validated (Corbett et al., 2017; Uzdensky, 2018). Briefly, mice were anaesthetized by 2% isoflurane during surgical procedure on a temperature controlled (37˚C ± 1) stereotaxic frame. The skull was exposed by incision of the skin along the midline of the scalp. Rose Bengal (200 µl, 10 mg/ml solution in sterile saline, Sigma-Aldrich, USA) was injected intraperitoneally. After 8 min, the skull was illuminated for 15 min by a 4.5 mm diameter cold light source positioned at 2.2 mm left lateral of Bregma 0.0mm, targeting the left motor and somatosensory cortices. For the sham group, the same surgical

procedure was applied except Rose Bengal was replaced with 200 µl of sterile saline (0.9% NaCl, Pfizer, Australia).

Visual Discrimination (VD) task

Mouse touchscreen operant chambers were used in the cognitive testing as described with modifications (Horner et al., 2013), and were conducted in a blinded and randomised manner. Mice were calorie restricted overnight before cognitive testing (allowed access to food after cognitive testing for 5 hours, between 12:00 – 17:00 h). A liquid reward (strawberry milkshake) was provided to motivate the performance of the mice. Mice were introduced to a series of habituation and basic training tasks where they learn to associate a nose poke of the touchscreen and the delivery of a liquid reward. Over 10 days all mice learnt to perform the task with a minimum correct rate of 70%. Following general touchscreen training, mice underwent photothrombotic occlusion surgery. Three days post-surgery, mice commenced the VD task. Briefly, the procedure entailed simultaneous presentation of two stimuli; one was programmed as being correct (S+) and one as being incorrect (S-). Whether the S+ was on the right or left was determined pseudorandomly. When the mouse made a correct choice, S+, a tone was triggered, the food tray was illuminated and the food reward was delivered (a correct trial was recorded). If the mouse touched the incorrect image, S-, there was no reward delivery, no tone, and the house light was turned on for 5s and a correction trial was initiated. Correction trials consisted of repeated presentation of the previous trial until a correct response was made and were not counted towards the trial limit or number of correct responses. In each VD session, the testing ended once a mouse successfully completed 30 trials or reached a 60 min time limit, whichever occurred first. All mice completed a total of 10 sessions.

Paw asymmetry assessment using the cylinder task

Motor function was evaluated by a cylinder test as previously described (Schaar et al., 2010). Briefly, one day before stroke (day -1) and day 14 post-stroke, each mouse was placed in a glass cylinder 9 cm diameter and 15 cm in height, and movements were recorded from both sides for 10 min. Paw placement was determined by a researcher blinded to the experimental condition. The first forelimb to contact the wall during a full rear was recorded as an independent wall placement for that limb. The simultaneous contact of both the left and right forelimbs to the wall during a full rear was considered as one placement for both limbs. A total of 20 touches were scored. A final asymmetry score was calculated as the ratio of non-impaired forelimb movement minus impaired forelimb movement to total forelimb movement.

Protein extraction and Western blotting

The peri-infarct territory (2 mm^2 around infarct core, Bregma +1.0 to -1.0mm), the thalamus (Bregma -1.2 to -2.2mm) and the hippocampus (Bregma -1.2 to -2.5mm) were punched using a 1 mm tissue punch. Samples were sonicated in 300 µl lysis buffer (50 mM TRIS buffer pH7.4, 1 mM EDTA, 1 mM DTT, 80 µM ammonium molybdate, 1 mM sodium pyrophosphate, 1 mM sodium vanadate, 5 mM b-glycerolphosphate, 1 protease inhibitor cocktail tablet, 1 phosphatase inhibitor cocktail tablet, final concentration) and centrifuged at 14000g for 20 min at 4°C. The supernatant fractions were collected and pellet fractions were resuspended in 100 µL of sodium dodecyl sulfate buffer (2% SDS, 50 mM Tris pH 7.4). Protein concentrations were determined by Pierce BCA protein assay kit (Thermo Fisher Scientific, USA) according to the manufacturer's instructions. Samples were mixed with sample buffer (2% SDS, 50 mM Tris, 10% glycerol, 1% DTT, 0.1% bromophenol blue, pH 6.8). 15 µg of total tissue protein samples were electrophoresed into Biorad Criterion TGC Stain-Free 4–20% gels. Gels were transferred to PVDF membranes. PVDF membranes were washed in Tris-buffered saline with tween (TBST) (150 mM NaCl, 10 mM Tris, 0.075% Tween-20, pH 7.5) and incubated in 5%

skim milk powder in TBST for 1 h at room temperature. Membranes were incubated with primary antibodies (amyloid-β, α-synuclein, NeuN, AQP4, GFAP, ADLH1L1, α-syntrophin or dystrophin) overnight at 4°C and secondary antibody for 1 h at room temperature (see Suppl. Table 1 for antibodies concentration). In between each incubation step, membranes were washed in TBST. Membranes were visualized on an Amersham Imager 600 using Luminata Classico or Luminata Forte western blotting detection reagents. The density of the bands was measured using Amersham Imager 600 analysis software.

Histology Analysis

Cresyl Violet staining was performed as previously described (Ong et al., 2018). For immunoperoxidase labelling and immunofluorescence, free-floating fixed sections corresponding to peri-infarct (Bregma 0.0mm), and thalamus and hippocampus (Bregma -1.5mm) were immunostained as described (Zhao et al., 2017). Images were acquired using Aperio AT2 (Leica, Germany) or Leica TCS SP8 confocal microscope. ImageJ (1.50, National Institutes of Health) and Matlab (R2015a, MathWorks) were used to estimate tissue loss and to analyse intensity and area coverage of immunolabeling. AQP4 polarity analysis were performed as previously described (Wang et al., 2012). In this case, each image was thresholded uniformly at two different levels: a high and a low stringency threshold (Supplementary Figure 3(e)). The low stringency threshold defined the overall area of AQP4 immunoreactivity, whereas the high-stringency threshold defined the area of intense AQP4 immunoreactivity that in control mice is localized to perivascular end-feet of the astrocytes. The ratio of the low-stringency area to the high-stringency area was used to generate a value defined as "AQP4 polarity". The higher the AQP4 polarity, the greater proportion on immunoreactivity was restricted to perivascular regions, whereas the lower the proportion, the more evenly distributed immunoreactivity was between the perivascular end-feet and the soma. (For detailed image analysis see Supplementary material).

Statistics

All data were expressed as mean±SD and were analyzed using GraphPad Prism v7.02. The primary outcome measurement was differences between sham and stroke. Data from ELISA, tissue loss, western blotting, immunohistochemistry and immunofluorescence labelling were analyzed using 2-tailed t test. VD task (10 sessions temporal analysis) and motor test were analyzed using 2-way ANOVA, followed by Sidak multiple comparisons. A p value <0.05 was considered statistically significant.

Results

Cortical stroke induces cognitive impairment and motor deficits

Three days after the induction of the stroke targeting the motor and sensory cortex, the cognitive performance of the mice were assessed using a mouse touchscreen platform for VD task during 10 consecutive days (Fig. 1A). The first cohort of mice (sham n=10, stroke n=11) was evaluated using two images with a low similarity index ('marble-fan' pair). We observed a significant time effect ($F_{(4, 76)}=14.35$, $p<0.0001$) but no significant differences in the % correct trials in stroked mice compared with sham (Fig. 1B). The second cohort (sham n=10, stroke n=11) were subjected to the same VD task, however images were substituted for a high similarity index pair ('ovals-rectangles' pair). We found a significant decrease in % correct trials in stroked mice compared to sham ($F_{(1, 19)}=23.74$, $p=0.0001$) and a significant time effect ($F_{(4, 76)}=7.81$, $p<0.0001$). In addition, post hoc analysis indicated a significant decrease in rate of % correct trials at the fourth and fifth block of sessions in stroke mice compared to sham ($p=0.0179$ and $p=0.043$, respectively) (Fig 1C). A range of metrics from the VD task were also

collected for temporal analysis. There was no significant effect in the number of trials completed within 60 minutes nor in time to complete 30 trials, however, there was a significant increase in the number of total correction trials completed in stroke mice compared to sham (p=0.0426) (Supplementary Fig. 2A, B and C).

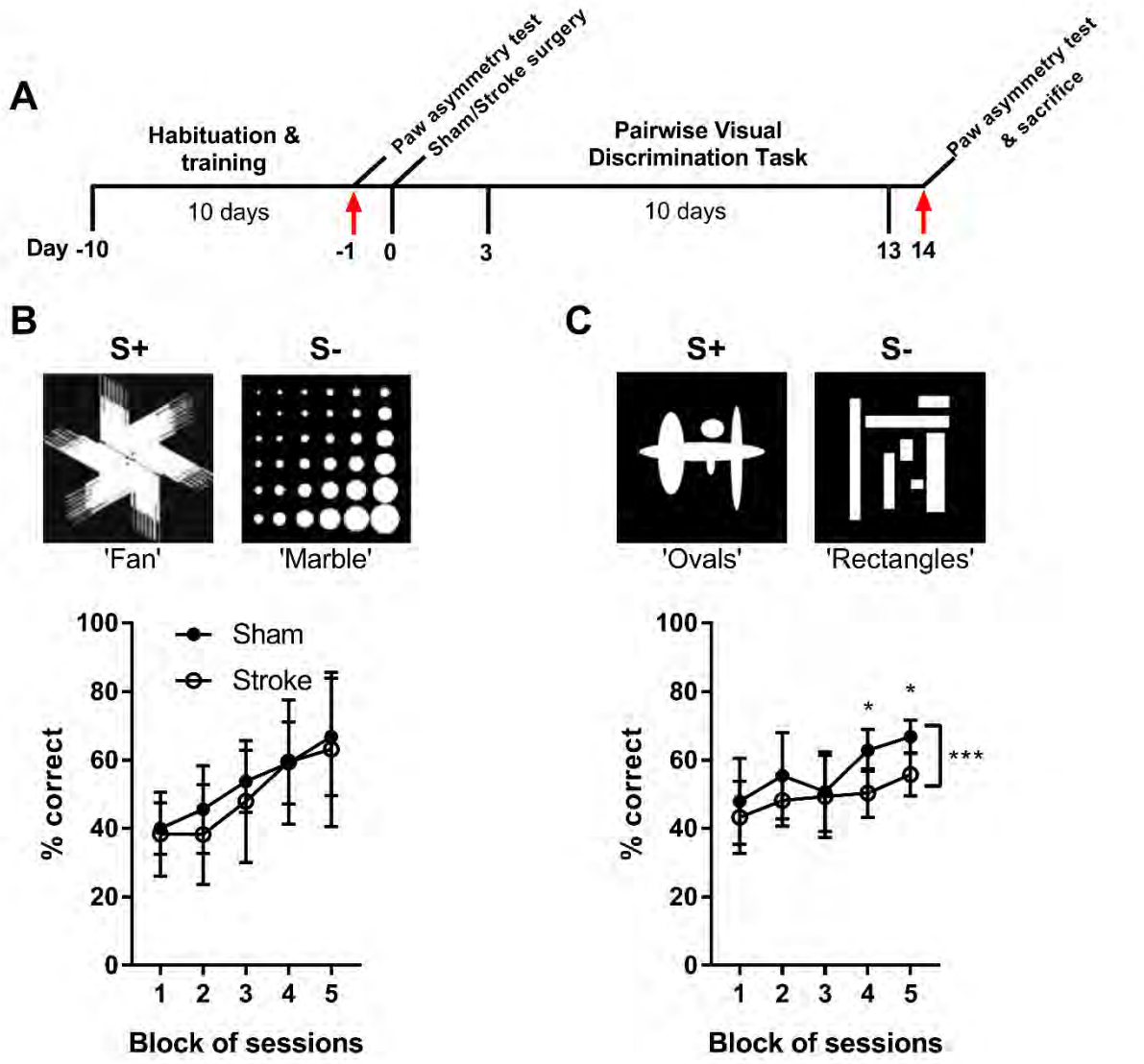

Fig. 1. Cortical stroke affects mice ability to discriminate between two images with a high similarity index, but not with low similarity index. (A) Experimental design timeline. (B) The first cohort of mice (sham n=10, stroke n=11) were subjected to VD task using two images with a low similarity index ('marble-fan' pair) (S+ correct and S- incorrect). No significant differences were found in the % correct responses between sham and stroke mice. (C) A second cohort (sham n=10, stroke n=11) was evaluated using a high similarity index pair ('ovals-rectangles' pair). We found a significant decrease in % correct responses in stroked mice compared to sham at fourth and fifth block of session. 1 block is the average of 2 sessions. Mean ± SD (two-way ANOVA and Sidak's multiple comparisons). *p<0.05; ***p<0.001.

The second cohort of mice were also tested for motor deficits one day before stroke and at 14 days post stroke. Locomotor asymmetry was evaluated using a cylinder task. Specifically, this

evaluates the paw preference that mice exhibit for stabilising themselves while rearing within a cylinder. Data on asymmetry scores indicated that there were no significant differences in paw preference prior to stroke. However, at day 14 the stroke group exhibited a significantly stronger preference for using their unaffected paw (the paw not connected to the damaged hemisphere) relative to sham ($p<0.0001$) (Fig. 2A).

Cortical stroke induces neuronal loss in the peri-infarct region and in SND sites

In order to assess the damage that the cortical stroke induced in the brain, we first estimated the tissue loss at bregma 0.0mm level using Cresyl Violet staining. We observed that the stroke group had significantly increased levels of tissue loss relative to the sham group ($p<0.0001$) (Fig. 2B).

To investigate whether neuronal loss occurs in the primary infarct area and in SND sites, we evaluated the protein levels of the mature neuronal marker (NeuN) in the peri-infarct, thalamus and hippocampus using Western blotting. Our analysis indicated a significant decrease in NeuN levels in the peri-infarct ($p=0.0003$), thalamus ($p=0.0023$) and hippocampus ($p=0.0093$) (Fig. 2C).

We further confirmed the protein data using immunohistochemistry NeuN staining. We performed automated $NeuN^+$ cell count in peri-infarct and thalamus (Supplementary Fig. 3A). Data showed a significant decrease in $NeuN^+$ cells in both the peri-infarct ($p<0.0001$) and thalamus ($p<0.0001$) in stroke mice (Fig. 2D and E). In the hippocampus area, cell bodies are very densely packed making $NeuN^+$ cell count difficult. Instead, optical density was assessed using thresholding analyses (Supplementary Fig. 3B) in three different sub-regions of the hippocampus: CA1, CA3 and dentate gyrus (DG). We found a significant decrease in threshold material for NeuN only in the CA1 sub-region of stroke mice compared with sham ($p=0.0138$) (Fig. 2D and E).

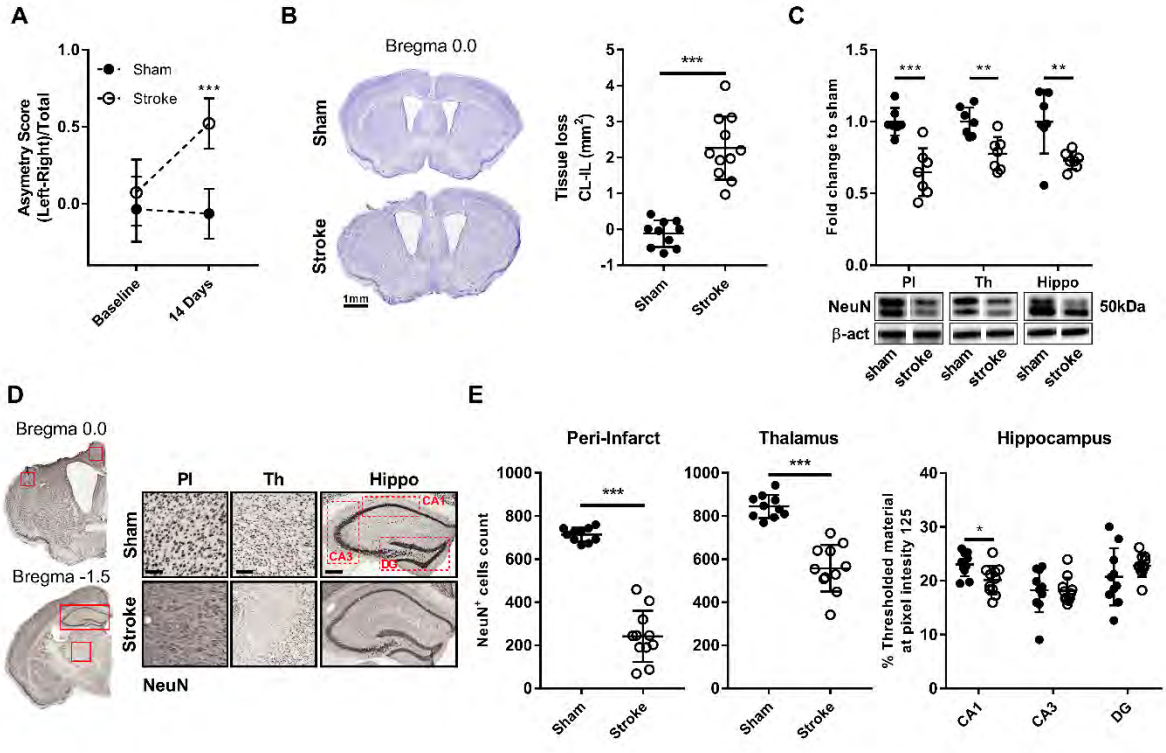

Fig. 2. Cortical stroke induces motor deficits and neuronal loss in the peri-infarct and in SND sites at 14 days. (A) Locomotor asymmetry was evaluated at baseline (one day before stroke induction) and at 14 days post-stroke using cylinder task (two-way ANOVA and Sidak's multiple comparisons). (B) Representative images of Cresyl violet staining at Bregma 0.0mm. Tissue loss was calculated as contralateral (CL) hemisphere area−ipsilateral (IL) hemisphere area. (C) Representative western blot and quantification of NeuN protein levels within the peri-infarct (PI), thalamus (Th) and hippocampus (Hippo) for sham and stroke mice and loading control β-actin (β-act). (D). Representative immunohistochemistry labelling for NeuN. Left panel: red squares indicate the location of the peri-infarct, thalamus and hippocampus regions examined. Right panels: higher magnification images (PI scale bar = 100µm, Th scale bar = 200µm, Hippo scale bar = 300µm). Dash area indicate the sub-regions of the hippocampus studied (CA1, CA3 and dentate gyrus (DG)). **(e)** Quantification of NeuN-positve cell within peri-infarct and thalamus. In the hippocampus area, optical density of NeuN staining was assessed using thresholding analyses. Mean ± SD (2-tailed t-test) * $p < 0.05$, ** $p < 0.01$ *** $p < 0.001$.

Cortical stroke leads to aggregation and accumulation of neurotoxic proteins

α-Synuclein: The supernatant and pellet fractions were analysed by western blotting for the levels of α-Syn. We evaluated the monomer (14kDa), dimer (28kDa) and trimer (42kDa) levels. In the peri-infarct region, we found a significant increase in α-Syn dimer and trimer levels in both the supernatant and pellet fraction (supernatant dimer $p<0.0001$; supernatant trimer $p=0.0003$; pellet dimer $p=0.0005$; pellet trimer $p=0.0085$). In the thalamus, a significant reduction of monomer levels, and a corresponding significant increase in α-Syn trimer levels were observed in the supernatant fraction only (supernatant monomer $p=0.0021$; supernatant trimer $p=0.015$). No changes were detected in the pellet. In the hippocampus, we found no significant changes in the supernatant, however, we identified a significant increase in both monomer and trimer levels in the pellet fraction (pellet monomer $p=0.0002$, pellet trimer $p=0.0094$) (Fig. 3A and B).

To further validate the western blot results and understand the spatial distribution of α-Syn accumulation brain sections from different bregma regions corresponding with the peri-infarct region (Bregma 0.0mm), thalamus and hippocampus (Bregma -1.5mm) were analysed by immunohistochemistry using an antibody against α-Syn. Optical density of α-Syn staining was quantitatively assessed using the threshold analysis. Using ImageJ software, we identified that pixel intensity 120 detected genuine α-Syn immunoreactive material (Supplementary Fig. 3C).We found a significant increase in α-Syn accumulation in the peri-infarct ($p=0.0198$), thalamus ($p=0.0064$) and hippocampus (CA1 $p=0.0037$, CA3 $p=0.0004$, DG $p=0.0004$) of stroked mice compared to sham (Fig. 3C). Pearson correlation analysis showed no significant correlation between the extent of α-Syn accumulation and cognitive performance within the stroke group ($r = -0.04335$, $P_{(Y = -0.01792*X + 54.22)} = 0.8893$).

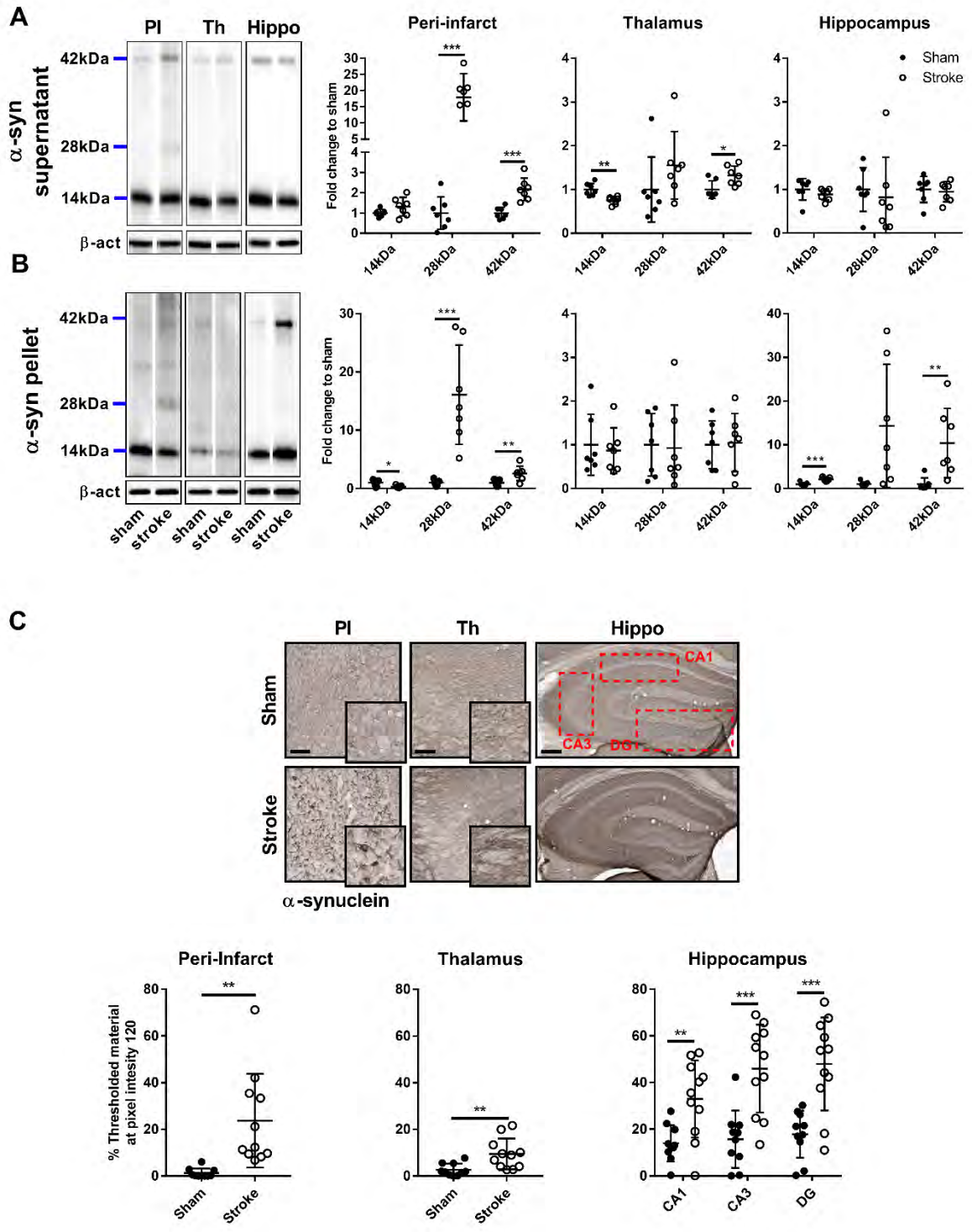

Fig. 3. Cortical stroke leads to aggregation and accumulation of α-Synuclein (α-Syn) at 14 days post-stroke. Representative western blot and quantification of α-synuclein expression profile within the peri-infarct (PI), thalamus (Th) and hippocampus (hippo) in the supernatant (A) and pellet (B) fraction. Our analyses focused on the monomer (14kDa), dimer (28kDa) and trimer (42kDa). (C) Representative images of α-Syn immunostaining and high magnification detail (PI scale bar = 100µm, Th scale bar = 200µm, Hippo scale bar = 300µm). Dash area indicate the sub-regions of the hippocampus studied (CA1, CA3 and dentate gyrus (DG)). Quantification of material thresholded at the pixel intensity 120 shows an increased deposition of α-Syn. Mean ± SD (2-tailed t-test). * $p < 0.05$, ** $p < 0.01$ *** $p < 0.001$.

Amyloid-β: We investigated the Aβ aggregation status in both supernatant and pellet fractions. Specifically, we quantitated the pentamer (25kDa), intermediate size oligomers (30kDa), decamer (50kDa) and dodecamer (56kDa). In the peri-infarct area, we observed a significant increase in all of the supernatant and pellet oligomers in stroke mice compared with sham mice (supernatant pentamer $p=0.00015$; supernatant intermediate size oligomer $p=0.0032$; supernatant decamer $p<0.0001$; supernatant dodecamer $p=0.00096$; pellet pentamer $p=0.0032$ and pellet decamer $p=0.0008$). In the thalamus, we found a significant increase in the decamer both in the supernatant and pellet fraction (supernatant decamer $p<0.0001$; pellet decamer $p=0.0463$). In the hippocampus, we observed a significant increase in the intermediate size oligomers, decamer and dodecamer in the supernatant fraction (supernatant intermediate size oligomer $p=0.0059$; supernatant decamer $p=0.0033$; supernatant dodecamer $p=0.00039$) and decamer in the pellet fraction (pellet decamer $p=0.0003$) (Fig. 4A and B)

We also found a significant increase in Aβ immunolabelling at pixel intensity 120 (Supplementary Fig. 3C) in the peri-infarct ($p<0.0001$), thalamus ($p=0.0378$) and hippocampus (CA1 $p=0.0003$; CA3 $p=0.0077$; DG $p=0.0085$) in stroke mice compared with sham (Fig. 4C). Pearson correlation analysis showed no significant correlation between the extent of Aβ accumulation and cognitive performance within the stroke group ($r = -0.1866$, $P_{(Y = -0.08497*X + 57.46)} = 0.5828$).

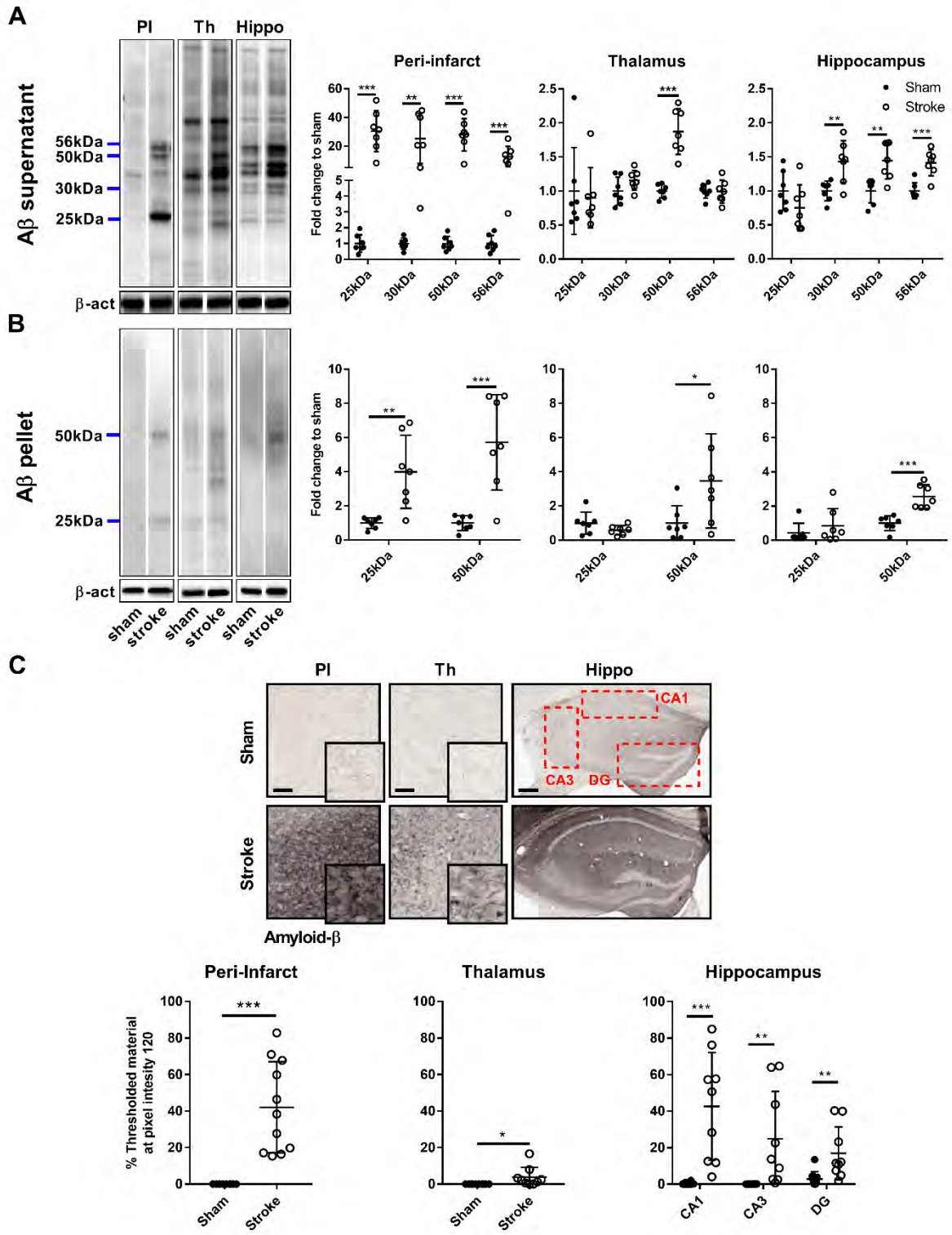

Fig. 4. Cortical stroke leads to aggregation and accumulation of Amyloid-β (Aβ) at 14 days post-stroke. Representative western blot and quantification of Aβ expression profile within the peri-infarct (PI), thalamus (Th) and hippocampus (hippo) in the supernatant (A) and pellet (B) fraction. Our analyses focused on different molecular weight oligomers (25kDa, 30kDa, 50kDa and 56kDa). Our results showed a significant increase in different molecular weight oligomers and accumulation after stroke. We observed a consistent increased of the 50kDa oligomer. (C) Representative images of Aβ immunostaining and high magnification detail (PI scale bar = 100µm, Th scale bar = 200µm, Hippo scale bar = 300µm). Dash area indicate the sub-regions

of the hippocampus studied (CA1, CA3 and dentate gyrus (DG)). Quantification of material thresholded at the pixel intensity 120 shows an increased deposition of Aβ. Mean ± SD (2-tailed t-test). * $p < 0.05$, ** $p < 0.01$ *** $p < 0.001$.

Cortical stroke promotes astrogliosis and AQP4 dysregulation primarily in the peri-infarct region and thalamus

We next analysed the expression of astrocytic markers (ALDH1L1 and GFAP) in the peri-infarct region, thalamus and hippocampus at 14 days after stroke. Western blotting data revealed a significant increase in both ALDH1L1 and GFAP in the peri-infarct (ALDH1L1 p=0.0024; GFAP p=0.0001), thalamus (ALDH1L1 p=0.00031; GFAP p=0.0001) and hippocampus (ALDH1L1 p=0.0126; GFAP p=0.0108) in stroke mice compared to sham (Fig. 5A and B). We further confirmed the protein data using immunofluorescence, and found that stroke mice exhibited a significant increase in the GFAP-positive area in the peri-infarct region (p<0.0001), thalamus (p<0.0001) and in all the hippocampal sub-regions studied (CA1 p<0.0001; CA3 p<0.0001; DG p=0.0037) (Fig. 6B, E and H).

Then, we analysed if stroke induced disturbances in the AQP4 water channel. Here, we observed a significant decreased in the AQP4 protein expression within the peri-infarct area (p<0.0001) in stroke mice compared with sham. However, there were no significant changes of AQP4 protein levels in the thalamus or hippocampus (Fig. 5C). These analyses provided us with information about the protein expression profile. However, it is necessary to investigate whether AQP4 remains polarised to perivascular astrocytic end-feet domains after stroke to ensure proper clearance and water distribution. Therefore, we carried out complementary immunofluorescence analyses co-labelling GFAP and AQP4. In sham animals, we observed that AQP4 is highly polarised to the end-feet of the astrocytes, however, after stroke we observed a clear mislocalisation of AQP4 (Fig. 6A, D and G). In addition to this qualitative analysis, we also measured AQP4 polarity as described previously (Wang et al., 2012). Higher AQP4 polarity values reflected expression levels of AQP4 in perivascular end-feet being greater than in surrounding tissue, while lower AQP4 polarity reflected a more even distribution between the perivascular end-feet and the soma. Our analysis revealed a loss of AQP4 polarity in the peri-infarct (p=0.002) and thalamus (p=0.0103) regions of mice receiving stroke compared with sham, but there were no significant changes in the hippocampus (Fig. 6C, F and I).

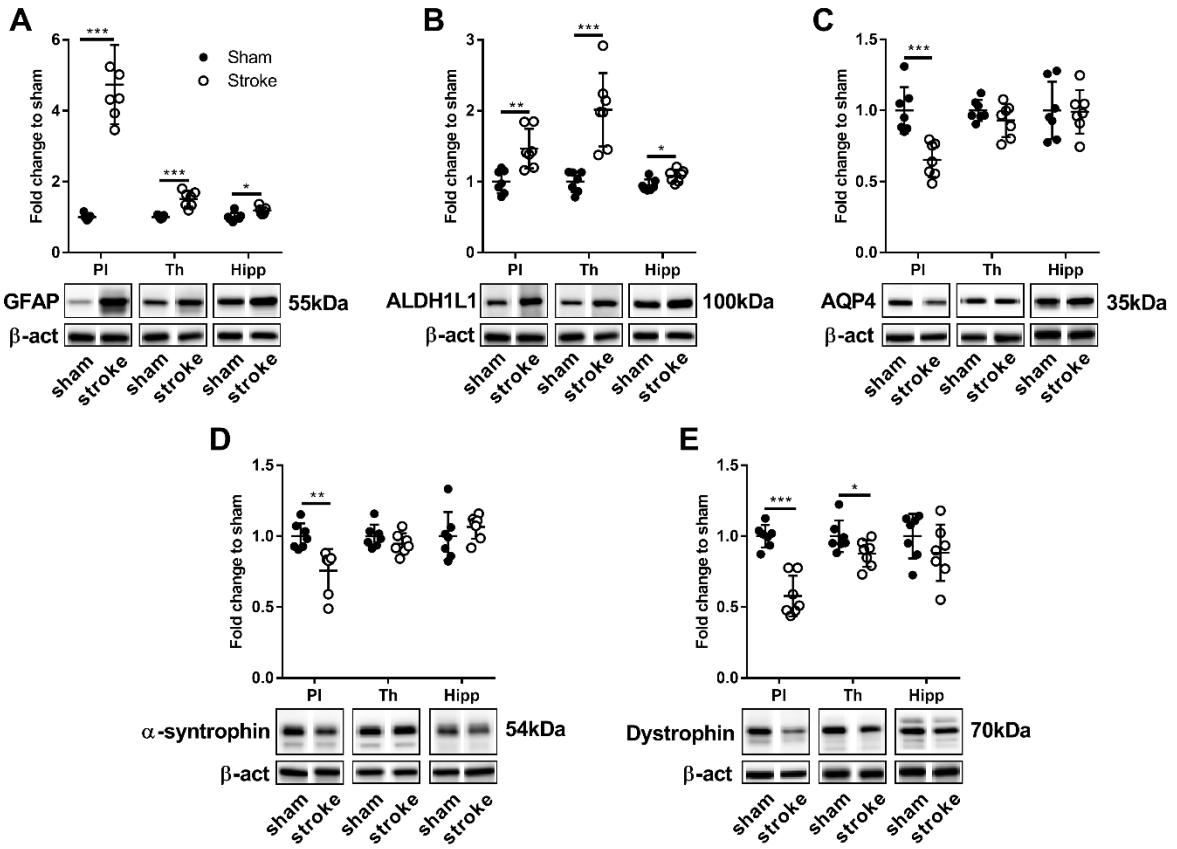

Fig. 5. Cortical stroke promote astrogliosis, AQP4 dysregulation and disturbance in the proteins of the dystrophin-associated complex at 14 days. Representative western blot and quantification of astrocytic markers (GFAP (A) and ALDH1L1 (B) within the peri-infarct (PI), thalamus (Th) and hippocampus (hippo). (C) Representative western blot and quantification of aquaporin 4 (AQP4) water channel. Representative western blot and quantification of α-syntrophin (D) and dystrophin (E) within the peri-infarct (PI), thalamus (Th) and hippocampus (hippo). Mean ± SD (2-tailed t-test). * $p < 0.05$, ** $p < 0.01$ *** $p < 0.001$.

Finally, we investigated the protein expression profile of dystrophin and α-syntrophin, which are proteins of the dystrophin-associated complex responsible for maintaining AQP4 polarisation to the end-feet of the astrocytes (Amiry-Moghaddam et al., 2004; Amiry-Moghaddam et al., 2003; Neely et al., 2001; Nicchia et al., 2008). Western blot analysis revealed a significant reduction in α-syntrophin within the peri-infarct ($p=0.0054$) and a significant reduction in dystrophin within peri-infarct ($p<0.0001$) and thalamus ($p=0.0464$) territories in stroked mice compared to sham (Fig. 5D and E).

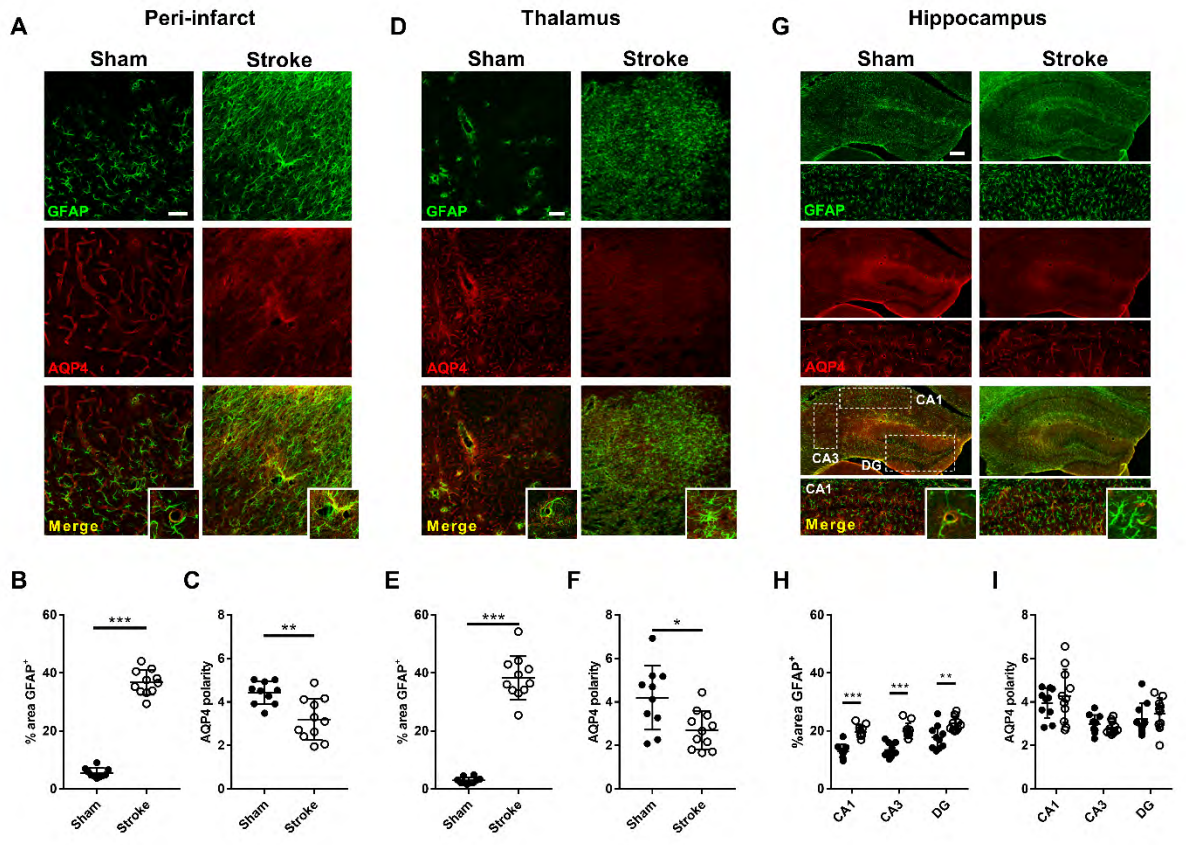

Fig. 6. Cortical stroke promote astrogliosis and AQP4 dysregulation. Representative immunofluorescence images of peri-infarct (A), thalamus (D) and hippocampus (G) co-labelled with GFAP (green) and AQP4 (red) (PI scale bar = 50µm, Th scale bar = 100µm, Hippo scale bar = 200µm). White dash area indicate the sub-regions of the hippocampus studied (CA1, CA3 and dentate gyrus (DG)). Quantification of reactive astrogliosis (% area of $GFAP^+$) in the peri-infarct (B), thalamus (E) and hippocampus (H). (C, F and I) Changes in AQP4 polarity were also measured in these same regions. In sham animals, AQP4 is highly polarised to perivascular end-feet of astrocytes. We observed a partial loss of the AQP4 polarity in the peri-infarct and thalamus area but not in the hippocampus at 14 days post-stroke. Mean ± SD (2-tailed t-test). * $p < 0.05$, ** $p < 0.01$ *** $p < 0.001$.

Discussion

We showed for the first time that photothrombotic vascular occlusion of the motor and somatosensory cortex has a significant impact on the ability of the mice to learn how to discriminate between two different stimuli, as evaluated by a mouse touchscreen platform for VD task. Secondly, we observed a significant loss of neuronal cells post-stroke in the peri-infarct region and in SND sites, such as the thalamus and the CA1 sub-region of the hippocampus. We then focused our investigation on α-Syn and Aβ, which have previously been linked to cognitive impairment and neurodegenerative conditions. We identified an increase in the accumulation and aggregation of these neurotoxic proteins in the peri-infarct, thalamus and hippocampus. Finally, we demonstrated that stroke induces astrogliosis, AQP4 dysregulation and disturbances in the dystrophin-associated complex. Collectively, these results suggest that the cognitive impairment seen post-stroke might be due to an increased accumulation of

neurotoxic proteins as a result of a failure of the clearance mechanisms to remove these waste products from the brain.

We utilised a photothrombotic stroke model in combination of a touchscreen platform to advance our understanding in post-stroke cognitive impairment (Bussey et al., 2008). Classically, the Morris water maze has been the gold-standard test for assessing cognition, however, in the context of stroke recovery, this task is cofounded by motor impairment and a ceiling effect that reduce its sensitivity in assessing cognition (Balkaya et al., 2018; Morris, 1984; Shepherd et al., 2016). Further, this task could be perceived as a stressful condition, a factor that negatively affect cognition (Ong et al., 2017b; Zhao et al., 2017). To assess these deficits, we chose a more sensitive and translationally relevant platform, utilising touchscreen testing (Balkaya et al., 2018; Horner et al., 2013; Schaar et al., 2010; Shepherd et al., 2016). Specifically, we focused on the VD task, in which mice must learn to consistently respond to one of two visual stimuli to be rewarded. One of the critical variables that we wished to determine was the relative difficulty of the stimuli presented. To address this, we considered two image sets (low similarity and high similarity). When the low similarity pair was tested ('marble vs fan' pair, typically used in previous studies (Morton et al., 2006; Romberg et al., 2013)), no differences in cognitive performance were observed between stroked and sham mice. We then considered the performance of mice using the high similarity pair ('oval-rectangles' pair). In this case, we observed a significant decrease in the % of correct trials between 10 to 14 days post-stroke in stroke mice compared to sham. Together, this data identified that the sensitivity of the VD task to unmask cognitive deficits varies as a function of the similarity of the image sets.

One important factor to consider in interpreting the VD performance data is the dependence of the task on motor function. Clearly, the touchscreen tasks require intact motor function such that subjects are able to traverse the testing chamber, respond to the screen, and collect a reward (Horner et al., 2013). As such, one possible interpretation of the data we have reported is that they reflect a motor impairment of the mice rather than a cognitive deficit. In favour of this explanation, we did observe that stroked mice exhibited a stronger preference for using their unaffected paw during a spontaneous rearing task, which is consistent with prior findings (Zalewska et al., 2018; Zhao et al., 2017). However, despite this data, we could find no evidence of a motor deficit impacting the VD task as neither the number of trials completed within 60 minutes nor the time taken to complete 30 trials were statistically significant between the sham and stroke groups. This result indicates that any motor deficits present did not meaningfully affect the assessment of cognitive performance. This is consistent with a previous observation from our group that stroke does not alter the distance covered using the open field task (Zalewska et al., 2018). Given these results, we suggest that stroke affects the ability of the mice to discriminate between two different stimuli with a high similarity index, and these cognitive deficits are independent of the motor impairment caused by the photothrombotic stroke.

We then examined tissue loss and neuronal loss in order to assess the damage that the cortical stroke induced in the brain. Stroke mice exhibited a significant increase in tissue loss around the infarct site, which is consistent with previous observations (Zalewska et al., 2017; Zhao et al., 2017). The tissue loss after stroke includes loss of neurons (Karl et al., 2010), and neuronal loss is expected in the primary infarct site and in SND sites (Baumgartner et al., 2018; Tamura et al., 1991; Zhang et al., 2012b). Here, we identified a significant decrease in NeuN-positive cells in the peri-infarct region, thalamus and also the CA1 sub-region of the hippocampus. The decrease in the number of neurons in the hippocampus is an important finding that could

explain the cognitive impairment seen after stroke and reinforces the idea that stroke induces alterations in remote regions that are functionally connected to the primary ischemic area (Wang et al., 2004; Xie et al., 2011). A recent study by Baumgartner et al. (2018) also supports this idea by providing *in vivo* evidence that a sensorimotor stroke induces a dysfunction in the hippocampal-thalamic network.

In terms of further considering the mechanisms involved in this neuronal loss and cognitive impairment, we investigated whether stroke altered the aggregation and accumulation of two neurotoxic proteins. First, we studied α-Syn, which is a natively soluble unfolded protein that undergoes spontaneous aggregation under different environmental conditions and plays a central role in chronic neurodegenerative diseases (Breydo et al., 2012; Stoica et al., 2012). In the context of stroke, previous studies have shown that an ischemic insult in adult mice lead to increased levels of α-Syn in the cortex (Kim et al., 2016; Unal-Cevik et al., 2011) and a knockdown or knockout of α-Syn significantly decreased infarct volume and promoted better motor recovery (Kim et al., 2016). To investigate the aggregation of α-Syn, we analysed both supernatant and pellet protein fractions using western blotting. We observed an increase in α-Syn oligomerization in all regions of neuronal loss. We further confirmed this observation using immunohistochemistry. Oligomeric forms of α-Syn have been previously described to be crucial structures underlying neuronal death and cognitive deficits in neurodegenerative diseases through several mechanisms such as inflammation, oxidative stress and autophagy (Dias et al., 2013; Pacheco et al., 2012). Interestingly, all these mechanism have been found to mediate post-stroke neuronal death and therefore it is reasonable to hypothesise that α-Syn might also play an important role in cognitive impairment after stroke.

A second protein extensively implicated in neurodegeneration is Aβ (Haass and Selkoe, 2007; Lesne et al., 2006; Lesne et al., 2013). Here, we studied how stroke alters the Aβ aggregation status in multiple regions of the brain. Previous studies have mainly focused on the Aβ deposition in the peri-infarct region (Garcia-Alloza et al., 2011) and the thalamus (Ong et al., 2017a; van Groen et al., 2005; Zhao et al., 2018). Our results showed a significant increased oligomerization in these two regions and in the hippocampus after stroke. Interestingly, we observed a consistent increase of the 50kDa oligomer within the supernatant and pellet fraction of all the brain regions. Several studies have indicated that these Aβ oligomers, rather than the monomers or insoluble fibrils, may be responsible for the cellular pathology and cognitive decline in Alzheimer's disease (Lesne et al., 2006; Lesne et al., 2013). We also investigated whether the plasma levels of Aβ40 and Aβ42 could be used as a predictor for cognitive impairment after stroke; however, we did not observe significant differences (Supplementary Fig. 4A and B). This is consistent with previous studies where blood levels of Aβ were only increased in the first 3 days after stroke, and decreased to baseline levels by day 7 (Liu et al., 2015b) and day 30 post-stroke (Howe et al., 2018).

Taking our findings on α-Syn and Aβ together, we suggest that that the aggregation and accumulation of neurotoxic protein after stroke may be more widespread than expected, involving regions far from the primary infarct. The association of neuronal loss and protein aggregation suggest that greater levels of α-Syn and Aβ accumulation seen in the brain, especially in the hippocampus, might be responsible for neuronal death and cognitive impairment seen after stroke. In studies of neurodegenerative diseases, Wilson et al. (Wilson et al., 2017) investigated the impact of the early Aβ accumulation on visual discrimination dysfunction in an Alzheimer's disease (AD) rat model. They observed an intraneuronal accumulation of Aβ soluble oligomers occurring in the hippocampus and neocortex. This accumulation of Aβ altered synaptic plasticity through persistent inhibition of long-term

potentiation in the CA1 area of the hippocampus which, in turn, severely impaired the visual discrimination learning. This similar effect might be also happening in the context of stroke.

There are several possible mechanisms to explain this increase in neurotoxic protein load: an increase in the rate of production, a decrease in the rate of degradation, or impaired clearance. Here, we focused particularly on the role of the clearance mechanisms in the accumulation of these neurotoxic proteins. It is well documented that the astrocytes have end-feet processes which wrap around the cerebral blood vessels, with a highly localised channel protein, AQP4 (Iliff et al., 2012; Mestre et al., 2018). AQP4 allows the bidirectional movement of water, which allows the exchange of the CSF with the ISF of the parenchyma, and forms a gradient for the removal of interstitial solutes (Verkman and Mitra, 2000). Reactive astrogliosis has been associated with the loss of perivascular AQP4 polarization in several brain injury models (Iliff et al., 2014; Ren et al., 2013; Wang et al., 2012). Therefore, we investigated whether the reactive astrogliosis and AQP4 dysfunction were present in the primary infarct area and in sites of SND. In this study, we found that widespread astrogliosis was evident throughout all the regions studied in the brains of stroke mice, consistent with our previous study (Patience et al., 2015). Our analysis also showed decreased levels of the AQP4 protein in the peri-infarct region of stroke mice but no significant differences were found in the thalamus or hippocampus. It should be noted that the assessment of AQP4 protein levels alone cannot conclusively determine whether AQP4 remains polarised to perivascular astrocytic end-feet. We therefore performed immunofluorescence analysis co-labelling GFAP and AQP4. AQP4 polarization was assessed by image analysis as previously described (Wang et al., 2012). In the peri-infarct and thalamus territories, AQP4 polarity was significantly reduced 14 days after stroke, however, no significant differences were found in the hippocampus. The disturbances in AQP4 reported here are consistent with previous studies in stroke and different neuropathological conditions (Ren et al., 2013; Wang et al., 2012; Zhao et al., 2018) and supports our hypothesis that loss of perivascular AQP4 polarization might impair the clearance of neurotoxic proteins away from the brain environment. AQP4 could represent a potential therapeutic target to improve neurotoxic protein clearance. Previous pre-clinical studies have shown that the accumulation of Aβ after stroke could be ameliorated using different therapeutic interventions targeting the Aβ production or clearance pathways (Sarajarvi et al., 2012; Zhang et al., 2012a; Zhang et al., 2011). This reduction has also been linked to an improvement in functional outcomes.

The investigation of AQP4 related proteins, such as the dystrophin-associated complex proteins, showed significantly reduced expression of both α-syntrophin and dystrophin in the peri-infarct area, and also significantly reduced dystrophin expression in the thalamus. These proteins position AQP4 to the perivascular astrocytic end-feet membrane allowing the bidirectional movement of water and solutes (Amiry-Moghaddam et al., 2004; Neely et al., 2001; Nicchia et al., 2008). Previous studies have reported that α-syntrophin knockout (Amiry-Moghaddam et al., 2003; Neely et al., 2001) and dystrophin-null (Vajda et al., 2002) mice exhibited a dramatic reduction of AQP4 in astroglial end-feet surrounding blood vessels and interfered with the transport of water across the brain-blood interface. Our results were consistent with the immunofluorescence analyses that showed a reduction in AQP4 polarity exclusively in the peri-infract and thalamus, indicating a possible role of α-syntrophin and dystrophin in the AQP4 polarization disturbances and therefore the solute clearance after stroke. One important consideration is that we did not directly quantify CSF clearance, and future functional tests using in vivo/advanced imaging techniques are warranted to confirm the role of AQP4 in neurotoxic proteins clearance after stroke.

Our results have some limitations. Firstly, this is a cross-sectional study at 14 days post-stroke. We cannot conclusively answer which of these processes has occurred first or identify any underlying cause. In addition to the observed neuronal loss, accumulation of neurotoxic proteins and dysregulation of astrocytic AQP4, well documented mechanisms such as trans-synaptic apoptosis are most likely involved in the cascade of processes resulting in SND. This warrants further investigation. Critically, this study is an important first step in building an understanding of the post-stroke mechanisms affecting cognitive impairment. To gain a further understanding of related mechanisms, a longitudinal investigation would be necessary. Secondly, we have only examined discrimination learning and therefore other cognitive domains such as executive function, working memory and attention should be investigated in future studies. In addition, it would certainly be worthwhile to assess whether these cognitive deficits persist long-term.

In conclusion, this study demonstrates that the induction of stroke in the motor and sensory cortex induces cognitive deficits, specifically the ability to discriminate between stimuli with a high degree of similarity. This provides further evidence that cognitive impairment induced by stroke could be due to a series of secondary mechanisms, leading to the death of neuronal cells at the thalamus and the CA1 sub-region of the hippocampus. Our findings of increased α-Syn and Aβ in the peri-infarct region, thalamus and hippocampus post-stroke suggest that these neurotoxic proteins are likely to contribute to post-stroke cognitive impairment. Finally, we also demonstrated that disturbances in the AQP4 polarization might play an important role in the failure of removing these neurotoxic proteins from the brain environment. Therapeutic strategies to improve brain waste clearance may be promising approaches to prevent post-stroke cognitive impairment.

Acknowledgements
This study was supported by Hunter Medical Research Institute (HMRI 896), Faculty of Health and Medicine Pilot Grant, Priority Research Centre for Stroke and Brain Injury Research Support Grant, Mary Costello Alzheimer's Pilot Grant and The University of Newcastle, Australia. LKO and SSB also acknowledge support from Research Advantage for ECR Higher Degree by Research (HDR) Scholarship and Greaves Family Postgraduate Scholarships in Medical Research (HMRI 1054)

Declaration of conflicting interests
The author(s) declared no potential conflicts of interest with respect to the research, authorship, and/or publication of this article.

References

Aho, L., Jolkkonen, J., Alafuzoff, I., 2006. Beta-amyloid aggregation in human brains with cerebrovascular lesions. Stroke 37, 2940-2945. 10.1161/01.Str.0000248777.44128.93
Amiry-Moghaddam, M., Frydenlund, D.S., Ottersen, O.P., 2004. Anchoring of aquaporin-4 in brain: molecular mechanisms and implications for the physiology and pathophysiology of water transport. Neuroscience 129, 999-1010. 10.1016/j.neuroscience.2004.08.049
Amiry-Moghaddam, M., Otsuka, T., Hurn, P.D., Traystman, R.J., Haug, F.M., Froehner, S.C., Adams, M.E., Neely, J.D., Agre, P., Ottersen, O.P., Bhardwaj, A., 2003. An alpha-syntrophin-dependent pool of AQP4 in astroglial end-feet confers bidirectional water flow between blood and brain. Proc Natl Acad Sci U S A 100, 2106-2111. 10.1073/pnas.0437946100
Arbel-Ornath, M., Hudry, E., Eikermann-Haerter, K., Hou, S., Gregory, J.L., Zhao, L., Betensky, R.A., Frosch, M.P., Greenberg, S.M., Bacskai, B.J., 2013. Interstitial fluid drainage

is impaired in ischemic stroke and Alzheimer's disease mouse models. Acta Neuropathol 126, 353-364. 10.1007/s00401-013-1145-2
Balkaya, M.G., Trueman, R.C., Boltze, J., Corbett, D., Jolkkonen, J., 2018. Behavioral outcome measures to improve experimental stroke research. Behav Brain Res 352, 161-171. 10.1016/j.bbr.2017.07.039
Baumgartner, P., El Amki, M., Bracko, O., Luft, A.R., Wegener, S., 2018. Sensorimotor stroke alters hippocampo-thalamic network activity. Scientific reports 8, 15770. 10.1038/s41598-018-34002-9
Breydo, L., Wu, J.W., Uversky, V.N., 2012. Alpha-synuclein misfolding and Parkinson's disease. Biochim Biophys Acta 1822, 261-285. 10.1016/j.bbadis.2011.10.002
Bussey, T.J., Padain, T.L., Skillings, E.A., Winters, B.D., Morton, A.J., Saksida, L.M., 2008. The touchscreen cognitive testing method for rodents: how to get the best out of your rat. Learning & memory (Cold Spring Harbor, N.Y.) 15, 516-523. 10.1101/lm.987808
Corbett, D., Carmichael, S.T., Murphy, T.H., Jones, T.A., Schwab, M.E., Jolkkonen, J., Clarkson, A.N., Dancause, N., Wieloch, T., Johansen-Berg, H., Nilsson, M., McCullough, L.D., Joy, M.T., 2017. Enhancing the alignment of the preclinical and clinical stroke recovery research pipeline: Consensus-based core recommendations from the Stroke Recovery and Rehabilitation Roundtable translational working group. International journal of stroke : official journal of the International Stroke Society 12, 462-471. 10.1177/1747493017711814
Dias, V., Junn, E., Mouradian, M.M., 2013. The role of oxidative stress in Parkinson's disease. J Parkinsons Dis 3, 461-491. 10.3233/jpd-130230
Garcia-Alloza, M., Gregory, J., Kuchibhotla, K.V., Fine, S., Wei, Y., Ayata, C., Frosch, M.P., Greenberg, S.M., Bacskai, B.J., 2011. Cerebrovascular lesions induce transient beta-amyloid deposition. Brain 134, 3697-3707. 10.1093/brain/awr300
Gottesman, R.F., Hillis, A.E., 2010. Predictors and assessment of cognitive dysfunction resulting from ischaemic stroke. Lancet Neurol 9, 895-905. 10.1016/s1474-4422(10)70164-2
Haass, C., Selkoe, D.J., 2007. Soluble protein oligomers in neurodegeneration: lessons from the Alzheimer's amyloid beta-peptide. Nat Rev Mol Cell Biol 8, 101-112. 10.1038/nrm2101
Horner, A.E., Heath, C.J., Hvoslef-Eide, M., Kent, B.A., Kim, C.H., Nilsson, S.R., Alsio, J., Oomen, C.A., Holmes, A., Saksida, L.M., Bussey, T.J., 2013. The touchscreen operant platform for testing learning and memory in rats and mice. Nat Protoc 8, 1961-1984. 10.1038/nprot.2013.122
Howe, M.D., Atadja, L.A., Furr, J.W., Maniskas, M.E., Zhu, L., McCullough, L.D., Urayama, A., 2018. Fibronectin induces the perivascular deposition of cerebrospinal fluid-derived amyloid-beta in aging and after stroke. Neurobiol Aging 72, 1-13. 10.1016/j.neurobiolaging.2018.07.019
Iizuka, H., Sakatani, K., Young, W., 1990. Neural damage in the rat thalamus after cortical infarcts. Stroke 21, 790-794.
Iliff, J.J., Chen, M.J., Plog, B.A., Zeppenfeld, D.M., Soltero, M., Yang, L., Singh, I., Deane, R., Nedergaard, M., 2014. Impairment of glymphatic pathway function promotes tau pathology after traumatic brain injury. The Journal of neuroscience : the official journal of the Society for Neuroscience 34, 16180-16193. 10.1523/jneurosci.3020-14.2014
Iliff, J.J., Wang, M., Liao, Y., Plogg, B.A., Peng, W., Gundersen, G.A., Benveniste, H., Vates, G.E., Deane, R., Goldman, S.A., Nagelhus, E.A., Nedergaard, M., 2012. A paravascular pathway facilitates CSF flow through the brain parenchyma and the clearance of interstitial solutes, including amyloid beta. Sci Transl Med 4, 147ra111. 10.1126/scitranslmed.3003748
Karl, J.M., Alaverdashvili, M., Cross, A.R., Whishaw, I.Q., 2010. Thinning, movement, and volume loss of residual cortical tissue occurs after stroke in the adult rat as identified by histological and magnetic resonance imaging analysis. Neuroscience 170, 123-137. 10.1016/j.neuroscience.2010.06.054

Kim, T., Mehta, S.L., Kaimal, B., Lyons, K., Dempsey, R.J., Vemuganti, R., 2016. Poststroke Induction of alpha-Synuclein Mediates Ischemic Brain Damage. The Journal of neuroscience : the official journal of the Society for Neuroscience 36, 7055-7065. 10.1523/jneurosci.1241-16.2016
Kluge, M.G., Abdolhoseini, M., Zalewska, K., Ong, L.K., Johnson, S.J., Nilsson, M., Walker, F.R., 2018. Spatiotemporal analysis of impaired microglia process movement at sites of secondary neurodegeneration post-stroke. Journal of cerebral blood flow and metabolism : official journal of the International Society of Cerebral Blood Flow and Metabolism, 271678x18797346. 10.1177/0271678x18797346
Kuzma, E., Lourida, I., Moore, S.F., Levine, D.A., Ukoumunne, O.C., Llewellyn, D.J., 2018. Stroke and dementia risk: A systematic review and meta-analysis. Alzheimers Dement 14, 1416-1426. 10.1016/j.jalz.2018.06.3061
Lesne, S., Koh, M.T., Kotilinek, L., Kayed, R., Glabe, C.G., Yang, A., Gallagher, M., Ashe, K.H., 2006. A specific amyloid-beta protein assembly in the brain impairs memory. Nature 440, 352-357. 10.1038/nature04533
Lesne, S.E., Sherman, M.A., Grant, M., Kuskowski, M., Schneider, J.A., Bennett, D.A., Ashe, K.H., 2013. Brain amyloid-beta oligomers in ageing and Alzheimer's disease. Brain 136, 1383-1398. 10.1093/brain/awt062
Levine, D.A., Galecki, A.T., Langa, K.M., Unverzagt, F.W., Kabeto, M.U., Giordani, B., Wadley, V.G., 2015. Trajectory of Cognitive Decline After Incident Stroke. Jama 314, 41-51. 10.1001/jama.2015.6968
Liu, W., Wong, A., Au, L., Yang, J., Wang, Z., Leung, E.Y., Chen, S., Ho, C.L., Mok, V.C., 2015a. Influence of Amyloid-beta on Cognitive Decline After Stroke/Transient Ischemic Attack: Three-Year Longitudinal Study. Stroke 46, 3074-3080. 10.1161/strokeaha.115.010449
Liu, Y.H., Cao, H.Y., Wang, Y.R., Jiao, S.S., Bu, X.L., Zeng, F., Wang, Q.H., Li, J., Deng, J., Zhou, H.D., Wang, Y.J., 2015b. Serum Abeta is predictive for short-term neurological deficits after acute ischemic stroke. Neurotox Res 27, 292-299. 10.1007/s12640-015-9518-z
Makinen, S., van Groen, T., Clarke, J., Thornell, A., Corbett, D., Hiltunen, M., Soininen, H., Jolkkonen, J., 2008. Coaccumulation of calcium and beta-amyloid in the thalamus after transient middle cerebral artery occlusion in rats. Journal of cerebral blood flow and metabolism : official journal of the International Society of Cerebral Blood Flow and Metabolism 28, 263-268. 10.1038/sj.jcbfm.9600529
Mestre, H., Hablitz, L.M., Xavier, A.L., Feng, W., Zou, W., Pu, T., Monai, H., Murlidharan, G., Castellanos Rivera, R.M., Simon, M.J., Pike, M.M., Pla, V., Du, T., Kress, B.T., Wang, X., Plog, B.A., Thrane, A.S., Lundgaard, I., Abe, Y., Yasui, M., Thomas, J.H., Xiao, M., Hirase, H., Asokan, A., Iliff, J.J., Nedergaard, M., 2018. Aquaporin-4-dependent glymphatic solute transport in the rodent brain. Elife 7. 10.7554/eLife.40070
Morris, R., 1984. Developments of a water-maze procedure for studying spatial learning in the rat. J Neurosci Methods 11, 47-60.
Morton, A.J., Skillings, E., Bussey, T.J., Saksida, L.M., 2006. Measuring cognitive deficits in disabled mice using an automated interactive touchscreen system. Nat Methods 3, 767. 10.1038/nmeth1006-767
Neely, J.D., Amiry-Moghaddam, M., Ottersen, O.P., Froehner, S.C., Agre, P., Adams, M.E., 2001. Syntrophin-dependent expression and localization of Aquaporin-4 water channel protein. Proc Natl Acad Sci U S A 98, 14108-14113. 10.1073/pnas.241508198
Nicchia, G.P., Rossi, A., Nudel, U., Svelto, M., Frigeri, A., 2008. Dystrophin-dependent and -independent AQP4 pools are expressed in the mouse brain. Glia 56, 869-876. 10.1002/glia.20661
Ong, L.K., Chow, W.Z., TeBay, C., Kluge, M., Pietrogrande, G., Zalewska, K., Crock, P., Aberg, N.D., Bivard, A., Johnson, S.J., Walker, F.R., Nilsson, M., Isgaard, J., 2018. Growth

Hormone Improves Cognitive Function After Experimental Stroke. Stroke 49, 1257-1266. 10.1161/strokeaha.117.020557
Ong, L.K., Walker, F.R., Nilsson, M., 2017a. Is Stroke a Neurodegenerative Condition? A Critical Review of Secondary Neurodegeneration and Amyloid-beta Accumulation after Stroke. Aims Med Sci 4, 1-16.
Ong, L.K., Zhao, Z., Kluge, M., Walker, F.R., Nilsson, M., 2017b. Chronic stress exposure following photothrombotic stroke is associated with increased levels of Amyloid beta accumulation and altered oligomerisation at sites of thalamic secondary neurodegeneration in mice. Journal of cerebral blood flow and metabolism : official journal of the International Society of Cerebral Blood Flow and Metabolism 37, 1338-1348. 10.1177/0271678x16654920
Pacheco, C., Aguayo, L.G., Opazo, C., 2012. An extracellular mechanism that can explain the neurotoxic effects of alpha-synuclein aggregates in the brain. Front Physiol 3, 297. 10.3389/fphys.2012.00297
Patience, M.J., Zouikr, I., Jones, K., Clarkson, A.N., Isgaard, J., Johnson, S.J., Walker, F.R., Nilsson, M., 2015. Photothrombotic stroke induces persistent ipsilateral and contralateral astrogliosis in key cognitive control nuclei. Neurochem Res 40, 362-371. 10.1007/s11064-014-1487-8
Peng, W., Achariyar, T.M., Li, B., Liao, Y., Mestre, H., Hitomi, E., Regan, S., Kasper, T., Peng, S., Ding, F., Benveniste, H., Nedergaard, M., Deane, R., 2016. Suppression of glymphatic fluid transport in a mouse model of Alzheimer's disease. Neurobiol Dis 93, 215-225. 10.1016/j.nbd.2016.05.015
Ren, Z., Iliff, J.J., Yang, L., Yang, J., Chen, X., Chen, M.J., Giese, R.N., Wang, B., Shi, X., Nedergaard, M., 2013. 'Hit & Run' model of closed-skull traumatic brain injury (TBI) reveals complex patterns of post-traumatic AQP4 dysregulation. Journal of cerebral blood flow and metabolism : official journal of the International Society of Cerebral Blood Flow and Metabolism 33, 834-845. 10.1038/jcbfm.2013.30
Romberg, C., Horner, A.E., Bussey, T.J., Saksida, L.M., 2013. A touch screen-automated cognitive test battery reveals impaired attention, memory abnormalities, and increased response inhibition in the TgCRND8 mouse model of Alzheimer's disease. Neurobiol Aging 34, 731-744. 10.1016/j.neurobiolaging.2012.08.006
Saczynski, J.S., Sigurdsson, S., Jonsdottir, M.K., Eiriksdottir, G., Jonsson, P.V., Garcia, M.E., Kjartansson, O., Lopez, O., van Buchem, M.A., Gudnason, V., Launer, L.J., 2009. Cerebral infarcts and cognitive performance: importance of location and number of infarcts. Stroke 40, 677-682. 10.1161/strokeaha.108.530212
Sahathevan, R., Linden, T., Villemagne, V.L., Churilov, L., Ly, J.V., Rowe, C., Donnan, G., Brodtmann, A., 2016. Positron Emission Tomographic Imaging in Stroke: Cross-Sectional and Follow-Up Assessment of Amyloid in Ischemic Stroke. Stroke 47, 113-119. 10.1161/strokeaha.115.010528
Sarajarvi, T., Lipsanen, A., Makinen, P., Peraniemi, S., Soininen, H., Haapasalo, A., Jolkkonen, J., Hiltunen, M., 2012. Bepridil decreases Abeta and calcium levels in the thalamus after middle cerebral artery occlusion in rats. Journal of cellular and molecular medicine 16, 2754-2767. 10.1111/j.1582-4934.2012.01599.x
Schaar, K.L., Brenneman, M.M., Savitz, S.I., 2010. Functional assessments in the rodent stroke model. Exp Transl Stroke Med 2, 13. 10.1186/2040-7378-2-13
Shepherd, A., Tyebji, S., Hannan, A.J., Burrows, E.L., 2016. Translational Assays for Assessment of Cognition in Rodent Models of Alzheimer's Disease and Dementia. J Mol Neurosci 60, 371-382. 10.1007/s12031-016-0837-1
Stoica, G., Lungu, G., Bjorklund, N.L., Taglialatela, G., Zhang, X., Chiu, V., Hill, H.H., Schenk, J.O., Murray, I., 2012. Potential role of alpha-synuclein in neurodegeneration: studies

in a rat animal model. Journal of neurochemistry 122, 812-822. 10.1111/j.1471-4159.2012.07805.x
Sun, J.H., Tan, L., Yu, J.T., 2014. Post-stroke cognitive impairment: epidemiology, mechanisms and management. Ann Transl Med 2, 80. 10.3978/j.issn.2305-5839.2014.08.05
Tamura, A., Tahira, Y., Nagashima, H., Kirino, T., Gotoh, O., Hojo, S., Sano, K., 1991. Thalamic atrophy following cerebral infarction in the territory of the middle cerebral artery. Stroke 22, 615-618.
Unal-Cevik, I., Gursoy-Ozdemir, Y., Yemisci, M., Lule, S., Gurer, G., Can, A., Muller, V., Kahle, P.J., Dalkara, T., 2011. Alpha-synuclein aggregation induced by brief ischemia negatively impacts neuronal survival in vivo: a study in [A30P]alpha-synuclein transgenic mouse. Journal of cerebral blood flow and metabolism : official journal of the International Society of Cerebral Blood Flow and Metabolism 31, 913-923. 10.1038/jcbfm.2010.170
Uzdensky, A.B., 2018. Photothrombotic Stroke as a Model of Ischemic Stroke. Translational stroke research 9, 437-451. 10.1007/s12975-017-0593-8
Vajda, Z., Pedersen, M., Fuchtbauer, E.M., Wertz, K., Stodkilde-Jorgensen, H., Sulyok, E., Doczi, T., Neely, J.D., Agre, P., Frokiaer, J., Nielsen, S., 2002. Delayed onset of brain edema and mislocalization of aquaporin-4 in dystrophin-null transgenic mice. Proc Natl Acad Sci U S A 99, 13131-13136. 10.1073/pnas.192457099
van Groen, T., Puurunen, K., Maki, H.M., Sivenius, J., Jolkkonen, J., 2005. Transformation of diffuse beta-amyloid precursor protein and beta-amyloid deposits to plaques in the thalamus after transient occlusion of the middle cerebral artery in rats. Stroke 36, 1551-1556. 10.1161/01.STR.0000169933.88903.cf
Verkman, A.S., Mitra, A.K., 2000. Structure and function of aquaporin water channels. Am J Physiol Renal Physiol 278, F13-28. 10.1152/ajprenal.2000.278.1.F13
Wang, M., Ding, F., Deng, S., Guo, X., Wang, W., Iliff, J.J., Nedergaard, M., 2017. Focal Solute Trapping and Global Glymphatic Pathway Impairment in a Murine Model of Multiple Microinfarcts. The Journal of neuroscience : the official journal of the Society for Neuroscience 37, 2870-2877. 10.1523/jneurosci.2112-16.2017
Wang, M., Iliff, J.J., Liao, Y., Chen, M.J., Shinseki, M.S., Venkataraman, A., Cheung, J., Wang, W., Nedergaard, M., 2012. Cognitive deficits and delayed neuronal loss in a mouse model of multiple microinfarcts. The Journal of neuroscience : the official journal of the Society for Neuroscience 32, 17948-17960. 10.1523/jneurosci.1860-12.2012
Wang, W., Redecker, C., Bidmon, H.J., Witte, O.W., 2004. Delayed neuronal death and damage of GDNF family receptors in CA1 following focal cerebral ischemia. Brain Res 1023, 92-101. 10.1016/j.brainres.2004.07.034
Wilson, E.N., Abela, A.R., Do Carmo, S., Allard, S., Marks, A.R., Welikovitch, L.A., Ducatenzeiler, A., Chudasama, Y., Cuello, A.C., 2017. Intraneuronal Amyloid Beta Accumulation Disrupts Hippocampal CRTC1-Dependent Gene Expression and Cognitive Function in a Rat Model of Alzheimer Disease. Cerebral cortex (New York, N.Y. : 1991) 27, 1501-1511. 10.1093/cercor/bhv332
Xie, M., Yi, C., Luo, X., Xu, S., Yu, Z., Tang, Y., Zhu, W., Du, Y., Jia, L., Zhang, Q., Dong, Q., Zhu, W., Zhang, X., Bu, B., Wang, W., 2011. Glial gap junctional communication involvement in hippocampal damage after middle cerebral artery occlusion. Ann Neurol 70, 121-132. 10.1002/ana.22386
Zalewska, K., Ong, L.K., Johnson, S.J., Nilsson, M., Walker, F.R., 2017. Oral administration of corticosterone at stress-like levels drives microglial but not vascular disturbances post-stroke. Neuroscience 352, 30-38. 10.1016/j.neuroscience.2017.03.005
Zalewska, K., Pietrogrande, G., Ong, L.K., Abdolhoseini, M., Kluge, M., Johnson, S.J., Walker, F.R., Nilsson, M., 2018. Sustained administration of corticosterone at stress-like levels

after stroke suppressed glial reactivity at sites of thalamic secondary neurodegeneration. Brain Behav Immun 69, 210-222. 10.1016/j.bbi.2017.11.014
Zhang, J., Zhang, Y., Li, J., Xing, S., Li, C., Li, Y., Dang, C., Fan, Y., Yu, J., Pei, Z., Zeng, J., 2012a. Autophagosomes accumulation is associated with beta-amyloid deposits and secondary damage in the thalamus after focal cortical infarction in hypertensive rats. Journal of neurochemistry 120, 564-573. 10.1111/j.1471-4159.2011.07496.x
Zhang, J., Zhang, Y., Xing, S., Liang, Z., Zeng, J., 2012b. Secondary neurodegeneration in remote regions after focal cerebral infarction: a new target for stroke management? Stroke 43, 1700-1705. 10.1161/strokeaha.111.632448
Zhang, Y., Xing, S., Zhang, J., Li, J., Li, C., Pei, Z., Zeng, J., 2011. Reduction of beta-amyloid deposits by gamma-secretase inhibitor is associated with the attenuation of secondary damage in the ipsilateral thalamus and sensory functional improvement after focal cortical infarction in hypertensive rats. Journal of cerebral blood flow and metabolism : official journal of the International Society of Cerebral Blood Flow and Metabolism 31, 572-579. 10.1038/jcbfm.2010.127
Zhao, Z., Ong, L.K., Johnson, S., Nilsson, M., Walker, F.R., 2017. Chronic stress induced disruption of the peri-infarct neurovascular unit following experimentally induced photothrombotic stroke. Journal of cerebral blood flow and metabolism : official journal of the International Society of Cerebral Blood Flow and Metabolism 37, 3709-3724. 10.1177/0271678x17696100
Zhao, Z., Ong, L.K., Pietrogrande, G., Sanchez Bezanilla, S., Warren, K., Ilicic, M., Kluge, M.G., TeBay, C., Ottersen, O.P., Johnson, S.J., Nilsson, M., Walker, F.R., 2018. Low oxygen post conditioning improves stroke-induced cognitive impairment. bioRxiv. 10.1101/483453

SUPPLEMENTARY MATERIAL

Visual discrimination impairment after experimental stroke is associated with disturbances in the polarisation of the astrocytic aquaporin-4 and increased accumulation of neurotoxic proteins

Authors:
Sonia Sanchez-Bezanilla [a, b], Clifford TeBay[a], Michael Nilsson[a, b, c, d, e] , Frederick R Walker[a, b, c, d], Lin Kooi Ong[a, b, c]

Authors affiliations:
a - School of Biomedical Sciences and Pharmacy and Priority Research Centre for Stroke and Brain Injury, University of Newcastle, Callaghan, NSW, Australia.

b - Hunter Medical Research Institute, New Lambton, Heights, NSW, Australia.

c - NHMRC Centre of Research Excellence Stroke Rehabilitation and Brain Recovery, Heidelberg, VIC, Australia.

d - Centre for Rehab Innovations, University of Newcastle, Callaghan, NSW, Australia.

e - LKC School of Medicine, Nanyang Technological University, Singapore

Corresponding author
Lin Kooi Ong
School of Biomedical Sciences and Pharmacy and the Priority Research Centre for Stroke and Brain Injury, University of Newcastle, Callaghan, NSW, Australia. Hunter Medical Research Institute, Newcastle, NSW, Australia.
Phone: +61 492 15736
E-mail: lin.ong@uon.edu.au

Supplementary Methods

Animals

C57BL/6 male mice (10 weeks old) were obtained from the Animal Services Unit at the University of Newcastle. Mice were maintained in a temperature- (21˚C±1) and humidity-controlled environment with food and water available ad libitum. Lighting was on a 12:12h reverse light–dark cycle (lights on 19:00h) with all procedures conducted in the dark phase. In all experiments, mice were acclimatised to the environment for a minimum of seven days prior to the start of the experiment. Mice were housed between 2 to 4 per cage.

Tissue processing

At day 14, mice were deeply anaesthetised with sodium pentabarbitol. Blood samples (approximately 400 mL) were collected transcardially using a 0.5ml syringe coated with 0.1M EDTA and then centrifuged at 5000g for 10 min at 4°C. Plasma was collected, aliquoted and kept in a -80°C freezer for further analyses. Following blood collection, mice were perfused via the ascending aorta with ice cold 0.9% saline followed by ice cold 4% paraformaldehyde (pH 7.4) for histological analysis. Brains were dissected and post-fixed for 4 hours in the same fixative then transferred to a 12.5% sucrose solution in 0.1M PBS for storage and cyroprotection. Serial coronal sections were sliced on a freezing microtome (Leica, North Ryde, NSW, Australia) at a thickness of 30µm. For western blotting, mice were deeply anesthetized via intraperitoneal injection of sodium pentobarbital and transcardially perfused with ice cold 0.1 % diethylpyrocarbonate in 0.9 % saline for 3 mins. Brains were dissected and rapidly frozen in -80˚C isopentane. Sections were sliced using a cryostat (-20°C) at a thickness of 200µm. The peri-infarct territory (2 mm^2 around infarct core, Bregma +1.0 to -1.0mm), the thalamus (Bregma -1.2 to -2.2mm) and the hippocampus (Bregma -1.2 to -2.5mm) were punched using a 1 mm tissue punch. Samples were stored frozen in -80˚C until further analysis.

ELISA

The plasma were measured for amyloid-β 40 and amyloid-β 42 levels using commercially available human/rat βAmyloid (40) ELISA kit (29464701, FUJIFILM Wako) and human/rat βAmyloid (42) ELISA kit (29264501, FUJIFILM Wako) respectively, according to the manufacturer's instruction.

Cresyl Violet staining

Cresyl Violet staining was performed as previously described (Ong et al., 2018). Fixed sections at bregma 0.0mm (one per mice) were mounted on glass slides and air-dried. Sections were defatted in chloroform:ethanol solution for 8 min, followed by rehydration in a series ethanol solutions: absolute (1 min), 95% (1 min) and 70% (1 min). Sections were stained in Cresyl Violet solution for 15 min. Then, sections were washed in 70% ethanol (1 min), 95% ethanol (1 min), differentiating solution (2 min) and absolute ethanol (3 x 1 min). Finally, the sections were cleared in xylene (3 x 1 min) and cover slipped.

Immunohistochemistry

Free-floating fixed sections were immunostained as previously described (Zhao et al., 2017). Peri-infarct (bregma 0.0mm), and thalamus and hippocampus sections (bregma -1.5mm) were rinsed with 0.1 M PBS and incubated in 0.9% hydrogen peroxide for 30 min, followed by 3% normal horse serum. Sections were incubated in primary antibody (amyloid-β, α-synuclein or NeuN) for 72h at 4°C and then incubated with a biotinylated secondary antibody of corresponding species for 2h at room temperature (see Supplementary Table 1 for antibodies concentrations). Next, brain sections were incubated for 2h at 25°C with avidin–biotin-

peroxidase complex and finally developed using a nickel-enhanced 3, 3'-diaminobenzidine (DAB) peroxidase substrate. Tissues were processed simultaneously from both experimental groups, and the DAB reactions were developed for exactly the same length of time following the addition of glucose oxidase. After processing was completed, sections were washed and then mounted onto chrome alum-coated slides and cover slipped.

Immunofluorescence

Free-floating fixed sections were co-immunostained using standard protocols as previously described (Kluge et al., 2017; Tynan et al., 2013). Sections were rinsed, and non-specific binding sites were blocked using 3% bovine serum albumin. Sections were incubated in both primary antibodies (GFAP and AQP4) overnight at 4˚C, followed by 2h incubation in secondary antibodies for 2h at 25˚C (see Suppl. Table 1 for antibodies concentration). Brain sections were washed with PBS in between each incubation step and subsequently mounted and cover slipped.

Image acquisition and analysis

Cresyl Violet staining: Images were acquired at 20x using Aperio AT2 (Leica, Germany). The estimated tissue loss area [area of contralateral hemisphere – area of ipsilateral hemisphere] was determined on Cresyl Violet stained sections with ImageJ software 1.50 a, NIH. The quantitative analysis was undertaken specifically in the peri-infarct territory (Bregma 0.0mm).

Immunohistochemistry: Images of immunolabeling were obtained and analysed as described previously (Ong et al., 2018; Ong et al., 2017). Briefly, images were taken at 20x magnification by using an Aperio AT2. Whole mosaic SVS images were converted into TIFF images in Matlab v2018b. Then, the mosaic images were cropped in the peri-infarct, thalamus and hippocampus. For analysis of the cropped images of amyloid-β and α-synuclein labelling, pixel intensity level considered to be optimal for detecting genuine differences in immunoreactive signal was determined using ImageJ software to visualise thresholding of cropped regions at individual pixel intensities. This threshold level was used to investigate group differences for all labels (Supplementary Fig. 3(C)). Exhaustive automated NeuN cell counts were undertaken in the cropped images corresponding to peri-infarct and thalamus using ImageJ software (Supplementary Fig. 3(A)). In the hippocampus area, cell bodies are very densely packed making automated NeuN cell count difficult in this brain region. Instead, we performed thresholding analyses and chose the optimal pixel intensity that clearly reflected the immunolabelled signal (Supplementary Fig. 3(B)).

Immunofluorescence: For AQP4/GFAP double labelling, high resolution confocal images of immunolabeled brain sections were taken on a Leica TCS SP8 confocal microscope with a Leica HC PLC APO 20x/0.70 (peri-infarct) and 10x/0.40 (thalamus and hippocampus) objectives. For each region of interest, 30 μm z-stacks with a step size of 1 μm were taken. Imaging parameters (laser power, resolution and gain) were held constant throughout all imaging sessions. To measure reactive gliosis (GFAP immunoreactivity), the emission channels were split and the GFAP emission image was uniformly thresholded at a high stringency (Supplementary Fig. 3(D)). The area of GFAP immunoreactivity was expressed as a percentage of the overall field of view (ImageJ Software). We calculated the AQP4 polarity for each image as previously described (Wang et al., 2012) (Supplementary Fig. 3(E)).

Supplementary Table 1: List of antibodies used for western blot, immunohistochemistry and immunofluorescence analyses.

Target	Sources of antibodies	Application	Dilution
Amyloid-β	Biolegend, anti-Amyloid-β (6E10), # SIG-39320	WB	1:1000
		IHC	1:1000
NeuN	Cell Signaling, anti-NeuN (D3S31), #12943	WB	1:2000
	Millipore, anti-NeuN (clone A60), #MAB377	IHC	1:2000
α-Synuclein	BD Bioscience, anti-α-Synuclein, #610787	WB	1:1000
		IHC	1:1000
AQP4	Millipore, anti-aquaporin 4, #AB2218	WB	1:2000
		IF	1:1000
GFAP	Cell Signaling, anti- Glial Fibrillary Acidic Protein (GA5), #3670	WB	1:5000
	Sigma-Aldrich, Anti-Glial Fibrillary Acidic Protein (GA5), #G3893	IF	1:1000
ALDH1L1	Millipore, anti-ALDH1L1 (N103/39), #MABN495	WB	1:2000
α-Syntrophin	abcam, anti- α-Syntrophin alpha 1, #ab11187	WB	1:3000
Dystrophin	abcam, anti-dystrophin, #ab15277	WB	1:1000
β-actin	Sigma-Aldrich, Monoclonal Anti-β-actin-HRP antibody, A3854	WB	1:50000
Rabbit IgG	Biorad, Anti-Rabbit-HRP antibody, #170-6515	WB	1:7500
	ThermoFisher Scientific, anti-Rabbit IgG (H+L) Highly Cross-Adsorbed Secondary Antibody, Alexa Fluor 488, #A21206	IF	1:400
Mouse IgG	Biorad, Anti-Mouse-HRP antibody, #170-6516	WB	1:10000
	Jackson ImmunoReseach, Anti-Mouse-Biotin, #115-065-003	IHC	1:500
	ThermoFisher Scientific, anti-Mouse IgG (H+L) Highly Cross-Adsorbed Secondary Antibody, Alexa Fluor 594, #A21203	IF	1:400

WB, western blot; IHC, immunohistochemistry; IF, immunofluorescence

Supplementary Figures and Figure Legends

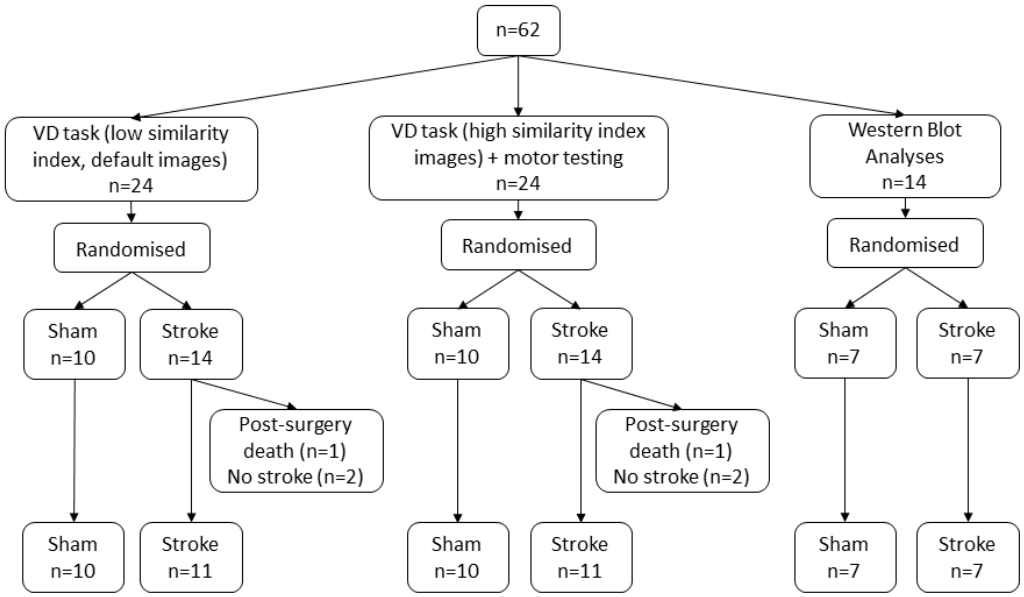

Supplementary Fig. 1. Diagram for inclusion and exclusion of mice in this study. Mice were removed from the study if we histologically identified that the stroke had not occurred. A total of 24 sham mice were used for visual discrimination (VD) task using images with low similarity index (Sham n=10; Stroke n=14). A total of 24 sham mice were used for VD task using images with high similarity index (Sham n=10; Stroke n=14). This second cohort was also used to assess motor function, blood were collected and the brains were used for histology analysis. Finally, a total of 14 stroke mice were used for protein analysis of the brains (Stroke n=7; Sham n=7).

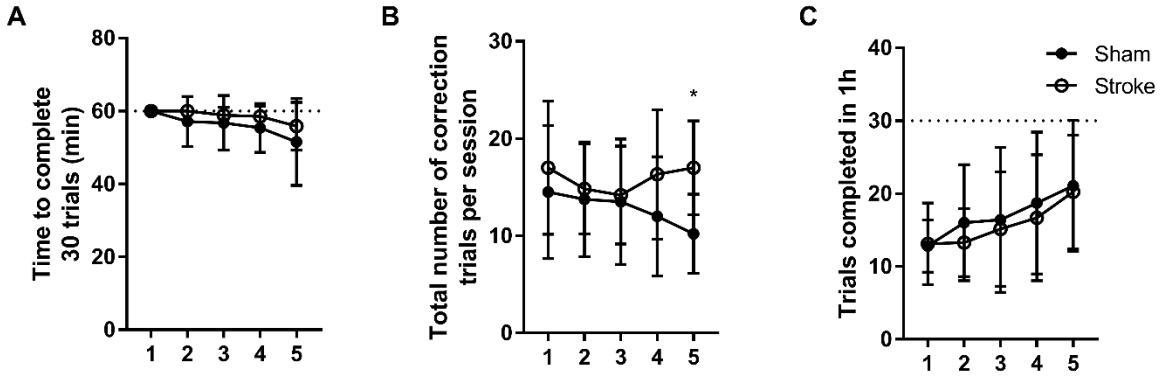

Supplementary Fig. 2. Metrics of the visual discrimination (VD) task for the high similarity index pair ('ovals-rectangles' pair). There is no statistically significant between sham and stroke mice in time to complete 30 trials (A) or number of trials completed within 60 min (C). However, stroke mice perform significantly more correction trials (B) during VD than sham. Mean±SD (two-way ANOVA and Sidak's multiple comparisons). * $p<0.05$.

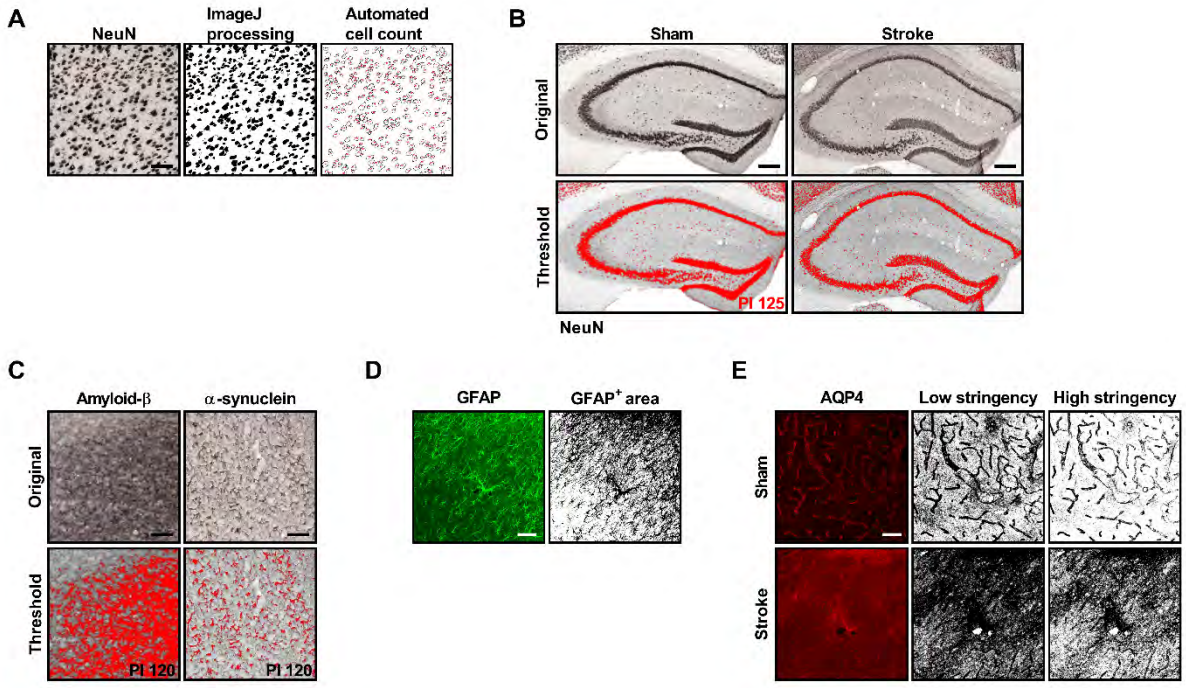

Supplementary Fig. 3. Image procesing and analysis. (A) Automated NeuN cell counts were undertaken in the peri-infarct and thalamus using ImageJ software. The original image (left) were converted into a binary image (middle) and the black particles were counted (right) (scale bar = 100µm). (B) In the hippocampus area, we performed thresholding analyses and chose the optimal pixel intensity that clearly reflected the immunolabelled signal using ImageJ. The top panels represent the original images. The bottom panels show material thresholded at the pixel intensity (PI) 125. The number of pixels that were captured at and below PI 125 were then expressed as a percentage of the total number of pixels in each image and this data were used to investigate group differences (scale bar = 300µm). (C) The same thereholding analysis were performed for amyloid-β and α-synuclein labelling. Top panels represent the original images and bottom panels represents material thresholded at PI 120 (scale bar = 100µm). (D) To measure GFAP immunoreactivity, confocal images (left) were uniformly thresholded at a high stringency (right) using ImageJ. The area of GFAP immunoreactivity was expressed as a percentage of the overall field of view. (E) To analyse AQP4 polarization, AQP4 confocal images were uniformly thresholded at two levels: low stringency and high stringency. Low stringency included all AQP4-immunoreactive pixels within the image. High-stringency threshold defined the area of intense AQP4 immunoreactivity that in sham mice is localized to perivascular end-feet. "AQP4 polarity" was calculated as the ratio between low stringency and high stringency areas. Higher AQP4 polarity values reflected expression levels of AQP4 in perivascular end-feet being greater than in surrounding tissue, while lower AQP4 polarity values reflected greater parity between perivascular and non-perivascular AQP4 expression.

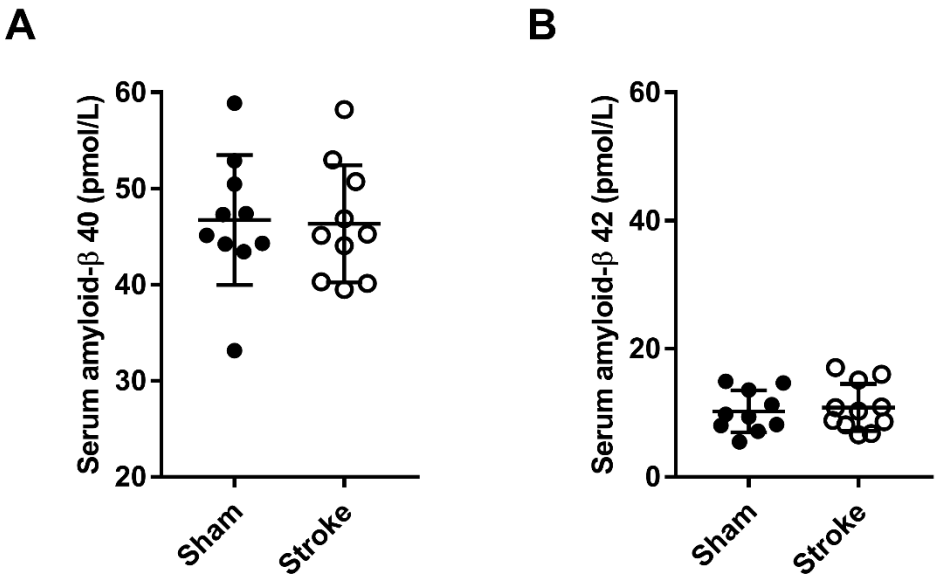

Supplementary Fig. 4. Stroke does not affect the levels of Amyloid-β in plasma. Plasma levels of Aβ40 (A) and Aβ42 (B) were assesed using ELISA. Mean ± SD (2-tailed t-test).

.

Supplementary references

Kluge, M.G., Kracht, L., Abdolhoseini, M., Ong, L.K., Johnson, S.J., Nilsson, M., Walker, F.R., 2017. Impaired microglia process dynamics post-stroke are specific to sites of secondary neurodegeneration. Glia 65, 1885-1899. 10.1002/glia.23201

Ong, L.K., Chow, W.Z., TeBay, C., Kluge, M., Pietrogrande, G., Zalewska, K., Crock, P., Aberg, N.D., Bivard, A., Johnson, S.J., Walker, F.R., Nilsson, M., Isgaard, J., 2018. Growth Hormone Improves Cognitive Function After Experimental Stroke. Stroke 49, 1257-1266. 10.1161/strokeaha.117.020557

Ong, L.K., Zhao, Z., Kluge, M., TeBay, C., Zalewska, K., Dickson, P.W., Johnson, S.J., Nilsson, M., Walker, F.R., 2017. Reconsidering the role of glial cells in chronic stress-induced dopaminergic neurons loss within the substantia nigra? Friend or foe? Brain Behav Immun 60, 117-125. 10.1016/j.bbi.2016.10.001

Tynan, R.J., Beynon, S.B., Hinwood, M., Johnson, S.J., Nilsson, M., Woods, J.J., Walker, F.R., 2013. Chronic stress-induced disruption of the astrocyte network is driven by structural atrophy and not loss of astrocytes. Acta Neuropathol 126, 75-91. 10.1007/s00401-013-1102-0

Wang, M., Iliff, J.J., Liao, Y., Chen, M.J., Shinseki, M.S., Venkataraman, A., Cheung, J., Wang, W., Nedergaard, M., 2012. Cognitive deficits and delayed neuronal loss in a mouse model of multiple microinfarcts. J Neurosci 32, 17948-17960. 10.1523/jneurosci.1860-12.2012

Zhao, Z., Ong, L.K., Johnson, S., Nilsson, M., Walker, F.R., 2017. Chronic stress induced disruption of the peri-infarct neurovascular unit following experimentally induced photothrombotic stroke. J Cereb Blood Flow Metab 37, 3709-3724. 10.1177/0271678x17696100

CHAPTER 4: PUBLICATION 2

More than motor impairment: A spatiotemporal analysis of cognitive impairment and associated neuropathological changes following cortical photothrombotic stoke.

As per the peer-review paper submitted to: Journal of Cerebral Blood Flow & Metabolism

CONTRIBUTIONS

We, the co-authors, attest the Research Higher Degree candidate, Sonia Sanchez Bezanilla, contributed to the paper entitled **"More than motor impairment: A spatiotemporal analysis of cognitive impairment and associated neuropathological changes following cortical photothrombotic stoke"** as outlined below:

- 70% Conception and design of research;
- 85% Experimental procedures;
- 75% Analysis and interpretation of the findings;
- 75% Writing and critical appraisal of the content

Rebecca J. Hood		*10/03/2020*
Name of Co-author	*Signature*	*Date*
Michael Nilsson		*19/02/2020*
Name of Co-author	*Signature*	*Date*
Frederick R. Walker		*19/02/2020*
Name of Co-author	*Signature*	*Date*
Lin Kooi Ong		*19/02/2020*
Name of Co-author	*Signature*	*Date*

Lesley MacDonald-Wicks

Assistant Dean Research Training

10/3/2020

More than motor impairment: A spatiotemporal analysis of cognitive impairment and associated neuropathological changes following cortical photothrombotic stoke.

Sonia Sanchez-Bezanilla[1,2], Rebecca J. Hood[1,2], Lyndsey E. Collins-Praino[3], Renée J. Turner[3], Frederick R. Walker[1,2,4,5], Michael Nilsson[1,2,4,5,6] and Lin Kooi Ong[1,2,4,7]

1. School of Biomedical Sciences and Pharmacy and the Priority Research Centre for Stroke and Brain Injury, The University of Newcastle, Australia, Callaghan, NSW, Australia
2. Hunter Medical Research Institute, Newcastle, NSW, Australia
3. Department of Medical Sciences, Adelaide Medical School, University of Adelaide, Adelaide SA 5005, Australia
4. NHMRC Centre of Research Excellence Stroke Rehabilitation and Brain Recovery, Heidelberg, VIC, Australia
5. Centre for Rehab Innovations, The University of Newcastle, Callaghan, NSW, Australia
6. LKC School of Medicine, Nanyang Technological University, Singapore
7. Monash University Malaysia, Bandar Sunway, Selangor, Malaysia

Correspondence:
Lin Kooi Ong
School of Pharmacy, Monash University Malaysia, Jalan Lagoon Selatan, 47500, Bandar Sunway, Selangor, Malaysia.
E-mail: ong.linkooi@monash.edu

Running title: Post-stroke cognitive deficits and hippocampal SND

Abstract
There is emerging evidence suggesting that a cortical stroke can cause delayed and remote hippocampal dysregulation, leading to cognitive impairment. In this study, we aimed to investigate motor and cognitive outcomes after experimental stroke, and their association with secondary neurodegenerative processes. Specifically, we used a photothrombotic stroke model targeting the motor and somatosensory cortices of mice. Motor function was assessed using the cylinder and grid walk tasks. Changes in cognition were assessed using a mouse touchscreen platform. Neuronal loss, gliosis and amyloid-β accumulation were investigated in the peri-infarct and hippocampal regions at 7, 28 and 84 days post-stroke. Our findings showed persistent impairment in cognitive function post-stroke, whilst there was a modest spontaneous motor recovery over the investigated period of 84 days. In the peri-infarct region, we detected a reduction in neuronal loss and decreased neuroinflammation over time post-stroke, which potentially explains the spontaneous motor recovery. Conversely, we observed persistent neuronal loss together with concomitant increased neuroinflammation and amyloid-β accumulation in the hippocampus, which likely accounts for the persistent cognitive dysfunction. Our findings indicate that cortical stroke induces secondary neurodegenerative processes in the hippocampus, a region remote from the primary infarct, potentially contributing to the progression of post-stroke cognitive impairment.

Key words: Cognitive impairment, Secondary neurodegeneration, Stroke, Neuroinflammation, Amyloid-β

Introduction

Stroke is the second most common cause of death in the world, and the leading cause of acquired disability [1, 2]. Of those who survive, over half remain physically dependent and approximately two-thirds have some form of neurological impairment in the years following stroke [3-6]. While motor impairments are the most common and widely recognised post-stroke complications [7], the neurological deficits caused by stroke go well beyond motor outcomes, with up to 80% of stroke survivors suffering from cognitive impairment [8-10]. Such cognitive impairment may persist long-term after the ischemic injury, and affect different cognitive domains such as memory, learning and executive functions [11]. Concerningly, a previous history of stroke is known to be a major risk factor for development of dementia [12]. In a recent report from the Oxford Vascular Study, the one-year standardized morbidity ratio for incidence of dementia was found to be 47.3% in survivors of a severe stroke, 5.8% following a minor stroke and 3.5% in those with a transient ischaemic attack compared to age and sex matched population [13]. Given this, a better understanding of the neural mechanisms that underlie the development of persistent cognitive impairment following stroke is crucial for both early detection as well as development of targeted treatments.

It has been previously identified that stroke triggers a wave of secondary damage that causes the progressive and inexorable loss of brain tissue at sites connected to the area damaged by the initial infarction, a phenomenon known as secondary neurodegeneration (SND) [14, 15]. SND develops within days after the primary infarction but may continue for some weeks, months and even years after the initial stroke event [15, 16], and has been observed in both rodents and humans [17-22]. SND has recently been implicated as a potential modulator to a number of late phase functional disturbances [23, 24]. The key hallmarks of SND include neuronal loss, neuroinflammation and accumulation of neurotoxic proteins [15]. Previous studies from our group and others have consistently reported the ocurrence of these observations in the thalamus and substantia nigra [17-21, 25-29]. While hippocampal atrophy has been reported after ischemic stroke [22, 30, 31], little is known about the underlying molecular and cellular mechanisms. This is significant, as the hippocampus is known to be highly interconnected with both the cerebral cortex [32] and thalamus [33], making it a potential key site for SND following stroke.

Recently, our group has identified that photothrombotic stroke within the motor and somatosensory cortex produces significant impairment in a hippocampal-dependent visual discrimination task using touchscreen based assessment at 14 days post-stroke [34]. Interestingly, although our cortical stroke model does not cause direct damage to the hippocampus, we identified neuronal loss, astrogliosis and increased accumulation of neurotoxic proteins within the hippocampus at 14 days post-stroke. These results clearly demonstrated that, despite the primary infarct being confined to the cortex, the disturbances extended well beyond this to include remote areas such as the hippocampus. While being an important landmark study to build an understanding of the mechanisms behind post-stroke cognitive impairment, this study left a number of important questions unanswered. Firstly, what is the timeline of progression of cognitive deficits following stroke? Secondly, what is the association between post-stroke functional outcomes and the key hallmarks of SND processes? In order to answer these questions, a longitudinal study encompassing both longer time-points and a battery of different cognitive tasks is necessary.

As such, in the present study, we comprehensively assessed both the functional and neuropathological outcomes up to 84 days after cortical photothrombotic stroke. Specifically, we assessed motor function using the cylinder and grid walk task, associative memory and

learning using the paired associate learning task (PAL) and cognitive flexibility using visual discrimination reversal task (VDR). The progress of brain tissue loss was assessed throughout the rostrocaudal extent of the ischemic lesion. Furthermore, we investigated the pattern of spatiotemporal changes of neuronal loss, gliosis and accumulation of amyloid-beta (Aβ) within both the primary cortical infarction sites and remote hippocampal regions at 7, 28 and 84 days post-stroke.

Materials and methods

The data that supports the findings for this study are available from the corresponding author upon reasonable request. See supplementary materials and methods for detailed protocols.

Animals
C57BL/6 male mice (10 weeks old) were obtained from the Animal Services Unit at the University of Newcastle. Mice were maintained in a temperature- (21˚C±1) and humidity-controlled environment with food and water available *ad libitum*. Lighting was on a 12:12h reverse light–dark cycle (lights on 19:00h) with all procedures conducted in the dark phase. In all experiments, mice were acclimatised to the environment for a minimum of seven days prior to the start of the experiment. Mice were housed between 2 to 4 per cage.

Experimental design
Animal research was undertaken in accordance with the Animal Research: Reporting of *In Vivo* Experiments (ARRIVE) guidelines. Experiments were approved by the University of Newcastle Animal Care and Ethics Committee (A-2013-340) and conducted in accordance with the New South Wales Animals Research Act and the Australian Code of Practice for the use of animals for scientific purposes. All the experimental groups were randomized, and all outcome analyses were performed in a blinded manner. A total of 85 mice (C57BL/6 male, 10 weeks old) were used in this study (Figure 1A). Details on animal numbers for each experiment and inclusion/exclusion criteria are included in the supplementary material (Supplementary figure 1). The first cohort (sham n=10, stroke n=14) were assessed on the VDR task and the brain tissue was used for protein analyses. The second cohort (sham n=10, stroke n=14) were assessed using a mouse touchscreen platform for the PAL task and underwent motor testing. The brain tissue from this cohort was used for histological analyses. For both cohorts, at day 0, mice were subjected to either photothrombotic occlusion or sham surgery. At day 7 post-stroke, mice were assessed on a mouse touchscreen platform on either the PAL task or VDR task. Upon completion of the task, mice were allowed to rest for one month (extinction period). At day 56 after stroke, the VDR task or PAL task was re-started. Motor tests were performed on second cohort one day before stroke/sham surgery and at days 7, 28 and 84 post-stroke. Finally, mice were sacrificed at day 84 post-stroke. A third cohort of mice were sacrificed at either 1 week (stroke n=18) or 1 month (stroke n=19) post-stroke, and the brains used for subsequent protein or histological analyses. This cohort was not subjected to functional testing, and the brains were used as representative for the 1 week or 1 month time points.

Sample Size Calculation
Sample size was estimated using G*Power 3.1 software. We required n=10 per group for the first and second cohorts, with an estimated standard deviation, SD=7 and an effect size of Cohen's d=1.7 allowing a type 1 error of 5% with the power of 80%.

Photothrombotic occlusion
Photothrombotic occlusion was performed as previously described [35-37].

Cognitive testing
Mouse touchscreen operant chambers (Campden Instruments Ltd., UK) were used in the cognitive testing as described with modifications [38, 39], and testing was conducted in a blinded and randomised manner. Specifically, associative memory and cognitive flexibility was assessed using the PAL task and the VDR task respectively.

Motor test
Cylinder test and grid walk test were chosen as motor assessments [40]. Motor tests were performed one day before stroke surgery and at days 7, 28 and 84 after stroke.

Tissue processing
Mice were sacrificed at different time points after surgery: 7, 28 or 84 days. Brains were either paraformaldehyde fixed (histological analyses) or fresh frozen (western blotting) as previously described [34, 41].

Histological Analysis
Cresyl Violet and Sudan black staining was performed as previously described [34, 35]. Free-floating fixed sections were used for immunofluorescence and were co-immunostained using standard protocols as previously described [26, 27].

Image acquisition and analysis
Cresyl Violet and Sudan Black stain imaging. Images were acquired at 20x using Aperio AT2 (Leica, Germany). The estimated tissue loss area [area of contralateral hemisphere – area of ipsilateral hemisphere] was determined on Cresyl Violet stained sections with ImageJ software 1.50 a, NIH. The quantitative analysis was undertaken specifically in the peri-infarct territory (Bregma 0.0 mm). The estimated corpus callosum loss area was determined using ImageJ software [area of contralateral hemisphere - area of ipsilateral hemisphere].

Immunofluorescence. High resolution confocal images of immunolabeled brain sections were taken on a Leica TCS SP8 confocal microscope with a Leica HC PLC APO 20x/0.70 (peri-infarct) and 10x/0.40 (hippocampus) objectives. For each region of interest, 30 µm z-stacks with a step size of 1 µm were taken. Imaging parameters (laser power, resolution and gain) were held constant throughout all imaging sessions.

- For NeuN labelling, extensive automated NeuN cell counts were performed using ImageJ software in the peri-infarct area. In the hippocampus, cell bodies are very densely packed, making automated NeuN cell count difficult in this brain region. Instead, we performed thresholding analyses and chose the optimal pixel intensity that clearly reflected the immunolabelled signal [34].
- The area of GFAP immunoreactivity was expressed as a percentage of the overall field of view (ImageJ Software) [34].
- Microglia morphological analysis was performed using Iba-1 labelled images. Quantitative analysis of soma and branch parameters was performed using a combined multi-level thresholding and minimum spanning tree skeleton tracing approach as described in Abdolhoseini et al. [42].

Protein extraction and Western blotting
Protein homogenates from the peri-infarct and the hippocampus samples were obtained and Western blotting performed as previously described [34, 35, 43].

Statistics

All data were analysed using GraphPad Prism v7.02. The primary outcome measurement was differences between sham, 7 days, 28 days and 84 days post-stroke. All values reported are mean±SD. Data from tissue loss, western blotting and immunofluorescence labelling were analysed using a one-way analysis of variance (ANOVA) followed by Tukey's post hoc comparison. Cognitive tests and motor tests were analysed using a 2-way ANOVA, followed by Sidak multiple comparisons. $P<0.05$ was considered statistically significant.

Results

Cognitive flexibility is impaired long-term after photothrombotic stroke

Seven days after the induction of the stroke targeting the motor and sensory cortex, mice underwent assessment on a mouse touchscreen platform for VDR task to assess cognitive flexibility. The task was performed for 25 consecutive days (sub-acute phase, 7-28 day), followed by a one month rest period (extinction period). Then, the VDR task was re-initiated at 56 days post-stroke (chronic phase, 56-84 day) (Figure 1A).

During the sub-acute phase, we found a significant decrease in the percentage of correct trials in stroked mice compared to shams ($F_{(1,19)}=11.99$, $p=0.0026$), a significant time effect ($F_{(21,399)}=10.72$, $p<0.0001$) and no significant interaction effect ($F_{(21, 399)}= 1.367$, $p=0.1300$). In addition, post hoc analysis indicated a significant decrease in the percentage of correct trials in the last two days of the VDR task ($p=0.0407$ and $p=0.0243$) in stroked mice compared to shams. During the chronic phase, we also found a significant decrease in the percentage of correct trials in stroked mice compared to shams ($F_{(1,19)}=7.867$, $p=0.0113$), a significant time effect ($F_{(18,342)}=11.37$, $p<0.0001$), and no significant interaction effect ($F_{(18,342)}=1.083$, $p=0.3673$). Post hoc analysis indicated a significant decrease in the percentage of correct trials in the last two days of VDR task ($p=0.0411$ and $p=0.0349$) in stroked mice compared to shams (Figure 1C). A range of metrics from the VDR task were also collected for temporal analysis. There were no significant differences between groups either in time to complete 36 trials, the number of total correction trials completed, or the number of trials completed within 60 min (Supplementary figure 2C and D).

Associative memory is impaired long-term after photothrombotic stroke

Associative memory was assessed using the PAL task at sub-acute (7-28 day) and chronic phases (56-84 day), as described above (Figure 1A). During the sub-acute phase, we found a significant decrease in the percentage of correct trials in stroked mice compared to sham ($F_{(1,20)}=4.855$, $p=0.0394$), a significant time effect ($F_{(4,80)}=42.31$, $p<0.0001$), and no significant interaction effect ($F_{(4,80)=}1.888$, $p=0.1207$). In addition, post hoc analysis indicated a significant decrease in the percentage of correct trials on the last day of the PAL task in stroked mice compared to shams ($p=0.0295$; Figure 1B). During the chronic phase, we also found a significant decrease in the percentage of correct trials in stroked mice compared to shams ($F_{(1,20)}=9.925$, $p=0.0050$), a significant time effect ($F_{(4,80)}=16.74$, $p<0.0001$), and significant interaction effect ($F_{(4,80)}=3.261$, $p=0.0157$). Post hoc analysis indicated a significant decrease in the percentage of correct trials at the last six days of the PAL task ($p=0.0063$; $p=0.0440$; $p=0.0265$; $p=0.0461$; $p=0.0409$ and $p=0.0129$, respectively) in stroked mice compared to shams (Figure 1B). A range of metrics from the PAL task were also collected for temporal analysis. There was no significant effect either in time to complete 36 trials or in the number of total correction trials completed. There was, however, a significant decrease in the number of trials completed within 60 minutes in the sub-acute phase in stroked mice compared to shams (Supplementary figure 2A and B).

Motor deficits are persistent long-term after photothrombotic stroke, with only modest spontaneous recovery over time

The progression of motor deficits long-term after photothrombotic stroke was assessed using two motor tests: the cylinder task and the grid walk task. We performed these tests prior to stroke to establish a baseline, and at 7, 28 and 84 days post-stroke. Locomotor asymmetry was evaluated using a cylinder task to evaluate the paw preference mice exhibit for stabilising themselves whilst rearing within a cylinder. Data on asymmetry scores indicated that there were no significant differences in paw preference prior to stroke. However, at day 7, 28 and 84 post-stroke, the stroke group exhibited a significantly stronger preference for using their unaffected paw relative to sham ($p=0.001$ at day 7, $p<0.0001$ at day 28 and $p=0.0004$ at day 84) (Figure 2A). Motor function was further assessed using the grid walk task, evaluating the ability of mice to effectively place their paws on an elevated grid during locomotion. There was no difference in the number of foot faults before stroke. At day 7, 28 and 84 post-stroke, the number of foot faults on the affected side (contralateral) was significantly higher in stroked mice compared to shams ($p<0.0001$ at day 7, 28 and 84) (Figure 2B).

Photothrombotic stroke causes persistent brain tissue and neuronal loss

We used Cresyl Violet staining to estimate the tissue loss at Bregma 1.0 mm, 0.0 mm, -1.0 mm and -1.5 mm. Rostrocaudal analysis of tissue loss revealed a significant increase in tissue loss at Bregma 0.0 mm, 1.0 mm, -1.0 mm and -1.5 mm at all time points compared to sham (Figure 3A). Peak tissue loss was observed at 7 days post-stroke and then gradually reduced, suggesting some spontaneous recovery from ischemic brain injury. We also evaluated the effect of stroke on white matter tract loss using Sudan Black staining of myelin, given that stroke-induced SND is a disruption of connections between the cortex and hippocampus. Specifically, we focused on the corpus callosum between Bregma 1.0 mm and -1.5 mm, and assessed white matter tract loss as the difference between the contralateral (CL) and ipsilateral (IL) hemispheric area (mm^2). We found a significant increase in white matter structural loss in the corpus callosum at Bregma 0.0 mm at 7, 28 and 84 days post-stroke compared to shams. Additionally, we observed white matter loss at Bregma -1.0 mm and -1.5 mm in stroked mice compared to shams at both 7 and 28 days, but not 84 days, post-stroke (Supplementary figure 3).

We performed immunofluorescence-based cell counting within the primary infarct area and hippocampus using the mature neuronal marker (NeuN) to investigate post-stroke neuronal loss. We performed automated NeuN+ cell count in peri-infarct. Data showed a significant decrease in NeuN+ cells in the peri-infarct of stroked mice at all time points compared to shams ($p=0.0003$ at 7 days, $p<0.0001$ at 28 days and $p=0.0173$ at 84 days) (Figure 3B). In the hippocampus cell bodies are very densely packed, making NeuN+ cell counting difficult. Therefore, optical density was assessed using thresholding analyses in both the CA1 and dentate gyrus (DG) subregions of the hippocampus. We found a significant decrease in threshold material for NeuN in the CA1 subregion at 28 ($p=0.0424$) and 84 days ($p=0.0082$) in stroked mice compared with shams, however, there were no significant differences within the DG (Figure 3C).

Stroke induces transient astrogliosis in the peri-infarct and hippocampus

To study the dynamic change of reactive astrocytes, we immunostained brain samples corresponding to the peri-infarct region (Bregma 0.0 mm) and hippocampus (Bregma -1.5 mm) using the astrocytic marker GFAP. Under normal conditions, astrocytes in the mouse cortex usually express little GFAP. As expected, at 7 and 28 days post-stroke mice exhibited a significant increase in the GFAP-positive area within the peri-infarct region compared to shams ($p<0.0001$) (Figure 4A). However, there were no statistically significant differences between

shams and stroke mice at 84 days post-stroke in the peri-infarct. It should be noted that the glial scar is observed in this region. In the CA1 subregion of the hippocampus, we observed a significant increase at days 7 ($p=0.0003$) and 28 ($p=0.0318$), but it was reduced to basal levels by day 84 (Figure 4B). In the DG, we only observed a significant increase in the % of area covered by GFAP at 7 days post-stroke ($p=0.0021$) (Supplementary figure 4A)

Persistent microglia activation long-term after stroke in peri-infarct and hippocampus

We performed immunofluorescence labelling of Iba-1, a widely used microglial/macrophage marker, to investigate the long-term changes in microglial activation. High-resolution confocal images were taken, and microglia morphological analyses were subsequently undertaken within the peri-infarct area and CA1 and DG subregions of the hippocampus. Further, we analysed the expression of a (CD11b) (microglial transmembrane protein and myeloid cells marker) using western blotting.

In the peri-infarct area, morphological analysis indicated that the microglia had undergone a shift toward a classically activated phenotype. Parameters indicating morphological microglial activation (increase in cell number and increased soma area) peaked at 7 days post-stroke (Figure 5A), with similar changes in microglial activation parameters also seen at 28 and 84 days post-stroke. At day 84, parameters including cell number and soma area were not significantly different to sham mice; however, there was a significant difference in all other parameters. These results indicate that there is persistent microglial activation up to 84 days post-stroke in the peri-infarct region. CD11b protein levels were significantly increased at 7 days post-stroke, but were reduced to basal levels by day 28, and further deceased at 84 days post-stroke (Supplementary figure 6A).

Within the hippocampus, microglial morphology analysis also revealed activated microglia within this region. Relative to the sham group, following stroke the microglia within the CA1 area exhibited changes in all the parameters studied. Peak activation was observed between days 14 and 28 post-stroke, with activation persistent up to 84 days post-stroke (Figure 5B). Regarding the DG, we observed a significant increase in the number of cells but there were no significant changes in other parameters (Supplementary figure 4B). Western blotting analysis indicated that CD11b protein levels were significantly increased at 7 and 28 days post-stroke compared with sham mice (Supplementary figure 6B).

Photothrombotic stroke leads to oligomerisation and accumulation of amyloid-β both in the peri-infarct zone and in the hippocampus

We investigated Aβ oligomerisation status using protein homogenates taken from the peri-infarct and the hippocampus. Specifically, we quantitated the pentamer (25 kDa), intermediate size oligomers (30 kDa), decamer (50 kDa) and dodecamer (56 kDa) forms of Aβ. These Aβ oligomers are linked to cellular pathology and cognitive decline [44, 45]. In the peri-infarct area, we observed a significant increase in pentamer, decamer and dodecamer in stroked mice compared with shams at 7, 28 and 84 days (around 10-20 fold increase) (Figure 6A). In the hippocampus, we observed a significant increase in dodecamer at all time points in stroked mice compared to shams (around 2 fold increase) (Figure 6B).

To further qualitatively assess the spatial distribution of Aβ, we immunostained brain sections from different Bregma regions corresponding with the peri-infarct region and hippocampus using an antibody against Aβ. As expected, no immunofluorescence signal was observed within the peri-infarct region in shams. However, in this same region, we observed a peak of Aβ immunofluorescence at 7 days post-stroke, which was reduced at day 28. At day 84, we

identified a change in the Aβ distribution pattern, from a scattered distribution to accumulation around the cerebral vessels (Figure 7A). In the CA1 subregion of the hippocampus, we detected a peak of immunofluorescence at 7 and 28 days post-stroke, and a reduction at 84 days. At day 84, Aβ was observed to accumulate around the cerebral vessels in the CA1 subregion of the hippocampus, but to a lesser degree compared to the peri-infarct region (Figure 7B). The immunofluorescence signal appeared to be consistent in the DG throughout all experimental groups (Supplementary figure 5).

Discussion

The main finding of the present study is that cortical photothrombotic stroke gives rise to a persistent impairment in associative memory and learning, as well as in cognitive flexibility, up to 84 days after the initial stroke. Cognition, as assessed by a mouse touchscreen platform for the PAL and VDR tasks, showed significant and persistent deficits long-term following stroke. In contrast, motor impairment slightly improved over time after the cortical photothrombotic stroke. Secondly, we observed significant tissue and neuronal loss post-stroke that persisted for at least 84 days in both the peri-infarct region and in CA1 subregion of the hippocampus. We also investigated the involvement of neuroinflammation post-stroke and found that microglia activation persisted for up to 84 days, while astrogliosis peaked at 7 days and then decreased overtime. Lastly, we showed an increase in Aβ soluble oligomers in both regions following stroke, and a shift in the spatial distribution of these aggregates towards the cerebral vasculature. Collectively, these novel observations provide compelling evidence that stroke affects multiple cognitive domains and that these deficits are persistent, whereas motor function shows modest recovery overtime. Such cognitive deficits were associated with concomitant neuropathology in the hippocampus, including neuronal loss, activation of microglia and accumulation of Aβ, despite of this region being remote from the site of primary infarct.

We used a photothrombotic stroke model targeting the motor and somatosensory cortices of mice. As expected, cortical photothrombotic stroke resulted in a clear impairment of motor function at 7, 28 and 84 days post-stroke, which is consistent with previous studies [46]. Following stroke, mice showed preferential use of the unaffected forelimb and an increase in foot faults when using the impaired limb, with the greatest motor deficits observed on post-stroke days 7 (grid walk task) and 28 (paw asymmetry). At post-stroke day 84, we observed a modest spontaneous recovery of motor function. Concomitantly, Cresyl Violet staining showed peak tissue loss at day 7 post-stroke, before being reduced thereafter. We also observed a gradual loss of neurons in the peri-infarct area up to day 28, and then a gradual increase at day 84. This is consistent with the functional remapping of the sensorimotor cortex that we hypothesise to be responsible for the slight recovery in motor function seen in the chronic phase post-stroke in our model. Such remapping within the peri-infarct region is driven both by axonal sprouting of new connections and by the birth of new neurons, which migrate from the subventricular zone to the cortex of the peri-infarct region [47]. Indeed, neurogenesis can be stimulated by cerebral ischemia, with previous work demonstrating that the number of neural progenitor cells is significantly increased in the peri-infarct region at 3-7 days post-stroke in the photothrombotic model [48, 49]. Further, at 56 days following photothrombotic stroke, mice showed a functional reorganization of the sensory cortical maps for both the forelimb and hindlimbs, as well as a modest but significant increase in motor neuron sprouting has been observed [50]. This was accompanied by the recovery of performance on a skilled reaching task, although interestingly, in contrast to the current study, deficits on both the cylinder and grid-walking task remained evident, suggesting that different types of sensorimotor function may recover at different rates depending on stroke size and location [51].

Neuroinflammation is an important process that occurs in the brain after cerebral ischemia, encompassing the activation of astrocytes and microglia. This response is at first beneficial and necessary to promote brain repair; however, it becomes detrimental when it is prolonged [52-55]. In this study, we observed an intense astrogliosis response, as characterized by the excessive expression of GFAP, at 7 and 28 days post-injury in the peri-infarct region, which subsided by day 84. Indeed, astrogliosis is an early response in the days following stroke, which evolves to form the mature glial scar forms to wall off the infarcted tissue [56]. Next, we comprehensively assessed the alterations of microglial morphology using Iba-1 immunolabeling and complemented these results by analysing the expression levels of CD11b, which is a marker commonly used to label microglia but also myeloid cells. Our in-depth analysis of the microglial response revealed that microglial activation status peaked at 7 days post-stroke in the peri-infarct region, before shifting to a less activated state by day 84, a similar pattern to the observed astrocytic response. We observed a concomitant loss of neurons in the peri-infarct area up to day 28, and then a gradual increase at day 84. The close temporal correlation between the activation of astrocytes and microglia and neuronal loss highlights the potential importance of astroglial- and microglial-mediated neuroinflammatory responses as a modulator of neuronal survival. These results suggest that reduced neuroinflammation as well as brain tissue and neuronal recovery in the peri-infarct region over time most certainty contribute to the spontaneous motor recovery.

Next, we examined the long-term impact of cortical stroke on cognition. In our previous study, we demonstrated that our stroke model induced impairment in the ability of mice to discriminate between two images with a high degree of similarity at 14 days post-stroke [34]. Further, this photothrombotic stroke model has been reported to elicit long-term deficits in learning and memory, as assessed by the Morris water maze [57]. Critically, given that stroke affects a range of cognitive domains, and these effects are known to be persistent long-term [58, 59] we sought to further understand the devastating effects of stroke on cognition, by using a mouse touchscreen platform [60]. This mouse touchscreen platform is recognised to avoid some of the limitations associated with classical assessments. For instance, the "classical gold standard" Morris water maze is hampered by significant interpretational challenges, the aversive nature of the protocol, and shares limited resemblances with human cognitive assessments [40, 61, 62]. Specifically, in the current study, we used the translationally relevant mouse touchscreen platform to assess different cognitive domains. The PAL task assesses associative memory and learning domains [63]. This task has been extensively used in the clinical assessment of cognition [64], and the task available for rodents is analogous to the one used in clinical research [65]. On the other hand, the VDR task includes both visual discrimination and reversal learning [39, 66], with discrimination learning providing a measure of perceptual ability to discriminate between two stimuli, while reversal learning has been used to examine cognitive flexibility [39, 67, 68]. One of the critical variables that we were interested in evaluating in this study is whether the cognitive deficits observed at the subacute phase (7-28 day) would persist or further decline when mice were tested in the chronic phase (56-84 day). We observed a significant decrease in the percentage of correct trials in the subacute phase in stroked mice. Furthermore, when these mice were tested in the chronic phase months after stroke, we detected an even greater reduction in the percentage of correct trials in stroked mice compared to shams. While we observed modest spontaneous motor recovery after stroke in mice, a novel and important observation is that a stroke within the motor and somatosensory cortex resulted in persistent cognitive impairment (up to 84 days). Such progressive and persistent impairment in cognitive function mirrors that observed in stroke patients [8, 12, 69, 70]. For instance, Levine et al.

demonstrated that stroke was associated with long-term cognitive dysfunction over 6 years after the event [8].

Previous research has shown that the PAL task is dependent on the dorsal hippocampus [71], while the hippocampus is also known to play a role in the VDR task [72]. The hippocampus receives highly processed multi-modal sensory information from the cortex via its connections with the entorhinal cortex, making it a potential key site for the development of SND pathology [32]. Additionally, the hippocampus is also highly inter-connected with nuclei of the thalamus, such as the anterior and mediodorsal nuclei, which are known to play a critical role in cognitive function [33]. Given that the thalamus is known to be a key site for SND pathology, it is possible that Wallerian degeneration from the thalamus to the hippocampus may drive the development of SND in this area. Although, currently little is known about the importance of SND processes in the hippocampus long-term after stroke. Previous studies, including ours, have focused on other SND sites, such as the thalamus, or on earlier post-stroke time points [17, 18, 25, 27, 29]. In our recent study, we documented a reduction in NeuN-positive cells in the CA1 region at 14 days following stroke [34]. Based on this result, we hypothesised that this reduction in neurons in the hippocampus might be an indicator of the persistent cognitive deficits observed post-stroke. Indeed, with the findings of this study we have confirmed this hypothesis, demonstrating persistent neuronal loss at 28 and 84 days post-stroke in the CA1 sub-region of the hippocampus. The persistent loss of neurons over time in the CA1 subregion is a critical finding, due to the integral role that this region plays in cognitive processes such as learning and memory [73, 74]. Furthermore, although most strokes do not directly affect the hippocampus, it is well established that the CA1 sub-region of the hippocampus is more sensitive to hypoxia-ischemia insults and neurodegeneration than other areas of the brain [30, 31, 75]. Interestingly, we observed the DG sub-region of the hippocampus to be spared, which could be due to stimulation of neural cell proliferation within the DG after stroke [76]. Together these results support an important role for SND processes in the hippocampus and may contribute to the ongoing cognitive impairment observed after stroke.

There are several possible contributors to the observed persistent loss of CA1 neurons. We examined neuroinflammation in the hippocampus, observing a peak in reactive astrogliosis at 7 days post-stroke, which returned to basal levels by day 84 in the CA1 sub-region, similar pattern as observed in the peri-infarct region. These results suggest that astrocytes might play a role in neuroinflammation in the early stages post-stroke, but this effect is dampened in chronic phase following stroke. In contrast, microglial activation followed a different pattern, at least within the CA1 subregion of the hippocampus, with activated microglia observed to peak between day 7 and 28, and the activated morphology remaining at day 84 post-stroke. Together, these findings show that neuroinflammation driven by microglia lasts long-term after stroke, whereas the astrocytic response appears to resolve. Interestingly, in the hippocampus, microglial activation was already detectable by day 7 post-stroke. However, we did not observe hippocampal neuronal loss at that time point, suggesting that microglial activation might contribute to the delayed neuronal death within the hippocampus by creating a pro-inflammatory microenvironment, where microglial-induced neuroinflammation precedes neuronal loss. It is well described that brain injury and cerebral ischemia switch microglia into a prime state, where they have an increased pro-inflammatory response to secondary damage signals [77]. This is supported by previous experimental stroke studies demonstrating that chronic activation of microglia is detrimental to the survival of new hippocampal neurons and impairs cognition, whereas inhibition of microglial activation improves neurogenesis and cognitive performance [78, 79]. Together, this evidence suggests that a potential exaggerated and prolonged

microglial response might contribute to neuronal dysfunction and degeneration within the hippocampus, manifesting as post-stroke cognitive impairment.

Taken together, we have identified important differences between the processes occurring in the primary injury site (peri-infarct) and SND sites (hippocampus). In the peri-infarct region, neuronal loss and neuroinflammation peaked early after stroke and spontaneously recovered at later time points, which could explain the observed motor improvements. Contrary to this, in the hippocampus, a region remote from the primary infarct, neuronal loss and neuroinflammation persisted out to 84 days post-stroke, supporting our findings of long-term cognitive deficits after stroke.

Furthermore, previous studies have linked Aβ accumulation with cognitive impairment and neurodegenerative conditions [44, 45, 80]. Numerous clinical and experimental studies have now described that Aβ deposition occurs in the peri-infarct region [81] and the thalamus [82, 83] post-stroke, and that such accumulation of neurotoxic proteins is highly associated with cognitive impairment in stroke patients [45, 84, 85]. Indeed, we have recently reported increased levels of Aβ in the hippocampus at 14 days post-stroke [34]. In the current study we found significantly increased Aβ oligomerization in both the peri-infarct and hippocampal regions after stroke. Interestingly, we observed a consistent increase of the 56 kDa oligomer at all time points in both regions, in keeping with multiple studies which have suggested that these soluble Aβ oligomers, and not the plaques, are linked to cognitive decline in the context of Alzheimer's disease [45, 80]. There is emerging evidence suggesting that Aβ oligomers are responsible for neuronal loss after experimental stroke via an uncontrolled feedforward neurodegeneration loop [82, 86, 87]. Aβ oligomers released from ischemic cells can trigger pathological activation of microglia through various pathways, which in turn induce a pro-inflammatory and high oxidative stress microenvironment, both of which lead to neuronal death [88]. It should be noted that Aβ oligomers can also evoke pericyte-mediated constriction of cerebral capillaries, and cause cerebrovascular dysregulation [89]. In addition to our protein analyses, we assessed the spatial distribution of these Aβ oligomers using immunostaining. Strikingly, we observed that the distribution of Aβ seemed to slightly shift over time. At day 7 and 28 the Aβ adopted a scattered distribution in the brain parenchyma, whereas at 84 days post-stroke the Aβ was mainly accumulating around the cerebral vessels, although some Aβ remained also in the brain parenchyma. Aβ deposits around the cerebral vessels was observed in the peri-infarct region, and a lesser degree in the CA1 subregion of the hippocampus. Our results complement a previous study by Howe et al. which demonstrated that stroke induces increased perivascular deposition of Aβ, and this effect is aggravated in aged mice at 30 days post-injury [90]. Our findings suggest that Aβ oligomers are not merely a consequence of stroke, but also actively contribute to the damage of neurovascular unit and dysregulation of the brain waste clearance systems, leading to post-stroke cognitive impairment.

In conclusion, here we demonstrated that cortical photothrombotic stroke causes impairments in associative memory, learning and cognitive flexibility which persist for months after the initial cortical infarction. Additionally, our spatiotemporal analyses provide further critical insights regarding the cellular and molecular events leading to this impairment in cognition. We demonstrate that there is persistent neuronal loss in an area critical in cognition, the CA1 subregion of the hippocampus. Such neuronal loss and cognitive impairment was associated with persistent neuroinflammation and increased Aβ oligomerization that creates a hostile microenvironment for neuronal survival and proliferation, which come together to create a "perfect storm" of SND post-stroke. Our findings thus highlight the critical importance of microglia and Aβ as potential key mediators in the progression of secondary damage post-

stroke. Additionally, we observed a modest spontaneous recovery of the motor function during the chronic phase, which was linked to brain recovery processes occurring in the peri-infarct area. This may be drive spontaneous functional remapping of the peri-infarct region following stroke. This spatiotemporal study has clear advantages by tracking translationally relevant functional outcomes and associated neuropathological changes long-term after experimental stroke. Nevertheless, further research is required to fully elucidate the brain mechanisms that underlie the persistent cognitive deficits seen post-stroke, including how these are related to the development of SND. As such, therapeutic strategies targeting neuroinflammation and neurotoxic protein accumulation may be promising approaches to promote brain recovery and enhance functional outcomes post-stroke.

Acknowledgements
LKO, FRW and MN acknowledge ongoing support from NHMRC Centre for Research Excellence in Stroke Recovery and Rehabilitation. LKO and SSB acknowledge support from Research Advantage for ECR Higher Degree by Research (HDR) Scholarship and Greaves Family Postgraduate Scholarships in Medical Research (HMRI 1054). LKO acknowledge support from IBRO-APRC Travel & Short Stay Grant and Monash University Malaysia. LECP and RJT acknowledge support from NeuroSurgical Research Foundation and Perpetual.

Authors' contributions
SSB and LKO designed the research. SSB performed the majority of the experiments with assistance and contributions from RJH and LKO. The study was supervised by LKO, FRW and MN. SSB, RJH and LKO analysed the data. All authors contributed to interpretation of the results. SSB and LKO prepared the first draft of the manuscript. All authors provided critical review and editing of subsequent drafts of the manuscript. All authors have read and approved the final version of the manuscript.

Declaration of conflicting interests
The author(s) declared no potential conflicts of interest with respect to the research, authorship, and/or publication of this article.

Funding
This study was supported by Hunter Medical Research Institute (HMRI 896), Faculty of Health and Medicine Pilot Grant, Priority Research Centre for Stroke and Brain Injury Research Support Grant, Mary Costello Alzheimer's Pilot Grant and The University of Newcastle, Australia.

Supplementary material
Supplementary material for this paper can be found at the journal website: http://journals.sagepub.com/home/jcb

ORCID
Sonia Sanchez-Bezanilla https://orcid.org/0000-0003-2753-2691
Rebecca J. Hood https://orcid.org/0000-0001-7485-4883
Lyndsey E. Collins-Praino https://orcid.org/0000-0002-4380-7600
Renée J. Turner https://orcid.org/0000-0003-4278-8302
Michael Nilsson https://orcid.org/0000-0002-8826-1621
Lin Kooi Ong http://orcid.org/0000-0001-8664-0540

References

1. Mendis S. Stroke disability and rehabilitation of stroke: World Health Organization perspective. *Int J Stroke* 2013; 8: 3-4. DOI: 10.1111/j.1747-4949.2012.00969.x.
2. Katan M and Luft A. Global Burden of Stroke. *Semin Neurol* 2018; 38: 208-211. 2018/05/23. DOI: 10.1055/s-0038-1649503.
3. Feigin VL, Barker-Collo S, Parag V, et al. Auckland Stroke Outcomes Study. Part 1: Gender, stroke types, ethnicity, and functional outcomes 5 years poststroke. *Neurology* 2010; 75: 1597-1607. DOI: 10.1212/WNL.0b013e3181fb44b3.
4. Wolfe CDA, Crichton SL, Heuschmann PU, et al. Estimates of outcomes up to ten years after stroke: analysis from the prospective South London Stroke Register. *PLoS Med* 2011; 8: e1001033-e1001033. 2011/05/17. DOI: 10.1371/journal.pmed.1001033.
5. Schnitzler A, Woimant F, Tuppin P, et al. Prevalence of self-reported stroke and disability in the French adult population: a transversal study. *PLoS One* 2014; 9: e115375-e115375. DOI: 10.1371/journal.pone.0115375.
6. Hendricks HT, van Limbeek J, Geurts AC, et al. Motor recovery after stroke: a systematic review of the literature. *Archives of physical medicine and rehabilitation* 2002; 83: 1629-1637. 2002/11/08. DOI: 10.1053/apmr.2002.35473.
7. Cramer SC, Nelles G, Benson RR, et al. A functional MRI study of subjects recovered from hemiparetic stroke. *Stroke* 1997; 28: 2518-2527. DOI: 10.1161/01.str.28.12.2518.
8. Levine DA, Galecki AT, Langa KM, et al. Trajectory of Cognitive Decline After Incident Stroke. *JAMA* 2015; 314: 41-51. DOI: 10.1001/jama.2015.6968.
9. Weinstein G, Preis SR, Beiser AS, et al. Cognitive performance after stroke--the Framingham Heart Study. *Int J Stroke* 2014; 9 Suppl A100: 48-54. 2014/04/30. DOI: 10.1111/ijs.12275.
10. Sun J-H, Tan L and Yu J-T. Post-stroke cognitive impairment: epidemiology, mechanisms and management. *Ann Transl Med* 2014; 2: 80-80. DOI: 10.3978/j.issn.2305-5839.2014.08.05.
11. Al-Qazzaz NK, Ali SH, Ahmad SA, et al. Cognitive impairment and memory dysfunction after a stroke diagnosis: a post-stroke memory assessment. *Neuropsychiatric disease and treatment* 2014; 10: 1677-1691. 2014/09/18. DOI: 10.2147/ndt.S67184.
12. Mijajlović MD, Pavlović A, Brainin M, et al. Post-stroke dementia - a comprehensive review. *BMC Med* 2017; 15: 11-11. DOI: 10.1186/s12916-017-0779-7.
13. Pendlebury ST and Rothwell PM. Incidence and prevalence of dementia associated with transient ischaemic attack and stroke: analysis of the population-based Oxford Vascular Study. *Lancet Neurol* 2019; 18: 248-258. 2019/02/21. DOI: 10.1016/s1474-4422(18)30442-3.
14. Block F, Dihné M and Loos M. Inflammation in areas of remote changes following focal brain lesion. *Prog Neurobiol* 2005; 75: 342-365. DOI: 10.1016/j.pneurobio.2005.03.004.
15. Zhang J, Zhang Y, Xing S, et al. Secondary neurodegeneration in remote regions after focal cerebral infarction: a new target for stroke management? *Stroke* 2012; 43: 1700-1705. 2012/04/05. DOI: 10.1161/STROKEAHA.111.632448.
16. Gerhard A, Schwarz J, Myers R, et al. Evolution of microglial activation in patients after ischemic stroke: a [11C](R)-PK11195 PET study. *Neuroimage* 2005; 24: 591-595. 2004/11/18. DOI: 10.1016/j.neuroimage.2004.09.034.
17. Wei L, Ying D-J, Cui L, et al. Necrosis, apoptosis and hybrid death in the cortex and thalamus after barrel cortex ischemia in rats. *Brain Res* 2004; 1022: 54-61. DOI: 10.1016/j.brainres.2004.06.080.
18. Dihné M, Grommes C, Lutzenburg M, et al. Different mechanisms of secondary neuronal damage in thalamic nuclei after focal cerebral ischemia in rats. *Stroke* 2002; 33: 3006-3011. DOI: 10.1161/01.str.0000039406.64644.cb.
19. Ogawa T, Yoshida Y, Okudera T, et al. Secondary thalamic degeneration after cerebral infarction in the middle cerebral artery distribution: evaluation with MR imaging. *Radiology* 1997; 204: 255-262. DOI: 10.1148/radiology.204.1.9205256.
20. Nakane M, Tamura A, Sasaki Y, et al. MRI of secondary changes in the thalamus following a cerebral infarct. *Neuroradiology* 2002; 44: 915-920. 2002/09/10. DOI: 10.1007/s00234-002-0846-3.

21. Nakane M, Teraoka A, Asato R, et al. Degeneration of the ipsilateral substantia nigra following cerebral infarction in the striatum. *Stroke* 1992; 23: 328-332. DOI: 10.1161/01.str.23.3.328.
22. Brodtmann A, Khlif MS, Egorova N, et al. Dynamic Regional Brain Atrophy Rates in the First Year After Ischemic Stroke. *Stroke* 2020: Strokeaha120030256. DOI: 10.1161/strokeaha.120.030256.
23. Chen Y, Garcia GE, Huang W, et al. The involvement of secondary neuronal damage in the development of neuropsychiatric disorders following brain insults. *Front Neurol* 2014; 5: 22-22. DOI: 10.3389/fneur.2014.00022.
24. Fernández-Andújar M, Doornink F, Dacosta-Aguayo R, et al. Remote thalamic microstructural abnormalities related to cognitive function in ischemic stroke patients. *Neuropsychology* 2014; 28: 984-996. 2014/06/02. DOI: 10.1037/neu0000087.
25. Iizuka H, Sakatani K and Young W. Neural damage in the rat thalamus after cortical infarcts. *Stroke* 1990; 21: 790-794. DOI: 10.1161/01.str.21.5.790.
26. Kluge MG, Abdolhoseini M, Zalewska K, et al. Spatiotemporal analysis of impaired microglia process movement at sites of secondary neurodegeneration post-stroke. *J Cereb Blood Flow Metab* 2019; 39: 2456-2470. 2018/09/11. DOI: 10.1177/0271678X18797346.
27. Kluge MG, Kracht L, Abdolhoseini M, et al. Impaired microglia process dynamics post-stroke are specific to sites of secondary neurodegeneration. *Glia* 2017; 65: 1885-1899. 2017/08/24. DOI: 10.1002/glia.23201.
28. Nakajima M, Hirano T, Terasaki T, et al. Signal change of the substantia nigra on diffusion-weighted imaging following striatal infarction. *Intern Med* 2010; 49: 65-68. 2010/01/01. DOI: 10.2169/internalmedicine.49.2694.
29. Zalewska K, Pietrogrande G, Ong LK, et al. Sustained administration of corticosterone at stress-like levels after stroke suppressed glial reactivity at sites of thalamic secondary neurodegeneration. *Brain Behav Immun* 2018; 69: 210-222. 2017/11/21. DOI: 10.1016/j.bbi.2017.11.014.
30. Wang W, Redecker C, Bidmon H-J, et al. Delayed neuronal death and damage of GDNF family receptors in CA1 following focal cerebral ischemia. *Brain Res* 2004; 1023: 92-101. DOI: 10.1016/j.brainres.2004.07.034.
31. Gemmell E, Bosomworth H, Allan L, et al. Hippocampal neuronal atrophy and cognitive function in delayed poststroke and aging-related dementias. *Stroke* 2012; 43: 808-814. 2011/12/31. DOI: 10.1161/strokeaha.111.636498.
32. Canto CB, Wouterlood FG and Witter MP. What does the anatomical organization of the entorhinal cortex tell us? *Neural plasticity* 2008; 2008: 381243. 2008/09/05. DOI: 10.1155/2008/381243.
33. Wolff M and Vann SD. The Cognitive Thalamus as a Gateway to Mental Representations. *The Journal of neuroscience : the official journal of the Society for Neuroscience* 2019; 39: 3-14. 2018/11/06. DOI: 10.1523/jneurosci.0479-18.2018.
34. Sanchez-Bezanilla S, TeBay C, Nilsson M, et al. Visual discrimination impairment after experimental stroke is associated with disturbances in the polarization of the astrocytic aquaporin-4 and increased accumulation of neurotoxic proteins. *Exp Neurol* 2019; 318: 232-243. 2019/05/09. DOI: 10.1016/j.expneurol.2019.05.001.
35. Pietrogrande G, Zalewska K, Zhao Z, et al. Low oxygen post conditioning prevents thalamic secondary neuronal loss caused by excitotoxicity after cortical stroke. *Sci Rep* 2019; 9: 4841. 2019/03/21. DOI: 10.1038/s41598-019-39493-8.
36. Zhao Z, Ong LK, Johnson S, et al. Chronic stress induced disruption of the peri-infarct neurovascular unit following experimentally induced photothrombotic stroke. *J Cereb Blood Flow Metab* 2017; 37: 3709-3724. 2017/03/18. DOI: 10.1177/0271678x17696100.
37. Sanchez-Bezanilla S, Nilsson M, Walker FR, et al. Can We Use 2,3,5-Triphenyltetrazolium Chloride-Stained Brain Slices for Other Purposes? The Application of Western Blotting. *Frontiers in molecular neuroscience* 2019; 12: 181. 2019/08/17. DOI: 10.3389/fnmol.2019.00181.
38. Ong LK, Chow WZ, TeBay C, et al. Growth Hormone Improves Cognitive Function After Experimental Stroke. *Stroke* 2018; 49: 1257-1266. 2018/04/11. DOI: 10.1161/strokeaha.117.020557.

39. Horner AE, Heath CJ, Hvoslef-Eide M, et al. The touchscreen operant platform for testing learning and memory in rats and mice. *Nat Protoc* 2013; 8: 1961-1984. 2013/09/19. DOI: 10.1038/nprot.2013.122.
40. Schaar KL, Brenneman MM and Savitz SI. Functional assessments in the rodent stroke model. *Exp Transl Stroke Med* 2010; 2: 13-13. DOI: 10.1186/2040-7378-2-13.
41. Sanchez-Bezanilla S, Åberg ND, Crock P, et al. Growth Hormone Treatment Promotes Remote Hippocampal Plasticity after Experimental Cortical Stroke. *International journal of molecular sciences* 2020; 21 2020/07/02. DOI: 10.3390/ijms21124563.
42. Abdolhoseini M, Kluge MG, Walker FR, et al. Segmentation, Tracing, and Quantification of Microglial Cells from 3D Image Stacks. *Sci Rep* 2019; 9: 8557. 2019/06/14. DOI: 10.1038/s41598-019-44917-6.
43. Sanchez-Bezanilla S, Åberg ND, Crock P, et al. Growth Hormone Promotes Motor Function after Experimental Stroke and Enhances Recovery-Promoting Mechanisms within the Peri-Infarct Area. *International journal of molecular sciences* 2020; 21 2020/01/23. DOI: 10.3390/ijms21020606.
44. Haass C and Selkoe DJ. Soluble protein oligomers in neurodegeneration: lessons from the Alzheimer's amyloid beta-peptide. *Nat Rev Mol Cell Biol* 2007; 8: 101-112. DOI: 10.1038/nrm2101.
45. Lesné SE, Sherman MA, Grant M, et al. Brain amyloid-β oligomers in ageing and Alzheimer's disease. *Brain* 2013; 136: 1383-1398. 2013/04/09. DOI: 10.1093/brain/awt062.
46. Aswendt M, Pallast N, Wieters F, et al. Lesion Size- and Location-Dependent Recruitment of Contralesional Thalamus and Motor Cortex Facilitates Recovery after Stroke in Mice. *Transl Stroke Res* 2020 2020/03/14. DOI: 10.1007/s12975-020-00802-3.
47. Carmichael ST. Cellular and molecular mechanisms of neural repair after stroke: making waves. *Annals of neurology* 2006; 59: 735-742. 2006/04/25. DOI: 10.1002/ana.20845.
48. Kang SS, Kook JH, Hwang S, et al. Inhibition of matrix metalloproteinase-9 attenuated neural progenitor cell migration after photothrombotic ischemia. *Brain Res* 2008; 1228: 20-26. 2008/07/12. DOI: 10.1016/j.brainres.2008.06.056.
49. Li H, Zhang N, Lin HY, et al. Histological, cellular and behavioral assessments of stroke outcomes after photothrombosis-induced ischemia in adult mice. *BMC neuroscience* 2014; 15: 58. 2014/06/03. DOI: 10.1186/1471-2202-15-58.
50. Clarkson AN, López-Valdés HE, Overman JJ, et al. Multimodal examination of structural and functional remapping in the mouse photothrombotic stroke model. *J Cereb Blood Flow Metab* 2013; 33: 716-723. 2013/02/07. DOI: 10.1038/jcbfm.2013.7.
51. Jeffers MS, Touvykine B, Ripley A, et al. Poststroke Impairment and Recovery Are Predicted by Task-Specific Regionalization of Injury. *The Journal of neuroscience : the official journal of the Society for Neuroscience* 2020; 40: 6082-6097. 2020/07/02. DOI: 10.1523/jneurosci.0057-20.2020.
52. Ceulemans A-G, Zgavc T, Kooijman R, et al. The dual role of the neuroinflammatory response after ischemic stroke: modulatory effects of hypothermia. *J Neuroinflammation* 2010; 7: 74-74. DOI: 10.1186/1742-2094-7-74.
53. Lakhan SE, Kirchgessner A and Hofer M. Inflammatory mechanisms in ischemic stroke: therapeutic approaches. *J Transl Med* 2009; 7: 97-97. DOI: 10.1186/1479-5876-7-97.
54. Huang J, Upadhyay UM and Tamargo RJ. Inflammation in stroke and focal cerebral ischemia. *Surg Neurol* 2006; 66: 232-245. DOI: 10.1016/j.surneu.2005.12.028.
55. Wang Q, Tang XN and Yenari MA. The inflammatory response in stroke. *J Neuroimmunol* 2007; 184: 53-68. 2006/12/26. DOI: 10.1016/j.jneuroim.2006.11.014.
56. Choudhury GR and Ding S. Reactive astrocytes and therapeutic potential in focal ischemic stroke. *Neurobiology of disease* 2016; 85: 234-244. 2015/05/20. DOI: 10.1016/j.nbd.2015.05.003.
57. Schmidt A, Diederich K, Strecker JK, et al. Progressive cognitive deficits in a mouse model of recurrent photothrombotic stroke. *Stroke* 2015; 46: 1127-1131. 2015/03/07. DOI: 10.1161/strokeaha.115.008905.

58. Schaapsmeerders P, Maaijwee NAM, van Dijk EJ, et al. Long-term cognitive impairment after first-ever ischemic stroke in young adults. *Stroke* 2013; 44: 1621-1628. 2013/05/07. DOI: 10.1161/STROKEAHA.111.000792.
59. Mellon L, Brewer L, Hall P, et al. Cognitive impairment six months after ischaemic stroke: a profile from the ASPIRE-S study. *BMC Neurol* 2015; 15: 31-31. DOI: 10.1186/s12883-015-0288-2.
60. Bussey TJ, Padain TL, Skillings EA, et al. The touchscreen cognitive testing method for rodents: how to get the best out of your rat. *Learn Mem* 2008; 15: 516-523. DOI: 10.1101/lm.987808.
61. Balkaya MG, Trueman RC, Boltze J, et al. Behavioral outcome measures to improve experimental stroke research. *Behav Brain Res* 2018; 352: 161-171. 2017/07/29. DOI: 10.1016/j.bbr.2017.07.039.
62. Shepherd A, Tyebji S, Hannan AJ, et al. Translational Assays for Assessment of Cognition in Rodent Models of Alzheimer's Disease and Dementia. *J Mol Neurosci* 2016; 60: 371-382. 2016/09/16. DOI: 10.1007/s12031-016-0837-1.
63. Kim CH, Heath CJ, Kent BA, et al. The role of the dorsal hippocampus in two versions of the touchscreen automated paired associates learning (PAL) task for mice. *Psychopharmacology (Berl)* 2015; 232: 3899-3910. 2015/05/13. DOI: 10.1007/s00213-015-3949-3.
64. Barnett JH, Blackwell AD, Sahakian BJ, et al. The Paired Associates Learning (PAL) Test: 30 Years of CANTAB Translational Neuroscience from Laboratory to Bedside in Dementia Research. *Curr Top Behav Neurosci* 2016; 28: 449-474. DOI: 10.1007/7854_2015_5001.
65. Nithianantharajah J, McKechanie AG, Stewart TJ, et al. Bridging the translational divide: identical cognitive touchscreen testing in mice and humans carrying mutations in a disease-relevant homologous gene. *Sci Rep* 2015; 5: 14613-14613. DOI: 10.1038/srep14613.
66. Turner KM, Simpson CG and Burne THJ. BALB/c Mice Can Learn Touchscreen Visual Discrimination and Reversal Tasks Faster than C57BL/6 Mice. *Front Behav Neurosci* 2017; 11: 16-16. DOI: 10.3389/fnbeh.2017.00016.
67. Brigman JL, Graybeal C and Holmes A. Predictably irrational: assaying cognitive inflexibility in mouse models of schizophrenia. *Front Neurosci* 2010; 4: 13. DOI: 10.3389/neuro.01.013.2010.
68. Graybeal C, Bachu M, Mozhui K, et al. Strains and stressors: an analysis of touchscreen learning in genetically diverse mouse strains. *PLoS One* 2014; 9: e87745-e87745. DOI: 10.1371/journal.pone.0087745.
69. Pendlebury ST and Rothwell PM. Prevalence, incidence, and factors associated with pre-stroke and post-stroke dementia: a systematic review and meta-analysis. *Lancet Neurol* 2009; 8: 1006-1018. 2009/09/24. DOI: 10.1016/S1474-4422(09)70236-4.
70. Gorelick PB, Scuteri A, Black SE, et al. Vascular contributions to cognitive impairment and dementia: a statement for healthcare professionals from the american heart association/american stroke association. *Stroke* 2011; 42: 2672-2713. 2011/07/21. DOI: 10.1161/STR.0b013e3182299496.
71. Kim M, Kwak C, Yu N-K, et al. Optimization of the touchscreen paired-associate learning (PAL) task for mice and its dorsal hippocampal dependency. *Animal Cells and Systems* 2016; 20: 229-236. DOI: 10.1080/19768354.2016.1221855.
72. Vilà-Balló A, Mas-Herrero E, Ripollés P, et al. Unraveling the Role of the Hippocampus in Reversal Learning. *The Journal of neuroscience : the official journal of the Society for Neuroscience* 2017; 37: 6686-6697. 2017/06/09. DOI: 10.1523/jneurosci.3212-16.2017.
73. Ward R, Valenzuela JP, Li W, et al. Poststroke cognitive impairment and hippocampal neurovascular remodeling: the impact of diabetes and sex. *Am J Physiol Heart Circ Physiol* 2018; 315: H1402-H1413. 2018/08/17. DOI: 10.1152/ajpheart.00390.2018.
74. Jarrard LE. On the role of the hippocampus in learning and memory in the rat. *Behav Neural Biol* 1993; 60: 9-26. DOI: 10.1016/0163-1047(93)90664-4.
75. Chen J, Zhu RL, Nakayama M, et al. Expression of the apoptosis-effector gene, Bax, is up-regulated in vulnerable hippocampal CA1 neurons following global ischemia. *J Neurochem* 1996; 67: 64-71. DOI: 10.1046/j.1471-4159.1996.67010064.x.

76. Lichtenwalner RJ and Parent JM. Adult neurogenesis and the ischemic forebrain. *J Cereb Blood Flow Metab* 2006; 26: 1-20. 2005/06/17. DOI: 10.1038/sj.jcbfm.9600170.
77. Li JW, Zong Y, Cao XP, et al. Microglial priming in Alzheimer's disease. *Ann Transl Med* 2018; 6: 176. 2018/06/29. DOI: 10.21037/atm.2018.04.22.
78. Takamura R, Watamura N, Nikkuni M, et al. All-trans retinoic acid improved impaired proliferation of neural stem cells and suppressed microglial activation in the hippocampus in an Alzheimer's mouse model. *Journal of neuroscience research* 2017; 95: 897-906. 2016/07/23. DOI: 10.1002/jnr.23843.
79. Liu Z, Fan Y, Won SJ, et al. Chronic treatment with minocycline preserves adult new neurons and reduces functional impairment after focal cerebral ischemia. *Stroke* 2007; 38: 146-152. 2006/11/24. DOI: 10.1161/01.STR.0000251791.64910.cd.
80. Lesné S, Koh MT, Kotilinek L, et al. A specific amyloid-beta protein assembly in the brain impairs memory. *Nature* 2006; 440: 352-357. DOI: 10.1038/nature04533.
81. Garcia-Alloza M, Gregory J, Kuchibhotla KV, et al. Cerebrovascular lesions induce transient β-amyloid deposition. *Brain* 2011; 134: 3697-3707. 2011/11/26. DOI: 10.1093/brain/awr300.
82. Ong LK, Walker FR and Nilsson M. Is Stroke a Neurodegenerative Condition? A Critical Review of Secondary Neurodegeneration and Amyloid-beta Accumulation after Stroke. *AIMS Medical Science* 2017; 4: 1-16. DOI: 10.3934/medsci.2017.1.1.
83. van Groen T, Puurunen K, Mäki H-M, et al. Transformation of diffuse beta-amyloid precursor protein and beta-amyloid deposits to plaques in the thalamus after transient occlusion of the middle cerebral artery in rats. *Stroke* 2005; 36: 1551-1556. 2005/06/02. DOI: 10.1161/01.STR.0000169933.88903.cf.
84. Liu W, Wong A, Au L, et al. Influence of Amyloid-β on Cognitive Decline After Stroke/Transient Ischemic Attack: Three-Year Longitudinal Study. *Stroke* 2015; 46: 3074-3080. 2015/09/17. DOI: 10.1161/STROKEAHA.115.010449.
85. Popa-Wagner A, Schröder E, Walker LC, et al. beta-Amyloid precursor protein and ss-amyloid peptide immunoreactivity in the rat brain after middle cerebral artery occlusion: effect of age. *Stroke* 1998; 29: 2196-2202. DOI: 10.1161/01.str.29.10.2196.
86. Martins AH, Zayas-Santiago A, Ferrer-Acosta Y, et al. Accumulation of Amyloid Beta (Aβ) Peptide on Blood Vessel Walls in the Damaged Brain after Transient Middle Cerebral Artery Occlusion. *Biomolecules* 2019; 9 2019/08/11. DOI: 10.3390/biom9080350.
87. Ong LK, Zhao Z, Kluge M, et al. Chronic stress exposure following photothrombotic stroke is associated with increased levels of Amyloid beta accumulation and altered oligomerisation at sites of thalamic secondary neurodegeneration in mice. *J Cereb Blood Flow Metab* 2017; 37: 1338-1348. 2016/06/28. DOI: 10.1177/0271678x16654920.
88. Glass CK, Saijo K, Winner B, et al. Mechanisms underlying inflammation in neurodegeneration. *Cell* 2010; 140: 918-934. 2010/03/23. DOI: 10.1016/j.cell.2010.02.016.
89. Nortley R, Korte N, Izquierdo P, et al. Amyloid β oligomers constrict human capillaries in Alzheimer's disease via signaling to pericytes. *Science (New York, NY)* 2019; 365 2019/06/22. DOI: 10.1126/science.aav9518.
90. Howe MD, Atadja LA, Furr JW, et al. Fibronectin induces the perivascular deposition of cerebrospinal fluid-derived amyloid-β in aging and after stroke. *Neurobiol Aging* 2018; 72: 1-13. 2018/08/09. DOI: 10.1016/j.neurobiolaging.2018.07.019.

Figure legends

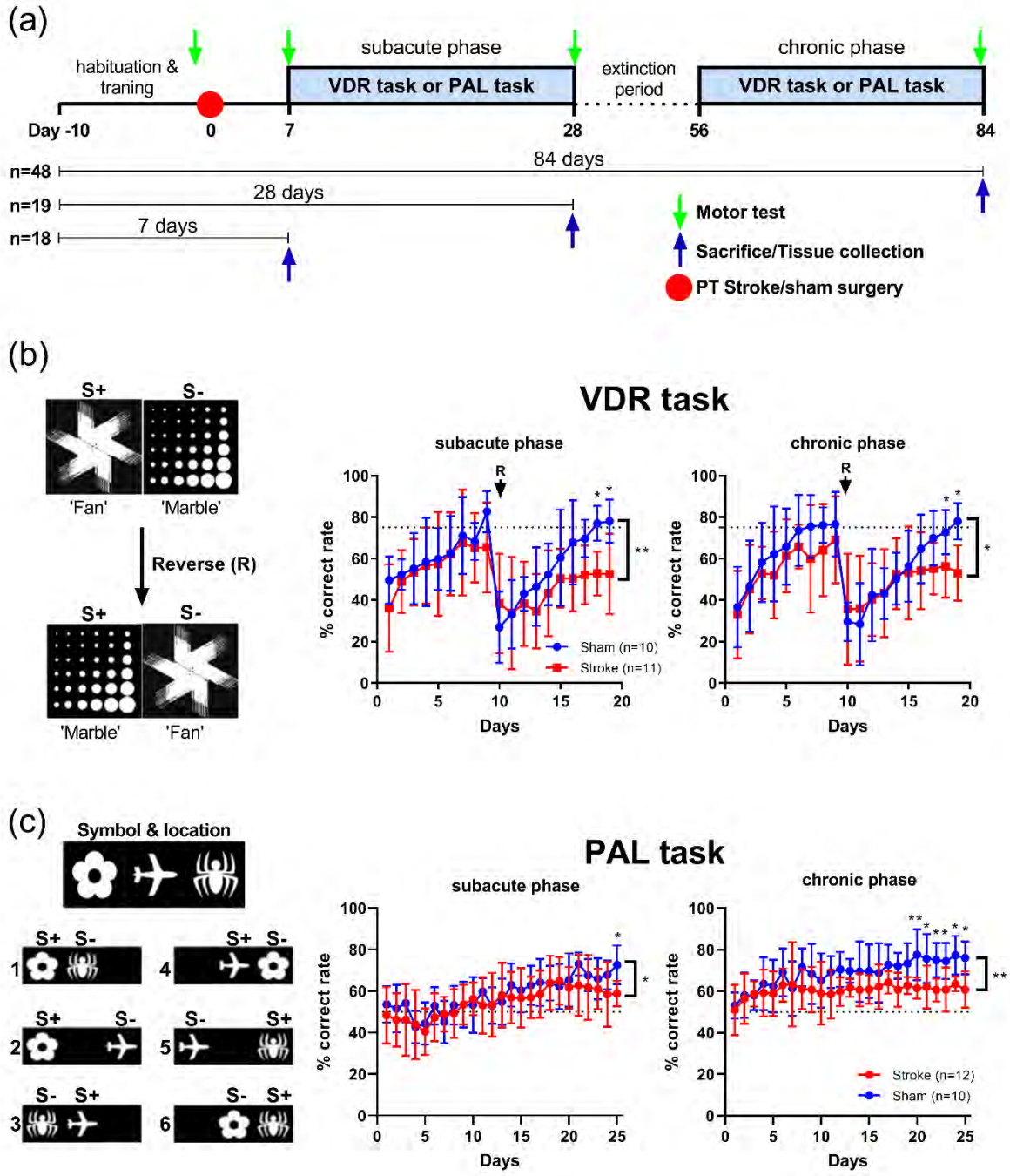

Figure 1. Cortical stroke impairs cognitive function. (A) Experimental design timeline. (B) First cohort of mice underwent assessment on a visual discrimination reversal (VDR) task during both the earlier (sub-acute phase) and later (chronic phase) stages post-stroke. We found a significant decrease in % correct responses in stroked mice compared to sham both in the subacute and chronic phase. (C) Second cohort of mice was assessed on the paired-associate learning (PAL) task in an earlier stage post-stroke (subacute phase) and at a later stage (chronic phase). We found a significant decrease in the % correct responses in stroked mice compared to shams, both in the sub-acute and chronic phases following stroke. Mean±SD (two-way ANOVA and Sidak's multiple comparisons). *p < 0.05; **p < 0.01. PT = photothrombotic

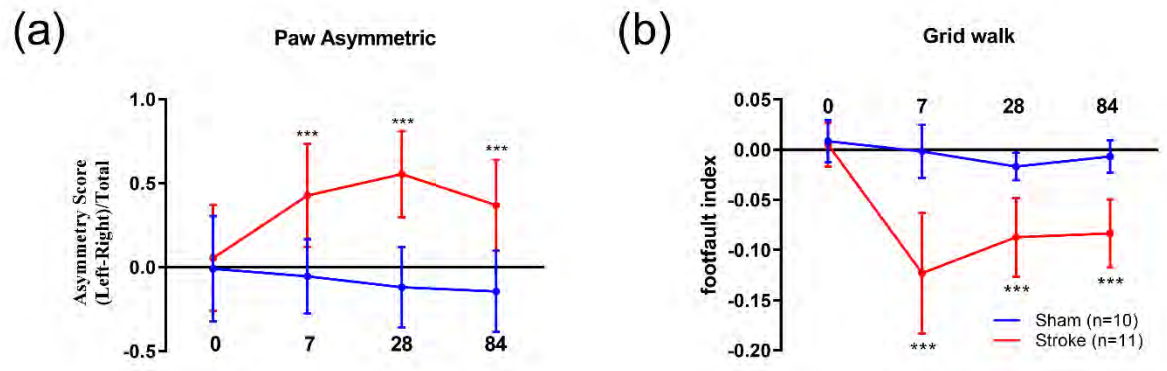

Figure 2. Cortical stroke impairs motor function. (A) Locomotor asymmetry was evaluated at baseline (one day before stroke induction) and at 7, 28 and 84 days post-stroke using the cylinder test. (B) Foot faults were also evaluated using the grid walk test. Stroked mice demonstrated significant deficits in both tests compared to shams, with a slight (non-significant) recovery over time. Mean±SD (two-way ANOVA and Sidak's multiple comparisons). ***$p < 0.001$.

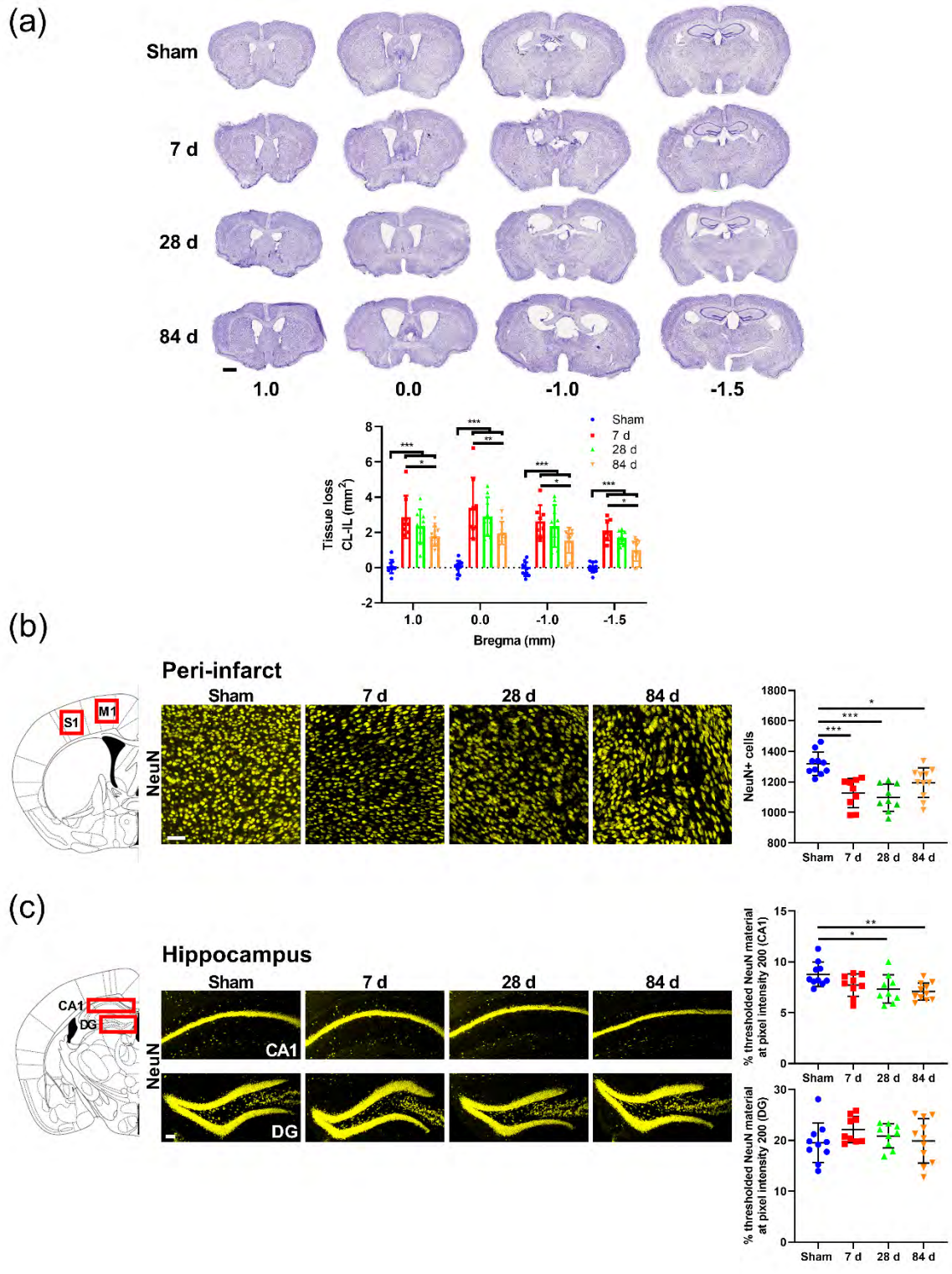

Figure 3. Cortical stroke induces neuronal loss within the peri-infarct area and hippocampus. (A) Representative images of Cresyl violet staining at Bregma 1.0, 0.0, -1.0, -1.5 mm. Tissue loss was calculated as contralateral (CL) hemisphere area−ipsilateral (IL) hemisphere area. Stroke significantly increased tissue loss at all Bregma levels (mm^2). (B) Representative immunofluorescence labelling for NeuN in the peri-infarct. Left panel: red squares indicate the location of motor (M1) and sensory cortex (S1) examined. Right panels: higher magnification images (scale bar=50 μm). (C) Representative immunofluorescence labelling for NeuN in the

hippocampus. Left panel: red squares indicate the location of CA1 and dentate gyrus (DG) examined. Right panels: higher magnification images (scale bar=100 μm). Mean±SD (Two-way ANOVA and Turkey's multiple comparison test). *p < 0.05; **p < 0.01; ***p < 0.001.

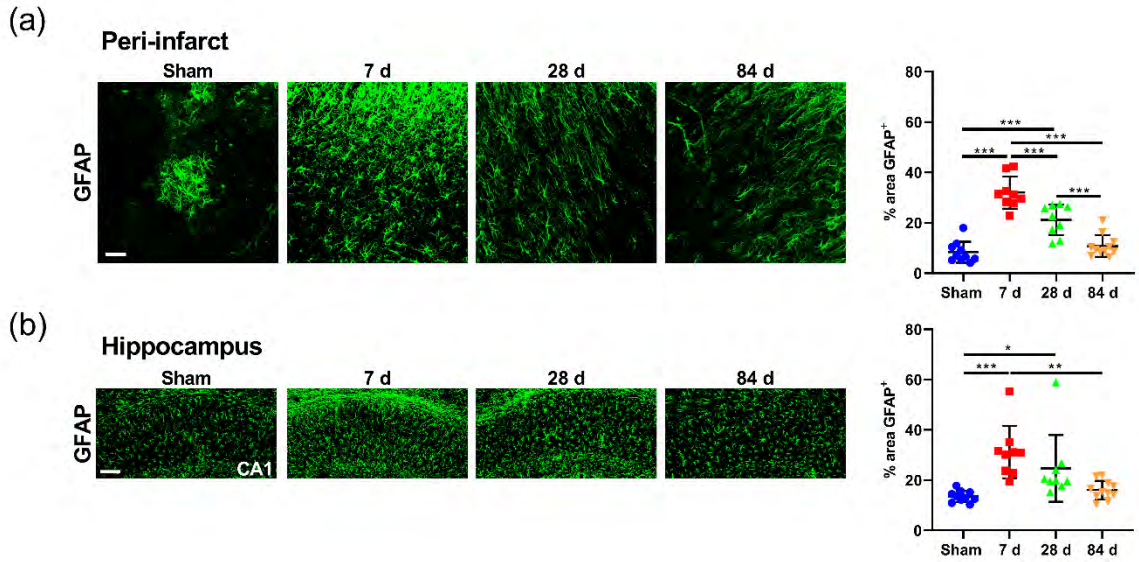

Figure 4. Cortical stroke promotes astrogliosis. (A) Representative immunofluorescence images of peri-infarct area labelled with GFAP (scale bar=50 μm) and quantification of reactive astrogliosis (% area of GFAP+). (B) Representative immunofluorescence images of the CA1 region of the hippocampus labelled with GFAP (scale bar=100 μm) and quantification of reactive astrogliosis. Reactive astrogliosis peaked at 7 days in both regions, which returned to basal levels by day 84. Mean±SD (Two-way ANOVA and Turkey's multiple comparison test). *p < 0.05; **p < 0.01; ***p < 0.001.

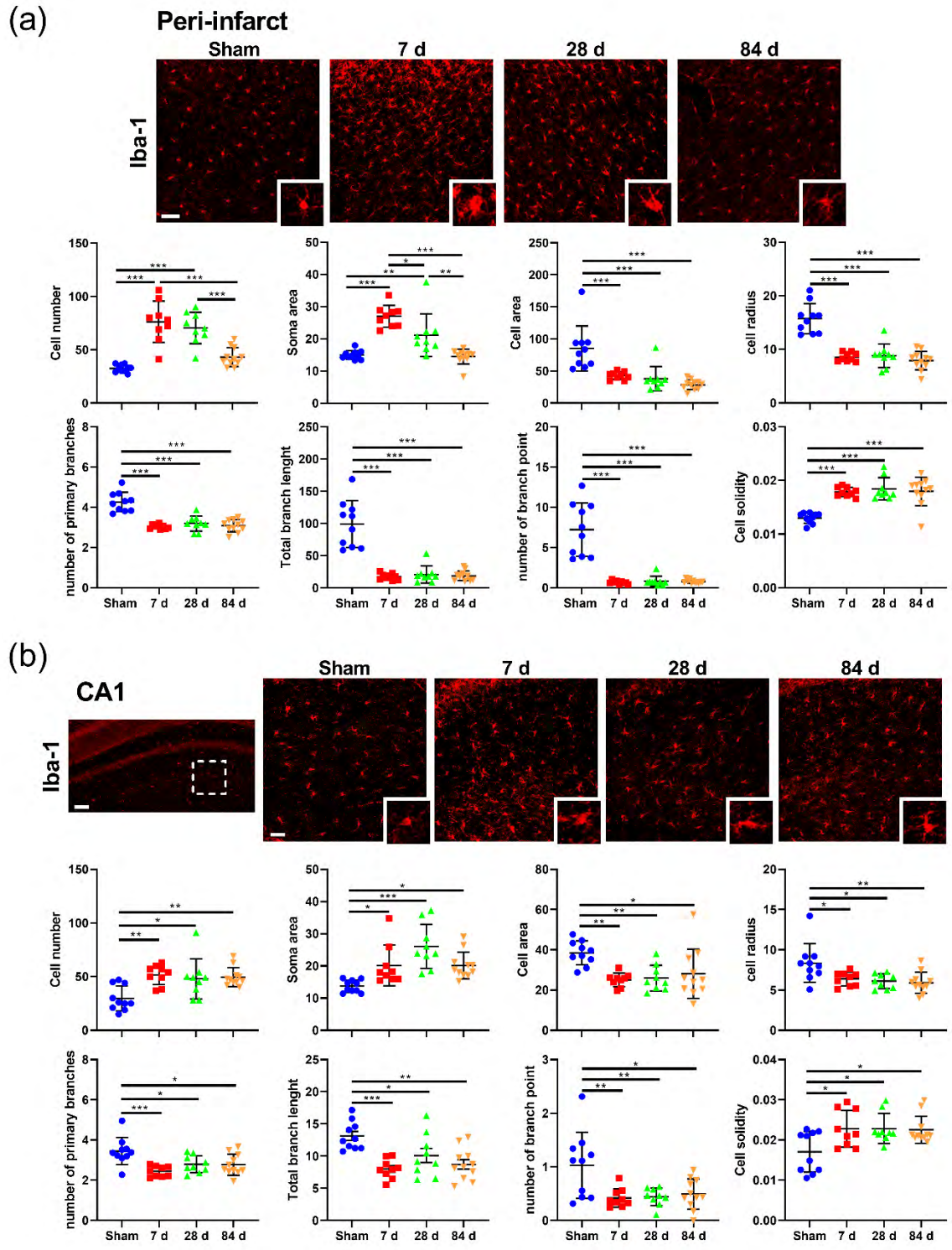

Figure 5. Cortical stroke induces microglial activation (A) Representative immunofluorescence images of the peri-infarct region and quantification of microglia morphology over time (scale bar=50 µm). (B) Representative immunofluorescence images of the CA1 region of the hippocampus and quantification of microglia morphology over time (scale bar=100 µm; scale bar of magnification=50 µm). White dotted square represents the area of morphological analysis. Mean±SD (Two-way ANOVA and Turkey's multiple comparison test). *p < 0.05; **p < 0.01; ***p < 0.001.

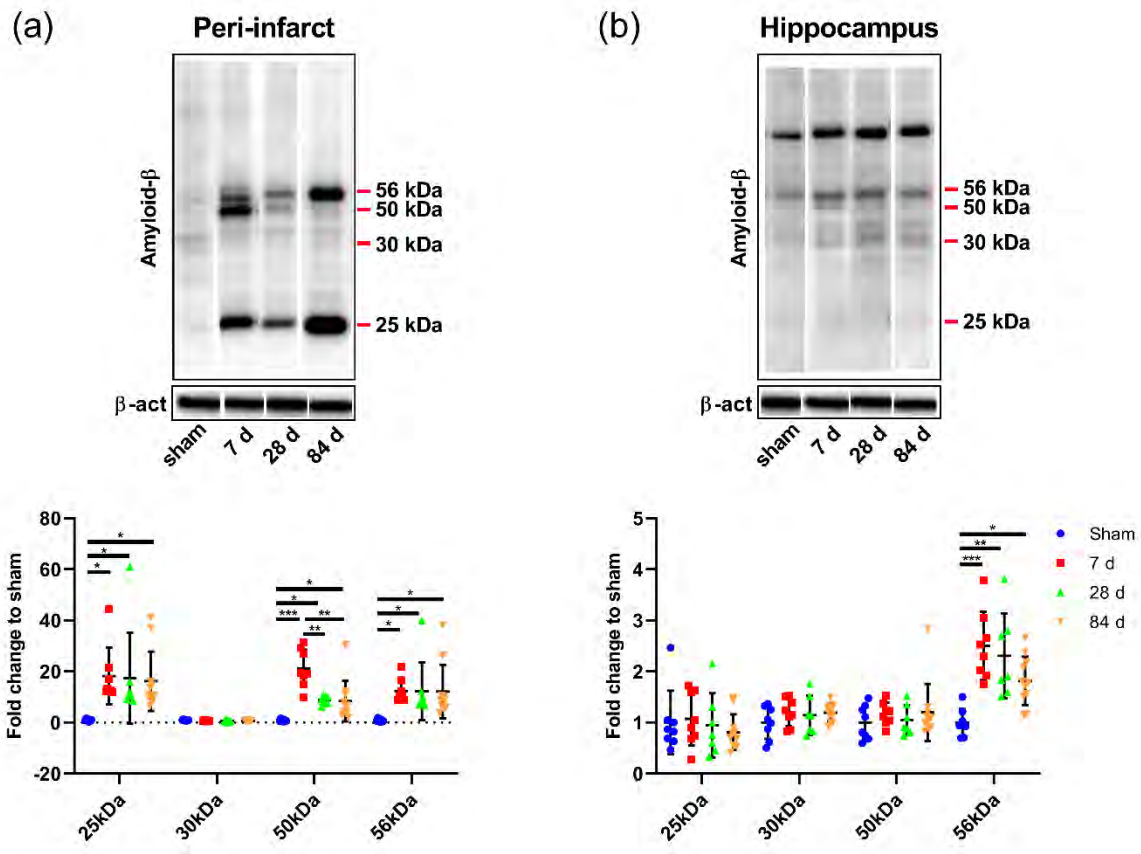

Figure 6. Stroke leads to amyloid-β (Aβ) oligomerization. Our analyses focused on different molecular weight oligomers (25 kDa, 30 kDa, 50 kDa and 56 kDa). (A) Representative western blot and quantification of Aβ expression profile within the peri-infarct region. Stroke leads to significant increase in Aβ 25 kDa, 50 kDa and 56 kDa at 7, 28 and 84 days. (B) Representative western blot and quantification of Aβ expression profile within the hippocampus. Stroke leads to significant increase in only Aβ 56 kDa at 7, 28 and 84 days. Mean±SD (Two-way ANOVA and Turkey's multiple comparison test). *$p < 0.05$; **$p < 0.01$; ***$p < 0.001$.

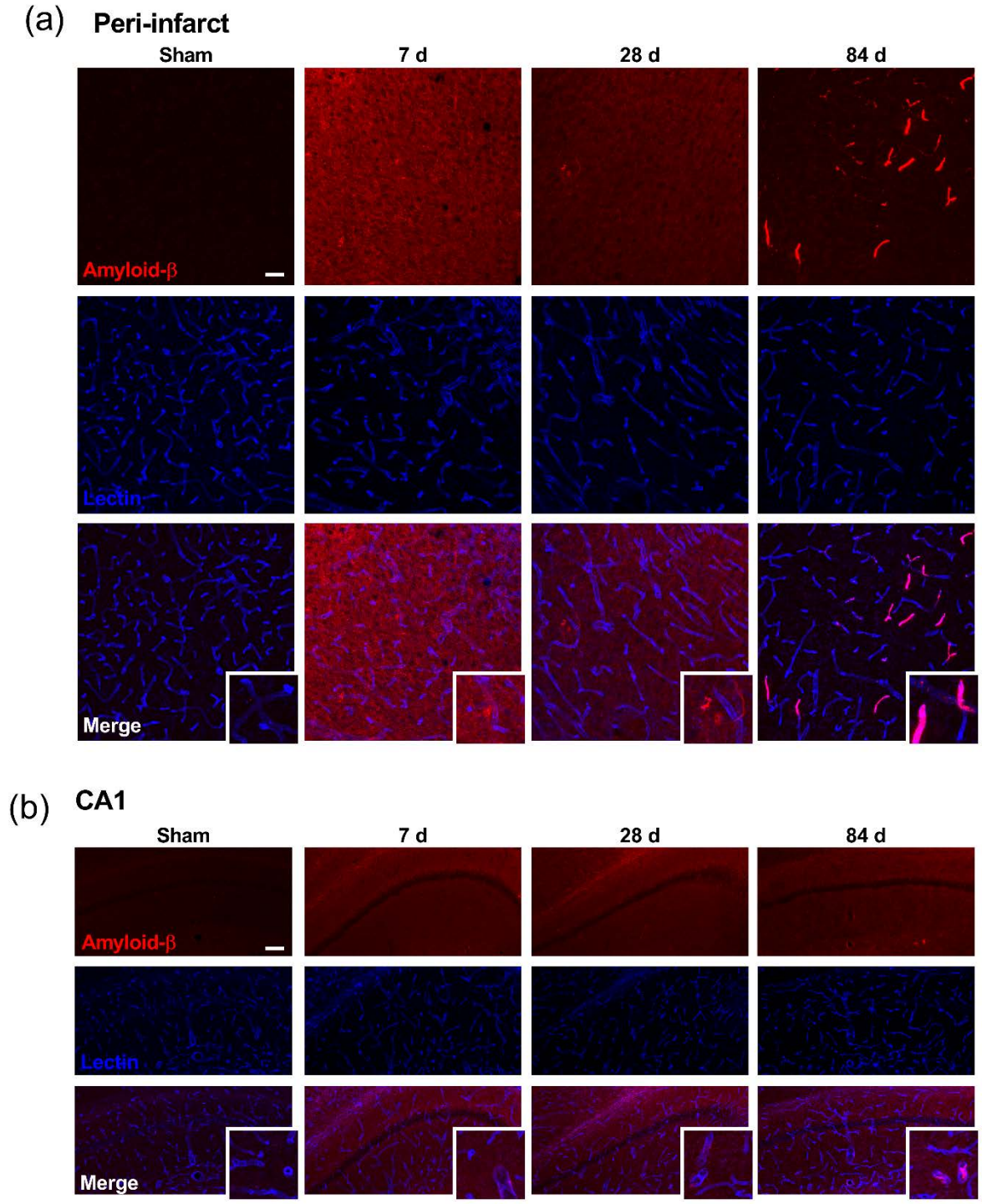

Figure 7. Stroke leads to amyloid-β (Aβ) aggregation which changes in distribution over time. (A and B) Representative immunofluorescence images of Aβ immunostaining (red) and Lectin (blue) and high magnification detail (peri-infarct scale bar=50 μm, CA1 scale bar=100 μm). Aβ expression switches from a scattered distribution in the parenchyma of the brain up to 28 days post-stroke to a localisation around the vessels at 84 days post-stroke in the peri-infarct region and in the CA1 sub-region of the hippocampus. At day 84, Aβ was observed to accumulate around the cerebral vessels in the peri-infarct region, and a lesser degree in the CA1 subregion of the hippocampus.

SUPPLEMENTARY MATERIAL

More than motor impairment: A spatiotemporal analysis of cognitive impairment and associated neuropathological changes following cortical photothrombotic stoke.

Sonia Sanchez-Bezanilla[1,2], Rebecca J. Hood[1,2], Lyndsey E. Collins-Praino[3], Renée J. Turner[3], Frederick R. Walker[1,2,4,5], Michael Nilsson[1,2,4,5,6] and Lin Kooi Ong[1,2,4,7]

1. School of Biomedical Sciences and Pharmacy and the Priority Research Centre for Stroke and Brain Injury, The University of Newcastle, Australia, Callaghan, NSW, Australia
2. Hunter Medical Research Institute, Newcastle, NSW, Australia
3. Department of Medical Sciences, Adelaide Medical School, University of Adelaide, Adelaide SA 5005, Australia
4. NHMRC Centre of Research Excellence Stroke Rehabilitation and Brain Recovery, Heidelberg, VIC, Australia
5. Centre for Rehab Innovations, The University of Newcastle, Callaghan, NSW, Australia
6. LKC School of Medicine, Nanyang Technological University, Singapore
7. Monash University Malaysia, Bandar Sunway, Selangor, Malaysia

Correspondence:
Lin Kooi Ong
School of Pharmacy, Monash University Malaysia, Jalan Lagoon Selatan, 47500, Bandar Sunway, Selangor, Malaysia.
E-mail: ong.linkooi@monash.edu

Supplementary materials and methods

Photothrombotic occlusion

Mice were anaesthetized by 2% isoflurane and maintained under general anaesthesia for the duration of the surgical procedure. Rose Bengal (200 µl, 10 mg/ml solution in sterile saline, Sigma-Aldrich, USA) was injected intraperitoneally and allowed to circulate for 8 min. The exposed skull was then illuminated for 15 min by a 4.5 mm diameter cold light source positioned at 2.2 mm left lateral of Bregma 0.0 mm, targeting the left motor and somatosensory cortices. For the sham group, the same surgical procedure was applied, except Rose Bengal was replaced with 200 µl of sterile saline (0.9% NaCl, Pfizer, Australia) (337). This stroke model produces relatively small penumbra area due to intense development of cell death in the infarction core. Nevertheless, in this study, we considered the peri-infarct region as the tissue that is in close proximity to the core infarct.

Motor test

Cylinder test. Spontaneous forelimb preference was evaluated by a cylinder test (338, 339). Each mouse was placed in a glass cylinder and the forelimb use during vertical exploration was evaluated. A final asymmetry score was calculated as the ratio of non-impaired forelimb movement minus impaired forelimb movement to total forelimb movement ([# non-impaired-# impaired movements]/total # movements).

Grid walk test. Sensorimotor function and motor coordination deficits during locomotion were assessed by the grid walk test (338, 339). Each mouse was placed on an elevated grid with

squares sized of approximately 2x2 cm. The number of "foot faults" made by the right and left limbs were counted. A foot fault index was calculated as the ratio of non-impaired forelimb foot faults minus impaired forelimb foot faults to total number of steps ([# non-impaired- # impaired steps]/total # steps).

Cognitive testing

Visual Discrimination reversal (VDR) task (271, 337)**.** Mice were calorie restricted overnight before cognitive testing (allowed access to food after cognitive testing for 5 hours, between 12:00 – 17:00 h). A liquid reward (strawberry milkshake) was provided to motivate the performance of the mice. Mice were introduced to a series of habituation and basic training tasks where they learned to associate a nose poke of the touchscreen with the delivery of a liquid reward. Basic training was performed over 10 days. During the training sessions, stimuli were displayed randomly on the screen one at a time. Stimuli consist of random shapes. One stimulus was presented at a time, on one side of the screen. The other side of the screen was left blank. The left or right position was chosen pseudorandomly, such that any image will not be displayed on the same side more than 3 times in a row. The mouse must touch the stimulus to elicit reward. If the mouse touched the blank screen, there was no response. All mice learned to perform the task with a minimum correct rate of 70%.

Following basic touchscreen training, mice underwent photothrombotic occlusion surgery. Seven days post-surgery, mice commenced the acquisition procedure of the VDR task. Briefly, the acquisition procedure entailed simultaneous presentation of two stimuli; one was programmed as being correct (S+; Fan) and one as being incorrect (S-; Marble). Whether the S+ was on the right or left was determined pseudorandomly. When the mouse made a correct choice, S+, a tone was triggered, the food tray was illuminated and the food reward was delivered and a correct trial was recorded. Conversely, if the mouse touched the incorrect image, S-, there was no reward delivery, no tone, and the house light was turned on for 5s and a correction trial was initiated. Correction trials consisted of repeated presentation of the previous trial until a correct response was made and were not counted towards the trial limit or number of correct responses. In each session, the testing ended once a mouse successfully completed 30 trials or reached a 60 min time limit, whichever occurred first. When the average percentage of correct trials of all mice reached an average of 70% correct answers, the reversal protocol started (at the 10^{th} session). The reversal sessions are identical to the acquisition, except that during reversal learning, the previously correct stimulus (S+) becomes the incorrect stimulus (S−; Fan), while the previously incorrect stimulus (S−) becomes correct (S+; Marble). All mice completed a total of 9 acquisition sessions, followed by a total of 10 reversal sessions. Once the VDR task was completed, the mice were allowed to rest for one month (extinction period). After the extinction period, mice performed the VDR task again.

Paired Associate Learning (PAL) task (271, 336)**.** The task consists of two distinct phases, basic training, whereby the animal learns the association between making contact with the screen and the actual PAL task. In the task, three stimuli images (a flower, plane and spider) were associated with a specific spatial location (left, centre, right respectively). In each trial, two images were displayed at the same time, one in its correct location (S+) and the other in an incorrect location (S-). All trials were mouse initiated and independent of the experimenter. If the mouse touched the image in its correct location, a reward was provided. If the animal touched the incorrect image or the correct image in its incorrect location, no reward (strawberry

milkshake) was given, the tone did not sound and the house light turned on for a 5s duration. Testing was stopped by finishing 36 trials or 1 hour (whichever happened first). All mice completed a total of 25 sessions. Once the PAL task was completed, the mice were allowed to rest for one month (extinction period) before performing the PAL task again.

Tissue processing

Mice were sacrificed at different time points after surgery: 7, 28 or 84 days. For histological analysis, mice were deeply anaesthetised with sodium pentabarbitol and perfused via the ascending aorta with approximately 10 ml ice-cold 0.9% saline followed by approximately 40 ml ice-cold 4% paraformaldehyde (pH 7.4). Brains were then dissected and post-fixed for 4 hours in 4% paraformaldehyde, then transferred to a 12.5% sucrose solution in 0.1 M PBS for storage and cryoprotection. Serial coronal 30 µm thick sections were sliced on a freezing microtome (Leica, North Ryde, NSW, Australia). For western blotting, mice were deeply anesthetized via intraperitoneal injection of sodium pentobarbital and transcardially perfused with ice-cold 0.1% diethylpyrocarbonate in 0.9% saline for 3 mins. Brains were rapidly dissected and frozen in -80 °C isopentane. Sections were sliced using a cryostat (-20 °C) at a thickness of 200 µm. The peri-infarct territory (2 mm2 around the infarct core, Bregma +1.0 to -1.0 mm) and the hippocampus (Bregma -1.2 to -2.5 mm) were isolated using a 1 mm tissue punch and samples were stored at -80 °C until further analysis (340).

Histological Analysis

Cresyl Violet. Fixed sections at Bregma 1.0, 0.0, -1.0 and -1.5 mm were mounted on glass slides and air-dried. Sections were defatted in chloroform:ethanol solution for 8 min, followed by rehydration in a series of ethanol solutions: absolute (1 min), 95% (1 min) and 70% (1 min). Sections were stained in Cresyl Violet solution for 15 min, then washed in 70% ethanol (1 min), 95% ethanol (1 min), differentiating solution (2 min) and absolute ethanol (3 x 1 min). Finally, the sections were cleared in xylene (3 x 1 min) and cover slipped (337).

Sudan black. Sections were mounted and rinsed with 70% ethanol, followed by 15 min incubation with Sudan Black B solution (Sigma-Aldrich, USA). After staining, sections were rinsed with 70% ethanol and water and counterstained with nuclear fast red solution for 5 min (Sigma-Aldrich, USA) (341).

Immunofluorescence. Free-floating fixed sections were co-immunostained using standard protocols (342). Sections were rinsed, and non-specific binding sites were blocked using 3% bovine serum albumin. Sections were incubated in primary antibodies (GFAP, Iba1, Aβ, NeuN) overnight at 4 ˚C, followed by a 2 hour incubation in corresponding secondary antibodies at 25 ˚C. For blood vessel detection, Lectin staining was performed together with the secondary antibody incubation (see Supplementary Table 1 for antibodies and concentrations). Brain sections were washed with PBS in between each incubation step and subsequently mounted and cover slipped.

Protein extraction and Western blotting

The peri-infarct territory (Bregma +1.0 to -1.0 mm) and the hippocampus (Bregma -1.2 to -2.5 mm) were isolated using a 1 mm tissue punch. Samples were sonicated in 300 µl lysis buffer (50 mM TRIS buffer pH 7.4, 1 mM EDTA, 1 mM DTT, 80 µM ammonium molybdate, 1 mM sodium pyrophosphate, 1 mM sodium vanadate, 5 mM b-glycerolphosphate, 1 protease

inhibitor cocktail tablet, 1 phosphatase inhibitor cocktail tablet, final concentration) and centrifuged at 14000 G for 20 min at 4˚C. The supernatant fractions were collected and protein concentrations determined using a Pierce BCA protein assay kit (Thermo Fisher Scientific, USA) according to the manufacturer's instructions. Samples were mixed with sample buffer (2% SDS, 50 mM Tris, 10% glycerol, 1% DTT, 0.1% bromophenol blue, pH 6.8). 15 µg of total tissue protein samples were electrophoresed into Biorad Criterion TGX Stain-Free 4–20% gels. Gels were transferred to PVDF membranes, washed in Tris-buffered saline with tween (TBST) (150 mM NaCl, 10 mM Tris, 0.075% Tween-20, pH 7.5) and incubated in 5% skim milk powder in TBST for 1 hour at room temperature. Membranes were incubated with primary antibodies (Aβ and CD11b) overnight at 4 °C and secondary antibody for 1 hour at room temperature (see Supplementary Table 1 for antibody concentration). In between each incubation step, membranes were washed in TBST. Membranes were visualized on an Amersham Imager 600 using Luminata Classico or Luminata Forte western blotting detection reagents. The density of the bands was measured using Amersham Imager 600 analysis software (337).

Supplementary Table 1: List of antibodies used for western blot and immunofluorescence analyses.

Target	Sources of antibodies	Application	Dilution
Amyloid-β	Biolegend, anti-Amyloid-β (6E10), # SIG-39320	WB IF	1:1000 1:1000
CD11b	Abcam, anti- CD11b, #ab75476	WB	1:2000
NeuN	Millipore, anti-NeuN (clone A60), #MAB377	IF	1:2000
Iba-1	WAKO, anti-Iba-1, #019-19741	IF	1:1000
GFAP	Sigma-Aldrich, Anti-Glial Fibrillary Acidic Protein (GA5), #G3893	IF	1:1000
Lectin	Vecton Laboratories, DyLight 649 Lycopersicon esculentum (Tomato) lectin #DL-1178	IF	1:1000
β-actin	Sigma-Aldrich, Monoclonal Anti-β-actin-HRP antibody, A3854	WB	1:50000
Rabbit IgG	Biorad, Anti-Rabbit-HRP antibody, #170-6515 ThermoFisher Scientific, anti-Rabbit IgG (H+L) Highly Cross-Adsorbed Secondary Antibody, Alexa Fluor 488, #A21206	WB IF	1:7500 1:400
Mouse IgG	Biorad, Anti-Mouse-HRP antibody, #170-6516 ThermoFisher Scientific, anti-Mouse IgG (H+L) Highly Cross-Adsorbed Secondary Antibody, Alexa Fluor 594, #A21203	WB IF	1:10000 1:400

WB, western blot; IF, immunofluorescence

Supplementary figures

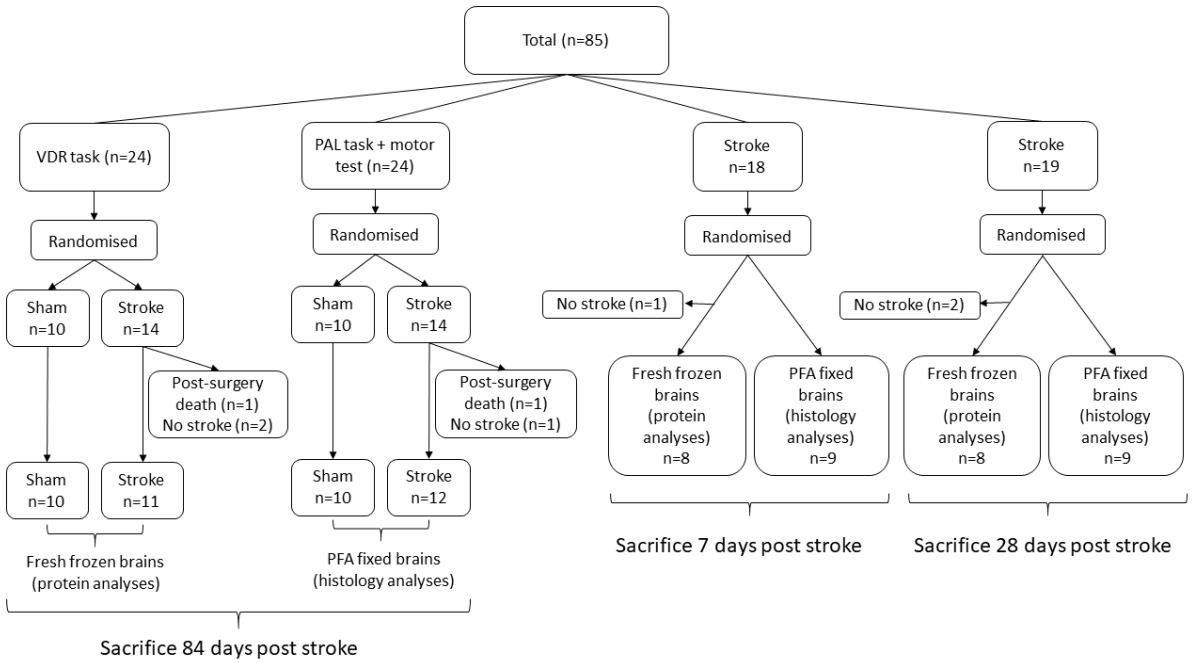

Supplementary Figure 1. Diagram for inclusion and exclusion of mice in this study. Mice were removed from the study if we histologically identified that the stroke had not occurred. A total of 85 mice were used in this study. A total of 24 mice were used for visual discrimination reversal (VDR) task and sacrificed at 84 days post-stroke to perform protein analysis of the brain. A total of 24 mice were used for paired-associate learning (PAL) task and sacrificed at 84 days post-stroke to perform histology analysis. A third cohort of mice were sacrificed at either 1 week (stroke n=18) or 1 month (stroke n=19) post-stroke, and the brains used for subsequent protein or histological analyses. This cohort was not subjected to functional testing, and the brains were used as representative for the 1 week or 1 month time points. A total of 18 and 19 mice were sacrificed at 7 and 28 days post stroke respectively. Brains were used for protein and histology analysis.

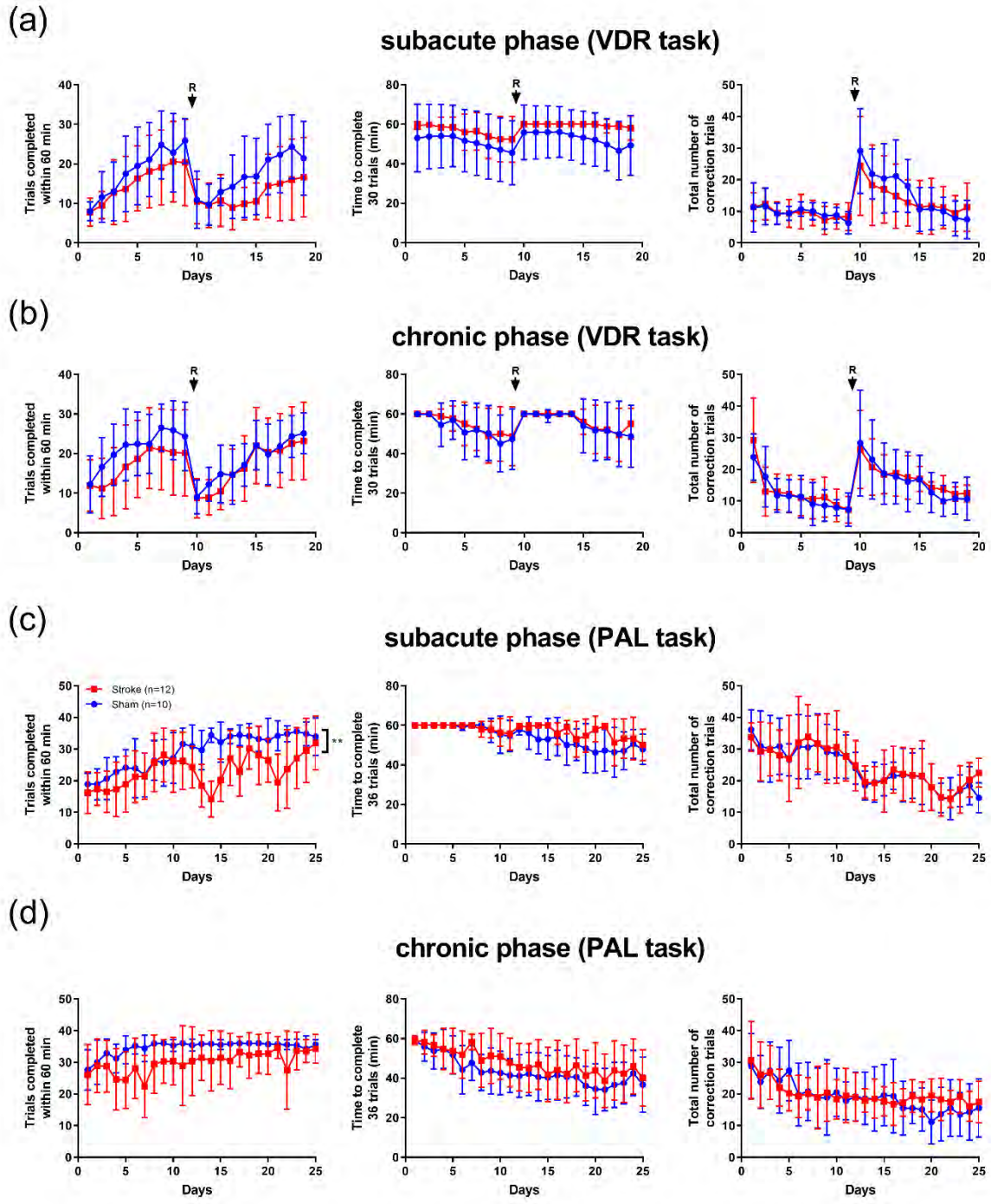

Supplementary figure 2. Metrics of the paired-associate learning (PAL) and visual discrimination (VD) task. For the VDR task, we measured number of trials completed within 60 min, time to complete 36 trials and total number of correction trials in the subacute (a) and chronic phase (b). The same metrics were measure for the PAL task during the subacute (c) and chronic phase (d). Mean±SD (two-way ANOVA and Sidak's multiple comparisons). ** $p<0.01$

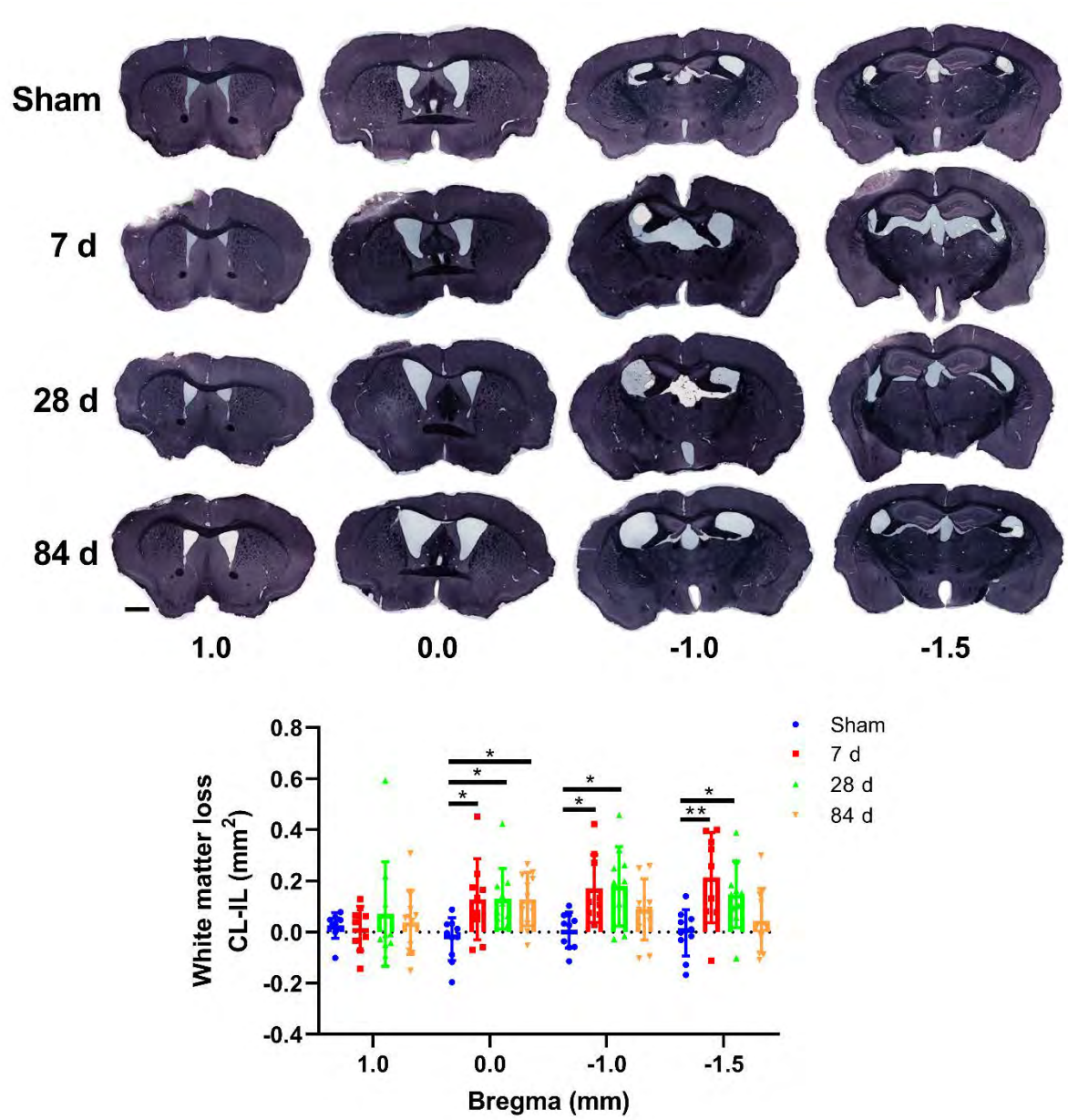

Supplementary figure 3. Stroke induces white matter tract loss. Images represent Sudan Black B staining at Bregma levels 1.0, 0.0, -1.0 and -1.5mm. Quantification of white matter loss was measured as a difference between the contralateral (CL) and ipsilateral (IL) hemisphere. We observed white matter loss at Bregma -1.0 mm and -1.5 mm in stroked mice compared to shams at both 7 and 28 days, but not 84 days, post-stroke. Mean±SD (Two-way ANOVA and Turkey's multiple comparison test). *$p < 0.05$; **$p < 0.01$.

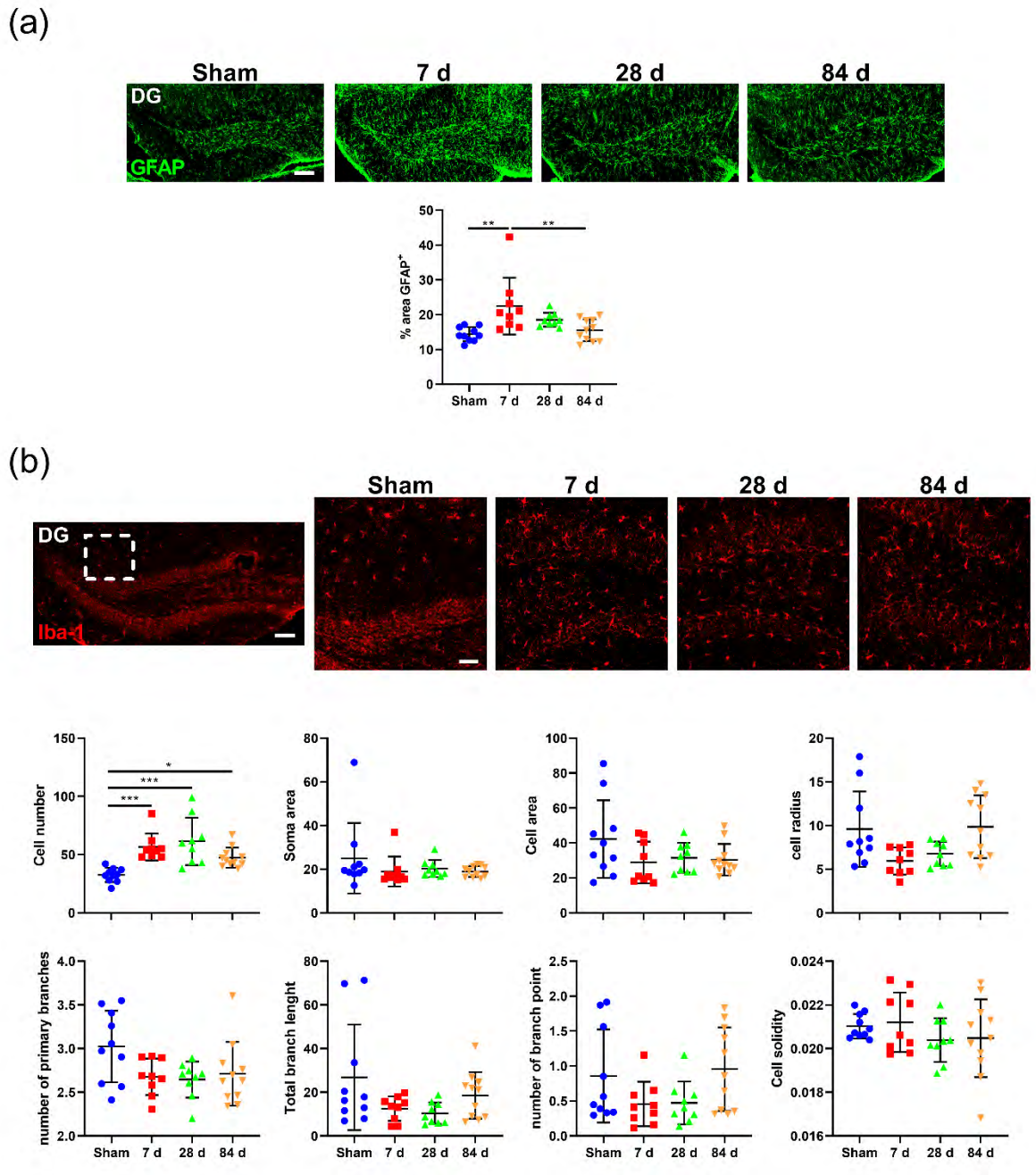

Supplementary figure 4. (a) Representative immunofluorescence images of DG region of the hippocampus labelled with GFAP (scale bar = 100 μm) and quantification of reactive astrogliosis (% area of GFAP+). (b) Representative immunofluorescence images of the DG region and quantification of microglia morphology over time (scale bar = 100 μm; scale bar of magnification = 50 μm). White dotted square represents the area of morphological analysis. We observed a significant increase in the number of cells but there were no significant changes in other parameters. Mean±SD (Two-way ANOVA and Turkey's multiple comparison test). *p < 0.05; **p < 0.01; ***p < 0.001.

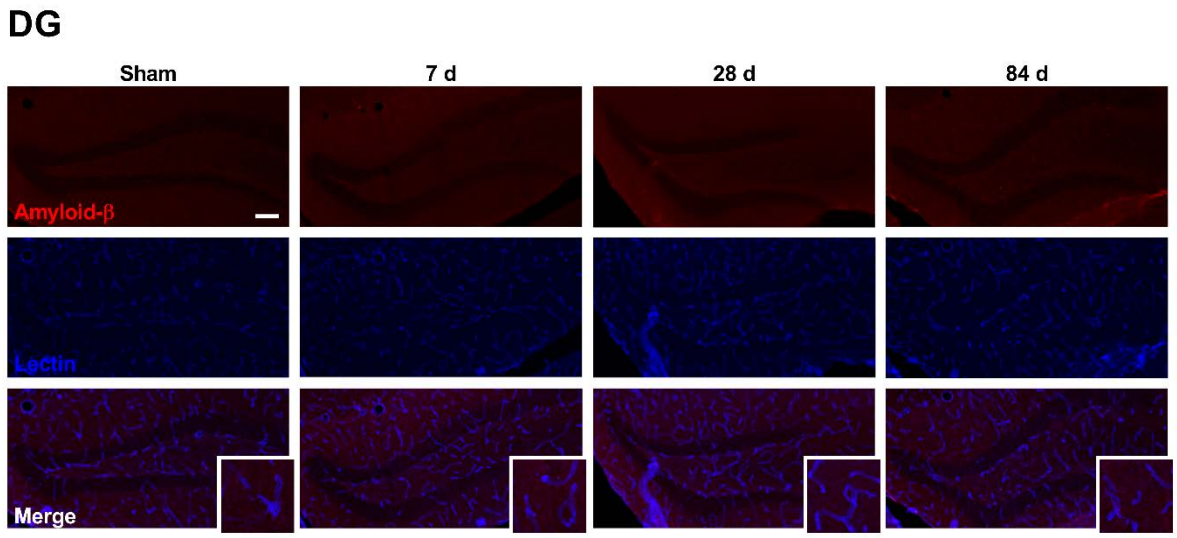

Supplementary figure 5. Representative immunofluorescence images of Aβ immunostaining (red) and Lectin (blue) and high magnification detail (scale bar=100 μm) in the DG region of the hippocampus. The immunofluorescence signal appeared to be consistent in the DG throughout all experimental groups**.**

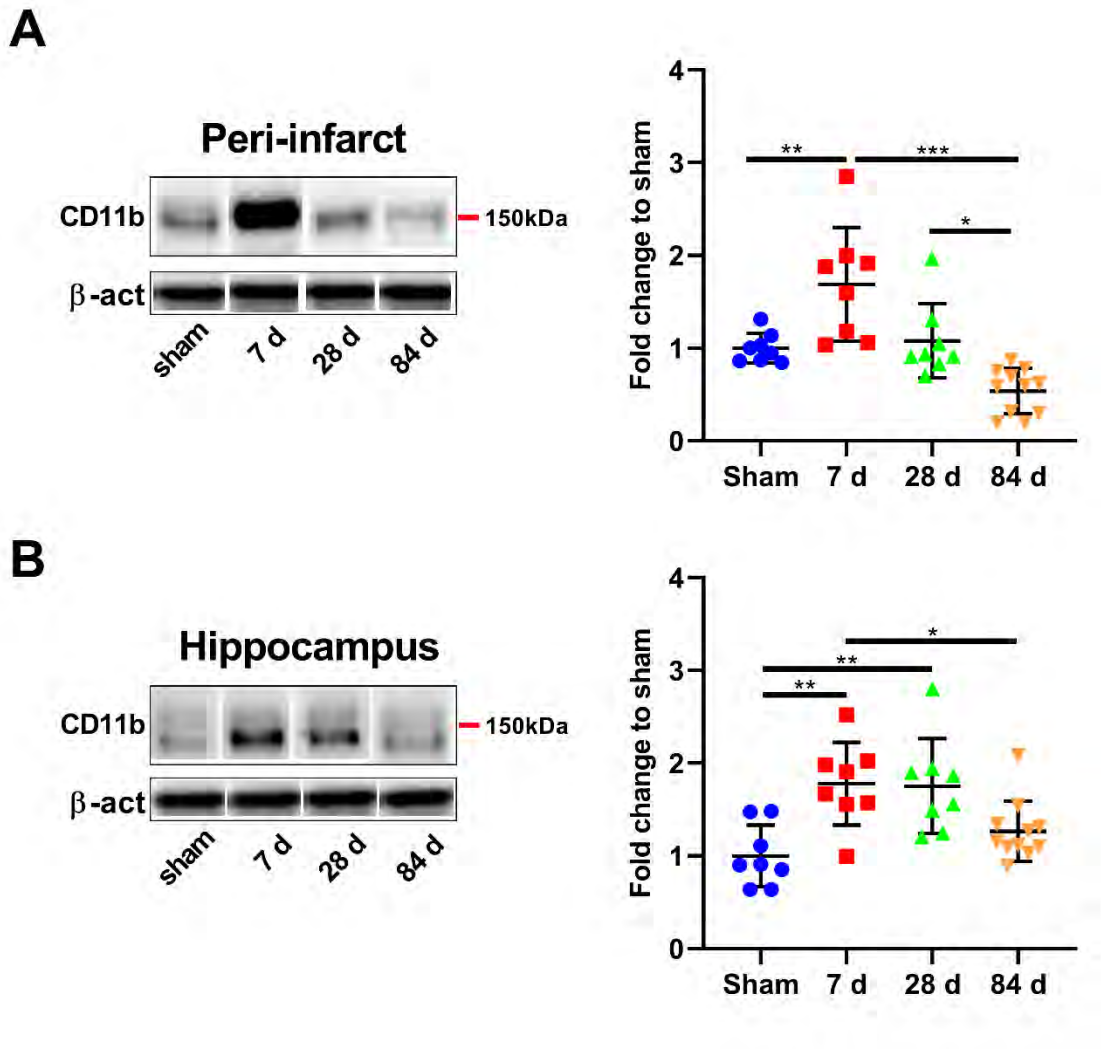

Supplementary figure 6. Stroke increases the expression of CD11b, a microglial activation marker. (A) Representative western blot and quantification of CD11b expression profile within the peri-infarct. (B) Representative western blot and quantification of CD11b expression profile within the hippocampus. Mean±SD (Two-way ANOVA and Turkey's multiple comparison test). *p < 0.05; **p < 0.01; ***p < 0.001.

References

1. Sanchez-Bezanilla S, TeBay C, Nilsson M, et al. Visual discrimination impairment after experimental stroke is associated with disturbances in the polarization of the astrocytic aquaporin-4 and increased accumulation of neurotoxic proteins. *Exp Neurol* 2019; 318: 232-243. 2019/05/09. DOI: 10.1016/j.expneurol.2019.05.001.

2. Schaar KL, Brenneman MM and Savitz SI. Functional assessments in the rodent stroke model. *Exp Transl Stroke Med* 2010; 2: 13-13. DOI: 10.1186/2040-7378-2-13.

3. Pietrogrande G, Zalewska K, Zhao Z, et al. Low Oxygen Post Conditioning as an Efficient Non-pharmacological Strategy to Promote Motor Function After Stroke. *Transl Stroke Res* 2019; 10: 402-412. 2018/08/28. DOI: 10.1007/s12975-018-0656-5.

4. Horner AE, Heath CJ, Hvoslef-Eide M, et al. The touchscreen operant platform for testing learning and memory in rats and mice. *Nat Protoc* 2013; 8: 1961-1984. 2013/09/19. DOI: 10.1038/nprot.2013.122.
5. Ong LK, Chow WZ, TeBay C, et al. Growth Hormone Improves Cognitive Function After Experimental Stroke. *Stroke* 2018; 49: 1257-1266. 2018/04/11. DOI: 10.1161/strokeaha.117.020557.
6. Sanchez-Bezanilla S, Åberg ND, Crock P, et al. Growth Hormone Treatment Promotes Remote Hippocampal Plasticity after Experimental Cortical Stroke. *International journal of molecular sciences* 2020; 21 2020/07/02. DOI: 10.3390/ijms21124563.
7. Pietrogrande G, Zalewska K, Zhao Z, et al. Low oxygen post conditioning prevents thalamic secondary neuronal loss caused by excitotoxicity after cortical stroke. *Sci Rep* 2019; 9: 4841. 2019/03/21. DOI: 10.1038/s41598-019-39493-8.
8. Kluge MG, Abdolhoseini M, Zalewska K, et al. Spatiotemporal analysis of impaired microglia process movement at sites of secondary neurodegeneration post-stroke. *J Cereb Blood Flow Metab* 2019; 39: 2456-2470. 2018/09/11. DOI: 10.1177/0271678X18797346.

CHAPTER 5: PUBLICATION 3

Growth hormone promotes motor function after experimental stroke and enhances recovery-promoting mechanisms within the peri-Infarct area

As per the peer-review paper accepted and published in: International Journal of Molecular Sciences

CONTRIBUTIONS

We, the co-authors, attest the Research Higher Degree candidate, Sonia Sanchez Bezanilla, contributed to the paper entitled **"Growth hormone promotes motor function after experimental stroke and enhances recovery-promoting mechanisms within the peri-infarct area"** as outlined below:

- 70% Conception and design of research;
- 70% Experimental procedures;
- 75% Analysis and interpretation of the findings;
- 75% Writing and critical appraisal of the content

N. David Åberg		*18/02/2020*
Name of Co-author	*Signature*	*Date*
Patricia Crock		*24/02/2020*
Name of Co-author	*Signature*	*Date*
Frederick R. Walker		*19/02/2020*
Name of Co-author	*Signature*	*Date*
Michael Nilsson		*19/02/2020*
Name of Co-author	*Signature*	*Date*
Jörgen Isgaard		*19/02/2020*
Name of Co-author	*Signature*	*Date*
Lin Kooi Ong		*19/02/2020*
Name of Co-author	*Signature*	*Date*

Lesley MacDonald-Wicks

Assistant Dean Research Training

10/3/2020

Article

Growth hormone promotes motor function after experimental stroke and enhances recovery-promoting mechanisms within the peri-infarct area

Sonia Sanchez-Bezanilla[1,2], N. David Åberg[3,4], Patricia Crock[2,5], Frederick R. Walker[1,2,6,7], Michael Nilsson[1,2,6,7,8], Jörgen Isgaard[1,3,4]*, Lin Kooi Ong[1,2,6,9]*

1. School of Biomedical Sciences and Pharmacy and the Priority Research Centre for Stroke and Brain Injury, the University of Newcastle, University Dr, Callaghan, 2308, NSW, Australia
2. Hunter Medical Research Institute, Lot 1, Kookaburra Cct, New Lambton Heights, 2305, NSW, Australia
3. University of Gothenburg, 405 30 Gothenburg, Sweden
4. Department of Internal Medicine, Region Västra Götaland, Sahlgrenska University Hospital, Blå stråket 5, 413 45 Gothenburg, Sweden.
5. Department of Paediatric Endocrinology and Diabetes, John Hunter Children's Hospital, Kookaburra Cct, New Lambton Heights, 2305, NSW, Australia
6. NHMRC Centre of Research Excellence Stroke Rehabilitation and Brain Recovery, 245 Burgundy Street, Heidelberg, 3084, VIC, Australia
7. Centre for Rehab Innovations, Lot 1, Kookaburra Cct, New Lambton Heights, 2305, NSW, Australia
8. LKC School of Medicine, Nanyang Technological University, 50 Nanyang Ave, 639798 Singapore
9. Monash University Malaysia, Bandar Sunway, 47500 Subang Jaya, Selangor, Malaysia

* Contributed equally to senior authorship
* Correspondence: ong.linkooi@monash.edu; jorgen.isgaard@medic.gu.se

Received: date; Accepted: date; Published: date

Abstract: Motor impairment is the most common and widely recognized clinical outcome after stroke. Current clinical practice in stroke rehabilitation focuses mainly on physical therapy, with no pharmacological intervention approved to facilitate functional recovery. Several studies have documented positive effects of growth hormone (GH) on cognitive function after stroke, but surprisingly the effects on motor function remain unclear. In this study, photothrombotic occlusion targeting the motor and sensory cortex was induced in adult male mice. Two days post-stroke, mice were administered with recombinant human GH or saline, continuing for 28 days, followed by evaluation of motor function. Three days after initiation of the treatment, bromodeoxyuridine was administered for subsequent assessment of cell proliferation. Known neurorestorative processes within the peri-infarct area were evaluated by histological and biochemical analyses at 30 days post-stroke. This study demonstrated that GH treatment improves motor function after stroke by 50-60%, as assessed using the cylinder and grid walk tests. Furthermore, the observed functional improvements occurred in parallel with a reduction in brain tissue loss, as well as increased cell proliferation, neurogenesis, increased synaptic plasticity and angiogenesis within the peri-infarct area. These findings provide new evidence about the potential therapeutic effects of GH in stroke recovery.

Keywords: Ischemic stroke, growth hormone, motor recovery, neurogenesis, neuronal plasticity, vascular remodeling

1. Introduction

Stroke is a leading cause of disability globally [1]. The most common and widely recognised neurological impairments caused by stroke are deficits in motor function [2]. Therefore, motor-based rehabilitation techniques have been developed to promote the recovery of motor impairments in stroke

patients [3-7]. Current clinical practice for impaired sensorimotor functions are mainly based on physical therapy starting within 48 hours of stroke onset, which can last for as long as months and years after the stroke [4,8]. Rehabilitation after stroke is often a long and slow process, and therefore the development of new effective therapeutic strategies that can enhance the recovery of brain function and improve functional outcomes are highly desirable. An innovative solution may be the use of a pharmacological strategy to promote a pro-restorative environment within the brain. One promising strategy in this regard is growth hormone (GH).

The therapeutic potential of GH on brain repair after brain injury or stroke has been considered in both human [9-18] and preclinical [19-24] studies. GH, a peptide hormone released from the anterior pituitary gland, plays an important role in brain growth, development and function [11]. Critically, prior work has documented the widespread expression of GH and GHR in the rat brain [25], and the ability of GH to stimulate the genesis of neuronal stem cells [26] and endothelial cells, as well as to promote synaptogenesis [27]. It is well known that any injury to the adult brain generates an adaptive brain repair response, which includes the proliferation of new cells and differentiation into different populations [28-31]. Previous experimental studies have shown that ischemic injury induces proliferation of newly born neurons in the subventricular zone, migration of these immature neurons, and localization within the peri-infarct region [31-36]. However, this self-repair mechanism operates only acutely after stroke and is insufficient to promote long-term recovery. Interestingly, several experimental studies have shown that GH can promote these neurorestorative or plasticity-promoting processes beyond what occurs with spontaneous recovery after brain injury or stroke, and this increased neurorestoration is closely linked with improvement in functional outcomes [9,11,15,18,37,38]. Despite the fact that the positive effects of GH in the adult brain have been extensively studied, it is still not clear whether GH could promote motor function after stroke.

In previous studies, we assessed the pro-cognitive effects of peripherally administered GH after experimental stroke and the possible underlying mechanisms leading to such effects. We found that GH treatment promotes cognitive recovery after stroke, however sensorimotor effects were not evaluated. In addition, we found an increased expression of neurotrophic factors, markers of synaptogenesis and myelination, and the formation of new blood vessels [39]. However, there is still a large gap in our understanding of whether GH treatment could also enhance motor function after stroke, and whether this is associated with neurorestorative processes within the peri-infarct regions.

In this study, we aimed to evaluate whether GH treatment could promote motor function after experimental stroke. Our primary hypothesis was that mice who received stroke that were then treated with recombinant human growth hormone (rhGH) for 28 days, starting at 48 hours post-stroke, would improve performance in motor tasks relative to non-rhGH-treated stroke mice. Our secondary hypothesis was that the rhGH–treated stroke mice would show an enhancement in known neurorestorative processes within the peri-infarct region. We assessed cellular and molecular changes using comprehensive and cross validated approaches including bromodeoxyuridine (BrdU) tagging, co-immunolabelling, and western blotting analyses.

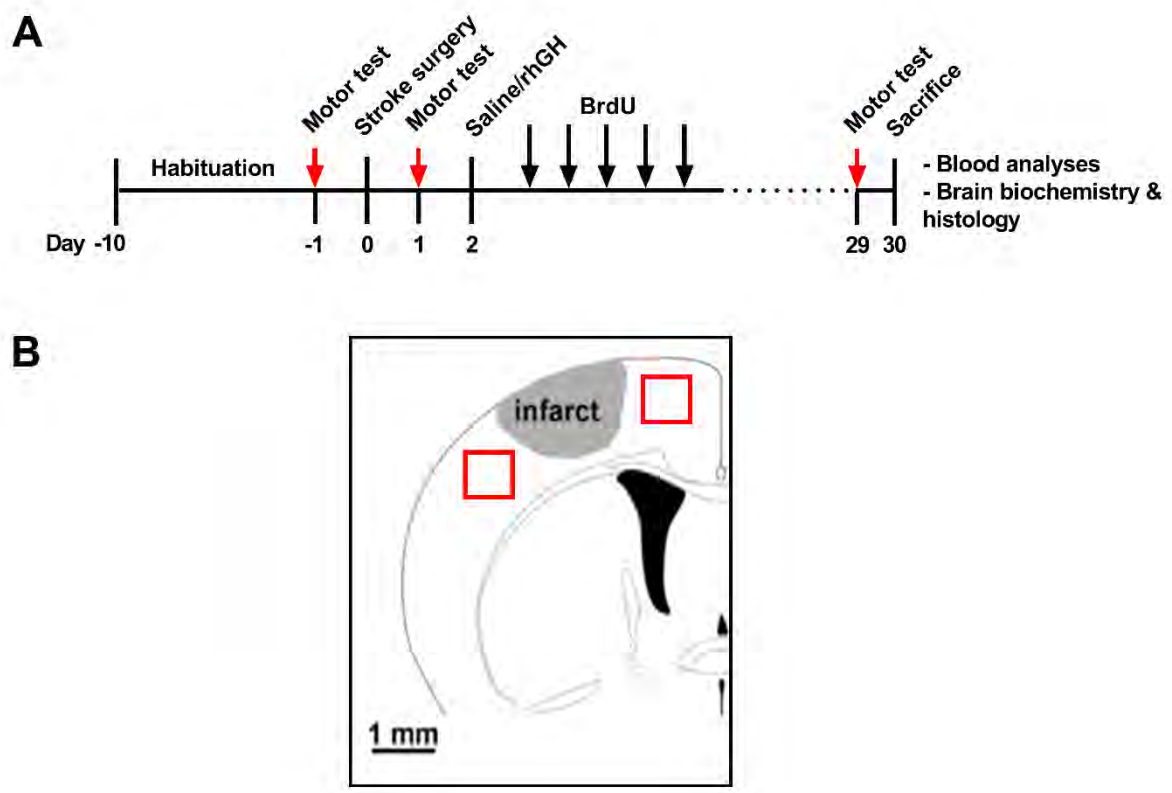

Figure 1. (A) Experimental timeline. Photothrombotic stroke was induced in all mice. Two days post-stroke, mice were randomly treated with either saline or rhGH via mini-osmotic pumps for 28 days. At day 3 mice were injected with BrdU for 5 consecutive days. Mice were assessed by motor tests at one day before stroke (pre-stroke), one day after stroke (post-stroke) and 29 days post-stroke (post-treatment). **(B)** Diagram illustrating the site of photothrombotic stroke induction (grey area) at Bregma 0.0 mm. Red squares represent the area of the peri-infarct region selected for immunofluorescence analyses. The peri-infarct territory, which is found in the 2 mm around the infarct core, was dissected for protein analysis. Bar = 1 mm.

2. Results

2.1. GH treatment improves motor function

We treated the mice with either saline (n=10) or rhGH (n=10) using a mini-osmotic pump, starting at 48 hours post-stroke for 28 days. Mice were assessed for motor deficits one day before stroke (pre-stroke), one day after stroke (post-stroke) and at 29 days post-stroke (post-treatment) (Figure 1). We used the cylinder task to evaluate locomotor asymmetry. This task evaluates the forelimb preference that mice utilise for upright postural support when rearing up on the cylinder wall. Data on the asymmetry scores indicated that there were no significant differences in forelimb preference prior to stroke. One day after stroke, all mice showed a significantly stronger preference for using their ipsilateral (unaffected) forelimb. At 29 days post-stroke, we found a significant motor improvement (50.32%, p=0.0123) in rhGH–treated stroke mice compared with saline-treated mice (Figure 2A). Motor function was also assessed using the grid walk task. This task evaluates the ability of mice to effectively

place their paws on an elevated grid during locomotion. As expected, there was no difference in the number of foot faults before stroke. One day after stroke, the number of foot faults on the contralateral (affected side) was significantly higher in all stroke mice. At 29 days post-stroke, there was a significant effect of rhGH treatment on motor function recovery (64.27%, p<0.0001; Figure 2B).

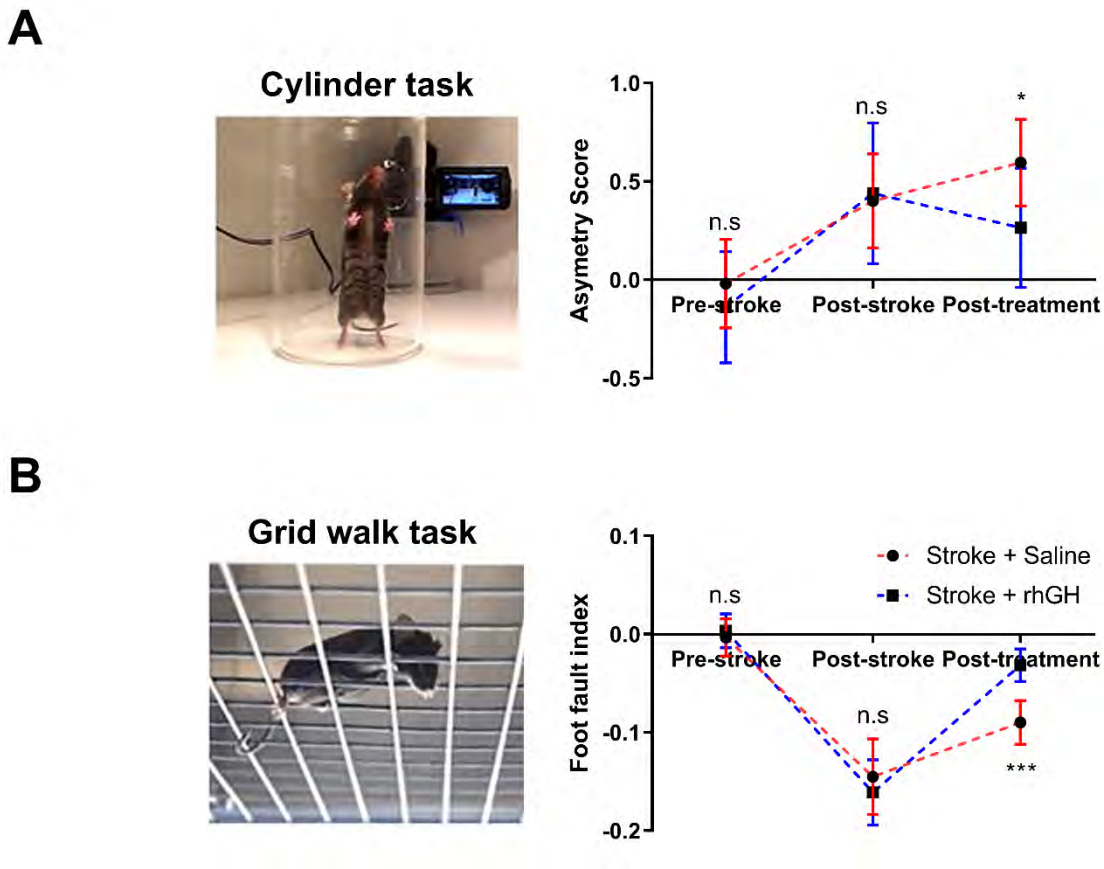

Figure 2. The effects of recombinant human growth factor (rhGH) treatment post-stroke on motor function. **(a)** Asymmetry scores were evaluated by the cylinder test, which shows that mice that received rhGH treatment significantly improve motor function. **(b)** A foot fault index was evaluated by the grid walk test, which also shows an improvement in motor function after rhGH treatment. In all panels, red colour designates saline treatment and blue designates rhGH treatment. Mean±SD. n.s = no significant**.** *p<0.05 and ***p<0.001.

2.2. GH treatment increases plasma IGF-1 levels

rhGH treatment administered post-stroke significantly increased IGF-1 (Saline treatment 289.9 ± 36.14 vs. rhGH treatment 433.5 ± 44.2 ng/ml, 49.51%, p<0.0001) and IGFBP-3 (Saline treatment 254.3 ± 50.06 vs. rhGH treatment 293.7 ± 26.1 ng/ml, 15.49%, p=0.0405) levels in plasma, assessed at time of sacrifice. These results have confirmed that commercially available rhGH has significant effects on mouse physiology when delivered subcutaneously via mini-osmotic pump. Further, we assessed the association between plasma IGF-1 and motor performance. A Pearson correlation analysis showed a significant positive correlation between plasma IGF-1 levels and cylinder task performance post rhGH treatment (r=-0.6789; $P_{(Y = -0.002513*X + 1.339)}$=0.0010) (Supplementary Figure 3a). There was also significant a

correlation between plasma IGF-1 levels and the grid walk task performance post rhGH treatment (r=0.8879; $P_{(Y = 0.0003785*X - 0.1977)}$<0.0001) (Supplementary Figure 3b).

2.3. GH treatment reduces tissue loss

Using Cresyl Violet staining we estimated the tissue loss at 0.0 mm and -2.0 mm from Bregma. We found a significant decrease in tissue loss at Bregma 0.0 mm at 30 days post stroke in mice treated with rhGH (29.89%, p= 0.0088; Figure 3).

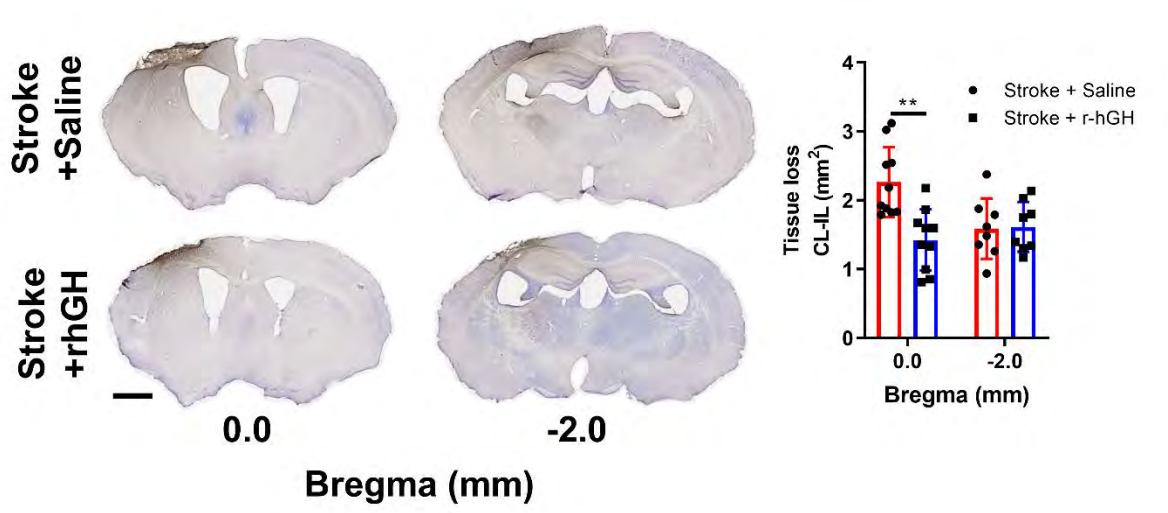

Figure 3. Cresyl violet staining of brain sections from Bregma 0.0 mm and -2.0 mm. Tissue loss was calculated as contralateral (CL) hemisphere area − ipsilateral (IL) hemisphere area (mm^2). *p<0.05 and ***p<0.001. Bar = 1 mm.

2.4. GH treatment promotes cell proliferation and neurogenesis within the peri-infarct region

We assessed several selected neurorestorative effects of rhGH after stroke using an immunolabelling approach. Firstly, we performed BrdU and NeuN co-labelling (Figure 4A). BrdU is an analogue of the nucleoside thymidine, which can be incorporated into replicating DNA and therefore can be used to identify proliferating cells [40]. In the peri-infarct region, we found a significant increase in the number of BrdU-positive cells in stroke mice treated with rhGH compared with saline treated mice (109.67%, p=0.0035; Figure 4B). We also observed an increase in the number of NeuN-positive neurons (9.10%, p = 0.0256) (Figure 4C). To assess whether these proliferating cells have differentiated into neurons, we analysed co-localisation of BrdU and NeuN labelling. rhGH treatment post-stroke significantly increased the number of BrdU-NeuN-positive cells (139.44%, p = 0.0073; Figure 4D).

Next, we analysed the levels of doublecortin (DCX), a marker of immature neurons [41]. DCX is a microtubule-associated protein, which is necessary in the proliferation of progenitor cells during neurogenesis [42,43]. Optical density of DCX immunofluorescence images within the peri-infarct were quantitatively assessed using a threshold analysis protocol. This immunofluorescence data revealed a significant increase in material thresholded for DCX (201.97%, p = 0.0115, at pixel intensity 225; Figure

5A) in stroke mice treated with rhGH compared with saline treatment. We further confirmed this histology data using a western blot protocol. The protein homogenates from the peri-infarct region of stroke+saline and stroke+rhGH cohorts were analysed along with a sham+saline cohort. We found a significant increase in DCX levels (0.44 fold, p = 0.0010; Figure 5C) after rhGH treatment.

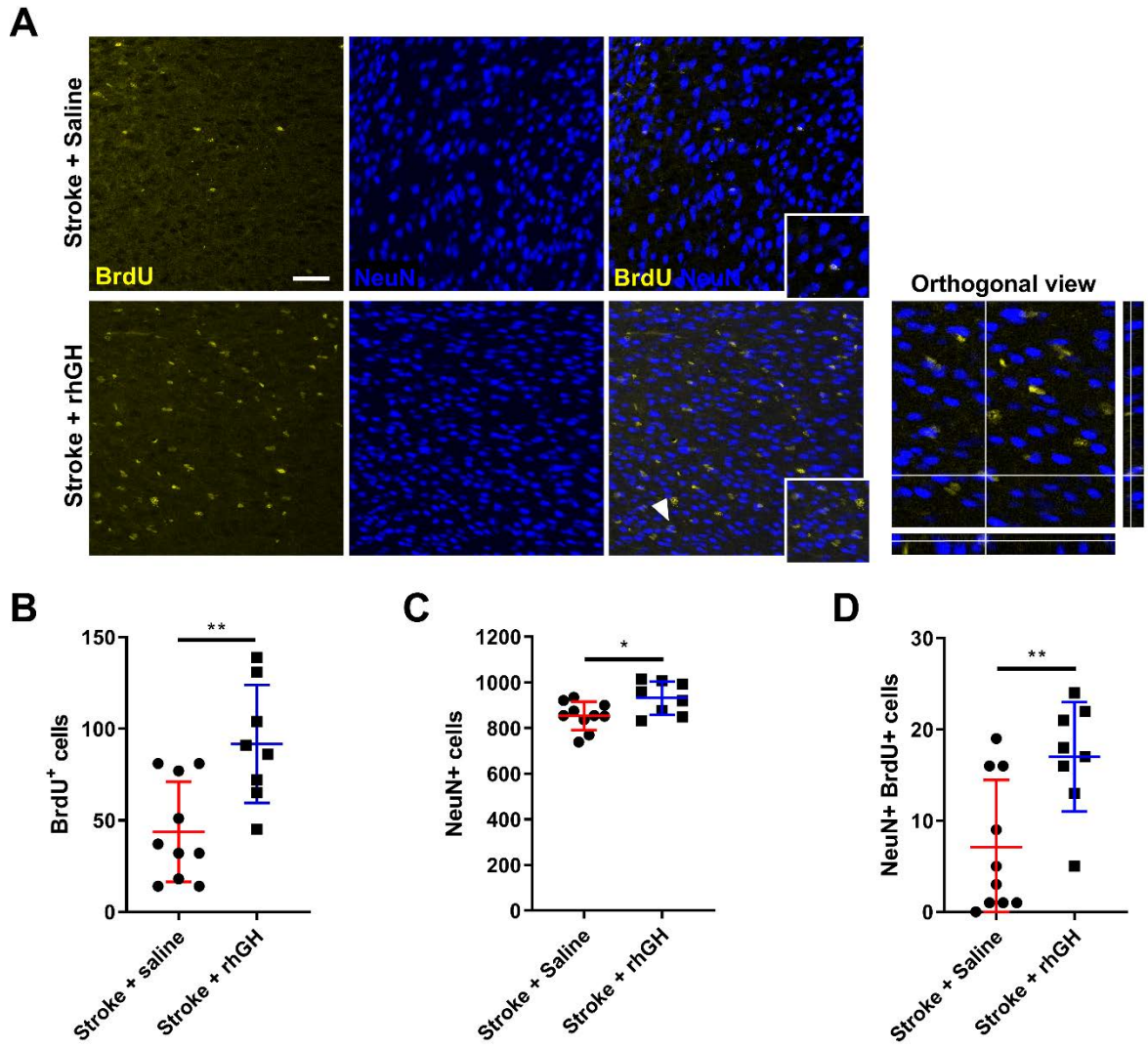

Figure 4. rhGH treatment promotes cell proliferation and neurogenesis in the peri-infarct region. **(A)** Representative immunofluorescence images, which are co-labelled with BrdU (yellow) and NeuN (blue), with orthogonal view also presented (far right). The white arrowhead shows a co-labelled cell visualized in orthogonal view. (Scale bar = 50 μm). rhGH treatment post-stroke significantly increased the number of BrdU-positive cells **(B)**, NeuN-positive cells **(C)** and BrdU-NeuN-positive cells **(D)**. Mean±SD. *p<0.05 and **p<0.01

2.5. GH treatment promotes expression of GluR1 within the peri-infarct region

We also assessed the levels of AMPA Receptor 1 (GluR1). GluR1 is a receptor implicated in synapse formation, stabilization, and plasticity [44]. The immunofluorescence data revealed a significant

increase in material thresholded for GluR1 (203.54%, p = 0.0003, at pixel intensity 220; Figure 5B) in stroke mice treated with rhGH compared with saline treated mice. The western blot data also shows a significant increase in GluR1 (0.49 fold, p = 0.001; Figure 5D) levels after rhGH treatment.

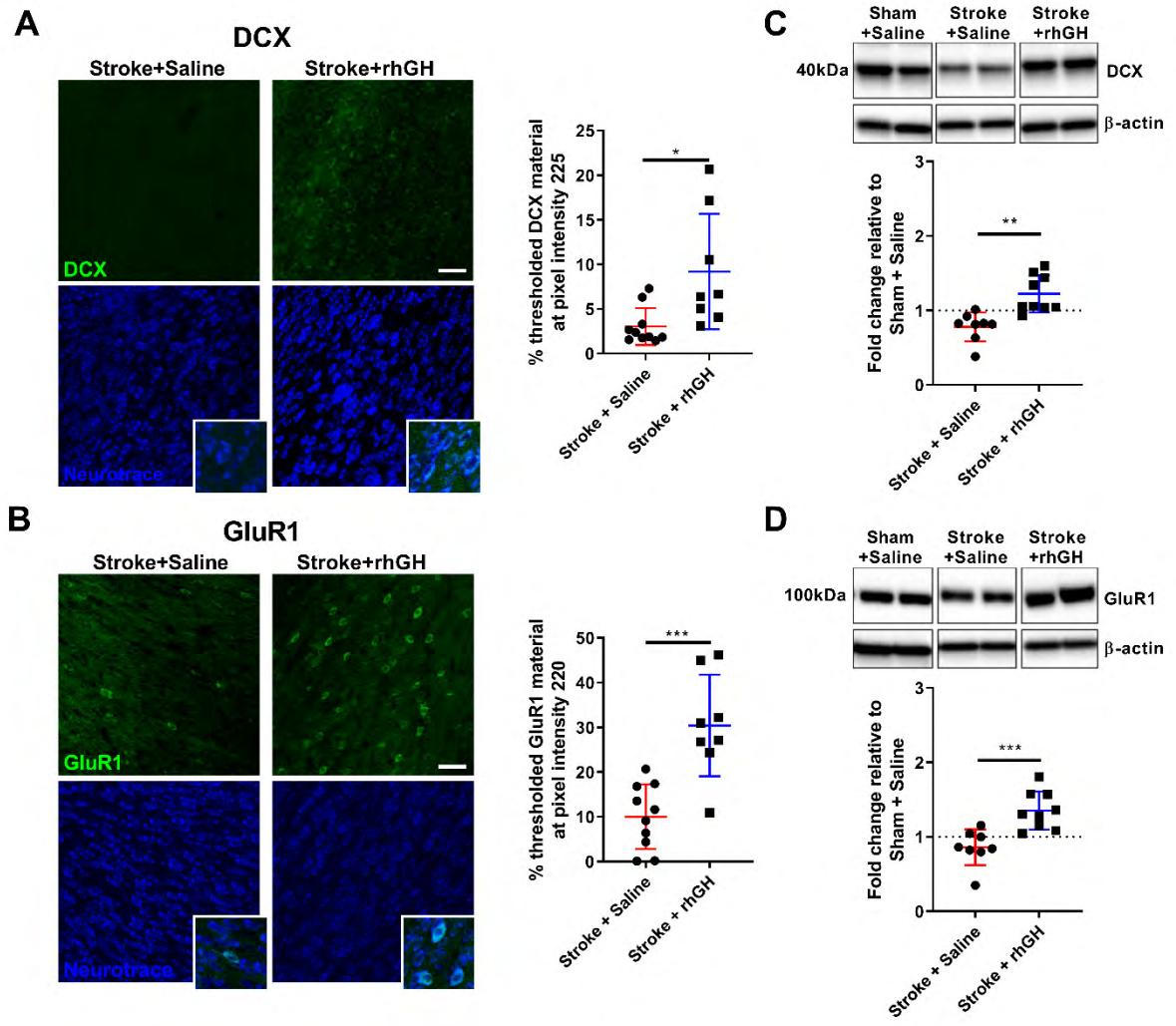

Figure 5. Increased expression of both DCX and GluR1 in the peri-infarct region after rhGH treatment. **(A)** Representative confocal images of peri-infarct areas co-labelled with DCX (green) and Neurotrace (blue) and high magnification (Scale bar = 50 μm). Quantification of material thresholded at the pixel intensity 225 shows an increase in DCX-positive structures after rhGH treatment. **(B)** Representative confocal images of peri-infarct areas co-labelled with GluR1 (green) and Neurotrace (blue), and high magnification (Scale bar = 50 μm). Quantification of material thresholded at the pixel intensity 220 shows increased GluR1-positive structures after rhGH treatment. **(C)** Representative western blot and quantification using anti-DCX antibody within the peri-infarct region. Quantification revealed increased expression of DCX in rhGH treated mice. **(D)** Representative western blot and quantification using anti-GluR1 antibody within the peri-infarct region. Quantification revealed increased expression of GluR1 in rhGH treated mice. Mean±SD. *p<0.05, **p<0.01 and ***p<0.001.

2.6. GH treatment promotes angiogenesis within the peri-infarct region

We next analysed the brain vasculature after rhGH treatment (Figure 6A). To assess vascular density, we used Lectin as a blood vessel staining and we performed a digital reconstruction of vessels for analysis of the immunofluorescence images. We found a significant increase in the percentage area covered by Lectin within the peri-infarct region in stroke mice treated with rhGH compared with saline treatment (18.20%, p = 0.0129; Figure 6B).

To assess whether the BrdU-positive cells have differentiated into endothelial cells, we performed co-labelling analyses of BrdU with Lectin. We found that rhGH treatment post-stroke significantly increased the number BrdU-Lectin-positive cells (98.91%, p = 0.0103; Figure 6C).

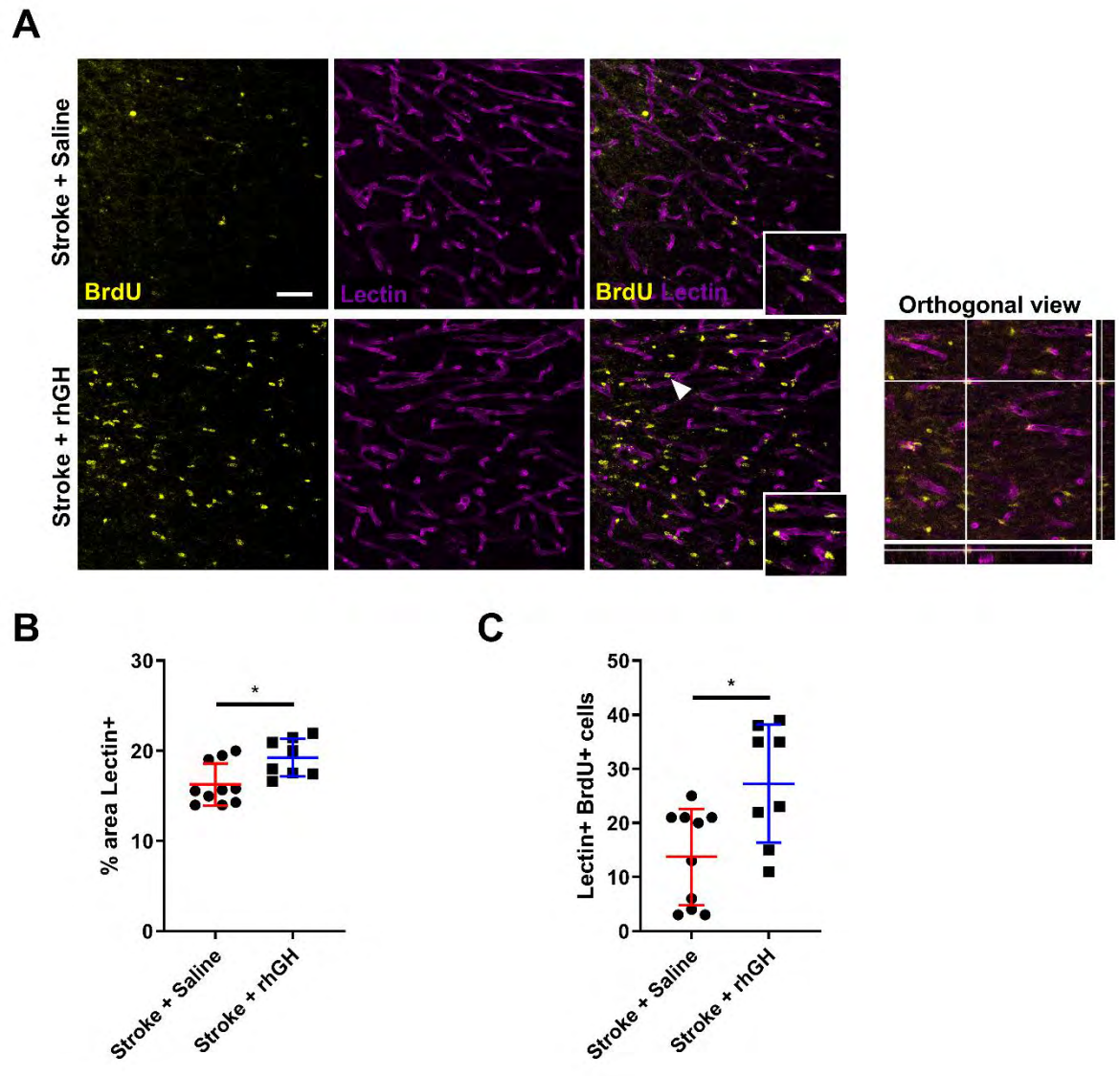

Figure 6. rhGH treatment promotes angiogenesis in the peri-infarct region post-stroke. **(A)** Representative immunofluorescence images of cells co-labelled with BrdU (yellow) and Lectin (purple) and orthogonal view (far right). The white arrowhead shows a cell visualized in orthogonal view. (Scale bar = 50 μm). rhGH treatment post-stroke significantly increased the % of area that was positive for Lectin (**B)** and the number of BrdU-Lectin-positive cells **(C).** Mean±SD. *p<0.05.

3. Discussion

The main finding of the present study is that GH treatment improves motor function after experimental stroke. Specifically, GH treatment for 28 days starting 48 hours post photothrombotic stroke significantly improved motor function, when compared with non–GH-treated stroke mice. Motor function was assessed using two different tasks; and in both tasks, GH treatment significantly improved motor deficits. GH treatment reduced the preference for spontaneous use of ipsilateral forelimbs during the cylinder task and decreased the number of foot-faults on grid walk task. Secondly, we studied selected neurorestorative processes, which have been previously linked to motor improvement. We observed an increased in proliferation of progenitor cells, neurogenesis, increased synaptic plasticity and angiogenesis within the peri-infarct area. Collectively, these results provide novel evidence supporting the use of GH after stroke to enhance known neurorestorative processes within the peri-infarct region, leading to an improvement in motor function.

In our previous study, we demonstrated that GH treatment post-stroke stimulates cognitive recovery in mice [39]. However, we did not investigate whether GH could improve motor function after stroke. Currently, therapies that promote functional motor recovery after stroke are exclusively limited to physical rehabilitation and secondary prevention, with only a modest degree of recovery [45]. While rehabilitation plays an important role in recovery from stroke, a pharmacological therapy to enhance this recovery would be highly desirable. GH is a particularly interesting option due its approval profile, efficacy and safety. Furthermore, there is now building evidence demonstrating that GH treatment in addition to standard rehabilitation can significantly contribute to the motor recovery of an acquired brain injury [9-24,37,46,47]. For instance, Heredia et al. [18,37] observed that administration of GH subcutaneously together with rehabilitation significantly improved motor function in rats as measured by the paw-reaching-for-food task. Therefore, we were motivated to extend the existing preclinical literature to consider GH treatment for its ability to ameliorate motor impairments after stroke [14].

In the present study, we aimed to investigate the effect of GH alone on motor function using a photothrombotic stroke model. Specifically, we utilised a battery of tests to assess the impact of GH on motor function. The cylinder and grid walk tests are standard motor function assessments, which have been extensively validated and used in experimental stroke studies [48]. As expected, photothrombotic vascular occlusion of the motor and somatosensory cortices resulted in a clear impairment of motor function at 1 day post-stroke which persisted for up to 30 days. The stroke mice showed preferential use of the unaffected forelimb and an increase in foot faults when using the impaired limb(s). Critically, GH treatment had a significant effect on enhancing recovery from these motor deficits at 30 days post-stroke, ameliorating the preferential use of the unaffected limb and reduction in the number of foot fault errors, thus confirming our primary hypothesis. It should be noted that our findings differ from the results from a study conducted by Pathipati et al. [14]. Although they found minor positive effects on motor recovery as assessed by a forepaw inhibition test, they did not observe any significant difference in forelimb asymmetry (cylinder task) after stroke between the GH and vehicle treatment groups. This discrepancy may be accounted for by different experimental stroke models (photothrombotic vs middle cerebral artery occlusion) and GH delivery (subcutaneous vs intracerebroventricular). In addition, we identified that GH treatment enhanced circulating levels of

IGF-1 and its primary circulating binding protein IGFBP-3. Previous studies have demonstrated the effect of IGF-1, a primary mediator of GH, on improving motor function after stroke [49,50]. Our data also suggests that higher circulatory levels of IGF-1 are associated with better motor outcomes.

To extend our understanding of the mechanisms behind the positive effects of GH on motor function, we also examined the impact of GH in known neurorestorative processes. Specifically, we focused on proliferation of progenitor cells, neurogenesis, synaptic plasticity and cerebrovascular remodelling. We observed a significant reduction in the tissue loss from the ipsilateral hemisphere at Bregma 0.0 mm in stroke mice treated with GH, which is consistent with our previous observation [39]. To interpret these results, we have to consider that in this study we started the GH treatment at 48h post-stroke. At this time point, most of the neurons within the infarct would have died [51] and therefore we would not link the decrease in tissue loss to a neuroprotective effect of GH. Instead, we would suggest that the reduction of tissue loss of the ipsilateral hemisphere is attributed to an increase in neurorestorative processes. To support our hypothesis, we used BrdU tagging to assess proliferating cells. We observed an increased number of BrdU-positive cells within the peri-infarct regions in stroke mice treated with GH, which is consistent with previous studies demonstrating that GH promotes cell proliferation within the central nervous system [52,53]. Critically, these progenitor cells are known to release neurotrophic factors to provide an environment which may contribute to neural network remodelling and functional recovery [54,55].

We then studied the fate of these newly proliferating cells. Firstly, we analysed the number of BrdU-NeuN-positive cells and we observed an increase in the number of these cells in stroke mice treated with GH. We would interpret that the new proliferating cells have differentiated (or matured) into neurons, supporting the idea that GH promotes neurogenesis after stroke [56]. Secondly, we considered the levels of expression of DCX, a protein mainly expressed by immature neurons in neurogenic niches [57-59]. Interestingly, previous studies have demonstrated that the number of DCX-positive cells positively correlates with recovery from functional deficits after stroke and, on the other hand, conditional ablation of DCX deteriorates both short- and long-term functional outcomes post-stroke [60-62]. Specifically, Jin et al. [61] showed that depletion of DCX exacerbated sensorimotor behavioural deficits measured by rotarod, limb placing, and elevated body swing tests. Here, we showed that GH treatment in stroke mice also resulted in a significant increase in DCX-positive structures and protein levels within the peri-infarct region. The ability for GH to promote neurogenesis within the peri-infarct region after stroke is a critical finding, as previous studies reported an association between functional motor recovery and the number of newly born neurons in the motor and somatosensory cortex after ischemic injury [63].

Synaptic plasticity is also known to play a critical role in recovery post-stroke [64]. We investigated the AMPA receptor subunit GluR1, which is implicated in synapse formation, stabilization, and plasticity [65-67]. Previous studies have indicated that an enhancement in synaptic plasticity, specifically AMPA signalling, promotes motor recovery after stroke [68]. Clarkson et al. [68] showed that positive allosteric modulators of AMPA receptors enhance motor recovery when administered after stroke, while AMPA receptor antagonists impair motor recovery in a photothrombotic stroke model. Here, we identified an increase in GluR1-positive structures and protein levels within the peri-infarct region post-stroke in the GH treated group. This finding further supports that GH plays an

important role in synaptogenesis after stroke, as we previously observed an increase in the protein levels and density of synapsin-1 after GH treatment in a stroke model [39].

Post-stroke angiogenesis is an essential process to restore brain function, leading to functional recovery [69]. Over several weeks after stroke, spontaneous proliferation of capillary endothelial cells and a gradual increase of revascularization has been observed [70-72]. Furthermore, most of the neurorestorative agents that improve functional outcomes after stroke or brain injury increase angiogenesis [73-77]. For instance, Chen et al. demonstrated that statins effectively enhanced motor function and this beneficial effect appeared to be mediated by an increased in angiogenesis, neurogenesis and synaptogenesis [76,78]. In addition, GH has been previously associated with angiogenesis in various areas of the brain. Sonntag et al. demonstrated that GH treatment increases cerebrocortical arteriolar density in aged rats [79]. It is therefore reasonable to propose that angiogenesis might be upregulated in the brain after GH treatment, and may contribute to the improvement in motor function. Here, we analysed vessel density in the peri-infarct area using immunofluorescence labelled tomato-Lectin, which binds to glycoproteins located in the glycocalyx and in the basal membrane of endothelial cells [80]. Our results indicate that GH increases vessel density and area coverage at day 30 days post-stroke. Critically, we observed an increase in the number of BrdU-Lectin-positive cells in the mice treated with GH following stroke, suggesting that GH has the ability to enhance angiogenesis. These findings align with our previous study where we showed that GH has a positive effect on cerebrovascular remodelling by increased density and area coverage of both cluster of differentiation 31 (CD31) and collagen-IV–positive cells, which are typical endothelial cells markers commonly used to identify blood vessels.

One potential limitation of this study is that we did not considered the effect of GH on inflammatory processes after stroke. It is well documented that neuroinflammation also plays an important role in the pathophysiology of acute brain ischemia. Such phenomena are characterized by rapid activation of microglia, astrogliosis, infiltration of peripheral immune cells and production of pro-inflammatory cytokines [81-87]. Interestingly, GH has been previously demonstrated to induce gliogenesis [11]. It would certainly be worthwhile to investigate the effect of GH on neuroinflammatory processes after stroke in future studies.

In conclusion, in this study we demonstrated that peripheral GH treatment improves motor function post-stroke. This motor improvement is associated with enhancement of neurorestorative processes such as cell proliferation, neurogenesis, synaptic plasticity and angiogenesis. Collectively our results reinforce the concept of using GH as a useful therapeutic tool in promoting brain recovery post-stroke. This may be clinically relevant as there are studies documenting high incidence of GH dysregulation after stroke [88-90]. While our results are encouraging and support earlier promising results from our group and others, further research should consider how long after the initial stroke we could start the treatment, what would be the optimal dose and timing required to promote functional recovery and how long after the cessation of the treatment do the positive outcomes persist for, as well as the interaction of the treatment with common comorbidities. Further, the usage of GH as an adjuvant during rehabilitation after stroke should be considered. We propose that GH appears to represent a promising therapeutic intervention after stroke and should be considered for clinical studies.

4. Materials and Methods

4.1. Animals

Male C57BL/6 mice (10 weeks; n = 48) were provided by the Animal Services Unit at the University of Newcastle. Mice were housed in cages with food and water available *ad libitum* in a temperature-(21˚C±1) and humidity-controlled environment. The room lighting was set on a 12:12 hour reverse light–dark cycle with lights on at 19:00. All animal procedures were conducted during the dark phase. Prior to the initiation of the experiments, mice were allowed to acclimatise to the environment for seven days. Experiments were approved by the University of Newcastle Animal Care and Ethics Committee (A-2014-432) and conducted in accordance with the New South Wales Animals Research Act and the Australian Code of Practice for the use of animals for scientific purposes. The ARRIVE guidelines (Animal Research: Reporting of In Vivo Experiments) were adhered for all animal procedures. Mice were randomized into the experimental groups. Behavioural assessments, histological and biochemistry analyses were performed in a blinded manner (see Supplementary Figure 1 for details about animal number and inclusion/exclusion criteria).

4.2. Sample size calculation

Sample size was estimated using G*Power 3.1 software. Calculations were made based on previous data on rhGH treatment after experimental stroke [39], we obtained an effect size of d=1.6. Allowing a type 1 error of 5%, α=0.05, with the power of 80%, β=0.2, we calculated a samples size of 8 animals per group.

4.3. Experimental design

The first cohort of mice (n=24) was used to investigate the neurorestorative effects of rhGH in promoting motor function recovery, and to explore the underlying mechanisms using histological analysis (see Figure 1A for timeline). Day 0, all mice underwent photothrombotic occlusion. Treatment with rhGH (1.4 mg/kg body weight per day) or saline began on Day 2. rhGH was delivered subcutaneously via mini-osmotic pumps and continued for 28 days. At day 3 post-stroke, mice were injected with BrdU (50 mg/kg body weight/day, Sigma-Aldrich, USA) continuing for 5 consecutive days. Motor function was assessed one day prior to stroke (pre-stroke), Day 2 (post-stroke) and at 29 days post-stroke (post-treatment). On day 30, mice were euthanized using sodium pentabarbitol. Plasma samples were collected for analysis of insulin-like growth factor 1 (IGF-1) and insulin-like growth factor-binding protein 3 (IGFBP-3) levels using ELISA kits. After blood was collected, mice were perfused and brains collected for histological analysis.

The second cohort of mice (n=24) was generated for protein biochemical analysis of the peri-infarct territory. Day 0, all mice were randomly allocated to receive either photothrombotic occlusion or sham surgery. Treatment with rhGH (1.4 mg/kg body weight per day, or saline control) or saline began on Day 2, subcutaneously via mini-osmotic pumps for 28 days. Mice were sacrificed on day 30 and brains collected for biochemical analysis.

4.4. Photothrombotic occlusion

Photothrombotic occlusion was performed as described previously [91-93]. Firstly, mice were anesthetized with 2% isoflurane and placed on a temperature controlled (37°C ± 1) stereotaxic frame. Mice received an intraperitoneal injection of Rose Bengal (200 μl, 10 mg/ml solution in sterile saline, Sigma-Aldrich, USA) or sterile saline (0.9% NaCl, Pfizer, Australia) before the skull was exposed by incision of the skin. At 8 min post-injection, a cold light source (4.5 mm diameter) was placed on the skull at 2.2 mm left lateral of Bregma 0.0 mm for 15 min.

4.5. Mini-osmotic pump placement

Mini-osmotic pump placement was performed as previously described [94]. Briefly, at 48 hours post-stroke, mice were anaesthetized with 2% isoflurane. An incision was made in the skin between the scapulae to create a subcutaneous space for the mini-osmotic pumps (Model 2004, Alzet, USA). The mini-osmotic pumps were filled with 200 μl of either rhGH (Somatropin 10 mg/1.5 mL, SciTropin A, SciGen, Australia) or sterile saline. The pumps deliver 0.25 μl/hour for 28 days (0.04 mg rhGH per day). After the pump was placed into the subcutaneous space, the skin incision was closed with staples. The surgical procedure was performed in a temperature- (37°C±1) controlled environment.

4.6. Motor test

As outlined in the experimental design, motor tests were performed one day pre-stroke, one day post-stroke and at 29 days post-stroke.

Forelimb asymmetry was assessed by a ***cylinder test*** as previously described [86,92,95]. Briefly, each mouse was placed in a glass cylinder. The locomotor activity was recorded using video cameras from two different angles. The first forelimb to touch the wall of the cylinder during a full rear was scored as a wall placement. When both forelimbs (left and right) simultaneously touched the wall of the cylinder, it was considered as one placement for each forelimb. A total of 20 forelimb placements per mouse were scored by a blinded researcher. The forelimb asymmetry score was calculated as the ratio of non-impaired forelimb placement minus impaired forelimb placement to total forelimb placement.

Deficits in limb placement were evaluated by ***grid walk test*** as previously described [92,95]. Briefly, each mouse was placed on a grid (2x2 cm^2) elevated from the ground. The locomotor activity was recorded using video cameras from two different angles. A 'foot fault' was scored when a mouse failed to place their paw on the bars of the grid. The number of foot faults on each side was counted over a total of 60 steps by a blinded researcher. A foot fault index was calculated as the ratio of non-impaired foot faults minus impaired foot faults to the total number of steps.

4.7. ELISA

Commercially available ELISA kits were used to measure plasma levels of IGF-1 (mouse/rat IGF-1 Quantikine ELISA (MG100; R&D systems, MN)) and IGFBP-3 (mouse IGFBP-3 ELISA (EMIGFBP3; Thermo Fisher Scientific)), according to the manufacturer's instructions.

4.8. Histological Analysis

The first cohort of mice were perfused transcardially using 0.9% saline followed by 4% paraformaldehyde (pH 7.4, both solutions kept in ice). Brains were collected and post-fixed for 4 hours in 4% paraformaldehyde. Brains were then transferred to a 12.5% sucrose solution in 0.1M PBS and stored until sliced. Brains were sliced (coronal sections) using a freezing microtome (Leica, North Ryde, NSW, Australia) at a thickness of 30 μm and kept in an antifreeze solution at 4°C. Fixed brains were later used for histological analyses.

Cresyl violet staining was performed as previously described [86]. Coronal brain sections (2 sections per brain, Bregma 0.0 and -2.0mm) were mounted on glass slides and allowed to dry for 1 hour. Sections were defatted in chloroform: consisting of submersion in ethanol solution for 8 min, followed by rehydration in absolute ethanol, 95% ethanol and 70% ethanol. Sections were stained in Cresyl Violet solution for 15 min. Then, sections were washed in 70% ethanol, 95% ethanol, differentiating solution and absolute ethanol. Finally, the sections were cleared in xylene and cover slipped.

Immunofluorescence staining performed as previously described [85,96]. Free-floating fixed sections were rinsed in PBS, and 3% bovine serum albumin was used to block non-specific binding. For BrdU staining, antigen retrieval was performed before the blocking step as follows: 10 min HCl (1M) incubation on ice, 10 min HCl (2M) incubation at room temperature, 20 min HCl (2M) incubation at 37°C, 10 min borate buffer (0.1M) incubation at room temperature and three washes in PBS + 0.1% triton. Sections were incubated with the appropriate primary antibody (DCX, GluR1, BrdU, NeuN) overnight at 4°C. After the primary antibody incubation, sections were washed and incubated in corresponding secondary antibodies for 2h at room temperature (see table 1 for antibody concentrations and acronym description). For blood vessel detection, lectin staining was performed together with the secondary antibody incubation. Finally, brain sections were mounted on glass slides, air-dried and cover slipped.

4.9. Image acquisition and analysis

Cresyl Violet images were acquired at 20x magnification using Aperio AT2 (Leica, Germany). The estimated tissue loss area was determined as the area of contralateral hemisphere - area of ipsilateral hemisphere using ImageJ software. Bregma levels 0.0 and -2.0 mm were used for analyses.

Co-immunofluorescence high resolution images of the peri-infarct area (Figure 1B) were taken on a Leica TCS SP8 confocal microscope with a Leica HC PLC APO 10x/0.40 objective. For the peri-infarct region of interest, 30 μm z-stacks with a step size of 1 μm were taken. Imaging parameters (laser power, resolution and gain) were held constant throughout all imaging sessions. Exhaustive automated BrdU and NeuN cell counts were performed using ImageJ software (Supplementary Figure 2A). For analysis of DCX and GluR1 labelling, we performed thresholding analyses and chose the optimal pixel intensity that clearly reflected the immunofluorescence signal (Supplementary Figure 2C). To measure vessel coverage (% Lectin-positive area), Lectin emission image was uniformly thresholded at a high stringency (Supplementary Figure 2B). The area of vessel coverage was expressed as a percentage of the overall image (ImageJ Software). For BrdU-NeuN-positive and BrdU-Lectin-positive co-labelling,

we used the plugin 'colocalization' for ImageJ. The colocalized points of two 8-bits images were highlighted by this plugin, and will appear as black points (Supplementary Figure 2D).

4.10. Protein extraction and western blotting

The second cohort of mice were transcardially perfused with cold 0.9% saline for 3 min. Brains were dissected, snap frozen in isopentane and stored at -80°C. A cryostat (-20°C) was used to slice the brains (coronal sections) at a thickness of 200 μm. The peri-infarct territory (2 mm^2 around infarct core, Bregma +1.0 to -1.0 mm) of each section was punched using a 1 mm tissue punch. Samples were stored in -80°C for further biochemical analysis.

Protein extraction and subsequent western blotting were performed as previously described [91,97,98]. Briefly, peri-infarct tissue samples (Figure 1B) were sonicated in 300 μl lysis buffer. The components of the lysis buffer were 1% SDS, 1 mM ethylenediaminetetraacetic acid, 1 mM dithiothreitol, 80 μM ammoniummolybdate, 1 mM sodium pyrophosphate, 1 mM sodium vanadate, 5 mM β-glycerolphosphate, 1 protease inhibitor cocktail tablet, 1 phosphatase inhibitor cocktail tablet in 50 mM TRIS buffer pH 7.4. The samples were centrifuged at 14000 G for 20 min at 4°C. Then, supernatants were collected into new tubes to separate from the pellet fractions. For determination of protein concentration, a Pierce BCA protein assay kit was used (Thermo Fisher Scientific, USA) per manufacturer's instructions. All supernatant samples were adjusted to 1.5mg/ml. The samples were mixed with sample buffer (2% SDS, 50 mM Tris, 10% glycerol, 1% DTT, 0.1% bromophenol blue, pH 6.8). For western blotting, 15 μg of lysate was loaded per lane and electrophoresed to Biorad Criterion TGC Stain-Free 4–20% gels. Gels were transferred to polyvinylidene fluoride membranes. After transferring, membranes were blocked with 5% skim milk for 1 h at room temperature. Then, membranes were incubated with the primary antibody (DCX or GluR1, see table 1 for antibody concentrations) in a rocking plate overnight at 4°C. The following day, membranes were washed with tris-buffered saline, 0.1% Tween and incubated with the appropriate secondary antibody for 1 h at room temperature. Membranes were visualized on an Amersham Imager 600 using Luminata Classico western blotting detection reagent. The Amersham Imager 600 analysis software was used to analyse the density of the bands.

4.11. Statistical analyses

All data were analysed using GraphPad Prism v7.02 and are expressed as mean ± SD. Tissue loss and motor test data were analysed using 2-way analysis of variance (ANOVA) followed by Sidak multiple comparisons. ELISA, western blotting and immunofluorescence labelling were analysed using 2-tailed t-tests. Pearson correlation was used to determine the association between motor performance and plasma IGF-1. A p value <0.05 was considered statistically significant.

Table 1. List of antibodies used for western blot and immunofluorescence analyses.

Targets	Description	Sources of Antibodies	Application	Dilution
BrdU	Bromodeoxyuridine (BrdU) is used as a marker for the proliferation of cells [40]. It is a synthetic nucleoside analog of thymidine that is incorporated into the DNA of actively replicating cells.	Sigma-Aldrich, mouse anti-BrdU, #B8434	IF	1:1000
NeuN	Neuronal nuclei (NeuN) is a nuclear protein expressed in most neurons of the nervous systems [99]. It is a marker for mature neurons.	Cell Signalling, rabbit anti-NeuN (D3S31), #12943	IF	1:1000
DCX	Doublecortin (DCX) is a microtubule associated protein that stabilises and bundles microtubules. It is expressed by neuronal precursor cells and immature neurons [41]	abcam, rabbit anti-doublecortin, #ab18723	WB IF	1:1000 1:1000
GluR1	AMPA receptor 1 (GluR1) is an ionotropic glutamate-gated ion channel. GluR1 is implicated in synapse formation, stabilisation and plasticity [44]. GluR1 is necessary for expression of long-term potentiation in the hippocampus and formation of short-term memory [100].	Cell Signalling, rabbit anti-AMPA Receptor 1 (GluA1), #13185	WB IF	1:2000 1:1000
β-actin	β-actin is a cytoskeletal housekeeping protein.	Sigma-Aldrich, Monoclonal Anti-β-actin-HRP antibody, A3854	WB	1:50000
NeuroTrace	NeuroTrace fluorescent Nissl stain is selective for the Nissl substance present in neurons [101]. Nissl substance is composed of ribosomal RNA associated with the rough endoplasmic reticulum in neuronal perikarya and dendrites.	ThermoFisher Scientific, NeuroTrace™ 640/660 Deep-Red Fluorescent Nissl Stain, #N21483	IF	1:1000
Lectin	Tomato lectin is a common stain for blood vessels. Lectin binds to carbohydrate components of endothelial cells [80].	Vecton Laboratories, DyLight 649 Lycopersicon esculentum (Tomato) lectin #DL-1178	IF	1:1000
Rabbit IgG	Secondary antibody.	Biorad, Anti-Rabbit-HRP antibody, #170-6515 ThermoFisher Scientific, anti-Rabbit IgG (H + L) Highly Cross-Adsorbed Secondary Antibody, Alexa Fluor 488, #A21206	WB IF	1:7500 1:400
Mouse IgG	Secondary antibody.	ThermoFisher Scientific, anti-Mouse IgG (H + L) Highly Cross-Adsorbed Secondary Antibody, Alexa Fluor 594, #A21203	IF	1:400

WB, western blot; IF, immunofluorescence.

Supplementary Materials: Supplementary materials can be found at www.mdpi.com/xxx/s1.

Author Contributions: All authors have read and agree to the published version of the manuscript. Conceptualization, S.S.B., J.I and L.K.O.; Data curation, S.S.B. and L.K.O; Formal analysis, S.S.B., J.I. and L.K.O.; Funding acquisition, F.R.W., M.N., J.I. and L.K.O.; Methodology, S.S.B. and L.K.O.; Supervision, F.RW., M.N., J.I. and L.K.O.; Writing – original draft, S.S.B and L.K.O.; Writing – review & editing, S.S.B., N.D.Å., P.C., F.R.W, M.N., J.I. and L.K.O.

Funding: This study was funded by the Swedish Government (ALFGBG-74390), University of Gothenburg, Hunter Medical Research Institute, Faculty of Health and Medicine Pilot Grant, Priority Research Centre for Stroke and Brain Injury Research Support Grant, Mary Costello Alzheimer's Pilot Grant and The University of Newcastle, Australia. LKO and SSB also acknowledge support from Research Advantage for ECR Higher Degree by Research (HDR) Scholarship and Greaves Family Postgraduate Scholarships in Medical Research. NDÅ was supported by grants from the Swedish state under the agreement between the Swedish Government (ALFGBG-719761, ALFGBG-751111).

Acknowledgments: We would like to acknowledge the insights and comments provided by Dr Rebecca Hood on early versions of the manuscript.

Conflicts of Interest: The authors declare no conflict of interest. The funders had no role in the design of the study; in the collection, analyses, or interpretation of data; in the writing of the manuscript, or in the decision to publish the results

Abbreviations

GH	Growth hormone
rhGH	Recombinant human growth hormone
BrdU	Bromodeoxyuridine
IGF-1	Insulin-like growth factor 1
IGFBP-3	Insulin-like growth factor-binding protein 3
CL	Contralateral
IL	Ipsilateral
NeuN	Neuronal nuclei
DCX	Doublecortin
GluR1	AMPA Receptor 1
CD31	Cluster of differentiation 31
ELISA	Enzyme-linked immunosorbent assay

References

1. Mackay, J.; Mensah, G.A. *The atlas of heart disease and stroke*; World Health Organization: 2004.
2. Hankey, G.J.; Jamrozik, K.; Broadhurst, R.J.; Forbes, S.; Anderson, C.S. Long-term disability after first-ever stroke and related prognostic factors in the Perth Community Stroke Study, 1989-1990. *Stroke* **2002**, *33*, 1034-1040, doi:10.1161/01.str.0000012515.66889.24.
3. Langhorne, P.; Bernhardt, J.; Kwakkel, G. Stroke rehabilitation. *Lancet* **2011**, *377*, 1693-1702, doi:10.1016/s0140-6736(11)60325-5.
4. Langhorne, P.; Coupar, F.; Pollock, A. Motor recovery after stroke: a systematic review. *The Lancet. Neurology* **2009**, *8*, 741-754, doi:10.1016/s1474-4422(09)70150-4.
5. Johansson, B.B. Current trends in stroke rehabilitation. A review with focus on brain plasticity. *Acta Neurol Scand* **2011**, *123*, 147-159, doi:10.1111/j.1600-0404.2010.01417.x.
6. Arya, K.N.; Pandian, S.; Verma, R.; Garg, R.K. Movement therapy induced neural reorganization and motor recovery in stroke: a review. *J Bodyw Mov Ther* **2011**, *15*, 528-537, doi:10.1016/j.jbmt.2011.01.023.
7. Brewer, L.; Horgan, F.; Hickey, A.; Williams, D. Stroke rehabilitation: recent advances and future therapies. *Qjm* **2013**, *106*, 11-25, doi:10.1093/qjmed/hcs174.

8. Efficacy and safety of very early mobilisation within 24 h of stroke onset (AVERT): a randomised controlled trial. *Lancet* **2015**, *386*, 46-55, doi:10.1016/s0140-6736(15)60690-0.
9. Scheepens, A.; Sirimanne, E.S.; Breier, B.H.; Clark, R.G.; Gluckman, P.D.; Williams, C.E. Growth hormone as a neuronal rescue factor during recovery from CNS injury. *Neuroscience* **2001**, *104*, 677-687, doi:10.1016/s0306-4522(01)00109-9.
10. Shin, D.H.; Lee, E.; Kim, J.W.; Kwon, B.S.; Jung, M.K.; Jee, Y.H.; Kim, J.; Bae, S.R.; Chang, Y.P. Protective effect of growth hormone on neuronal apoptosis after hypoxia-ischemia in the neonatal rat brain. *Neurosci Lett* **2004**, *354*, 64-68, doi:10.1016/j.neulet.2003.09.070.
11. Aberg, N.D.; Brywe, K.G.; Isgaard, J. Aspects of growth hormone and insulin-like growth factor-I related to neuroprotection, regeneration, and functional plasticity in the adult brain. *ScientificWorldJournal* **2006**, *6*, 53-80, doi:10.1100/tsw.2006.22.
12. Isgaard, J.; Aberg, D.; Nilsson, M. Protective and regenerative effects of the GH/IGF-I axis on the brain. *Minerva Endocrinol* **2007**, *32*, 103-113.
13. Christophidis, L.J.; Gorba, T.; Gustavsson, M.; Williams, C.E.; Werther, G.A.; Russo, V.C.; Scheepens, A. Growth hormone receptor immunoreactivity is increased in the subventricular zone of juvenile rat brain after focal ischemia: a potential role for growth hormone in injury-induced neurogenesis. *Growth hormone & IGF research : official journal of the Growth Hormone Research Society and the International IGF Research Society* **2009**, *19*, 497-506, doi:10.1016/j.ghir.2009.05.001.
14. Pathipati, P.; Surus, A.; Williams, C.E.; Scheepens, A. Delayed and chronic treatment with growth hormone after endothelin-induced stroke in the adult rat. *Behav Brain Res* **2009**, *204*, 93-101, doi:10.1016/j.bbr.2009.05.023.
15. Devesa, P.; Reimunde, P.; Gallego, R.; Devesa, J.; Arce, V.M. Growth hormone (GH) treatment may cooperate with locally-produced GH in increasing the proliferative response of hippocampal progenitors to kainate-induced injury. *Brain Inj* **2011**, *25*, 503-510, doi:10.3109/02699052.2011.559611.
16. Li, R.C.; Guo, S.Z.; Raccurt, M.; Moudilou, E.; Morel, G.; Brittian, K.R.; Gozal, D. Exogenous growth hormone attenuates cognitive deficits induced by intermittent hypoxia in rats. *Neuroscience* **2011**, *196*, 237-250, doi:10.1016/j.neuroscience.2011.08.029.
17. Alba-Betancourt, C.; Luna-Acosta, J.L.; Ramirez-Martinez, C.E.; Avila-Gonzalez, D.; Granados-Avalos, E.; Carranza, M.; Martinez-Coria, H.; Aramburo, C.; Luna, M. Neuro-protective effects of growth hormone (GH) after hypoxia-ischemia injury in embryonic chicken cerebellum. *Gen Comp Endocrinol* **2013**, *183*, 17-31, doi:10.1016/j.ygcen.2012.12.004.
18. Heredia, M.; Palomero, J.; de la Fuente, A.; Criado, J.M.; Yajeya, J.; Devesa, J.; Devesa, P.; Vicente-Villardon, J.L.; Riolobos, A.S. Motor Improvement of Skilled Forelimb Use Induced by Treatment with Growth Hormone and Rehabilitation Is Dependent on the Onset of the Treatment after Cortical Ablation. *Neural Plast* **2018**, *2018*, 6125901, doi:10.1155/2018/6125901.
19. Devesa, J.; Reimunde, P.; Devesa, A.; Souto, S.; Lopez-Amado, M.; Devesa, P.; Arce, V.M. Recovery from neurological sequelae secondary to oncological brain surgery in an adult growth hormone-deficient patient after growth hormone treatment. *J Rehabil Med* **2009**, *41*, 775-777, doi:10.2340/16501977-0416.
20. High, W.M., Jr.; Briones-Galang, M.; Clark, J.A.; Gilkison, C.; Mossberg, K.A.; Zgaljardic, D.J.; Masel, B.E.; Urban, R.J. Effect of growth hormone replacement therapy on cognition after traumatic brain injury. *J Neurotrauma* **2010**, *27*, 1565-1575, doi:10.1089/neu.2009.1253.
21. Reimunde, P.; Quintana, A.; Castanon, B.; Casteleiro, N.; Vilarnovo, Z.; Otero, A.; Devesa, A.; Otero-Cepeda, X.L.; Devesa, J. Effects of growth hormone (GH) replacement and cognitive rehabilitation in patients with cognitive disorders after traumatic brain injury. *Brain Inj* **2011**, *25*, 65-73, doi:10.3109/02699052.2010.536196.
22. Moreau, O.K.; Cortet-Rudelli, C.; Yollin, E.; Merlen, E.; Daveluy, W.; Rousseaux, M. Growth hormone replacement therapy in patients with traumatic brain injury. *J Neurotrauma* **2013**, *30*, 998-1006, doi:10.1089/neu.2012.2705.

23. Song, J.; Park, K.; Lee, H.; Kim, M. The effect of recombinant human growth hormone therapy in patients with completed stroke: a pilot trial. *Ann Rehabil Med* **2012**, *36*, 447-457, doi:10.5535/arm.2012.36.4.447.
24. Devesa, J.; Devesa, P.; Reimunde, P.; Arce, V. Growth hormone and kynesitherapy for brain injury recovery. In *Brain Injury-Pathogenesis, Monitoring, Recovery and Management*, IntechOpen: 2012.
25. Lobie, P.E.; Garcia-Aragon, J.; Lincoln, D.T.; Barnard, R.; Wilcox, J.N.; Waters, M.J. Localization and ontogeny of growth hormone receptor gene expression in the central nervous system. *Brain research. Developmental brain research* **1993**, *74*, 225-233, doi:10.1016/0165-3806(93)90008-x.
26. Blackmore, D.G.; Reynolds, B.A.; Golmohammadi, M.G.; Large, B.; Aguilar, R.M.; Haro, L.; Waters, M.J.; Rietze, R.L. Growth hormone responsive neural precursor cells reside within the adult mammalian brain. *Scientific reports* **2012**, *2*, 250, doi:10.1038/srep00250.
27. Bianchi, V.E.; Locatelli, V.; Rizzi, L. Neurotrophic and Neuroregenerative Effects of GH/IGF1. *Int J Mol Sci* **2017**, *18*, doi:10.3390/ijms18112441.
28. Ohab, J.J.; Carmichael, S.T. Poststroke neurogenesis: emerging principles of migration and localization of immature neurons. *Neuroscientist* **2008**, *14*, 369-380, doi:10.1177/1073858407309545.
29. Dancause, N.; Barbay, S.; Frost, S.B.; Plautz, E.J.; Chen, D.; Zoubina, E.V.; Stowe, A.M.; Nudo, R.J. Extensive cortical rewiring after brain injury. *J Neurosci* **2005**, *25*, 10167-10179, doi:10.1523/jneurosci.3256-05.2005.
30. Li, S.; Overman, J.J.; Katsman, D.; Kozlov, S.V.; Donnelly, C.J.; Twiss, J.L.; Giger, R.J.; Coppola, G.; Geschwind, D.H.; Carmichael, S.T. An age-related sprouting transcriptome provides molecular control of axonal sprouting after stroke. *Nat Neurosci* **2010**, *13*, 1496-1504, doi:10.1038/nn.2674.
31. Jin, K.; Minami, M.; Lan, J.Q.; Mao, X.O.; Batteur, S.; Simon, R.P.; Greenberg, D.A. Neurogenesis in dentate subgranular zone and rostral subventricular zone after focal cerebral ischemia in the rat. *Proceedings of the National Academy of Sciences of the United States of America* **2001**, *98*, 4710-4715, doi:10.1073/pnas.081011098.
32. Kannangara, T.S.; Carter, A.; Xue, Y.; Dhaliwal, J.S.; Beique, J.C.; Lagace, D.C. Excitable Adult-Generated GABAergic Neurons Acquire Functional Innervation in the Cortex after Stroke. *Stem Cell Reports* **2018**, *11*, 1327-1336, doi:10.1016/j.stemcr.2018.10.011.
33. Arvidsson, A.; Collin, T.; Kirik, D.; Kokaia, Z.; Lindvall, O. Neuronal replacement from endogenous precursors in the adult brain after stroke. *Nature medicine* **2002**, *8*, 963-970, doi:10.1038/nm747.
34. Parent, J.M.; Vexler, Z.S.; Gong, C.; Derugin, N.; Ferriero, D.M. Rat forebrain neurogenesis and striatal neuron replacement after focal stroke. *Annals of neurology* **2002**, *52*, 802-813, doi:10.1002/ana.10393.
35. Zhang, R.L.; Zhang, Z.G.; Zhang, L.; Chopp, M. Proliferation and differentiation of progenitor cells in the cortex and the subventricular zone in the adult rat after focal cerebral ischemia. *Neuroscience* **2001**, *105*, 33-41, doi:10.1016/s0306-4522(01)00117-8.
36. Gu, W.; Brannstrom, T.; Wester, P. Cortical neurogenesis in adult rats after reversible photothrombotic stroke. *Journal of cerebral blood flow and metabolism : official journal of the International Society of Cerebral Blood Flow and Metabolism* **2000**, *20*, 1166-1173, doi:10.1097/00004647-200008000-00002.
37. Heredia, M.; Fuente, A.; Criado, J.; Yajeya, J.; Devesa, J.; Riolobos, A.S. Early growth hormone (GH) treatment promotes relevant motor functional improvement after severe frontal cortex lesion in adult rats. *Behav Brain Res* **2013**, *247*, 48-58, doi:10.1016/j.bbr.2013.03.012.
38. Heredia, M.; Rodríguez, N.; Sánchez Robledo, V.; Criado, J.M.; de la Fuente, A.; Devesa, J.; Devesa, P.; Sánchez Riolobos, A. Factors Involved in the Functional Motor Recovery of Rats with Cortical Ablation after GH and Rehabilitation Treatment: Cortical Cell Proliferation and

Nestin and Actin Expressions in Striatum and Thalamus. . *Preprint* **2019**, 10.20944/preprints201910.0165.v1, doi:10.20944/preprints201910.0165.v1.
39. Ong, L.K.; Chow, W.Z.; TeBay, C.; Kluge, M.; Pietrogrande, G.; Zalewska, K.; Crock, P.; Aberg, N.D.; Bivard, A.; Johnson, S.J., et al. Growth Hormone Improves Cognitive Function After Experimental Stroke. *Stroke* **2018**, *49*, 1257-1266, doi:10.1161/strokeaha.117.020557.
40. Duque, A.; Rakic, P. Different effects of bromodeoxyuridine and [3H]thymidine incorporation into DNA on cell proliferation, position, and fate. *J Neurosci* **2011**, *31*, 15205-15217, doi:10.1523/jneurosci.3092-11.2011.
41. Brown, J.P.; Couillard-Despres, S.; Cooper-Kuhn, C.M.; Winkler, J.; Aigner, L.; Kuhn, H.G. Transient expression of doublecortin during adult neurogenesis. *J Comp Neurol* **2003**, *467*, 1-10, doi:10.1002/cne.10874.
42. Ayanlaja, A.A.; Xiong, Y.; Gao, Y.; Ji, G.; Tang, C.; Abdikani Abdullah, Z.; Gao, D. Distinct Features of Doublecortin as a Marker of Neuronal Migration and Its Implications in Cancer Cell Mobility. *Frontiers in molecular neuroscience* **2017**, *10*, 199, doi:10.3389/fnmol.2017.00199.
43. Couillard-Despres, S.; Winner, B.; Schaubeck, S.; Aigner, R.; Vroemen, M.; Weidner, N.; Bogdahn, U.; Winkler, J.; Kuhn, H.G.; Aigner, L. Doublecortin expression levels in adult brain reflect neurogenesis. *Eur J Neurosci* **2005**, *21*, 1-14, doi:10.1111/j.1460-9568.2004.03813.x.
44. Cull-Candy, S.; Kelly, L.; Farrant, M. Regulation of Ca2+-permeable AMPA receptors: synaptic plasticity and beyond. *Curr Opin Neurobiol* **2006**, *16*, 288-297, doi:10.1016/j.conb.2006.05.012.
45. Dobkin, B.H. Training and exercise to drive poststroke recovery. *Nat Clin Pract Neurol* **2008**, *4*, 76-85, doi:10.1038/ncpneuro0709.
46. Devesa, J.; Reimunde, P.; Devesa, P.; Barbera, M.; Arce, V. Growth hormone (GH) and brain trauma. *Horm Behav* **2013**, *63*, 331-344, doi:10.1016/j.yhbeh.2012.02.022.
47. Devesa, J.; Diaz-Getino, G.; Rey, P.; Garcia-Cancela, J.; Loures, I.; Nogueiras, S.; Hurtado de Mendoza, A.; Salgado, L.; Gonzalez, M.; Pablos, T., et al. Brain Recovery after a Plane Crash: Treatment with Growth Hormone (GH) and Neurorehabilitation: A Case Report. *Int J Mol Sci* **2015**, *16*, 30470-30482, doi:10.3390/ijms161226244.
48. Schaar, K.L.; Brenneman, M.M.; Savitz, S.I. Functional assessments in the rodent stroke model. *Exp Transl Stroke Med* **2010**, *2*, 13, doi:10.1186/2040-7378-2-13.
49. Liu, X.F.; Fawcett, J.R.; Thorne, R.G.; DeFor, T.A.; Frey, W.H., 2nd. Intranasal administration of insulin-like growth factor-I bypasses the blood-brain barrier and protects against focal cerebral ischemic damage. *J Neurol Sci* **2001**, *187*, 91-97, doi:10.1016/s0022-510x(01)00532-9.
50. Zhu, W.; Fan, Y.; Frenzel, T.; Gasmi, M.; Bartus, R.T.; Young, W.L.; Yang, G.Y.; Chen, Y. Insulin growth factor-1 gene transfer enhances neurovascular remodeling and improves long-term stroke outcome in mice. *Stroke* **2008**, *39*, 1254-1261, doi:10.1161/strokeaha.107.500801.
51. Buscemi, L.; Price, M.; Bezzi, P.; Hirt, L. Spatio-temporal overview of neuroinflammation in an experimental mouse stroke model. *Scientific reports* **2019**, *9*, 507, doi:10.1038/s41598-018-36598-4.
52. Aberg, N.D.; Johansson, I.; Aberg, M.A.; Lind, J.; Johansson, U.E.; Cooper-Kuhn, C.M.; Kuhn, H.G.; Isgaard, J. Peripheral administration of GH induces cell proliferation in the brain of adult hypophysectomized rats. *J Endocrinol* **2009**, *201*, 141-150, doi:10.1677/joe-08-0495.
53. David Aberg, N.; Lind, J.; Isgaard, J.; Georg Kuhn, H. Peripheral growth hormone induces cell proliferation in the intact adult rat brain. *Growth hormone & IGF research : official journal of the Growth Hormone Research Society and the International IGF Research Society* **2010**, *20*, 264-269, doi:10.1016/j.ghir.2009.12.003.
54. Li, B.; Piao, C.S.; Liu, X.Y.; Guo, W.P.; Xue, Y.Q.; Duan, W.M.; Gonzalez-Toledo, M.E.; Zhao, L.R. Brain self-protection: the role of endogenous neural progenitor cells in adult brain after cerebral cortical ischemia. *Brain research* **2010**, *1327*, 91-102, doi:10.1016/j.brainres.2010.02.030.
55. Zhao, L.R.; Willing, A. Enhancing endogenous capacity to repair a stroke-damaged brain: An evolving field for stroke research. *Progress in neurobiology* **2018**, *163-164*, 5-26, doi:10.1016/j.pneurobio.2018.01.004.

56. Lindvall, O.; Kokaia, Z. Neurogenesis following Stroke Affecting the Adult Brain. *Cold Spring Harbor perspectives in biology* **2015**, *7*, doi:10.1101/cshperspect.a019034.
57. Jin, K.; Sun, Y.; Xie, L.; Peel, A.; Mao, X.O.; Batteur, S.; Greenberg, D.A. Directed migration of neuronal precursors into the ischemic cerebral cortex and striatum. *Mol Cell Neurosci* **2003**, *24*, 171-189.
58. Keiner, S.; Witte, O.W.; Redecker, C. Immunocytochemical detection of newly generated neurons in the perilesional area of cortical infarcts after intraventricular application of brain-derived neurotrophic factor. *J Neuropathol Exp Neurol* **2009**, *68*, 83-93, doi:10.1097/NEN.0b013e31819308e9.
59. Kunze, A.; Achilles, A.; Keiner, S.; Witte, O.W.; Redecker, C. Two distinct populations of doublecortin-positive cells in the perilesional zone of cortical infarcts. *BMC Neurosci* **2015**, *16*, 20, doi:10.1186/s12868-015-0160-8.
60. Kunze, A.; Grass, S.; Witte, O.W.; Yamaguchi, M.; Kempermann, G.; Redecker, C. Proliferative response of distinct hippocampal progenitor cell populations after cortical infarcts in the adult brain. *Neurobiol Dis* **2006**, *21*, 324-332, doi:10.1016/j.nbd.2005.07.013.
61. Jin, K.; Wang, X.; Xie, L.; Mao, X.O.; Greenberg, D.A. Transgenic ablation of doublecortin-expressing cells suppresses adult neurogenesis and worsens stroke outcome in mice. *Proceedings of the National Academy of Sciences of the United States of America* **2010**, *107*, 7993-7998, doi:10.1073/pnas.1000154107.
62. Sun, F.; Wang, X.; Mao, X.; Xie, L.; Jin, K. Ablation of neurogenesis attenuates recovery of motor function after focal cerebral ischemia in middle-aged mice. *PLoS One* **2012**, *7*, e46326, doi:10.1371/journal.pone.0046326.
63. Ohab, J.J.; Fleming, S.; Blesch, A.; Carmichael, S.T. A neurovascular niche for neurogenesis after stroke. *J Neurosci* **2006**, *26*, 13007-13016, doi:10.1523/jneurosci.4323-06.2006.
64. Murphy, T.H.; Corbett, D. Plasticity during stroke recovery: from synapse to behaviour. *Nature reviews. Neuroscience* **2009**, *10*, 861-872, doi:10.1038/nrn2735.
65. Hollmann, M.; Heinemann, S. Cloned glutamate receptors. *Annu Rev Neurosci* **1994**, *17*, 31-108, doi:10.1146/annurev.ne.17.030194.000335.
66. Dingledine, R.; Borges, K.; Bowie, D.; Traynelis, S.F. The glutamate receptor ion channels. *Pharmacol Rev* **1999**, *51*, 7-61.
67. Lu, W.; Isozaki, K.; Roche, K.W.; Nicoll, R.A. Synaptic targeting of AMPA receptors is regulated by a CaMKII site in the first intracellular loop of GluA1. *Proceedings of the National Academy of Sciences of the United States of America* **2010**, *107*, 22266-22271, doi:10.1073/pnas.1016289107.
68. Clarkson, A.N.; Overman, J.J.; Zhong, S.; Mueller, R.; Lynch, G.; Carmichael, S.T. AMPA receptor-induced local brain-derived neurotrophic factor signaling mediates motor recovery after stroke. *J Neurosci* **2011**, *31*, 3766-3775, doi:10.1523/jneurosci.5780-10.2011.
69. Ergul, A.; Alhusban, A.; Fagan, S.C. Angiogenesis: a harmonized target for recovery after stroke. *Stroke* **2012**, *43*, 2270-2274, doi:10.1161/strokeaha.111.642710.
70. Li, Y.; Lu, Z.; Keogh, C.L.; Yu, S.P.; Wei, L. Erythropoietin-induced neurovascular protection, angiogenesis, and cerebral blood flow restoration after focal ischemia in mice. *Journal of cerebral blood flow and metabolism : official journal of the International Society of Cerebral Blood Flow and Metabolism* **2007**, *27*, 1043-1054, doi:10.1038/sj.jcbfm.9600417.
71. Hayashi, T.; Noshita, N.; Sugawara, T.; Chan, P.H. Temporal profile of angiogenesis and expression of related genes in the brain after ischemia. *Journal of cerebral blood flow and metabolism : official journal of the International Society of Cerebral Blood Flow and Metabolism* **2003**, *23*, 166-180, doi:10.1097/01.Wcb.0000041283.53351.Cb.
72. Yanev, P.; Seevinck, P.R.; Rudrapatna, U.S.; Bouts, M.J.; van der Toorn, A.; Gertz, K.; Kronenberg, G.; Endres, M.; van Tilborg, G.A.; Dijkhuizen, R.M. Magnetic resonance imaging of local and remote vascular remodelling after experimental stroke. *Journal of cerebral blood flow and metabolism : official journal of the International Society of Cerebral Blood Flow and Metabolism* **2017**, *37*, 2768-2779, doi:10.1177/0271678x16674737.

73. Zhang, Z.G.; Chopp, M. Neurorestorative therapies for stroke: underlying mechanisms and translation to the clinic. *The Lancet. Neurology* **2009**, *8*, 491-500, doi:10.1016/s1474-4422(09)70061-4.
74. Xiong, Y.; Mahmood, A.; Chopp, M. Angiogenesis, neurogenesis and brain recovery of function following injury. *Current opinion in investigational drugs (London, England : 2000)* **2010**, *11*, 298-308.
75. Zhang, Y.; Xiong, Y.; Mahmood, A.; Meng, Y.; Qu, C.; Schallert, T.; Chopp, M. Therapeutic effects of erythropoietin on histological and functional outcomes following traumatic brain injury in rats are independent of hematocrit. *Brain research* **2009**, *1294*, 153-164, doi:10.1016/j.brainres.2009.07.077.
76. Chen, J.; Zhang, Z.G.; Li, Y.; Wang, Y.; Wang, L.; Jiang, H.; Zhang, C.; Lu, M.; Katakowski, M.; Feldkamp, C.S., et al. Statins induce angiogenesis, neurogenesis, and synaptogenesis after stroke. *Annals of neurology* **2003**, *53*, 743-751, doi:10.1002/ana.10555.
77. Chopp, M.; Zhang, Z.G.; Jiang, Q. Neurogenesis, angiogenesis, and MRI indices of functional recovery from stroke. *Stroke* **2007**, *38*, 827-831, doi:10.1161/01.STR.0000250235.80253.e9.
78. Chen, J.; Zhang, C.; Jiang, H.; Li, Y.; Zhang, L.; Robin, A.; Katakowski, M.; Lu, M.; Chopp, M. Atorvastatin induction of VEGF and BDNF promotes brain plasticity after stroke in mice. *Journal of cerebral blood flow and metabolism : official journal of the International Society of Cerebral Blood Flow and Metabolism* **2005**, *25*, 281-290, doi:10.1038/sj.jcbfm.9600034.
79. Sonntag, W.E.; Lynch, C.D.; Cooney, P.T.; Hutchins, P.M. Decreases in cerebral microvasculature with age are associated with the decline in growth hormone and insulin-like growth factor 1. *Endocrinology* **1997**, *138*, 3515-3520, doi:10.1210/endo.138.8.5330.
80. Robertson, R.T.; Levine, S.T.; Haynes, S.M.; Gutierrez, P.; Baratta, J.L.; Tan, Z.; Longmuir, K.J. Use of labeled tomato lectin for imaging vasculature structures. *Histochem Cell Biol* **2015**, *143*, 225-234, doi:10.1007/s00418-014-1301-3.
81. Anrather, J.; Iadecola, C. Inflammation and Stroke: An Overview. *Neurotherapeutics : the journal of the American Society for Experimental NeuroTherapeutics* **2016**, *13*, 661-670, doi:10.1007/s13311-016-0483-x.
82. Tuttolomondo, A.; Pecoraro, R.; Casuccio, A.; Di Raimondo, D.; Butta, C.; Clemente, G.; Della Corte, V.; Guggino, G.; Arnao, V.; Maida, C., et al. Peripheral frequency of CD4+ CD28- cells in acute ischemic stroke: relationship with stroke subtype and severity markers. *Medicine* **2015**, *94*, e813, doi:10.1097/md.0000000000000813.
83. Tuttolomondo, A.; Pinto, A.; Corrao, S.; Di Raimondo, D.; Fernandez, P.; Di Sciacca, R.; Arnao, V.; Licata, G. Immuno-inflammatory and thrombotic/fibrinolytic variables associated with acute ischemic stroke diagnosis. *Atherosclerosis* **2009**, *203*, 503-508, doi:10.1016/j.atherosclerosis.2008.06.030.
84. Tuttolomondo, A.; Di Raimondo, D.; Pecoraro, R.; Casuccio, A.; Di Bona, D.; Aiello, A.; Accardi, G.; Arnao, V.; Clemente, G.; Corte, V.D., et al. HLA and killer cell immunoglobulin-like receptor (KIRs) genotyping in patients with acute ischemic stroke. *Journal of neuroinflammation* **2019**, *16*, 88, doi:10.1186/s12974-019-1469-5.
85. Kluge, M.G.; Kracht, L.; Abdolhoseini, M.; Ong, L.K.; Johnson, S.J.; Nilsson, M.; Walker, F.R. Impaired microglia process dynamics post-stroke are specific to sites of secondary neurodegeneration. *Glia* **2017**, *65*, 1885-1899, doi:10.1002/glia.23201.
86. Sanchez-Bezanilla, S.; TeBay, C.; Nilsson, M.; Walker, F.R.; Ong, L.K. Visual discrimination impairment after experimental stroke is associated with disturbances in the polarization of the astrocytic aquaporin-4 and increased accumulation of neurotoxic proteins. *Experimental neurology* **2019**, *318*, 232-243, doi:10.1016/j.expneurol.2019.05.001.
87. Jones, K.A.; Maltby, S.; Plank, M.W.; Kluge, M.; Nilsson, M.; Foster, P.S.; Walker, F.R. Peripheral immune cells infiltrate into sites of secondary neurodegeneration after ischemic stroke. *Brain, behavior, and immunity* **2018**, *67*, 299-307, doi:10.1016/j.bbi.2017.09.006.

88. Boehncke, S.; Ackermann, H.; Badenhoop, K.; Sitzer, M. Pituitary function and IGF-I levels following ischemic stroke. *Cerebrovascular diseases (Basel, Switzerland)* **2011**, *31*, 163-169, doi:10.1159/000321738.
89. Bondanelli, M.; Ambrosio, M.R.; Carli, A.; Bergonzoni, A.; Bertocchi, A.; Zatelli, M.C.; Ceruti, S.; Valle, D.; Basaglia, N.; degli Uberti, E.C. Predictors of pituitary dysfunction in patients surviving ischemic stroke. *The Journal of clinical endocrinology and metabolism* **2010**, *95*, 4660-4668, doi:10.1210/jc.2010-0611.
90. Lillicrap, T.; Garcia-Esperon, C.; Walker, F.R.; Ong, L.K.; Nilsson, M.; Spratt, N.; Levi, C.R.; Parsons, M.; Isgaard, J.; Bivard, A. Growth Hormone Deficiency Is Frequent After Recent Stroke. *Frontiers in neurology* **2018**, *9*, 713, doi:10.3389/fneur.2018.00713.
91. Ong, L.K.; Zhao, Z.; Kluge, M.; Walker, F.R.; Nilsson, M. Chronic stress exposure following photothrombotic stroke is associated with increased levels of Amyloid beta accumulation and altered oligomerisation at sites of thalamic secondary neurodegeneration in mice. *Journal of cerebral blood flow and metabolism : official journal of the International Society of Cerebral Blood Flow and Metabolism* **2017**, *37*, 1338-1348, doi:10.1177/0271678x16654920.
92. Zalewska, K.; Pietrogrande, G.; Ong, L.K.; Abdolhoseini, M.; Kluge, M.; Johnson, S.J.; Walker, F.R.; Nilsson, M. Sustained administration of corticosterone at stress-like levels after stroke suppressed glial reactivity at sites of thalamic secondary neurodegeneration. *Brain, behavior, and immunity* **2018**, *69*, 210-222, doi:10.1016/j.bbi.2017.11.014.
93. Pietrogrande, G.; Zalewska, K.; Zhao, Z.; Abdolhoseini, M.; Chow, W.Z.; Sanchez-Bezanilla, S.; Ong, L.K.; Johnson, S.J.; Nilsson, M.; Walker, F.R. Low oxygen post conditioning prevents thalamic secondary neuronal loss caused by excitotoxicity after cortical stroke. *Scientific reports* **2019**, *9*, 4841, doi:10.1038/s41598-019-39493-8.
94. Walser, M.; Hansen, A.; Svensson, P.A.; Jernas, M.; Oscarsson, J.; Isgaard, J.; Aberg, N.D. Peripheral administration of bovine GH regulates the expression of cerebrocortical beta-globin, GABAB receptor 1, and the Lissencephaly-1 protein (LIS-1) in adult hypophysectomized rats. *Growth hormone & IGF research : official journal of the Growth Hormone Research Society and the International IGF Research Society* **2011**, *21*, 16-24, doi:10.1016/j.ghir.2010.11.002.
95. Pietrogrande, G.; Zalewska, K.; Zhao, Z.; Johnson, S.J.; Nilsson, M.; Walker, F.R. Low Oxygen Post Conditioning as an Efficient Non-pharmacological Strategy to Promote Motor Function After Stroke. *Translational stroke research* **2019**, *10*, 402-412, doi:10.1007/s12975-018-0656-5.
96. Kluge, M.G.; Abdolhoseini, M.; Zalewska, K.; Ong, L.K.; Johnson, S.J.; Nilsson, M.; Walker, F.R. Spatiotemporal analysis of impaired microglia process movement at sites of secondary neurodegeneration post-stroke. *Journal of cerebral blood flow and metabolism : official journal of the International Society of Cerebral Blood Flow and Metabolism* **2018**, 10.1177/0271678x18797346, 271678x18797346, doi:10.1177/0271678x18797346.
97. Zhao, Z.; Ong, L.K.; Johnson, S.; Nilsson, M.; Walker, F.R. Chronic stress induced disruption of the peri-infarct neurovascular unit following experimentally induced photothrombotic stroke. *Journal of cerebral blood flow and metabolism : official journal of the International Society of Cerebral Blood Flow and Metabolism* **2017**, *37*, 3709-3724, doi:10.1177/0271678x17696100.
98. Sanchez-Bezanilla, S.; Nilsson, M.; Walker, F.R.; Ong, L.K. Can We Use 2,3,5-Triphenyltetrazolium Chloride-Stained Brain Slices for Other Purposes? The Application of Western Blotting. *Frontiers in molecular neuroscience* **2019**, *12*, 181, doi:10.3389/fnmol.2019.00181.
99. Mullen, R.J.; Buck, C.R.; Smith, A.M. NeuN, a neuronal specific nuclear protein in vertebrates. *Development* **1992**, *116*, 201-211.
100. Sanderson, D.J.; Good, M.A.; Seeburg, P.H.; Sprengel, R.; Rawlins, J.N.; Bannerman, D.M. The role of the GluR-A (GluR1) AMPA receptor subunit in learning and memory. *Prog Brain Res* **2008**, *169*, 159-178, doi:10.1016/s0079-6123(07)00009-x.
101. Benner, S.; Kakeyama, M.; Endo, T.; Yoshioka, W.; Tohyama, C. Application of NeuroTrace staining in the fresh frozen brain samples to laser microdissection combined with quantitative RT-PCR analysis. *BMC Res Notes* **2015**, *8*, 252, doi:10.1186/s13104-015-1222-9.

SUPPLEMENTARY MATERIAL

Growth hormone promotes motor function after experimental stroke and enhances recovery-promoting mechanisms within the peri-infarct area

Sonia Sanchez-Bezanilla[1,2], N. David Åberg[3,4], Patricia Crock[5], Frederick R. Walker[1,2,6,7], Michael Nilsson[1,2,6,7,8], Jörgen Isgaard[1,3,4]†, Lin Kooi Ong[1,2,6,9]†

1. School of Biomedical Sciences and Pharmacy and the Priority Research Centre for Stroke and Brain Injury, the University of Newcastle, University Dr, Callaghan, 2308, NSW, Australia
2. Hunter Medical Research Institute, Lot 1, Kookaburra Cct, New Lambton Heights, 2305, NSW, Australia
3. University of Gothenburg, 405 30 Gothenburg, Sweden
4. Department of Internal Medicine, Region Västra Götaland, Sahlgrenska University Hospital, Blå stråket 5, 413 45 Gothenburg, Sweden.
5. Department of Paediatric Endocrinology and Diabetes, John Hunter Children's Hospital, Kookaburra Cct, New Lambton Heights, 2305, NSW, Australia
6. NHMRC Centre of Research Excellence Stroke Rehabilitation and Brain Recovery, 245 Burgundy Street, Heidelberg, 3084, VIC, Australia
7. Centre for Rehab Innovations, Lot 1, Kookaburra Cct, New Lambton Heights, 2305, NSW, Australia
8. LKC School of Medicine, Nanyang Technological University, 50 Nanyang Ave, 639798 Singapore
9. Monash University Malaysia, Bandar Sunway, 47500 Subang Jaya, Selangor, Malaysia
† Contributed equally to senior authorship

Correspondence:
Lin Kooi Ong
School of Pharmacy, Monash University Malaysia, Jalan Lagoon Selatan, 47500, Bandar Sunway, Selangor, Malaysia.
E-mail: ong.linkooi@monash.edu

Jörgen Isgaard
Department of Internal Medicine University of Gothenburg and Sahlgrenska University Hospital, Gothenburg, Sweden.
E-mail jorgen.isgaard@medic.gu.se

Supplementary figures and legends

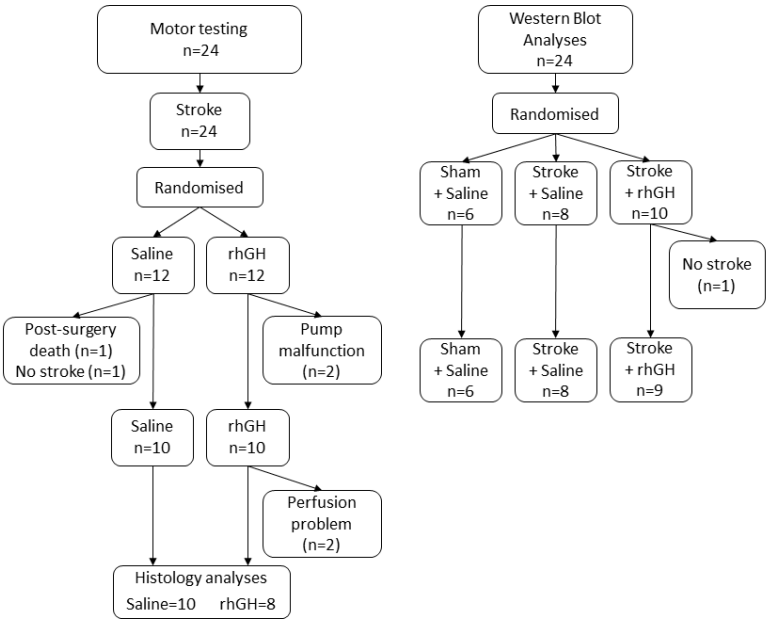

Supplementary Figure 1. Diagram for inclusion and exclusion of mice in this study. Mice were removed from the study if we histologically identified that the stroke had not occurred, or if malfunction of the mini-osmotic pumps had occurred. A total of 24 mice were used to assess motor function, and their brains were used for histological analysis (Stroke + Saline, n=12; Stroke + rhGH, n=12). A total of 24 sham mice were used for protein analysis of their brains (Sham + Saline, n=6; Stroke + Saline, n=8; Stroke + rhGH, n=10).

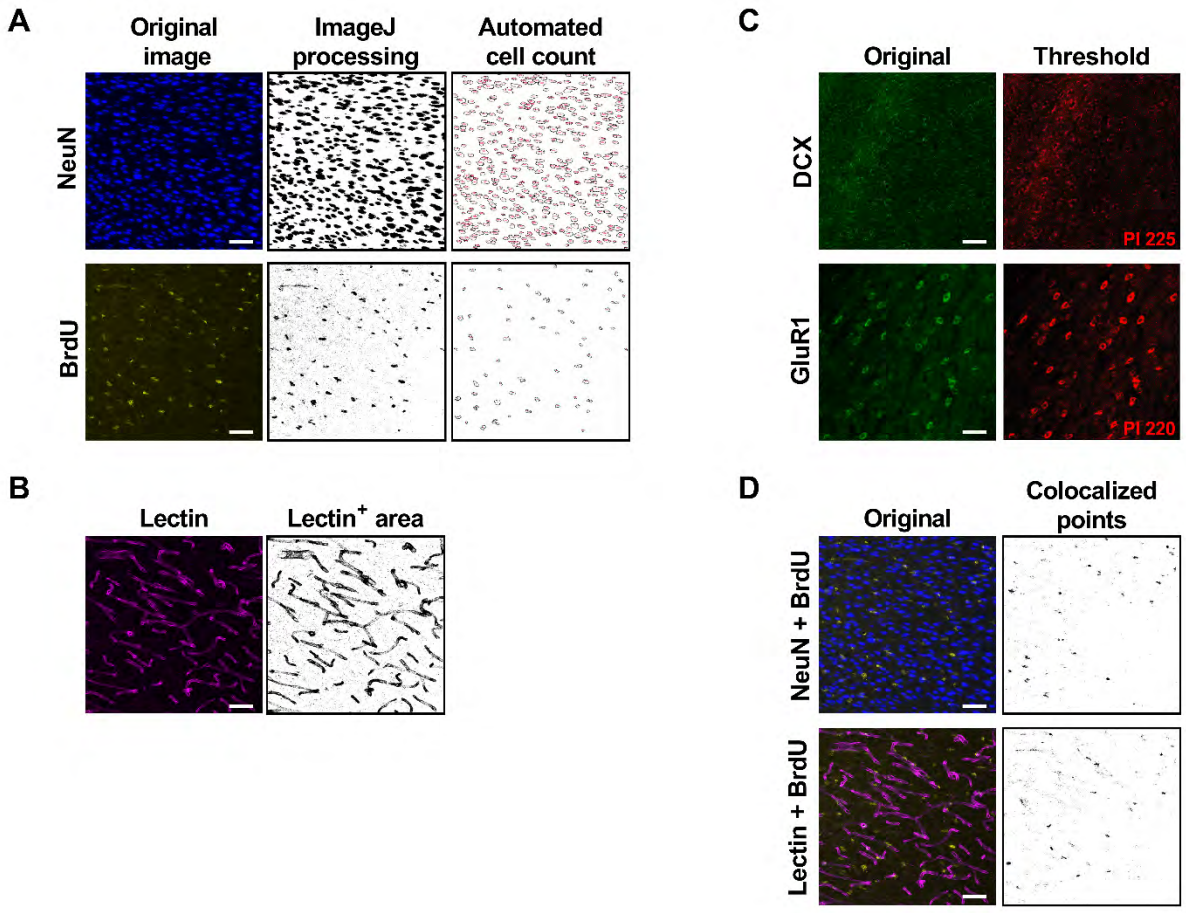

Supplementary Figure 2. Image processing and analysis. **(A)** Automated NeuN+ and BrdU+ cell counts were undertaken in the peri-infarct area using ImageJ software. The original images (left) were converted into a binary image (middle) and the black particles were counted (right). **(B)** To assess the area covered by vessels, we used lectin staining. Confocal images (left) were uniformly thresholded at a high stringency (right) using ImageJ. The Lectin+ area was expressed as a percentage of the overall field of view. **(C)** To analyse the DCX and GluR1 staining, we performed thresholding analyses and chose the optimal pixel intensity that clearly reflected the immunolabelled signal using ImageJ. The left panels represent the original images. The right panels show material thresholded at the pixel intensity (PI) 220 (DCX) and 225 (GluR1). The number of pixels that were captured at and below PI 125 were then expressed as a percentage of the total number of pixels in each image and this data was used to investigate group differences. **(D)** To assess the number of BrdU+ cells that have differentiated into neurons and blood vessels, we performed co-labelling analyses. Both channels (NeuN + BrdU or Lectin + BrdU) were merged together (left images). We then used the plugin 'colocalization' within ImageJ. This plugin highlights the colocalized points of two 8-bit images. The colocalized points appear in black (right images). The black particles were counted. Scale bar for all the images = 50µm.

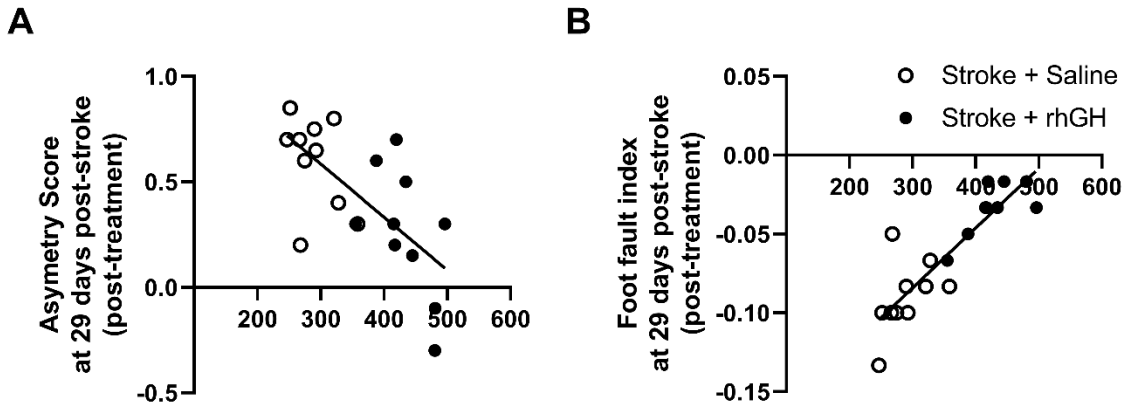

Supplementary Figure 3. Higher circulatory levels of IGF-1 are associated with better motor outcomes. **(A)** Pearson correlation analysis shows a significant positive correlation between serum IGF-1 levels and cylinder task performance post rhGH treatment (r=-0.6789; $P_{(Y = -0.002513*X + 1.339)}$=0.0010). **(B)** Pearson correlation analysis shows a significant correlation between serum IGF-1 levels and grid walk task performance post rhGH treatment (r=0.8879; $P_{(Y = 0.0003785*X - 0.1977)}$<0.0001). x-axis represents plasma IGF-1 (ng/mL).

CHAPTER 6: PUBLICATION 4

Growth hormone treatment promotes remote hippocampal plasticity after experimental cortical stroke

As per the peer-review paper accepted and published in: International Journal of Molecular Sciences

CONTRIBUTIONS

We, the co-authors, attest the Research Higher Degree candidate, Sonia Sanchez Bezanilla, contributed to the paper entitled **"Growth Hormone Treatment Promotes Remote Hippocampal Plasticity after Experimental Cortical Stroke"** as outlined below:

- 70% Conception and design of research;
- 70% Experimental procedures;
- 75% Analysis and interpretation of the findings;
- 75% Writing and critical appraisal of the content

N. David Åberg		*18/02/2020*
Name of Co-author	*Signature*	*Date*
Patricia Crock		*24/02/2020*
Name of Co-author	*Signature*	*Date*
Frederick R. Walker		*19/02/2020*
Name of Co-author	*Signature*	*Date*
Michael Nilsson		*19/02/2020*
Name of Co-author	*Signature*	*Date*
Jörgen Isgaard		*19/02/2020*
Name of Co-author	*Signature*	*Date*
Lin Kooi Ong		*19/02/2020*
Name of Co-author	*Signature*	*Date*

Lesley MacDonald-Wicks

Assistant Dean Research Training

10/3/2020

Article

Growth hormone treatment promotes remote hippocampal plasticity after experimental cortical stroke

Sonia Sanchez-Bezanilla[1,2], N. David Åberg[3,4], Patricia Crock[2,5], Frederick R. Walker[1,2,6,7], Michael Nilsson[1,2,6,7,8], Jörgen Isgaard[1,3,4]*, Lin Kooi Ong[1,2,6,9]*

1. School of Biomedical Sciences and Pharmacy and the Priority Research Centre for Stroke and Brain Injury, The University of Newcastle, NSW, Australia
2. Hunter Medical Research Institute, NSW, Australia
3. Institute of Medicine, The Sahlgrenska Academy, University of Gothenburg, Gothenburg, Sweden
4. Department of Internal Medicine, Region Västra Götaland, Sahlgrenska University Hospital, Gothenburg, Sweden.
5. Department of Paediatric Endocrinology and Diabetes, John Hunter Children's Hospital, NSW, Australia
6. NHMRC Centre of Research Excellence Stroke Rehabilitation and Brain Recovery, VIC, Australia
7. Centre for Rehab Innovations, The University of Newcastle, NSW, Australia
8. LKC School of Medicine, Nanyang Technological University, Singapore
9. Monash University Malaysia, Selangor, Malaysia

* Contributed equally to senior authorship
* Correspondence: ong.linkooi@monash.edu; jorgen.isgaard@medic.gu.se

Received: date; Accepted: date; Published: date

Abstract: Cognitive impairment is common after stroke, and disturbances in hippocampal function are often involved, even in remote non-hippocampal injuries. In terms of hippocampal function, growth hormone (GH) is known to affects plasticity and cognition. We aimed to investigate whether GH treatment after an experimental cortical stroke could enhance remote hippocampal plasticity and the hippocampal-dependent visual discrimination task. C57BL6 male mice were subjected to cortical photothrombotic stroke. Stroke mice were then treated with either saline or GH at 48hrs after occlusion for 28 days. We assessed learning and memory using mouse touchscreen platform for the visual discrimination task. We also evaluated markers of neural progenitor cells, synaptic plasticity and cerebrovascular remodelling in the hippocampal formation. GH treatment significantly improved the performance on visual discrimination task after stroke. We observed a concomitant increased number of bromodeoxyuridine-positive cells in the dentate gyrus of the hippocampus. We also detected increased protein levels and density of doublecortin, a neuronal precursor cells marker, as well as glutamate receptor 1 (GLuR1), a synaptic marker. These findings provide further neurobiological evidence for how GH treatment could be used to promote hippocampal plasticity, in a remote region from the initial cortical injury, and thus enhance cognitive recovery after stroke.

Keywords: Cognition, growth hormone, hippocampus, neurogenesis, synaptic plasticity, visual discrimination

1. Introduction

Stroke leads to cognitive impairment partly due to the disruption of hippocampal function. Recent studies provide evidence that stroke causes hippocampal structural changes and dysregulation of hippocampal networks, leading to memory decline in humans [1-5]. Interestingly, cerebral ischemia has been shown to stimulate proliferation of endogenous neural progenitor cells in animal models [6], and stroke patients [7]. Previous studies have suggested that ischemic stroke triggers increased proliferation of neural progenitor cells in hippocampal subgranular zone [8-14], and migration of these

cells to the damaged areas [15-18]. However, these potential self-repair mechanisms are thought to operate only for a restricted time period after stroke, with the number of newborn neurons being insufficient for full tissue repair and their existence being transitory [19]. Recent findings suggest that a significant portion of newborn neurons generated after stroke reveal aberrant morphology and fail to correctly integrate into pre-existing networks [20,21]. Given the capacity of this regenerative mechanism is limited, a therapeutic intervention that can stimulate neurogenesis and promote the integration of newborn neurons would be highly desirable to promote post-stroke recovery of cognition.

Interestingly, the pro-cognitive effects of growth hormone (GH) have been demonstrated in multiple neurological conditions, including traumatic brain injury [22]. GH has been shown to stimulate the genesis of neurons and endothelial cells, as well as to promote myelination and synaptogenesis [23]. Importantly, we have recently shown that GH treatment after photothrombotic vascular occlusion of the somatosensory and motor cortex, promoted a marked improvement in the performance of associative memory cognitive domain as measured by the paired-associate learning task [24]. We additionally found an enhancement of neurorestorative processes, such as increased cell proliferation, neurogenesis, increased synaptic plasticity, myelination and angiogenesis within the peri-infarct region, most likely contributing to the improvement of motor outcomes [24-28]. However, we did not investigate the pro-cognitive effects of GH treatment on other cognitive domains and possible neurorestorative changes in the hippocampus. Early studies by Pathipati at al. demonstrated that intracerebroventricular delivery of GH after experimental stroke improved spatial memory using the Morris water maze test, however, they did not investigate changes in the hippocampus [29]. Thus, there are limited studies documenting the role of GH on hippocampal plasticity in the context of stroke recovery.

Therefore, an important question that we wanted to address in the current study was how GH treatment could enhance neurorestorative processes within the hippocampus remote to a cortical stroke, thus leading to an improvement in overall post-stroke cognition. Specifically, we examined changes in the density, distribution and protein expression of markers of neural progenitor cells in the hippocampal formation, using bromodeoxyuridine (BrdU) tagging and doublecortin (DCX). We also examined changes in the AMPA receptor subunit glutamate receptor 1 (GluR1), which plays an important role in synaptic plasticity. In addition, we examined changes in cerebrovascular density, using Tomato Lectin, a blood vessel staining. We assessed the effect of GH treatment on learning and memory using mouse touchscreen platform for the hippocampal-dependent visual discrimination (VD) task [30,31].

2. Results

2.1. GH treatment improves cognitive function

Cognitive function was assessed by hippocampal-dependent VD task for 18 consecutive days (Fig. 1). We found a significant increase in % correct rate in r-hGH–treated stroke mice compared with saline ($F_{(1,18)}$=7.402, p=0.014), and a significant time effect ($F_{(5,90)}$=27.80, p<0.0001). Post hoc analysis indicated an increase in the % of correct rate at the fourth, fifth and sixth block of sessions in r-hGH–treated stroke mice (13.54%, p=0.036; 16.12%, p=0.007 and 18.52%, p=0.001, respectively). We also observed a significant increase in the number of trials completed within 60 minutes ($F_{(1,18)}$=13.00, p=0.002), and decrease in the time required to complete 30 trials ($F_{(1,18)}$=10.35, p=0.005) in r-hGH–treated stroke mice (Fig. 1B). Post hoc analysis indicated an increase in the number of trials completed within 60 minutes from the third to sixth block of sessions (11.60%, p=0.0002; 9.47%, p=0.0033; 9.80%, p=0.0022; 9.10%, p=0.0053), and a decrease in the time required to complete 30 trials from forth to sixth block of sessions (13.67%, p=0.0009; 14.28%, p=0.0005; 19.39%, p<0.0001) in r-hGH–treated stroke mice.

Pearson correlation analysis shows a significant correlation between plasma insulin-like growth factor 1 (IGF-1) levels and the performance of hippocampal-dependent VD task at the final session; percentage correct rate (r = 0.4492; P $_{(Y = 0.1102X + 30.84)}$ = 0.0469), trials completed within 60 min (r = 0.4536; P $_{(Y = 0.04704X + 7.385)}$ = 0.0446), and time to complete 30 trials (r = -0.6186; P $_{(Y = -0.1180X + 87.70)}$ = 0.0036).

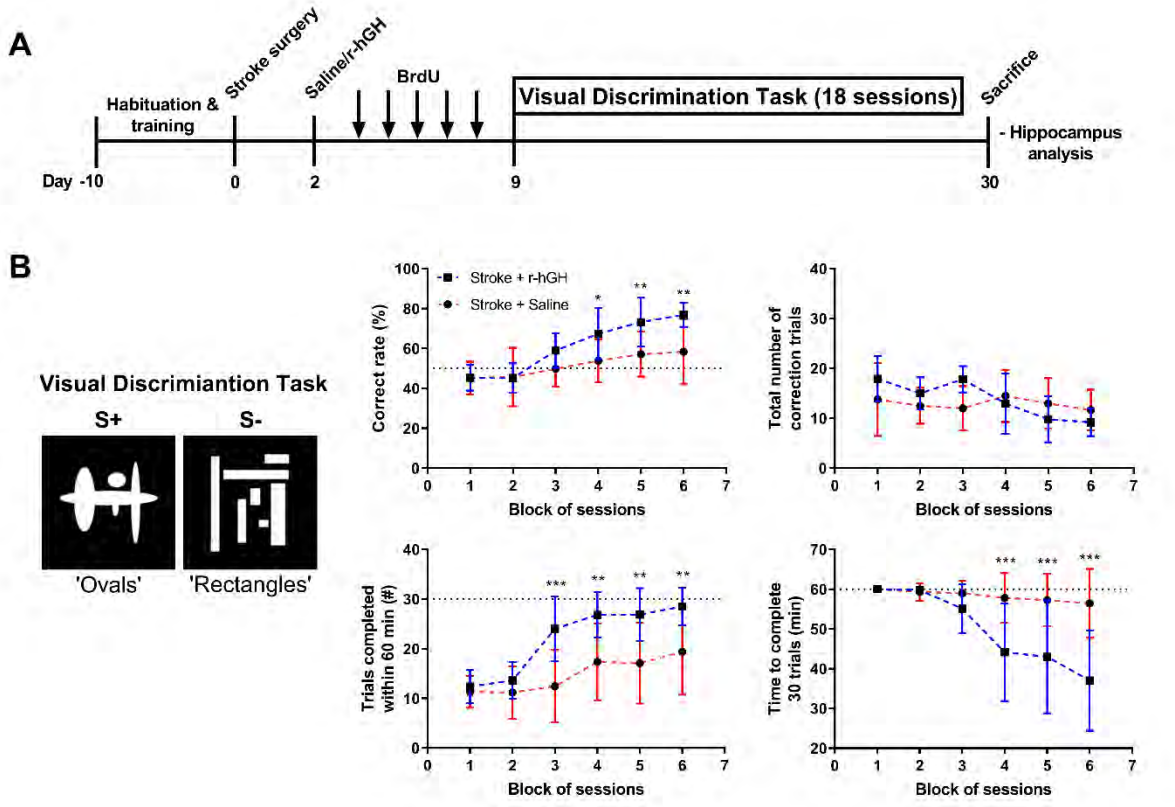

Figure 1. (A) Experimental design. **(B)** Illustration of the visual discrimination (VD) task. Images represent the pair of stimuli used for the task ('ovals-rectangles' pair) (S+ correct and S- incorrect). A variety of metrics were measured to assess cognitive performance in mice treated with recombinant human growth factor (r-hGH) compared to saline. Mean±SD (two-way ANOVA and Sidak's multiple comparisons). *p<0.05; **p<0.01 and ***p<0.001.

2.2. GH treatment promotes cell proliferation and neurogenesis in the dentate gyrus (DG)

We assessed BrdU/NeuN co-labelling and doublecortin (DCX) levels in two different sub-regions of the hippocampal formation: CA1 and DG (Fig. 2A). r-hGH treatment significantly increased the number of BrdU-positive cells in the DG (78.1%, p=0.004, Fig. 2B), but not in the CA1 (Fig. 2C). There were no differences in area of thresholded material for NeuN, NeuN protein levels and the number of BrdU-NeuN-positive cells (Fig. 2). r-hGH treatment significantly increased the material thresholded for DCX in the DG (82.0%, p=0.002, Fig. 3A). We also found a significant increase in DCX protein levels (0.25-fold, p=0.001; Fig. 3C) in r-hGH–treated stroke mice.

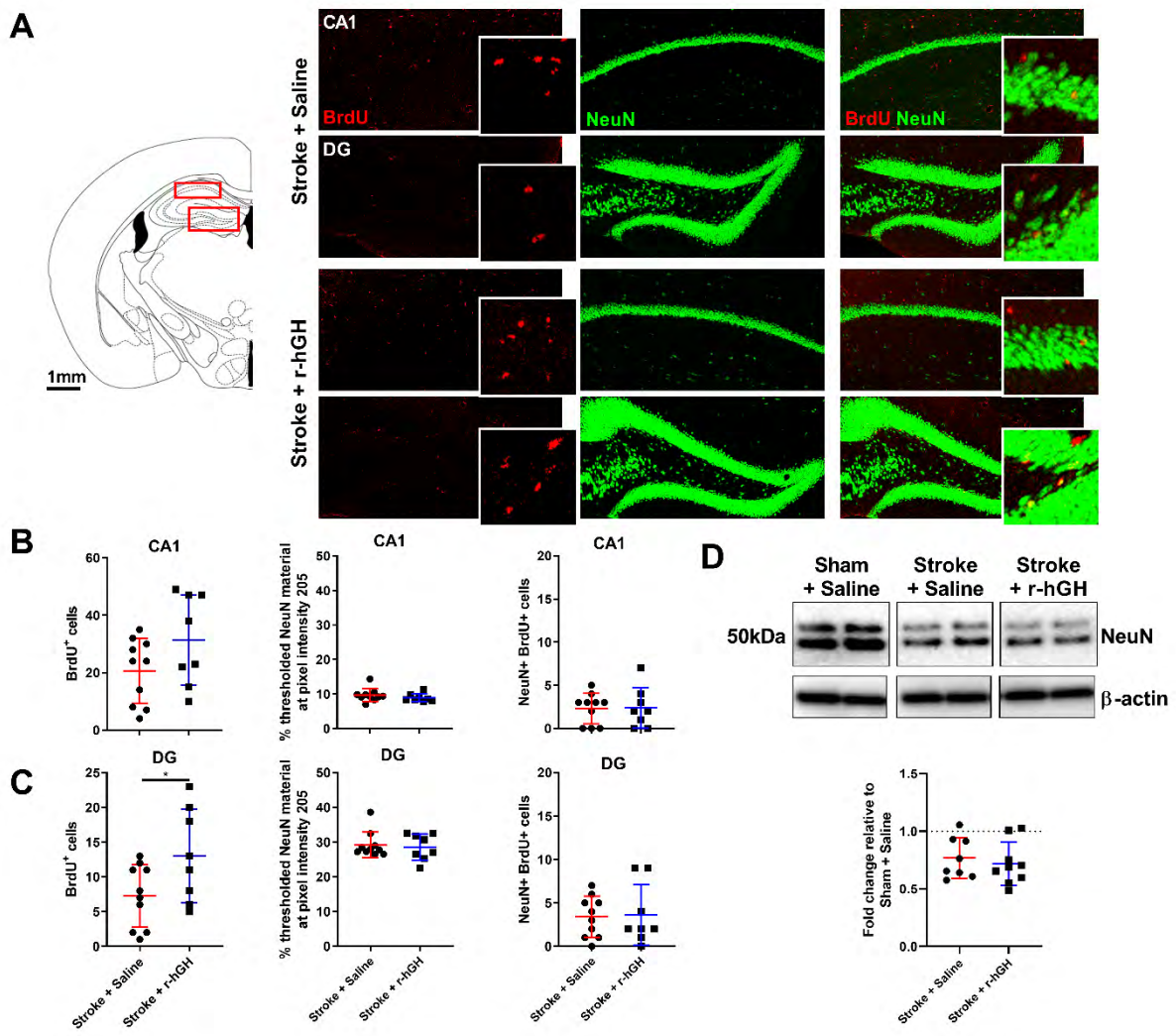

Figure 2. (A) Left panel: Schematic picture illustrating the location of the hippocampus region examined (CA1 and dentate gyrus (DG)). Right panel: Representative immunofluorescence images of bromodeoxyuridine (BrdU; red) and neuronal nuclei (NeuN; green) (scale bar=100 μm). **(B and C)** Quantification of BrdU-positive cells, thresholded NeuN material and BrdU-NeuN-positive cells in the CA1 and DG. **(D)** Representative western blot and quantification of NeuN protein levels in the hippocampus. For full immunoblots, see Supplementary Materials. Mean±SD (2-tailed t-test). *p<0.05.

2.3. GH treatment promotes expression of GluR1 within the hippocampal formation

We performed immunofluorescence analysis for a synaptic marker (GluR1) in the hippocampal formation. The immunofluorescence data revealed a significant increase in material thresholded for GluR1 in the CA1 (79.0%, p=0.007, at pixel intensity 220) and DG (113.3%, p=0.006, at pixel intensity 220) in r-hGH–treated stroke mice (Fig. 3B). Further, an increase in GluR1 protein levels (0.24-fold, p=0.001; Fig. 3D) was found in r-hGH–treated stroke mice.

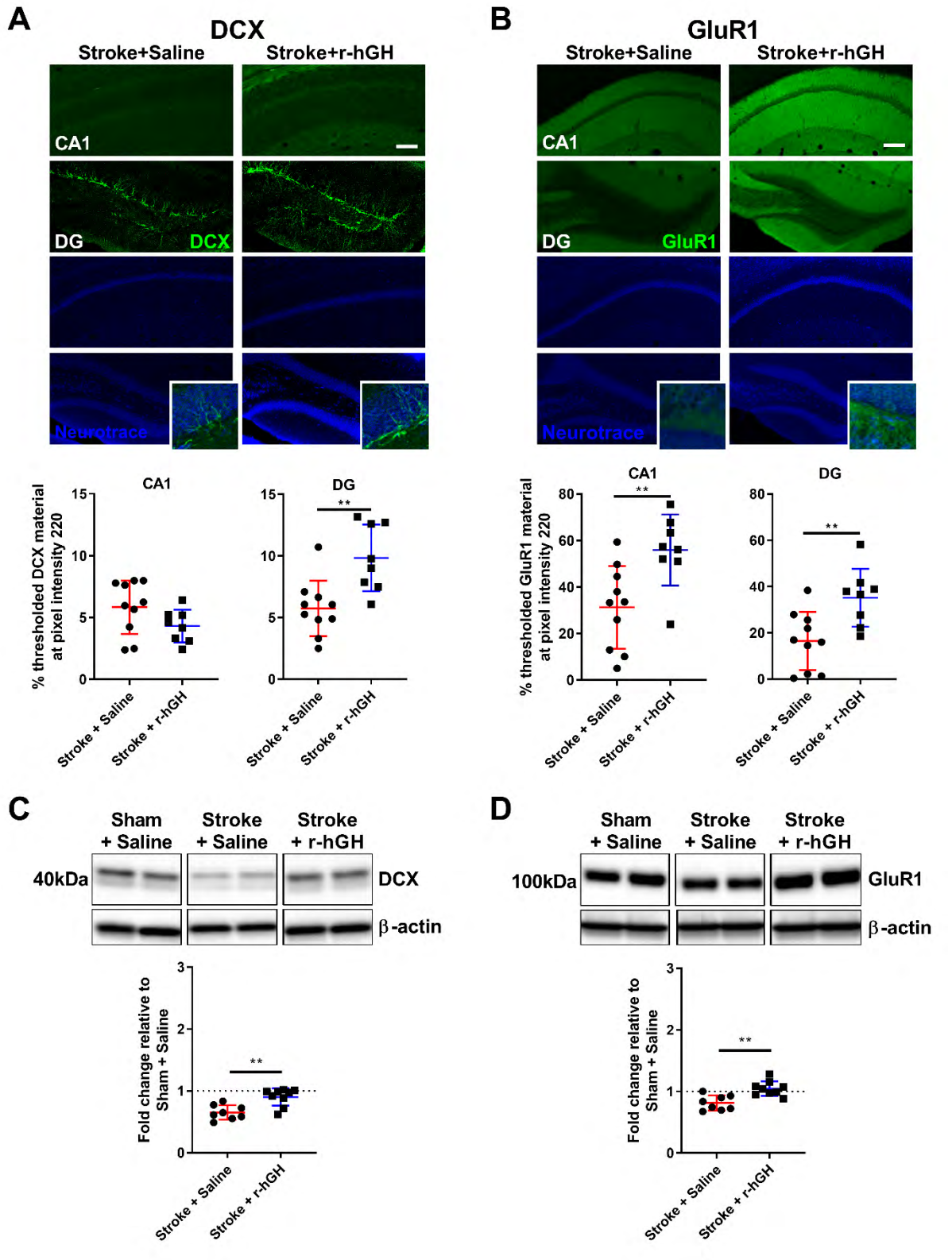

Figure 3. (A) Representative immunofluorescence images and quantification of doublecortin (DCX; green) in the CA1 and DG (scale bar=100 μm). (B) Representative immunofluorescence images and quantification of glutamate receptor 1 (GluR1; green) in the CA1 and DG (scale bar=100 μm). (C and D) Representative western blot and quantification of DCX and GluR1 protein levels in the hippocampus. For full immunoblots, see Supplementary Materials. Mean±SD (2-tailed t-test). **p<0.01.

2.4. GH treatment had no effect on the formation of cerebral vasculature within the hippocampal formation

We analysed the density of the brain vasculature in the hippocampal formation using immunofluorescence labelled Tomato Lectin, which binds to glycoproteins located in the glycocalyx and in the basal membrane of endothelial cells. We observed no statistically significant differences in the area covered by Tomato Lectin and the number BrdU-Lectin-positive cells in the hippocampal formation. Further, no significant changes in Collagen IV protein levels in r-hGH–treated stroke mice (Fig. 4).

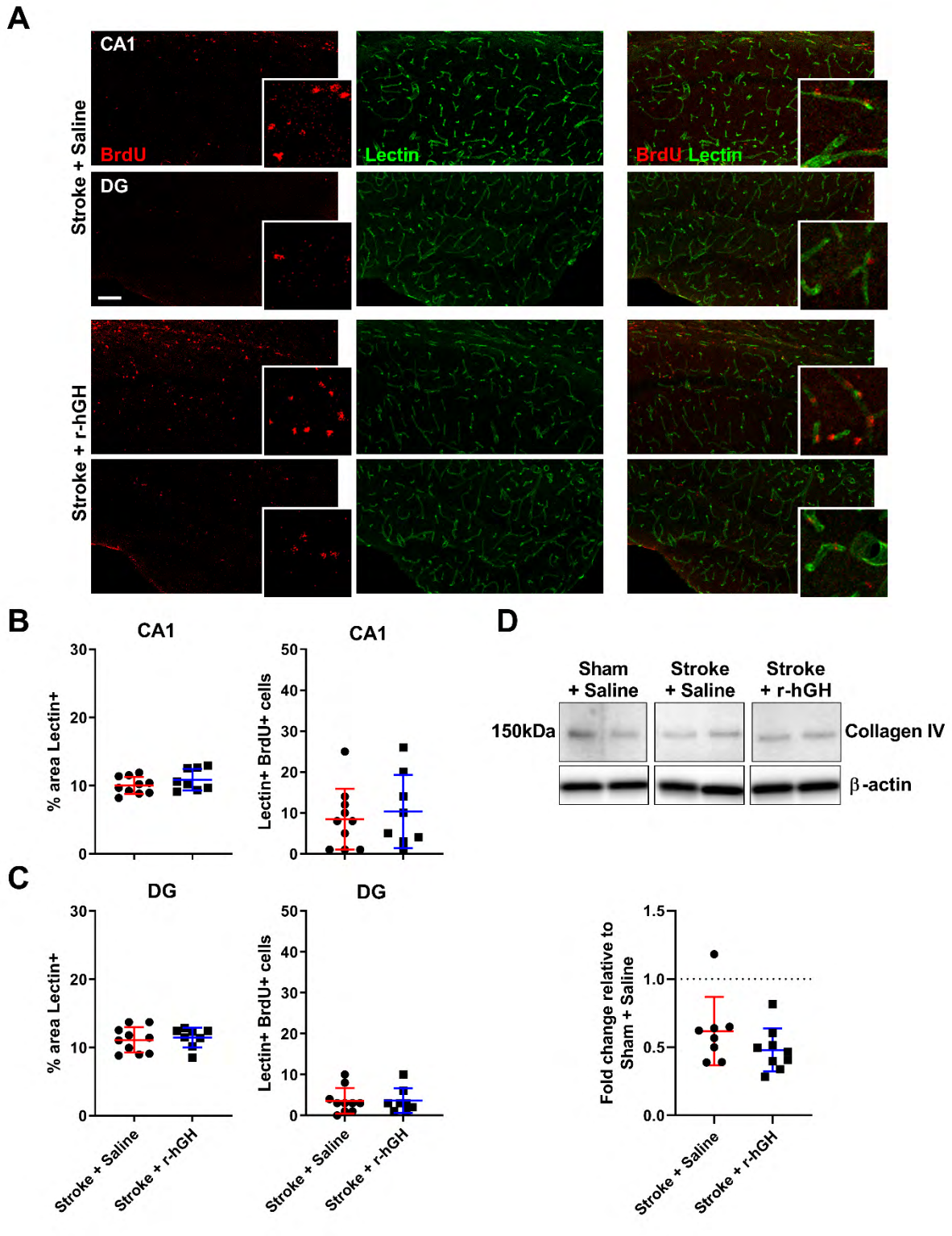

Figure 4. Analysis of cerebrovascular remodelling within the hippocampus region. **(A)** Representative immunofluorescence images of BrdU (red) and Tomato Lectin (green) and high magnification detail (scale bar=100μm) in the CA1 and DG subregion of the hippocampus. **(B)** Quantification of the number of BrdU-Lectin-positive cells and % of area covered by Tomato Lectin in the CA1. **(C)** Quantification of the number of BrdU-Lectin-positive cells and % of area covered by Tomato Lectin in the DG. There were no significant differences in any of the parameters between stroke mice treated with r-hGH and

the saline group. **(D)** Representative western blot and Collagen IV protein levels in the hippocampus. For full immunoblots, see Supplementary Materials. Mean±SD.

2.5. GH treatment promotes restoration of white matter disturbances

We evaluated white matter tract alterations in the corpus callosum using Sudan Black staining of myelin at Bregma 0.0mm and -2.0mm. We found a significant decrease in white matter structural loss in corpus callosum at Bregma 0.0mm (122.0%, p=0.036) and Bregma -2.0mm (54.4%, p=0.035) at 30 days post-stroke in r-hGH–treated stroke mice (Fig. 5).

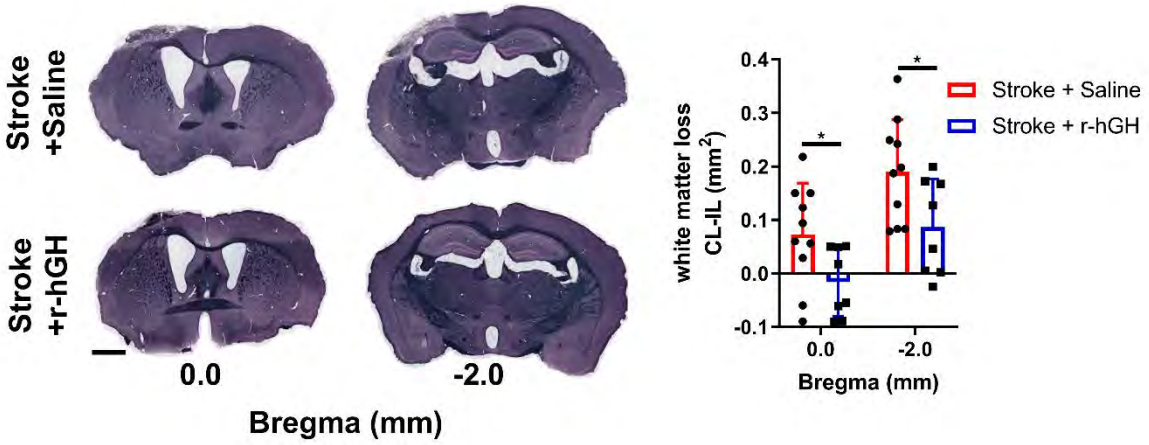

Figure 5. Sudan Black staining of white matter tracts from the corpus callosum (Bregma 0.0mm and -2.0mm). White matter loss was calculated as contralateral hemisphere area − ipsilateral hemisphere area (mm2). Mean±SD. *p<0.05. Sale bar=1mm.

3. Discussion

We demonstrated that GH treatment after experimental cortical stroke stimulates proliferation of neural progenitor cells and increases synaptic plasticity within the hippocampus, a remote region from the initial cortical injury, in parallel with improvements in hippocampal-dependent VD task. While long-term GH treatment after experimental stroke has been previously shown to improve cognitive function [24,29], this is the first study to our knowledge to comprehensively show both functional and hippocampal plasticity of GH treatment. Thus, the present study extends the understanding of how GH treatment acts on hippocampal plasticity to promote post-stroke cognitive recovery.

Our group recently established that cortical photothrombotic stroke impairs the ability of mice to discriminate between stimuli with a high degree of similarity [31]. Although our cortical stroke model does not cause a direct damage to the hippocampus, we observed an indirect significant decrease in the number of neurons within the hippocampus at 2 weeks post-stroke [31]. It should be noted that a cortical stroke could also induce a dysfunction in the hippocampal-thalamic network [32]. While cerebral ischemia causes persistent neuronal loss in remote regions that are functionally connected to the primary infarction site [33,34], interestingly, it also triggers a transient proliferation of endogenous neural progenitor cells in the DG of the hippocampus [6,35]. Importantly, we previously demonstrated that GH treatment after experimental stroke promotes associative memory cognitive domain as measured by the paired-associate learning task [24]. However, we only investigated the

neurorestorative effects of GH treatment within the peri-infarct regions [24]. The observed enhancement of recovery-promoting mechanisms within the peri-infarct area is most likely contributing to the improvement of motor outcomes [25], whereas the promotion of hippocampal neurogenesis and increased synaptic plasticity reported here are likely to be of importance for improved cognition.

The present study reports novel evidence that GH treatment promotes hippocampal neurogenesis, remotely from the cortical injury, and enhances the performance of hippocampal-dependent VD task. Our findings further suggested that higher levels of plasma IGF-1 are associated with better performance in hippocampal-dependent VD task, which is consistent with prior findings [24,36]. GH can exert its effects directly or indirectly via its mediator insulin-like growth factor 1 (IGF-1) on hippocampal plasticity [37]. Firstly, GH receptor expression is widespread in the brain and there are studies supporting a passage of GH over the blood-brain-barrier, therefore, GH may have direct effects on the brain [38]. Secondly, it is possible for GH to increase production and secretion of local IGF-1 in the brain [39,40]. Thirdly, GH induces the secretion of IGF-1 in the circulatory system, and peripheral IGF-1 can penetrate the blood-brain-barrier to exert effects on the brain [41,42]. However, it is not possible for our experimental design to specifically elucidate which mechanisms are involved. Nevertheless, we would suggest that it is most likely a combination of these pathways. We used BrdU tagging, to assess whether there is an increase in neural progenitor cells. We also evaluated the expression of DCX, a marker of immature neurons [43]. Our results showed an increased number of BrdU-positive cells and expression of DCX in the DG subregion in GH-treated stroke mice. Together, these findings of increase neurogenesis are critical, as recovery of the cognitive function following stroke depends on cellular plasticity in the hippocampal formation [14,44].

We also investigated other key neurorestorative processes in the hippocampal formation or in its vicinity. Firstly, we assessed synaptic plasticity by measuring the AMPA receptor subunit GluR1, which plays an important role in synapse formation, stabilization, and plasticity [45-47]. We found GluR1-positive structures and protein levels were increased in the hippocampus in GH treated mice. While the results might be an indication for higher synapse numbers or higher synaptic activity, it should be noted that GluR1 may be found also extrasynaptically [48]. Future comprehensive investigation on synaptic changes using co-immunolabelling of synaptic structures and high resolution microscopy is warranted. Secondly, given that stroke induced remote secondary neurodegeneration is a disruption of connections between cortex and hippocampus [31,32], we evaluated white matter tract disturbances. The results from Sudan Black staining suggest that GH treatment provides restorative effects on white matter structural loss. Together, these results are particularly interesting when considered in conjunction with the cognitive function findings. Thirdly, we explored the effect of GH treatment on cerebrovascular remodelling. In our previous studies, we showed that GH has the ability to enhance angiogenesis, and increases the density and area coverage of both CD31 and Collagen IV–positive cells in the peri-infarct region [24,25]. In the current study, we analysed vessel density in the hippocampus area using immunofluorescence labelled Tomato Lectin. However, GH treatment did not affect the % area covered by Tomato Lectin or the number of BrdU-Lectin-positive cells in the hippocampal formation, as we have previously shown in the peri-infarct area. These results suggest that some effects of GH appears to be global in the brain, while others are more brain region specific and cell type specific.

There are two important points regarding the experimental design of the current study that require consideration. Firstly, we used r-hGH for practical purposes and translational point of view. r-hGH is much accessible than mouse GH, and has been used in a wide setting of mouse experimental models with expected GH-related results. However, there some differences in the actions of r-hGH and mouse GH. Although r-hGH stimulates the GH receptor and an increase in serum IGF-I, there is also a potential minor stimulation of prolactin receptors [49,50]. Nonetheless, it appears that prolactin is not able to induce local IGF-I, at least not in the skeleton [51]. Therefore, this does not compromise the

results, but gives an alternative mechanism. Secondly, we administered r-hGH subcutaneously via mini-osmotic pumps for 28 days after experimental stroke, as we accounted for the impact of stress due to repeated injections. However, continuous infusion of GH may disrupt the endogenous GH pulsatile secretion, and different modes of GH administration can have minor different effects on the brain [52,53]. This warrants further investigation using programmable pumps.

4. Conclusion

We have shown that GH treatment can enhance neurogenesis and synaptic plasticity in the hippocampus, a remote region from a cortical injury, thus leading to improvement in cognition after stroke. Promisingly, small clinical studies have identified that GH treatment ameliorates cognitive impairment in stroke patients [36,54]. Further, due to the high incidence of GH deficiency in stroke survivors [55,56], GH treatment may represent a useful therapeutic intervention for many patients during stroke recovery.

5. Materials and Methods

5.1. Animals

All animal experiments were approved by the University of Newcastle Animal Care and Ethics Committee (A-2014-432) and undertaken in accordance to the Animal Research: Reporting of In Vivo Experiments guidelines. C57BL/6 mice (male, 10 weeks old, n=48) were obtained from the Animal Services Unit at the University of Newcastle. Mice were maintained in a 12:12h reverse light–dark cycle (lights on 19:00h). All procedures conducted in the dark phase.

5.2. Sample size calculation

Sample size was estimated using G*Power 3.1 software. Using previous and preliminary data [24,25], we obtained an effect size of d=1.6. Allowing a type 1 error of 5%, α=0.05, with the power of 80%, β=0.2, we calculated a samples size of 8 animals per group.

5.3. Experimental design

The experimental design of this study was as described in Figure 1A [24]. A total of 48 mice were used in this study. All the experimental groups are randomized, and all outcome analyses were performed in a blinded manner.

The first cohort of mice (n=24) was used to assess cognitive function, and brains were collected for histological analysis. At day 0 (D0), all mice were subjected to photothrombotic occlusion. At D2, mice were randomly allocated to receive either r-hGH or saline at 1.4 mg/kg body weight per day subcutaneously via mini-osmotic pumps for 28 days (Stroke+Saline n=12 and Stroke+r-hGH n=12). At D3 mice were injected with BrdU (50 mg/kg body weight) for 5 consecutive days. To evaluate cognitive function, mice were subjected to mouse touchscreen platform for visual discrimination (VD) task for 18 days (days 9 to 26 post-stroke). At D30, mice were euthanized and brains collected. Mice were excluded from the study if we histologically identified that the stroke had not occurred or malfunction of the mini-osmotic pumps. Within the saline group, one mouse had to be excluded due to post-surgery death and another one due to no stroke. Within the r-hGH group, we had to exclude one mouse due to pump malfunction and two mice due to a problem with the perfusion procedure.

The second cohort of mice (n=24) was used for biochemical analysis. At D0, mice were subjected to photothrombotic occlusion or sham surgery (Stoke n=18 and sham n=6). At D2, stroke mice received r-hGH or saline as described above (Sham+saline n=6, stroke+saline n=8 and stroke+r-hGH n=10). At D30, mice were euthanized and brains collected for western blotting. Within this second cohort, one mouse from the Stroke+r-hGH group had to be excluded for not having a stroke.

5.4. Photothrombotic occlusion

Photothrombotic occlusion was performed as described previously [31,57,58]. Briefly, mice were anesthetized by 2% isoflurane during surgical procedure on a temperature controlled (37˚C±1) stereotaxic frame. Rose Bengal (200µl, 10mg/ml solution in sterile saline, Sigma-Aldrich, USA) was injected intraperitoneally. At 8 min post-injection, the skull was exposed and illuminated for 15 min by cold light source positioned at 2.2mm left lateral of Bregma 0.0mm. For the sham group, the Rose Bengal injection was substituted with 200µl of sterile saline (0.9% NaCl, Pfizer, Australia).

5.5. Mini-osmotic pump placement

Mini-osmotic pump (Model 2004, Alzet, USA) placement was performed as preciously described [24,25,59]. At D2, the mini-osmotic pumps were implanted. An incision was made in the skin between the scapulae where the mini-osmotic pump was inserted. The pumps were filled with 200 µl of either recombinant human growth hormone (r-hGH, Somatropin 10mg/1.5mL, SciTropin A, SciGen, Australia) or sterile saline. The delivery rate of the pumps was 0.25µl/hr for 28 days (0.04 mg r-hGH per day).

5.6. Visual discrimination (VD) task

Mouse touchscreen operant chambers were used in the cognitive testing as described [30,31], and were conducted in a blinded and randomized manner. Briefly, mice were calorie restricted overnight before cognitive testing. Strawberry milkshake was used as a reward to motivate the performance of the mice. First, mice were trained to learn to associate a nose poke of the touchscreen and the delivery of the reward. Following training, mice underwent photothrombotic occlusion surgery. At D9, mice were subjected to the VD task. This task entailed simultaneous presentation of two stimuli; one correct (S+) and one incorrect (S-). The S+ stimulus appeared pseudo-randomly either in the right or left part of the touchscreen. When the mouse selected the correct choice, S+, a tone was triggered, the reward tray was illuminated, and strawberry milkshake was delivered to the tray. If the mouse selected the incorrect image, S-, there was no reward delivery, no tone, the house light was turned on for 5 s, and a correction trial was initiated. In each VD session, the testing ended once a mouse successfully completed 30 trials or reached a 60 min time limit, whichever occurred first. All mice were subjected to a total of 18 sessions.

5.7. Tissue processing

For the first cohort, mice were anaesthetised with sodium pentobarbital. Mice were perfused via the ascending aorta with ice-cold 0.9% saline followed by ice-cold 4% paraformaldehyde (pH 7.4). Brains were dissected and post-fixed for 4 hours in the same fixative then transferred to a 12.5% sucrose solution in 0.1M phosphate buffered saline (PBS) for storage and cryoprotection. Serial coronal sections were sliced on a freezing microtome (Leica, North Ryde, NSW, Australia) at a thickness of 30µm.

For the second cohort, mice were anaesthetised with sodium pentobarbital, and transcardially perfused with ice cold 0.9% saline. Brains were dissected and rapidly frozen in -80˚C isopentane. Brain sections were sliced using a cryostat (-20°C) at a thickness of 200µm. The hippocampal formation (Bregma -1.2 to -2.5mm) samples were dissected, and stored frozen in -80˚C until further analysis.

5.8. Immunofluorescence

Free-floating fixed sections were co-immunostained as previously described [60,61]. For BrdU staining, antigen retrieval was performed before the blocking step as follows: 10 min HCl (1M) incubation on ice, 10 min HCl (2M) incubation at room temperature, 20 min HCl (2M) incubation at 37˚C, 10 min borate buffer (0.1M) incubation at room temperature and three washes in PBS+0.1% Triton X. Sections were blocked using 3% bovine serum albumin, then incubated with appropriate primary antibody (DCX, GluR1, BrdU, NeuN) overnight at 4˚C, and followed by 2h incubation in corresponding

secondary antibodies at 25°C (see Table 1 for antibodies concentration). Tomato Lectin staining was performed together with the secondary antibody incubation. NeuroTrace was used to counterstain sections after immunocytochemical detection of DCX or GluR1. Brain sections were washed with PBS in between each incubation step.

5.9. Sudan black staining

Sudan black staining was performed as previously described [62]. Briefly, sections were mounted and rinsed with 70% ethanol followed by 15 min incubation with Sudan Black B solution (Sigma-Aldrich, USA). After staining sections were rinsed with 70% ethanol and water and 5 min counterstained with nuclear fast red solution (Sigma-Aldrich, USA).

5.10. Image acquisition and analysis

Immunofluorescence high-resolution confocal images were taken on a Leica TCS SP8 confocal microscope with a Leica HC PLC APO 10x/0.40 objective. For each region of interest, 30μm z-stacks with a step size of 1μm were taken. Imaging parameters (laser power, resolution and gain) were held constant throughout all imaging sessions. Exhaustive automated BrdU cell counts were performed using ImageJ software. For analysis of NeuN, DCX and GluR1 labelling, we performed thresholding analyses and chose the optimal pixel intensity that clearly reflected the immunofluorescence signal. To measure vessel coverage (% Lectin$^+$ area), the emission channels were split and the Lectin emission image was uniformly thresholded at a high stringency. The area of vessel coverage was expressed as a percentage of the overall field of view (ImageJ Software). For BrdU/NeuN and BrdU/Lectin co-labelling, we used the plugin 'colocalization' for ImageJ. This plugin highlights the colocalizated points of two 8-bits images. The colocalizated points appear black by default.

Sudan Black images were acquired at 20x using Aperio AT2 (Leica, Germany). Specifically, we focus on the corpus callosum and we assessed white matter loss as a difference between the contralateral and ipsilateral hemispheric area (mm2). The quantitative analysis was undertaken specifically in two sections (Bregma 0.0 and -2.0mm).

5.11. Protein extraction and western blotting

Protein extraction and western blotting were performed as previously described [63,64]. Hippocampus samples were sonicated in 300μl lysis buffer (50mM tris(hydroxymethyl)aminomethane buffer pH 7.4 containing 80μM ammoniummolybdate, 5mM β-glycerolphosphate, 1mM dithiothreitol, 1mM ethylenediaminetetraacetic acid, 1% sodium dodecyl sulfate, 1mM sodium pyrophosphate, 1mM sodium vanadate, 1 cOmplete™ protease inhibitor cocktail tablet, and 1 PhosSTOP™ phosphatase inhibitor cocktail tablet) and centrifuged at 14000g for 20 min at 4°C. Supernatants were collected and protein concentrations were estimated by Pierce BCA protein assay kit (Thermo Fisher Scientific, USA). Sample buffer (2% sodium dodecyl sulfate, 50mM tris(hydroxymethyl)aminomethane, 10% glycerol, 1% dithiothreitol, 0.1% bromophenol blue, pH 6.8) was added into the supernatants. To determine the protein levels of NeuN, DCX, GluR1 and Collagen IV, the protein homogenates from sham+saline (n=6), stroke+saline (n=8) and stroke+r-hGH (n=9) were analysed together on 26-well gels. 15μg of protein lysate was electrophoresed into Biorad Criterion TGX Stain-Free 4–20% gels and transferred to polyvinylidene fluoride membranes. The membranes were blocked with 5% skim milk in TBST for 1 h at room temperature and incubated overnight at 4°C with the appropriate primary antibody: NeuN, DCX, GluR1 and Collagen IV (see Table 1 for antibodies concentration). The next day, membranes were incubated with secondary antibody for 1 h at 25°C. In between each incubation step, membranes were washed in TBST. Chemiluminescence signals were detected on an Amersham Imager 600 using Luminata Classico western blotting detection reagent. The density of the bands was measured using Amersham Imager 600 analysis software. The protein markers were normalized to β-actin (as loading control), and were expressed as a fold change of mean±SD for each group relative to the mean of the sham+saline group.

5.12. Statistical analyses

All data were expressed as mean±SD, and were analysed using GraphPad Prism v7.02. The primary outcome measurement was differences between Stroke + Saline and Stroke + r-hGH. Data from western blotting, immunofluorescence labelling and white matter loss were analysed using 2-tailed t-test. VD task (18 sessions temporal analysis) was analysed using 2-way ANOVA, followed by Sidak multiple comparisons. A p value <0.05 was considered statistically significant.

Table 1: List of antibodies used for western blot and immunofluorescence analyses.

	Sources of antibodies	Application	Dilution
BrdU	Sigma-Aldrich, mouse anti-BrdU, #B8434	IF	1:1000
NeuN	Cell Signaling, rabbit anti-NeuN (D3S31), #12943	WB	1:2000
		IF	1:1000
DCX	abcam, rabbit anti-doublecortin, #ab18723	WB	1:1000
		IF	1:1000
GluR1	Cell Signaling, rabbit anti-AMPA Receptor 1 (GluA1), #13185	WB	1:2000
		IF	1:1000
Collagen IV	Abcam, rabbit anti-collagen IV, #ab6586	WB	1:1000
β-actin	Sigma-Aldrich, Monoclonal Anti-β-actin-HRP antibody, A3854	WB	1:50000
NeuroTrace	ThermoFisher Scientific, NeuroTrace™ 640/660 Deep-Red Fluorescent Nissl Stain, #N21483	IF	1:1000
Tomato Lectin	Vector Laboratories, DyLight 649 Lycopersicon esculentum (Tomato) Lectin #DL-1178	IF	1:1000
Rabbit IgG	Biorad, Anti-Rabbit-HRP antibody, #170-6515	WB	1:7500
	ThermoFisher Scientific, anti-Rabbit IgG (H+L) Highly Cross-Adsorbed Secondary Antibody, Alexa Fluor 488, #A21206	IF	1:400
Mouse IgG	Biorad, Anti-Mouse-HRP antibody, #170-6516	WB	1:10000
	ThermoFisher Scientific, anti-Mouse IgG (H+L) Highly Cross-Adsorbed Secondary Antibody, Alexa Fluor 594, #A21203	IF	1:400

WB, western blot; IF, immunofluorescence

Author Contributions: All authors have read and agree to the published version of the manuscript. Conceptualization, S.S.B., F.R.W., M.N., J.I. and L.K.O.; Data curation, S.S.B. and L.K.O; Formal analysis, S.S.B., F.R.W., M.N., J.I. and L.K.O.; Funding acquisition, F.R.W., M.N., J.I. and L.K.O.; Methodology, S.S.B. and L.K.O.; Supervision, F.RW., M.N., J.I. and L.K.O.; Writing – original draft, S.S.B., J.I. and L.K.O.; Writing – review & editing, S.S.B., N.D.Å., P.C., F.R.W, M.N., J.I. and L.K.O.

Funding: This study was supported by the Swedish Government (ALFGBG-74390), University of Gothenburg, Hunter Medical Research Institute, and the University of Newcastle, Australia. LKO and SSB were supported by Research Advantage Scholarship and Greaves Family Scholarship. LKO was supported by Monash University Malaysia. NDÅ was supported by the Swedish Government (ALFGBG-719761, ALFGBG-751111).

Acknowledgments: We would like to acknowledge the insights and comments provided by Dr Rebecca Hood on early versions of the manuscript.

Conflicts of Interest: The authors declare no conflict of interest. The funders had no role in the design of the study; in the collection, analyses, or interpretation of data; in the writing of the manuscript, or in the decision to publish the results.

Abbreviations

GH	Growth hormone
rhGH	Recombinant human growth hormone
BrdU	Bromodeoxyuridine
NeuN	Neuronal nuclei
DCX	Doublecortin
GluR1	AMPA Receptor 1
VD	Visual Discrimination
DG	Dentate Gyrus

References

1. Prins, N.D.; van Dijk, E.J.; den Heijer, T.; Vermeer, S.E.; Jolles, J.; Koudstaal, P.J.; Hofman, A.; Breteler, M.M. Cerebral small-vessel disease and decline in information processing speed, executive function and memory. *Brain : a journal of neurology* **2005**, *128*, 2034-2041, doi:10.1093/brain/awh553.
2. Blum, S.; Luchsinger, J.A.; Manly, J.J.; Schupf, N.; Stern, Y.; Brown, T.R.; DeCarli, C.; Small, S.A.; Mayeux, R.; Brickman, A.M. Memory after silent stroke: hippocampus and infarcts both matter. *Neurology* **2012**, *78*, 38-46, doi:10.1212/WNL.0b013e31823ed0cc.
3. Gemmell, E.; Bosomworth, H.; Allan, L.; Hall, R.; Khundakar, A.; Oakley, A.E.; Deramecourt, V.; Polvikoski, T.M.; O'Brien, J.T.; Kalaria, R.N. Hippocampal neuronal atrophy and cognitive function in delayed poststroke and aging-related dementias. *Stroke* **2012**, *43*, 808-814, doi:10.1161/strokeaha.111.636498.
4. Selnes, P.; Grambaite, R.; Rincon, M.; Bjørnerud, A.; Gjerstad, L.; Hessen, E.; Auning, E.; Johansen, K.; Almdahl, I.S.; Due-Tønnessen, P., et al. Hippocampal complex atrophy in poststroke and mild cognitive impairment. *J Cereb Blood Flow Metab* **2015**, *35*, 1729-1737, doi:10.1038/jcbfm.2015.110.
5. Khlif, M.S.; Werden, E.; Egorova, N.; Boccardi, M.; Redolfi, A.; Bird, L.; Brodtmann, A. Assessment of longitudinal hippocampal atrophy in the first year after ischemic stroke using automatic segmentation techniques. *NeuroImage. Clinical* **2019**, *24*, 102008, doi:10.1016/j.nicl.2019.102008.
6. Yagita, Y.; Kitagawa, K.; Ohtsuki, T.; Takasawa, K.; Miyata, T.; Okano, H.; Hori, M.; Matsumoto, M. Neurogenesis by progenitor cells in the ischemic adult rat hippocampus. *Stroke* **2001**, *32*, 1890-1896, doi:10.1161/01.str.32.8.1890.
7. Koh, S.-H.; Park, H.-H. Neurogenesis in Stroke Recovery. *Transl Stroke Res* **2017**, *8*, 3-13, doi:10.1007/s12975-016-0460-z.
8. Takagi, Y.; Nozaki, K.; Takahashi, J.; Yodoi, J.; Ishikawa, M.; Hashimoto, N. Proliferation of neuronal precursor cells in the dentate gyrus is accelerated after transient forebrain ischemia in mice. *Brain research* **1999**, *831*, 283-287, doi:10.1016/s0006-8993(99)01411-0.
9. Kee, N.J.; Preston, E.; Wojtowicz, J.M. Enhanced neurogenesis after transient global ischemia in the dentate gyrus of the rat. *Experimental brain research* **2001**, *136*, 313-320, doi:10.1007/s002210000591.
10. Tonchev, A.B.; Yamashima, T.; Zhao, L.; Okano, H. Differential proliferative response in the postischemic hippocampus, temporal cortex, and olfactory bulb of young adult macaque monkeys. *Glia* **2003**, *42*, 209-224, doi:10.1002/glia.10209.
11. Liu, J.; Solway, K.; Messing, R.O.; Sharp, F.R. Increased neurogenesis in the dentate gyrus after transient global ischemia in gerbils. *The Journal of neuroscience : the official journal of the Society for Neuroscience* **1998**, *18*, 7768-7778, doi:10.1523/jneurosci.18-19-07768.1998.

12. Lichtenwalner, R.J.; Parent, J.M. Adult neurogenesis and the ischemic forebrain. *J Cereb Blood Flow Metab* **2006**, *26*, 1-20, doi:10.1038/sj.jcbfm.9600170.
13. Kernie, S.G.; Parent, J.M. Forebrain neurogenesis after focal Ischemic and traumatic brain injury. *Neurobiology of disease* **2010**, *37*, 267-274, doi:10.1016/j.nbd.2009.11.002.
14. Cuartero, M.I.; de la Parra, J.; Pérez-Ruiz, A.; Bravo-Ferrer, I.; Durán-Laforet, V.; García-Culebras, A.; García-Segura, J.M.; Dhaliwal, J.; Frankland, P.W.; Lizasoain, I., et al. Abolition of aberrant neurogenesis ameliorates cognitive impairment after stroke in mice. *J Clin Invest* **2019**, *129*, 1536-1550, doi:10.1172/JCI120412.
15. Arvidsson, A.; Collin, T.; Kirik, D.; Kokaia, Z.; Lindvall, O. Neuronal replacement from endogenous precursors in the adult brain after stroke. *Nature medicine* **2002**, *8*, 963-970, doi:10.1038/nm747.
16. Parent, J.M.; Vexler, Z.S.; Gong, C.; Derugin, N.; Ferriero, D.M. Rat forebrain neurogenesis and striatal neuron replacement after focal stroke. *Annals of neurology* **2002**, *52*, 802-813, doi:10.1002/ana.10393.
17. Jin, K.; Sun, Y.; Xie, L.; Peel, A.; Mao, X.O.; Batteur, S.; Greenberg, D.A. Directed migration of neuronal precursors into the ischemic cerebral cortex and striatum. *Molecular and cellular neurosciences* **2003**, *24*, 171-189, doi:10.1016/s1044-7431(03)00159-3.
18. Zhang, R.; Zhang, Z.; Wang, L.; Wang, Y.; Gousev, A.; Zhang, L.; Ho, K.L.; Morshead, C.; Chopp, M. Activated neural stem cells contribute to stroke-induced neurogenesis and neuroblast migration toward the infarct boundary in adult rats. *J Cereb Blood Flow Metab* **2004**, *24*, 441-448, doi:10.1097/00004647-200404000-00009.
19. Bernal, G.M.; Peterson, D.A. Neural stem cells as therapeutic agents for age-related brain repair. *Aging cell* **2004**, *3*, 345-351, doi:10.1111/j.1474-9728.2004.00132.x.
20. Niv, F.; Keiner, S.; Krishna, K.; Witte, O.W.; Lie, D.C.; Redecker, C. Aberrant neurogenesis after stroke: a retroviral cell labeling study. *Stroke* **2012**, *43*, 2468-2475, doi:10.1161/STROKEAHA.112.660977.
21. Woitke, F.; Ceanga, M.; Rudolph, M.; Niv, F.; Witte, O.W.; Redecker, C.; Kunze, A.; Keiner, S. Adult hippocampal neurogenesis poststroke: More new granule cells but aberrant morphology and impaired spatial memory. *PLoS One* **2017**, *12*, e0183463-e0183463, doi:10.1371/journal.pone.0183463.
22. Bianchi, V.E.; Locatelli, V.; Rizzi, L. Neurotrophic and Neuroregenerative Effects of GH/IGF1. *Int J Mol Sci* **2017**, *18*, 2441, doi:10.3390/ijms18112441.
23. Aberg, N.D.; Brywe, K.G.; Isgaard, J. Aspects of growth hormone and insulin-like growth factor-I related to neuroprotection, regeneration, and functional plasticity in the adult brain. *TheScientificWorldJournal* **2006**, *6*, 53-80, doi:10.1100/tsw.2006.22.
24. Ong, L.K.; Chow, W.Z.; TeBay, C.; Kluge, M.; Pietrogrande, G.; Zalewska, K.; Crock, P.; Åberg, N.D.; Bivard, A.; Johnson, S.J., et al. Growth Hormone Improves Cognitive Function After Experimental Stroke. *Stroke* **2018**, *49*, 1257-1266, doi:10.1161/STROKEAHA.117.020557.
25. Sanchez-Bezanilla, S.; Åberg, N.D.; Crock, P.; Walker, F.R.; Nilsson, M.; Isgaard, J.; Ong, L.K. Growth Hormone Promotes Motor Function after Experimental Stroke and Enhances Recovery-Promoting Mechanisms within the Peri-Infarct Area. *Int J Mol Sci* **2020**, *21*, E606, doi:10.3390/ijms21020606.
26. Heredia, M.; Palomero, J.; de la Fuente, A.; Criado, J.M.; Yajeya, J.; Devesa, J.; Devesa, P.; Vicente-Villardón, J.L.; Riolobos, A.S. Motor Improvement of Skilled Forelimb Use Induced by Treatment with Growth Hormone and Rehabilitation Is Dependent on the Onset of the Treatment after Cortical Ablation. *Neural plasticity* **2018**, *2018*, 6125901, doi:10.1155/2018/6125901.
27. Heredia, M.; Rodríguez, N.; Sánchez Robledo, V.; Criado, J.M.; de la Fuente, A.; Devesa, J.; Devesa, P.; Sánchez Riolobos, A. Factors Involved in the Functional Motor Recovery of Rats with Cortical Ablation after GH and Rehabilitation Treatment: Cortical Cell Proliferation and

Nestin and Actin Expression in the Striatum and Thalamus. *Int J Mol Sci* **2019**, *20*, doi:10.3390/ijms20225770.

28. Heredia, M.; Fuente, A.; Criado, J.; Yajeya, J.; Devesa, J.; Riolobos, A.S. Early growth hormone (GH) treatment promotes relevant motor functional improvement after severe frontal cortex lesion in adult rats. *Behavioural brain research* **2013**, *247*, 48-58, doi:10.1016/j.bbr.2013.03.012.
29. Pathipati, P.; Surus, A.; Williams, C.E.; Scheepens, A. Delayed and chronic treatment with growth hormone after endothelin-induced stroke in the adult rat. *Behavioural brain research* **2009**, *204*, 93-101, doi:10.1016/j.bbr.2009.05.023.
30. Horner, A.E.; Heath, C.J.; Hvoslef-Eide, M.; Kent, B.A.; Kim, C.H.; Nilsson, S.R.O.; Alsiö, J.; Oomen, C.A.; Holmes, A.; Saksida, L.M., et al. The touchscreen operant platform for testing learning and memory in rats and mice. *Nat Protoc* **2013**, *8*, 1961-1984, doi:10.1038/nprot.2013.122.
31. Sanchez-Bezanilla, S.; TeBay, C.; Nilsson, M.; Walker, F.R.; Ong, L.K. Visual discrimination impairment after experimental stroke is associated with disturbances in the polarization of the astrocytic aquaporin-4 and increased accumulation of neurotoxic proteins. *Exp Neurol* **2019**, *318*, 232-243, doi:10.1016/j.expneurol.2019.05.001.
32. Baumgartner, P.; El Amki, M.; Bracko, O.; Luft, A.R.; Wegener, S. Sensorimotor stroke alters hippocampo-thalamic network activity. *Sci Rep* **2018**, *8*, 15770, doi:10.1038/s41598-018-34002-9.
33. Ong, L.K.; Walker, F.R.; Nilsson, M. Is Stroke a Neurodegenerative Condition? A Critical Review of Secondary Neurodegeneration and Amyloid-beta Accumulation after Stroke. *AIMS Medical Science* **2017**, *4*, 1-16, doi:10.3934/medsci.2017.1.1.
34. Zhang, J.; Zhang, Y.; Xing, S.; Liang, Z.; Zeng, J. Secondary neurodegeneration in remote regions after focal cerebral infarction: a new target for stroke management? *Stroke* **2012**, *43*, 1700-1705, doi:10.1161/STROKEAHA.111.632448.
35. Jin, K.; Minami, M.; Lan, J.Q.; Mao, X.O.; Batteur, S.; Simon, R.P.; Greenberg, D.A. Neurogenesis in dentate subgranular zone and rostral subventricular zone after focal cerebral ischemia in the rat. *Proc Natl Acad Sci U S A* **2001**, *98*, 4710-4715, doi:10.1073/pnas.081011098.
36. Feng, X.; Li, G.; Wu, W.; Xu, Y.; Lin, H.; Fan, J. Recombinant Human Growth Hormone Ameliorates Cognitive Impairment in Stroke Patients. *Journal of computer assisted tomography* **2020**, *44*, 255-261, doi:10.1097/rct.0000000000000990.
37. Nyberg, F.; Hallberg, M. Growth hormone and cognitive function. *Nature reviews. Endocrinology* **2013**, *9*, 357-365, doi:10.1038/nrendo.2013.78.
38. Pan, W.; Yu, Y.; Cain, C.M.; Nyberg, F.; Couraud, P.O.; Kastin, A.J. Permeation of growth hormone across the blood-brain barrier. *Endocrinology* **2005**, *146*, 4898-4904, doi:10.1210/en.2005-0587.
39. López-Fernández, J.; Sánchez-Franco, F.; Velasco, B.; Tolón, R.M.; Pazos, F.; Cacicedo, L. Growth hormone induces somatostatin and insulin-like growth factor I gene expression in the cerebral hemispheres of aging rats. *Endocrinology* **1996**, *137*, 4384-4391, doi:10.1210/endo.137.10.8828499.
40. Ye, P.; Umayahara, Y.; Ritter, D.; Bunting, T.; Auman, H.; Rotwein, P.; D'Ercole, A.J. Regulation of insulin-like growth factor I (IGF-I) gene expression in brain of transgenic mice expressing an IGF-I-luciferase fusion gene. *Endocrinology* **1997**, *138*, 5466-5475, doi:10.1210/endo.138.12.5600.
41. Reinhardt, R.R.; Bondy, C.A. Insulin-like growth factors cross the blood-brain barrier. *Endocrinology* **1994**, *135*, 1753-1761, doi:10.1210/endo.135.5.7525251.
42. Armstrong, C.S.; Wuarin, L.; Ishii, D.N. Uptake of circulating insulin-like growth factor-I into the cerebrospinal fluid of normal and diabetic rats and normalization of IGF-II mRNA content in diabetic rat brain. *Journal of neuroscience research* **2000**, *59*, 649-660, doi:10.1002/(sici)1097-4547(20000301)59:5<649::Aid-jnr8>3.0.Co;2-w.
43. Brown, J.P.; Couillard-Després, S.; Cooper-Kuhn, C.M.; Winkler, J.; Aigner, L.; Kuhn, H.G. Transient expression of doublecortin during adult neurogenesis. *The Journal of comparative neurology* **2003**, *467*, 1-10, doi:10.1002/cne.10874.

44. Pekna, M.; Pekny, M.; Nilsson, M. Modulation of neural plasticity as a basis for stroke rehabilitation. *Stroke* **2012**, *43*, 2819-2828, doi:10.1161/strokeaha.112.654228.
45. Hollmann, M.; Heinemann, S. Cloned glutamate receptors. *Annual review of neuroscience* **1994**, *17*, 31-108, doi:10.1146/annurev.ne.17.030194.000335.
46. Dingledine, R.; Borges, K.; Bowie, D.; Traynelis, S.F. The glutamate receptor ion channels. *Pharmacological reviews* **1999**, *51*, 7-61.
47. Lu, W.; Isozaki, K.; Roche, K.W.; Nicoll, R.A. Synaptic targeting of AMPA receptors is regulated by a CaMKII site in the first intracellular loop of GluA1. *Proc Natl Acad Sci U S A* **2010**, *107*, 22266-22271, doi:10.1073/pnas.1016289107.
48. Chater, T.E.; Goda, Y. The role of AMPA receptors in postsynaptic mechanisms of synaptic plasticity. *Frontiers in cellular neuroscience* **2014**, *8*, 401, doi:10.3389/fncel.2014.00401.
49. Mustafa, A.; Adem, A.; Roos, P.; Nyberg, F. Sex differences in binding of human growth hormone to rat brain. *Neuroscience research* **1994**, *19*, 93-99, doi:10.1016/0168-0102(94)90012-4.
50. Furigo, I.C.; Metzger, M.; Teixeira, P.D.; Soares, C.R.; Donato, J., Jr. Distribution of growth hormone-responsive cells in the mouse brain. *Brain structure & function* **2017**, *222*, 341-363, doi:10.1007/s00429-016-1221-1.
51. Nilsson, A.; Carlsson, B.; Isgaard, J.; Isaksson, O.G.; Rymo, L. Regulation by GH of insulin-like growth factor-I mRNA expression in rat epiphyseal growth plate as studied with in-situ hybridization. *The Journal of endocrinology* **1990**, *125*, 67-74, doi:10.1677/joe.0.1250067.
52. Walser, M.; Schiöler, L.; Oscarsson, J.; Åberg, M.A.; Wickelgren, R.; Svensson, J.; Isgaard, J.; Åberg, N.D. Mode of GH administration and gene expression in the female rat brain. *The Journal of endocrinology* **2017**, *233*, 187-196, doi:10.1530/joe-16-0656.
53. Walser, M.; Schiöler, L.; Oscarsson, J.; Aberg, M.A.; Svensson, J.; Aberg, N.D.; Isgaard, J. Different modes of GH administration influence gene expression in the male rat brain. *The Journal of endocrinology* **2014**, *222*, 181-190, doi:10.1530/joe-14-0223.
54. Song, J.; Park, K.; Lee, H.; Kim, M. The effect of recombinant human growth hormone therapy in patients with completed stroke: a pilot trial. *Annals of rehabilitation medicine* **2012**, *36*, 447-457, doi:10.5535/arm.2012.36.4.447.
55. Lillicrap, T.; Garcia-Esperon, C.; Walker, F.R.; Ong, L.K.; Nilsson, M.; Spratt, N.; Levi, C.R.; Parsons, M.; Isgaard, J.; Bivard, A. Growth Hormone Deficiency Is Frequent After Recent Stroke. *Front Neurol* **2018**, *9*, 713-713, doi:10.3389/fneur.2018.00713.
56. Kreber, L.A.; Ashley, M.J.; Masel, B.E.; Singh, C.K.; Randle, K.D.; Johnson, C.; Helvie, R.; Ashley, M.J.; Griesbach, G.S. Prevalence of growth hormone deficiency in middle-age adults recovering from stroke. *Brain injury* **2020**, *34*, 276-280, doi:10.1080/02699052.2019.1682195.
57. Zalewska, K.; Ong, L.K.; Johnson, S.J.; Nilsson, M.; Walker, F.R. Oral administration of corticosterone at stress-like levels drives microglial but not vascular disturbances post-stroke. *Neuroscience* **2017**, *352*, 30-38, doi:10.1016/j.neuroscience.2017.03.005.
58. Zhao, Z.; Ong, L.K.; Johnson, S.; Nilsson, M.; Walker, F.R. Chronic stress induced disruption of the peri-infarct neurovascular unit following experimentally induced photothrombotic stroke. *J Cereb Blood Flow Metab* **2017**, *37*, 3709-3724, doi:10.1177/0271678X17696100.
59. Walser, M.; Hansén, A.; Svensson, P.-A.; Jernås, M.; Oscarsson, J.; Isgaard, J.; Åberg, N.D. Peripheral administration of bovine GH regulates the expression of cerebrocortical beta-globin, GABAB receptor 1, and the Lissencephaly-1 protein (LIS-1) in adult hypophysectomized rats. *Growth Horm IGF Res* **2011**, *21*, 16-24, doi:10.1016/j.ghir.2010.11.002.
60. Kluge, M.G.; Abdolhoseini, M.; Zalewska, K.; Ong, L.K.; Johnson, S.J.; Nilsson, M.; Walker, F.R. Spatiotemporal analysis of impaired microglia process movement at sites of secondary neurodegeneration post-stroke. *J Cereb Blood Flow Metab* **2019**, *39*, 2456-2470, doi:10.1177/0271678X18797346.
61. Kluge, M.G.; Kracht, L.; Abdolhoseini, M.; Ong, L.K.; Johnson, S.J.; Nilsson, M.; Walker, F.R. Impaired microglia process dynamics post-stroke are specific to sites of secondary neurodegeneration. *Glia* **2017**, *65*, 1885-1899, doi:10.1002/glia.23201.

62. Pietrogrande, G.; Zalewska, K.; Zhao, Z.; Abdolhoseini, M.; Chow, W.Z.; Sanchez-Bezanilla, S.; Ong, L.K.; Johnson, S.J.; Nilsson, M.; Walker, F.R. Low oxygen post conditioning prevents thalamic secondary neuronal loss caused by excitotoxicity after cortical stroke. *Sci Rep* **2019**, *9*, 4841-4841, doi:10.1038/s41598-019-39493-8.
63. Ong, L.K.; Zhao, Z.; Kluge, M.; Walker, F.R.; Nilsson, M. Chronic stress exposure following photothrombotic stroke is associated with increased levels of Amyloid beta accumulation and altered oligomerisation at sites of thalamic secondary neurodegeneration in mice. *J Cereb Blood Flow Metab* **2017**, *37*, 1338-1348, doi:10.1177/0271678X16654920.
64. Sanchez-Bezanilla, S.; Nilsson, M.; Walker, F.R.; Ong, L.K. Can We Use 2,3,5-Triphenyltetrazolium Chloride-Stained Brain Slices for Other Purposes? The Application of Western Blotting. *Front Mol Neurosci* **2019**, *12*, 181-181, doi:10.3389/fnmol.2019.00181.

SUPPLEMENTARY MATERIAL

Growth hormone treatment promotes remote hippocampal plasticity after experimental cortical stroke

Sonia Sanchez-Bezanilla[1,2], N. David Åberg[3,4], Patricia Crock[5], Frederick R. Walker[1,2,6,7], Michael Nilsson[1,2,6,7,8], Jörgen Isgaard[1,3,4]†, Lin Kooi Ong[1,2,6,9]†

1. School of Biomedical Sciences and Pharmacy and the Priority Research Centre for Stroke and Brain Injury, the University of Newcastle, University Dr, Callaghan, 2308, NSW, Australia
2. Hunter Medical Research Institute, Lot 1, Kookaburra Cct, New Lambton Heights, 2305, NSW, Australia
3. University of Gothenburg, 405 30 Gothenburg, Sweden
4. Department of Internal Medicine, Region Västra Götaland, Sahlgrenska University Hospital, Blå stråket 5, 413 45 Gothenburg, Sweden.
5. Department of Paediatric Endocrinology and Diabetes, John Hunter Children's Hospital, Kookaburra Cct, New Lambton Heights, 2305, NSW, Australia
6. NHMRC Centre of Research Excellence Stroke Rehabilitation and Brain Recovery, 245 Burgundy Street, Heidelberg, 3084, VIC, Australia
7. Centre for Rehab Innovations, Lot 1, Kookaburra Cct, New Lambton Heights, 2305, NSW, Australia
8. LKC School of Medicine, Nanyang Technological University, 50 Nanyang Ave, 639798 Singapore
9. Monash University Malaysia, Bandar Sunway, 47500 Subang Jaya, Selangor, Malaysia
† Contributed equally to senior authorship

Correspondence:
Lin Kooi Ong
School of Pharmacy, Monash University Malaysia, Jalan Lagoon Selatan, 47500, Bandar Sunway, Selangor, Malaysia.
E-mail: ong.linkooi@monash.edu

Jörgen Isgaard
Department of Internal Medicine University of Gothenburg and Sahlgrenska University Hospital, Gothenburg, Sweden.
E-mail jorgen.isgaard@medic.gu.se

Supplementary figures and legends

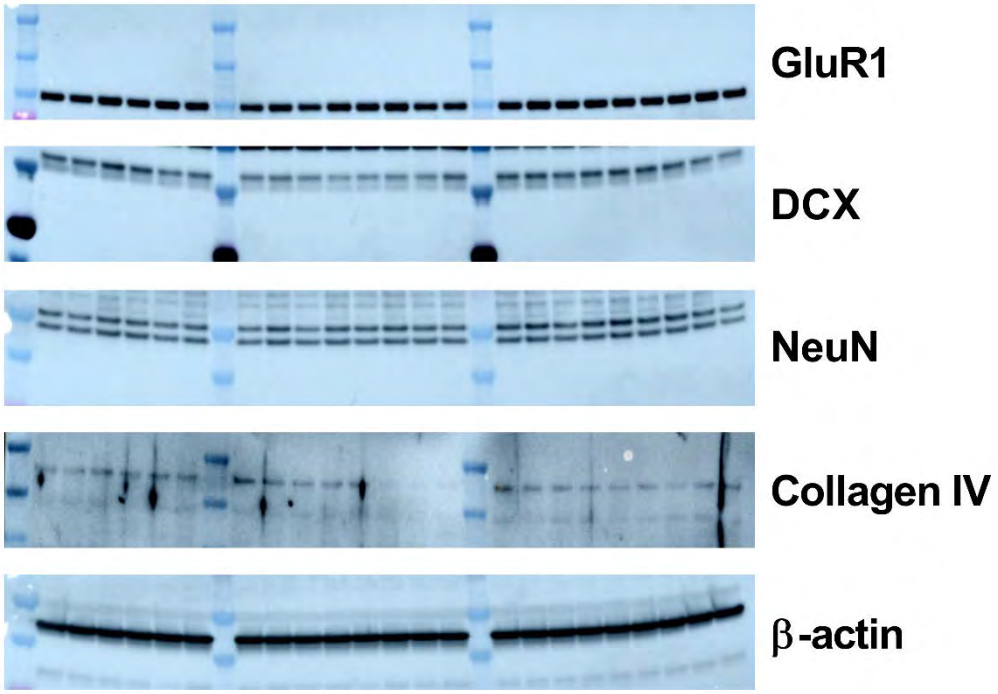

Supplementary Figure 1. Raw immunoblots corresponding to GluR1, DCX, NeuN, Collagen IV and β-actin.

CHAPTER 7: DISCUSSION

In this thesis, I have documented a number of novel findings and potential significant outcomes that may explain the underlying mechanisms of functional deficits post-stroke, with an emphasis on the subacute and chronic phases of the recovery. Critically, I have established how delayed exogenous administration of GH can modulate brain recovery and restore functional deficits. Firstly, in publication 1 (chapter 3), I identified that stroke at the motor and somatosensory cortex impairs the ability of mice to distinguish between two stimuli at 14 days post-stroke; I linked these deficits with SND processes occurring in the thalamus and hippocampus. Secondly, in publication 2 (chapter 4), I showed that stroke mice suffered from motor deficits and cognitive deficits that lasted during the follow-up period of 84 days after the initial ischemic injury; these deficits were associated with alterations in multiple molecular and cellular mechanisms in the peri-infarct and hippocampus. Thirdly, in publication 3 (chapter 5), I revealed that the motor deficits can be alleviated following a delayed administration of rhGH, starting at 48 hours post-stroke and continued for 28 days; these improvements were supported by enhanced neurorestorative processes in the peri-infarct region. Lastly, in publication 4 (chapter 6), I demonstrated that delayed administration of rhGH also enhances cognitive performance post-stroke, which is associated with cell proliferation, neurogenesis and synaptic plasticity within the hippocampus. The results presented provides platforms for the future direction of stroke research and potentially the pathways to overall long-term stroke recovery.

7.1. Cortical stroke not only causes motor deficits, but also delayed and persistent cognitive impairment

The primary aim of the chapters 3 and 4 was to investigate the effect of cortical stroke on functional outcomes over a period of 3 months, with particular emphasis on cognitive function. The importance of this study relies on the fact that cognitive impairment is a major stroke outcome that directly affects the quality of life of stroke survivors, however, the mechanisms

behind these deficits are yet to be elucidated. Characterisation of the temporal profile of the functional deficits is essential to facilitate investigations into the progression of stroke.

In these studies, the photothrombotic model of vascular occlusion was chosen to induce stroke. The advantages of this model are very relevant for the purposes of this research. Firstly, it is highly consistent, minimally invasive, relatively simple and a fast technique. Secondly, the motor and somatosensory cortex could be precisely targeted which is ideal for the study of SND processes and associated functional outcomes. Furthermore, other stroke models such as MCAo are known to be notoriously variable and can lead to damage in a number of locations such as the thalamus and hippocampus. Thirdly, I primarily focused on the recovery phase post-stroke and understanding the brain pathophysiological mechanisms during this phase and therefore the presence or absence of the penumbra was largely irrelevant. Considering everything, the photothrombotic model had many advantages over other preclinical stroke models. Therefore, this is the model I decided to use for all my experiments.

The stroke model chosen causes occlusion in the vessels of the left somatosensory and motor cortex, which would result in expected motor deficits. Therefore, I first investigated motor function. During the process of selecting a proper motor test, I gave importance to the least stressful, relatively shorter tests with no pre-training required and able to measure motor deficits long-term. Based on these pre-requisites, I chose two motor tests that fulfilled the aforementioned criteria: the cylinder test and the grid walk (343). As expected, both the cylinder and grid walk tests showed the significant impact of stroke on motor function. There was a spontaneous recovery of the motor function over time after stroke, which is consistent with previous evidence (64, 294, 344, 345).

Then, I investigated cognitive function in sham versus stroke mice. To assess cognitive function in rodents multiple tasks have been developed over the years. Rather than the classical maze-based tasks, here I chose the rodent touchscreen platform because it is a clinically and translationally relevant approach (270, 271). This platform is automated, highly

sensitive to deficits as well as improvements, requires minimal experimenter involvement, utilises food reward to motivate performance and most importantly is similar/analogous to the ones used in humans (271). Here I used a battery of different touchscreen tests to analyse different specific cognitive domains as it is well established that stroke survivors suffer from a variety of cognitive deficits. Additionally, as these deficits are known to last for years after an ischemic event, I analysed cognitive performance over a period of 3 months. The cognitive domains investigated were: ability to discriminate between two different stimuli (visual discrimination task (VD)) (271), associative memory and learning (paired-associate learning task (PAL)) (346, 347) and cognitive flexibility (visual discrimination reversal task (VDR)) (271, 348). All these tasks are based on the same principle where mice must choose the correct stimulus to be rewarded. These tasks have been previously validated for identifying complex cognitive deficits in rodents (349, 350).

The results collected from the VD task showed that stroke mice performed this task significantly worse than sham mice (as measured by the percentage of correct answers) only when the images presented had a high degree of similarity. Additionally, the data obtained from the PAL and VDR task also revealed that memory, learning and cognitive flexibility were severely impaired after stroke for at least 84 days. My findings expand on the existing literature showing that stroke patients suffer from impairments in a range of cognitive domains and these effects are known to be persistent long-term (189, 351-353). These findings are very important and suggest that, despite inducing stroke in the motor and sensory cortex, the functional deficits go beyond motor and/or sensory impairments.

These results regarding the functional outcomes after stroke are important as it demonstrates that there is a spontaneous recovery of motor function, but a persistent decline in various aspect of cognition for months after the initial infarction.

7.2. Cognitive impairment is associated with key hallmarks of SND

I have demonstrated in the chapter 3 and 4 that a cortical stroke at the motor and somatosensory cortex can cause persistent cognitive impairment, however the underlying mechanisms reigning these cognitive deficits are still unknown. Therefore, the second aim for chapter 3 and 4 was to investigate whether these deficits are associated with SND processes by using different time-points during the course of 3 months. These time-points ranged from the subacute phase (7 and 14 days after stroke) to the chronic phase (28 and 84 days post-stroke).

In the experiments undertaken, I analysed the molecular and cellular changes occurring in the brain after stroke in different regions, such as the peri-infarct territory and SND sites (thalamus and hippocampus). The peri-infarct territory is the area immediately adjacent to the infarct and the area where the most significant levels of repair processes can be observed (273). Thalamus is the main SND site and it is highly connected to the somatosensory cortex through a number of thalamocortical and corticothalamic projections (180). This area acts as a transfer centre for somatosensory signals to the somatosensory cortex (179). The hippocampus is the area where I specifically focused my attention on, as it is responsible for high cognitive processes such as learning and memory (354). The hippocampus is connected to the thalamus through hippocampal-thalamic connections, which has been demonstrated to be dysregulated after stroke (185).

In the peri-infarct, I observed a reduction in the NeuN labelling at earlier time points (day 7, 14 and 28) which then modestly increased at day 84. Similarly, tissue loss peaked at day 7 post-stroke before improving thereafter. These results suggest a proliferation of neuronal progenitor cells in this region. Microglial activation peaked in this area between day 7 and 28 after photothrombotic occlusion to then gradually subside at day 84. Furthermore, reactive astrogliosis peaked at 7 days and then was gradually reduced until it was indistinguishable from sham animals. These results on brain recovery in the motor and somatosensory cortex (peri-infarct area) over time, might explain the modest spontaneous motor recovery observed.

Then, I studied the cellular and molecular disturbances in SND sites. Previous studies from our group and others have mostly studied SND processes occurring in the thalamus after stroke (198, 204-206, 221, 249). Therefore, here I decided to mainly focus my attention on the hippocampus due to the lack of studies addressing the role of this region in the progression of cognitive impairment long-term after stroke. The observations were slightly different in the hippocampus compared to the peri-infarct area; specifically I found robust changes in the CA1 subregion. Neuronal loss started at 14 days post-stroke and persisted up to 84 days in the CA1 subregion. Microglia activation peaked around 28 days post-stroke and remained highly active after 84 days. Additionally, reactive astrogliosis peaked at 7 days and then was reduced to basal levels at 84 days. Interestingly, we observed the DG sub-region of the hippocampus to be spared, which could be due to stimulation of neural cell proliferation within the DG after stroke (355). The persistent neuronal loss over time and increased neuroinflammation in the CA1 subregion is a critical finding due to the role that this region plays in cognitive processes such as learning and memory. Further, it has been demonstrated that although most of strokes do not directly affect the hippocampus, the CA1 subregion of the hippocampus is more sensitive to ischemia than other areas of the brain (186, 356, 357). It should be noted that in my studies I found no evidence of direct hippocampal damage due to stroke, which suggests that stroke causes brain network dysregulation. Together these findings support the idea that SND processes in the hippocampus could be involved in the persistent cognitive deficits seen long-term after stroke.

In order to further understand the mechanisms involved in this neuronal loss and cognitive impairment, I investigated whether stroke altered the aggregation status and accumulation of neurotoxic proteins, which is another hallmark of SND. I analysed amyloid-β (Aβ) and α-synuclein (α-Syn), both of which have been previously associated with neurodegenerative diseases (212-214, 223, 358). I observed an increased oligomerization of both neurotoxic proteins in the peri-infarct and hippocampus. Assessment of Aβ using western blotting indicated that stroke was associated with a considerable elevation relative to sham,

specifically stroke mice exhibited greater levels of the 56 kDa oligomer in all the regions and it was persistent for months after stroke. Interestingly, the oligomeric forms of these neurotoxic proteins have previously been associated with cognitive deficits and neuronal loss in different brain diseases (213, 214, 229). The oligomers cause a variety of deleterious effects in neurons including disruption of cell membrane integrity, impairment of mitochondria function and neuroinflammation (218, 359-361). Therefore, the greater levels of α-Syn and Aβ observed in the stroke brain weeks after stroke, particularly in the hippocampus, could explain post-stroke cognitive impairment.

There are several potential explanations for the higher levels of α-Syn and Aβ seen in the brain after stroke. Stroke might induce fundamental disturbances in neurotoxic protein production, degradation or clearance. Here, I focused on the role of the clearance mechanisms. To examine this possibility, in the chapter 3 I analysed AQP4 polarization changes after stroke. It is well known that, under physiological conditions, AQP4 is localised in the astrocytic end-feet which wraps around the cerebral blood vessels, allowing the bidirectional movement of cerebrospinal fluid (CSF) and removes waste products from the brain (133, 362). After brain injury, reactive astrogliosis causes disturbances in the AQP4 polarization and impairs clearance (363-365). Here, I observed widespread astrogliosis throughout all the regions and a reduction in AQP4 polarity in the peri-infarct area. These results support the hypothesis that stroke induces a loss of AQP4 polarization, which impairs the clearance of neurotoxic proteins away from the brain environment and leads to neuronal loss and impairment in cognitive function.

In the chapter 4, I further demonstrated that the accumulation of Aβ is, at least partly, due to failure in its clearance. I performed immunohistochemistry analysis to assess the spatial distribution of Aβ within the brain tissue. These analyses revealed that in the peri-infarct region the distribution of Aβ shifted from a scattered distribution in the brain parenchyma to accumulation around the blood vessels at 3 months post-stroke. However, this effect was not as pronounced within the hippocampus. This finding is important as the accumulation of Aβ

around the vessels has been highly associated with the risk of developing vascular dementia (366, 367). These results together with the results presented in the chapter 3 provide more evidence to suggest that the accumulation of neurotoxic proteins could be due to a failure in clearance. This process together with neuronal loss and neuroinflammation might contribute to the development of cognitive impairment in stroke survivors.

While these studies are comprehensive and provide an important first step in building an understanding of the mechanisms behind post-stroke cognitive impairment, it should be documented that there are several limitations. One important consideration is that I did not directly quantify CSF clearance, and therefore I am unable to conclude that the accumulation of neurotoxic proteins is due to a failure in the CSF clearance. Future functional tests using *in vivo* imaging techniques are warranted to confirm the clearance disturbances after stroke. Additionally, to confirm the role of AQP4 in this clearance pathway, future studies should use AQP4 knockout mice or AQP4 blockers. The following has been added: Lastly, the photothrombotic stroke model produces relatively small penumbra area weakening its resemblance to human stroke. Therefore, future studies should use artery targeted photothrombotic models (which widens the penumbra) (368) to assess whether the presence of a penumbra influences SND and the associated mechanisms.

My results in addition to previous studies support the idea that the accumulation of neurotoxic proteins is most likely due to disturbances in clearance pathways after stroke (369). However, while the failure in the clearance of neurotoxic proteins is a plausible explanation, it is also worthwhile noting that the excessive production or decrease in degradation may play a role. Future studies should address the involvement of these potential mechanisms in the accumulation of neurotoxic proteins and the development of cognitive deficits.

Despite the presented limitations, these studies provide a detailed account of the SND processes occurring in the brain over the first 84 days post-stroke. My findings are important as they add to the growing body of literature linking SND with cognitive deficits after cortical stroke. Identification of these key mechanisms will provide guidance for future stroke research

and the development of pharmacologic intervention aimed at targeting these mechanisms (Summary of findings figure 10).

A

		7 days	14 days	28 days	84 days
Motor assessment	Cylinder task	↓ 43%	↓ 52%	↓ 55%	↓ 34%
	Grid walk task	↓ 17%	N/A	↓ 11%	↓ 10%
Cognitive assessment	Paired-associate learning task (PAL)	N/A	n.s.	↓ 13%	↓ 16%
	Visual discrimination reversal task (VDR)	N/A	n.s.	↓ 11%	↓ 23%
	Visual Discrimination task (VD)	N/A	↓ 13%*	N/A	N/A

B

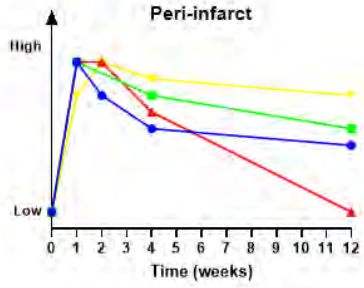

C

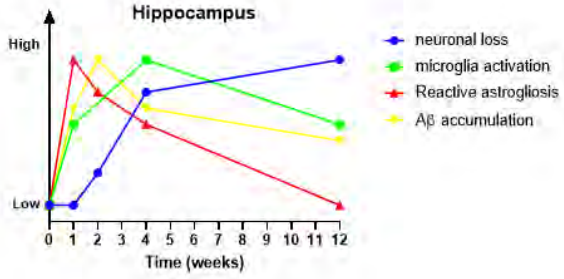

Figure 10. Summary of findings observed in chapter 3 and 4. **A.** Motor and cognitive performance at 7, 14, 28 and 84 days post-stroke. Motor function is slightly recovered long-term after stroke, while cognition remains impaired long-term. Results are presented as relative to sham. **B.** Schematic representation of processes occurring in the peri-infarct region (motor and sensory cortex) at 7, 14, 28 and 84 days post-stroke. All the processes peak around 1-2 weeks post-stroke to then be reduced in the following weeks. **C.** Schematic representation of processes occurring in the hippocampus after stroke. In this region, there is a delay in the response compared to peri-infarct. Neuronal loss starts around 2 weeks and persists for up to 3 months. Microglia activation peaks at 2 weeks and persists for up to 3 months. Aβ accumulation remains high for 3 months. Reactive astrogliosis is high in the first and second week after stroke and then reduced to basal levels. * VD task was significant when using images with a higher degree of similarity, but not when using images with a lower degree of similarity. N/A = not available. n.s. = not significant.

7.3. Growth hormone improve motor function after stroke

In chapters 3 and 4, I established the potential mechanisms involved in functional deficits after stroke. Here, I aimed to target these mechanisms to improve motor function and enhance brain repair using recombinant human growth hormone (rhGH). GH is widely known for its ability to promote growth in target tissues and cellular metabolism. However, GH has also been shown to play an important role in the central nervous system (CNS) functions, such as neurogenesis, synaptic plasticity and angiogenesis (299, 300).

In the experiments undertaken, all mice were subjected to photothrombotic stroke and then were randomly allocated to receive either rhGH or saline delivered subcutaneously *via* mini-osmotic pumps. Treatment started 48 hours post-stroke and continued for 28 consecutive days. Even though subcutaneously placement of mini-osmotic pumps required an extra surgical procedure, I chose this method over daily injections to reduce the stress caused on the mice due to the use of needles and the daily handling. Additionally, these osmotic pumps effectively deliver a pre-determined amount of rhGH daily for 28 days. To ensure that the rhGH was biologically active and it was being delivered properly, I analysed the levels of plasma IGF-1 at end-point and observed a significant increase in the GH group. The rhGH effect was also confirmed by the increased levels of plasma IGF-1 at end point. The treatment was commenced 48 hours post-stroke based on two major considerations. Firstly, I was interested in investigating the neurorestorative effects of GH, rather than neuroprotection as most of the neurons would have died after 48 hours. Secondly, I based my decision on preliminary data from our group (non-published). In these preliminary findings, we observed a transient increase in circulatory GH levels, peaking at 24 hours, which returned to basal levels at 72 hours post-stroke. Therefore, I decided to start after 48 hours to maintain GH at high levels levels. To evaluate motor function, I chose the same motor test as the ones outlined in chapter 4 (cylinder test and grid walk test). As expected, photothrombotic stroke significantly impaired motor function at one day after stroke and persisted for up to 30 days. Critically, rhGH treatment had a robust effect on enhancing motor recovery at 30 days post-stroke. This data

adds to the previous literature suggesting that GH treatment together with standard rehabilitation can significantly promote motor recovery after brain injury (322, 324, 335, 370).

To explore the possible underlying mechanisms contributing to the improved motor function following rhGH treatment, neurorestorative processes in the peri-infarct regions were firstly examined. Specifically, I focused on tissue loss, proliferation of progenitor cells, neurogenesis, synaptic plasticity and cerebrovascular remodelling. As predicted, stroke mice treated with rhGH demonstrated smaller infarct volume, relative to the stroke mice treated with saline. Further, to assess cell proliferation I used BrdU tagging. I observed an increased number of BrdU-positive cells within the peri-infarct regions.

I then studied the fate of these newly proliferating cells. I observed that part of the new cells had differentiated into neurons, supporting the idea that GH has a neurogenic effect after stroke. To support these findings, I also considered the expression of doublecortin (DCX), a protein mainly expressed by immature neurons. Mice treated with rhGH expressed higher levels of DCX reinforcing the idea that GH promotes neurogenesis. Interestingly, earlier studies have demonstrated that the number of DCX-positive cells positively correlates with recovery from functional deficits (371, 372), which could explain the ability of GH to improve motor function. Apart from proliferating and migrating to the damaged areas, these new neurons need to integrate as part of the exiting neuronal circuits. Therefore, I also analysed synaptic plasticity in this region. Specifically, I investigated the glutamate receptor 1 (GluR1), which plays an important role in synapse formation, stabilization, and plasticity, and have been previously linked with motor recovery after stroke (293, 373). I identified that GluR1 was elevated within the peri-infarct region post-stroke in the GH treated group.

Part of the newly proliferative cells also differentiated to form new blood vessels at 30 days post-stroke, suggesting that GH has the ability to promote angiogenesis. Additionally, GH increased vessel density and area coverage. Post-stroke angiogenesis is an essential process to restore the blood flow in the affected area and enhance brain function (374) and therefore greatly improves motor function recovery.

Apart from the above mentioned neurorestorative effects, it is well known that GH treatment promotes motor development and strength, by increasing muscle and bone growth (375, 376). This direct effect of GH on muscle mass and function might be also contributing to the improved motor function observed in those mice treated with GH. Ong *et al.* (336) documented an increase in body weight in stroke mice treated with GH compared to saline. However, they did not investigate whether this is due to an increased in muscle and/or bone growth.

These novel findings regarding the ability of GH to promote motor function after stroke are highly important as it could be used to boost recovery and improve the quality of life of stroke patients. Currently, the majority of stroke survivors are highly dependent and unable to perform tasks of daily living unassisted. These findings represent an important first step for the consideration of GH as a therapeutical intervention. This therapy could be used together with physical rehabilitation to accelerate the motor recovery, as shown in small and pilot clinical trials after TBI and stroke (316-318, 332).

7.4. Growth hormone improves cognitive function after stroke

In the previous study, I demonstrated the potential use of rhGH to improve motor function and promote neurorestorative processes in the peri-infarct area post-stroke. In addition to the physical disability, a high number of stroke survivors also suffer from cognitive impairment. Previous research conducted in our group showed that GH stimulates cognitive recovery, as measured by the paired-associate learning task (PAL) (336). Ong *et al.* (336) also reported that GH increased neurorestorative processes in the peri-infarct. However, they did not explore changes occurring in other cognitive-related brain regions. Therefore, I decided to further investigate the effect of rhGH on cognitive function and whether these improvements are associated with neurorestorative processes in the hippocampus.

It is well known that stroke affects different cognitive domains and therefore using a battery of tests to understand the complexity of the disease would be required. As mentioned earlier, in a previous study conducted by our group (336), we analysed the effect of GH on associative

memory and learning. Alternatively, to complement these findings, I decided to investigate visual discrimination (VD) using a touchscreen platform. The selection of this task was based on the results obtained in the chapter 3, where I already demonstrated that stroke leads to impairment in the VD task performance. Here, my results showed that stroke mice treated with rhGH performed the task significantly better than the saline group over a period of 18 days, as measured by the percentage of correct answers.

To extend our understanding of the positive effect of GH on cognitive function, I also examined the impact on neurorestorative processes, such as neurogenesis, synaptic plasticity and cerebrovascular remodelling in the hippocampus. I focused my attention on the hippocampus region, as previous studies have suggested that the hippocampus may be the primary region underlying the VD task (377-379).

My results showed an increased number of new proliferating cells in the dentate gyrus (DG) of the hippocampus in stroke mice treated with GH. The DG of the hippocampus, together with the subventricular zone (SVZ), is considered the main area of adult cell proliferation (380). Therefore, this result suggests that GH alone can affect hippocampal plasticity. These results are consistent with previous findings demonstrating that GH affects cell genesis both under brain injury and in the intact adult brain (324, 381-383). In addition to cell proliferation, I also observed increased neurogenesis and synaptic plasticity in the hippocampus as measured by the levels of DCX and GluR1 respectively.

The final mechanism that I explored was cerebrovascular remodelling. Previous studies showed that GH had a positive effect on angiogenesis by increasing vessel density and area covered in the peri-infarct region (336). However, here I found no significant differences in the area covered by blood vessels when comparing the hippocampus of mice that received GH treatment with mice that received saline. This result suggests that the hippocampus responds differently compared to the peri-infarct region. Angiogenesis in the peri-infarct (116) and thalamus (286) region have been previously confirmed after stroke. However, further studies are required to confirm whether this angiogenic effect also occurs in the hippocampus. This

region is not directly affected by the stroke itself and, as demonstrated in my previous chapter, the SND processes did not commence in this region until weeks after the primary infarction. Therefore, one month after stroke might be a very early time point to detect significant changes in angiogenesis. Future studies should analyse the angiogenic effect of GH in the hippocampus at later stages.

The results presented in this study expand on pre-existing literature showing that GH improves cognition in both health and disease populations (309, 310, 324, 332, 335, 336). Additionally, I demonstrated that GH has a wide range of neurorestorative effects that could have a potential role in a clinical setting.

Despite the promising results presented in chapters 5 and 6, additional work is required to improve our understanding of the effects of GH in the brain. For instance, the effect of GH in glia cells were not studied. Glia cells, including astrocytes and microglia, account for the majority of the brain's cells and play an important role in neuroinflammation. Therefore, future studies should consider these cell populations. Additionally, further studies regarding the appropriate time of administration, duration of the treatment and dosage as well as the interaction of the treatment with common comorbidities are still needed.

The safety and efficacy profile of GH has been widely documented (384). However, as with any medication, there are inherent risks of long-term morbidities that must be evaluated. A recent comprehensive review of available published data from GH registries, representing data from real-life clinical practice and covering over 150,000 patients from 1988-2016, identified that there was no evidence to indicate that GH treatment increases mortality, new malignancy, or stroke (314). Nevertheless, it is worthwhile to take into account other risk such as diabetes when considering the implementation of this therapy in future clinical trials. In summary, the results presented in chapters 5 and 6 support the idea that GH could be used as a pharmacological intervention to enhance motor and cognitive recovery. An important advantage presented in these studies is that rhGH can improve these functional outcomes when delivered days after stroke. This greatly increased the time window of treatment, which

currently is just limited to a couple of hours after the ischemic event (Summary of findings figure 11).

A

	Performance at 28 days post GH treatment
Cylinder Task	↑ 50%
Grid Walk Task	↑ 60%
Visual Discrimination Task	↑ 24%

B

	Peri-infarct (M1 and S1)	Dentate gyrus of hippocampus	CA1 of hippocampus
BrdU-positive cells	↑ 109%	↑ 78%	n.s.
NeuN-positive cells	↑ 10%	n.s.	n.s.
Doublecortin expression	↑ 200%	↑ 82%	n.s.
GluR1 expression	↑ 204%	↑ 113%	↑ 79%
% Area vessels	↑ 18%	n.s.	n.s.

Figure 11. Summary of findings observed in chapter 5 and 6. **A.** Motor and cognitive performance after rhGH treatment relative to saline treatment. **B.** Neurorestorative processes occurring in the brain after GH treatment in the peri-infarct and hippocampus relative to saline treatment. M1 = motor cortex S1 = somatosensory cortex. n.s. = not significant.

CHAPTER 8: CONCLUSIONS

In conclusion, the data presented in this thesis have demonstrated several novel and important findings:

- Stroke significantly impairs visual discrimination, learning, memory and behavioural flexibility in mice that continued during the follow-up period of 84 days.
- Stroke severely impaired motor function in the early stages and in later stages there is a modest spontaneous recovery.
- The cognitive impairment long-term after stroke is associated with SND processes in remote brain regions from the primary infarction.
- The accumulation of neurotoxic proteins in the stroke brain is associated with disturbances in the clearance mechanisms, as measured by the levels of AQP4 polarisation and the accumulation of Aβ around the vessels.
- rhGH treatment starting at 48 hours post-stroke significantly improves motor function. This improvement is associated with the enhancement of neurorestorative processes in the peri-infarct area.
- rhGH treatment starting at 48 hours post-stroke significantly improves visual discrimination. This improvement is associated with the enhancement of neurorestorative processes in the hippocampus.

The findings presented here may have significant clinical implications. Firstly, I developed a further understanding on the evolution of the functional deficits long-term after the ischemic onset. This thesis describes how cognitive impairment lasts for months after the initial stroke and affects a variety of cognitive domains, while the motor deficits slightly improve overtime. Secondly, I have described the potential cellular and molecular mechanisms involved in the pathophysiology of stroke during the recovery phase. Importantly, I found that stroke induces a continuous accumulation of neurotoxic proteins, persistent neuroinflammation and neuronal loss in different brain areas. The identification of these mechanisms in correlation with functional deficits strongly suggests an interaction and functional connection between the two.

An important consideration is that all these processes are key hallmarks of SND and develop in the weeks and months following stroke, which greatly prolongs the time course of therapeutic action. Therefore, these results point at SND as a promising therapeutic target to promote functional recovery.

Finally, in this thesis, I proposed GH as a new therapeutic intervention that has the ability to promote brain repair and improve functional outcomes. To date, the vast majority of pre-clinical research has focused on preventing tissue loss that occurs at the time of stroke (neuroprotection). Despite decades of research, very limited treatments for acute stroke have been developed and clinically approved. This suggests that new interventions should be directed at targeting mechanisms during the recovery phase of stroke and promote neurorestorative processes. Therefore, in this thesis I focused on investigating an intervention that could be delivered days after stroke and still have positive effects. I demonstrated that GH treatment (starting at 48 hours post-stroke) stimulates both motor and cognitive performance as well as promotes brain repair mechanisms in the peri-infarct and hippocampus. The presented evidence positions GH as a promising and useful therapeutic tool in the recovery phase after stroke. Future clinical studies are still necessary to confirm these pre-clinical findings.

In conclusion, the outcomes of this research are important in terms of furthering our understanding regarding the pathophysiology of stroke and in terms of new potential therapeutic interventions. Additionally, findings from this thesis are also likely to have implications more broadly in other neurological disorders such as TBI or subarachnoid haemorrhage. I anticipate that this evidence will hopefully be used to rethink the current approaches to the treatment of stroke, reduce disability in stroke patients and improve their quality of life.

CHAPTER 9: REFERENCES

1. Collaborators GBDCoD. Global, regional, and national age-sex specific mortality for 264 causes of death, 1980-2016: a systematic analysis for the Global Burden of Disease Study 2016. Lancet. 2017;390(10100):1151-1210.
2. World Health Organization. The atlas of heart disease and stroke / Judith Mackay and George Mensah ; with Shanthi Mendis and Kurt Greenland. Geneva: World Health Organization; 2004.
3. Kalaria RN, Akinyemi R, Ihara M. Stroke injury, cognitive impairment and vascular dementia. Biochim Biophys Acta. 2016;1862(5):915-925.
4. Economics DA. The economic impact of stroke in Australia. 2013.
5. Dewey HM, Thrift AG, Mihalopoulos C, Carter R, Macdonell RAL, McNeil JJ, et al. Lifetime cost of stroke subtypes in Australia: findings from the North East Melbourne Stroke Incidence Study (NEMESIS). Stroke. 2003;34(10):2502-2507.
6. Foundation S. Facts and figures about stroke. 2018.
7. Economics DA. No postcode untouched - Stroke in Australia. 2017.
8. Begg SJ, Vos T, Barker B, Stanley L, Lopez AD. Burden of disease and injury in Australia in the new millennium: measuring health loss from diseases, injuries and risk factors. Med J Aust. 2008;188(1):36-40.
9. Krishnamurthi RV, Feigin VL, Forouzanfar MH, Mensah GA, Connor M, Bennett DA, et al. Global and regional burden of first-ever ischaemic and haemorrhagic stroke during 1990-2010: findings from the Global Burden of Disease Study 2010. Lancet Glob Health. 2013;1(5):e259-e281.
10. Health AIo, Welfare. Cardiovascular disease mortality: trends at different ages. Canberra: AIHW; 2010.
11. Moskowitz MA, Lo EH, Iadecola C. The science of stroke: mechanisms in search of treatments. Neuron. 2010;67(2):181-198.
12. March EG. Towards Prevention and Early Recognition of Stroke: The Australian Context. Brain Impairment. 2011;12(3):223-230.
13. Deb P, Sharma S, Hassan KM. Pathophysiologic mechanisms of acute ischemic stroke: An overview with emphasis on therapeutic significance beyond thrombolysis. Pathophysiology. 2010;17(3):197-218.
14. Astrup J, Siesjö BK, Symon L. Thresholds in cerebral ischemia - the ischemic penumbra. Stroke. 1981;12(6):723-725.
15. Baron JC. Perfusion thresholds in human cerebral ischemia: historical perspective and therapeutic implications. Cerebrovasc Dis. 2001;11 Suppl 1:2-8.
16. Saver JL. Time is brain--quantified. Stroke. 2006;37(1):263-266.
17. Emberson J, Lees KR, Lyden P, Blackwell L, Albers G, Bluhmki E, et al. Effect of treatment delay, age, and stroke severity on the effects of intravenous thrombolysis with alteplase for acute ischaemic stroke: a meta-analysis of individual patient data from randomised trials. Lancet. 2014;384(9958):1929-1935.
18. National Institute of Neurological D, Stroke rt PASSG. Tissue plasminogen activator for acute ischemic stroke. N Engl J Med. 1995;333(24):1581-1587.
19. Sandercock P, Wardlaw JM, Lindley RI, Dennis M, Cohen G, Murray G, et al. The benefits and harms of intravenous thrombolysis with recombinant tissue plasminogen activator within 6 h of acute ischaemic stroke (the third international stroke trial [IST-3]): a randomised controlled trial. Lancet. 2012;379(9834):2352-2363.
20. Ma H, Campbell BCV, Parsons MW, Churilov L, Levi CR, Hsu C, et al. Thrombolysis Guided by Perfusion Imaging up to 9 Hours after Onset of Stroke. N Engl J Med. 2019;380(19):1795-1803.
21. Gilligan AK, Thrift AG, Sturm JW, Dewey HM, Macdonell RAL, Donnan GA. Stroke units, tissue plasminogen activator, aspirin and neuroprotection: which stroke intervention could provide the greatest community benefit? Cerebrovasc Dis. 2005;20(4):239-244.

22. Quain DA, Parsons MW, Loudfoot AR, Spratt NJ, Evans MK, Russell ML, et al. Improving access to acute stroke therapies: a controlled trial of organised pre-hospital and emergency care. Med J Aust. 2008;189(8):429-433.
23. Ciccone A, Valvassori L, Nichelatti M, Sgoifo A, Ponzio M, Sterzi R, et al. Endovascular treatment for acute ischemic stroke. N Engl J Med. 2013;368(10):904-913.
24. Nogueira RG, Jadhav AP, Haussen DC, Bonafe A, Budzik RF, Bhuva P, et al. Thrombectomy 6 to 24 Hours after Stroke with a Mismatch between Deficit and Infarct. N Engl J Med. 2018;378(1):11-21.
25. Albers GW, Marks MP, Kemp S, Christensen S, Tsai JP, Ortega-Gutierrez S, et al. Thrombectomy for Stroke at 6 to 16 Hours with Selection by Perfusion Imaging. N Engl J Med. 2018;378(8):708-718.
26. Berkhemer OA, Fransen PSS, Beumer D, van den Berg LA, Lingsma HF, Yoo AJ, et al. A randomized trial of intraarterial treatment for acute ischemic stroke. N Engl J Med. 2015;372(1):11-20.
27. Campbell BCV, Mitchell PJ, Kleinig TJ, Dewey HM, Churilov L, Yassi N, et al. Endovascular therapy for ischemic stroke with perfusion-imaging selection. N Engl J Med. 2015;372(11):1009-1018.
28. Goyal M, Demchuk AM, Menon BK, Eesa M, Rempel JL, Thornton J, et al. Randomized assessment of rapid endovascular treatment of ischemic stroke. N Engl J Med. 2015;372(11):1019-1030.
29. Saver JL, Goyal M, Bonafe A, Diener H-C, Levy EI, Pereira VM, et al. Stent-retriever thrombectomy after intravenous t-PA vs. t-PA alone in stroke. N Engl J Med. 2015;372(24):2285-2295.
30. Jovin TG, Chamorro A, Cobo E, de Miquel MA, Molina CA, Rovira A, et al. Thrombectomy within 8 hours after symptom onset in ischemic stroke. N Engl J Med. 2015;372(24):2296-2306.
31. Marmagkiolis K, Hakeem A, Cilingiroglu M, Gundogdu B, Iliescu C, Tsitlakidou D, et al. Safety and Efficacy of Stent Retrievers for the Management of Acute Ischemic Stroke: Comprehensive Review and Meta-Analysis. JACC Cardiovasc Interv. 2015;8(13):1758-1765.
32. Phan K, Zhao DF, Phan S, Huo YR, Mobbs RJ, Rao PJ, et al. Endovascular therapy including thrombectomy for acute ischemic stroke: A systematic review and meta-analysis with trial sequential analysis. J Clin Neurosci. 2016;29:38-45.
33. National stroke audit – acute services clinical audit report 2015.
34. Silvestrelli G, Parnetti L, Paciaroni M, Caso V, Corea F, Vitali R, et al. Early admission to stroke unit influences clinical outcome. Eur J Neurol. 2006;13(3):250-255.
35. Stroke Unit Trialists C. Organised inpatient (stroke unit) care for stroke. Cochrane Database Syst Rev. 2013;2013(9):CD000197-CD000197.
36. O'Donnell MJ, Xavier D, Liu L, Zhang H, Chin SL, Rao-Melacini P, et al. Risk factors for ischaemic and intracerebral haemorrhagic stroke in 22 countries (the INTERSTROKE study): a case-control study. Lancet. 2010;376(9735):112-123.
37. MacMahon S, Rodgers A. The Epidemiological Association between Blood Pressure and Stroke: Implications for Primary and Secondary Prevention. Hypertension Research. 1994;17(SupplementI):S23-S32.
38. Sandercock P, Gubitz G, Foley P, Counsell C. Antiplatelet therapy for acute ischaemic stroke. Cochrane Database Syst Rev. 2003(2):CD000029-CD000029.
39. Spence JD. Secondary stroke prevention. Nature reviews Neurology. 2010;6(9):477-486.
40. Hankey GJ, Jamrozik K, Broadhurst RJ, Forbes S, Anderson CS. Long-term disability after first-ever stroke and related prognostic factors in the Perth Community Stroke Study, 1989-1990. Stroke. 2002;33(4):1034-1040.
41. Dirnagl U, Iadecola C, Moskowitz MA. Pathobiology of ischaemic stroke: an integrated view. Trends Neurosci. 1999;22(9):391-397.

42. O'Collins VE, Macleod MR, Donnan GA, Horky LL, van der Worp BH, Howells DW. 1,026 experimental treatments in acute stroke. Ann Neurol. 2006;59(3):467-477.
43. Langhorne P, Bernhardt J, Kwakkel G. Stroke rehabilitation. Lancet. 2011;377(9778):1693-1702.
44. Krafft PR, Bailey EL, Lekic T, Rolland WB, Altay O, Tang J, et al. Etiology of stroke and choice of models. Int J Stroke. 2012;7(5):398-406.
45. Wentworth DA, Atkinson RP. Implementation of an acute stroke program decreases hospitalization costs and length of stay. Stroke. 1996;27(6):1040-1043.
46. Rijntjes M, Weiller C. Recovery of motor and language abilities after stroke: the contribution of functional imaging. Prog Neurobiol. 2002;66(2):109-122.
47. Opara JA, Jaracz K. Quality of life of post-stroke patients and their caregivers. J Med Life. 2010;3(3):216-220.
48. Sun J-H, Tan L, Yu J-T. Post-stroke cognitive impairment: epidemiology, mechanisms and management. Ann Transl Med. 2014;2(8):80-96.
49. Nys GMS, van Zandvoort MJE, de Kort PLM, Jansen BPW, Kappelle LJ, de Haan EHF. Restrictions of the Mini-Mental State Examination in acute stroke. Arch Clin Neuropsychol. 2005;20(5):623-629.
50. Patel M, Coshall C, Rudd AG, Wolfe CDA. Natural history of cognitive impairment after stroke and factors associated with its recovery. Clin Rehabil. 2003;17(2):158-166.
51. Serrano S, Domingo J, Rodríguez-Garcia E, Castro M-D, del Ser T. Frequency of cognitive impairment without dementia in patients with stroke: a two-year follow-up study. Stroke. 2007;38(1):105-110.
52. del Ser T, Barba R, Morin MM, Domingo J, Cemillan C, Pondal M, et al. Evolution of cognitive impairment after stroke and risk factors for delayed progression. Stroke. 2005;36(12):2670-2675.
53. Delavaran H, Jönsson AC, Lövkvist H, Iwarsson S, Elmståhl S, Norrving B, et al. Cognitive function in stroke survivors: A 10-year follow-up study. Acta Neurol Scand. 2017;136(3):187-194.
54. Claesson L, Lindén T, Skoog I, Blomstrand C. Cognitive impairment after stroke - impact on activities of daily living and costs of care for elderly people. The Göteborg 70+ Stroke Study. Cerebrovasc Dis. 2005;19(2):102-109.
55. Tatemichi TK, Desmond DW, Stern Y, Paik M, Sano M, Bagiella E. Cognitive impairment after stroke: frequency, patterns, and relationship to functional abilities. J Neurol Neurosurg Psychiatry. 1994;57(2):202-207.
56. Rasquin SMC, Lodder J, Verhey FRJ. Predictors of reversible mild cognitive impairment after stroke: a 2-year follow-up study. J Neurol Sci. 2005;229-230:21-25.
57. Levine DA, Galecki AT, Langa KM, Unverzagt FW, Kabeto MU, Giordani B, et al. Trajectory of Cognitive Decline After Incident Stroke. JAMA. 2015;314(1):41-51.
58. Barba R, Martínez-Espinosa S, Rodríguez-García E, Pondal M, Vivancos J, Del Ser T. Poststroke dementia : clinical features and risk factors. Stroke. 2000;31(7):1494-1501.
59. Simmonds F, Stevermuer T. The AROC annual report: the state of rehabilitation in Australia 2006. Aust Health Rev. 2008;32(1):85-110.
60. Langhorne P, Duncan P. Does the organization of postacute stroke care really matter? Stroke. 2001;32(1):268-274.
61. Langhorne P, Wu O, Rodgers H, Ashburn A, Bernhardt J. A Very Early Rehabilitation Trial after stroke (AVERT): a Phase III, multicentre, randomised controlled trial. Health technology assessment (Winchester, England). 2017;21(54):1-120.
62. Foundation NS. National Stroke Audit Rehabilitation Services 2010. Melbourne Australia. 2010.
63. Lin DJ, Finklestein SP, Cramer SC. New Directions in Treatments Targeting Stroke Recovery. Stroke. 2018;49(12):3107-3114.
64. Langhorne P, Coupar F, Pollock A. Motor recovery after stroke: a systematic review. Lancet Neurol. 2009;8(8):741-754.

65. Johansson BB. Current trends in stroke rehabilitation. A review with focus on brain plasticity. Acta Neurol Scand. 2011;123(3):147-159.
66. Brewer L, Horgan F, Hickey A, Williams D. Stroke rehabilitation: recent advances and future therapies. QJM. 2013;106(1):11-25.
67. Brainin M, Tuomilehto J, Heiss WD, Bornstein NM, Bath PMW, Teuschl Y, et al. Post-stroke cognitive decline: an update and perspectives for clinical research. Eur J Neurol. 2015;22(2):13-16.
68. Cumming TB, Tyedin K, Churilov L, Morris ME, Bernhardt J. The effect of physical activity on cognitive function after stroke: a systematic review. Int Psychogeriatr. 2012;24(4):557-567.
69. Mang CS, Campbell KL, Ross CJD, Boyd LA. Promoting neuroplasticity for motor rehabilitation after stroke: considering the effects of aerobic exercise and genetic variation on brain-derived neurotrophic factor. Phys Ther. 2013;93(12):1707-1716.
70. Hickey A MN, Bruen C, Mellon L, Bennett K, Williams D, Pender N, Doyle F. Psychological interventions for managing cognitive impairment after stroke. Cochrane Database of Systematic Reviews. 2019(Issue 8).
71. Hoffmann T, Bennett S, Koh C-L, McKenna K. A systematic review of cognitive interventions to improve functional ability in people who have cognitive impairment following stroke. Top Stroke Rehabil. 2010;17(2):99-107.
72. Grieb P. Neuroprotective properties of citicoline: facts, doubts and unresolved issues. CNS Drugs. 2014;28(3):185-193.
73. Alvarez-Sabín J, Román GC. Citicoline in vascular cognitive impairment and vascular dementia after stroke. Stroke. 2011;42(1 Suppl):S40-S43.
74. Cotroneo AM, Castagna A, Putignano S, Lacava R, Fantò F, Monteleone F, et al. Effectiveness and safety of citicoline in mild vascular cognitive impairment: the IDEALE study. Clin Interv Aging. 2013;8:131-137.
75. Alvarez-Sabín J, Ortega G, Jacas C, Santamarina E, Maisterra O, Ribo M, et al. Long-term treatment with citicoline may improve poststroke vascular cognitive impairment. Cerebrovasc Dis. 2013;35(2):146-154.
76. Wilkinson D, Doody R, Helme R, Taubman K, Mintzer J, Kertesz A, et al. Donepezil in vascular dementia: a randomized, placebo-controlled study. Neurology. 2003;61(4):479-486.
77. Black S, Román GC, Geldmacher DS, Salloway S, Hecker J, Burns A, et al. Efficacy and tolerability of donepezil in vascular dementia: positive results of a 24-week, multicenter, international, randomized, placebo-controlled clinical trial. Stroke. 2003;34(10):2323-2330.
78. Román GC, Salloway S, Black SE, Royall DR, Decarli C, Weiner MW, et al. Randomized, placebo-controlled, clinical trial of donepezil in vascular dementia: differential effects by hippocampal size. Stroke. 2010;41(6):1213-1221.
79. Rockwood K, Mitnitski A, Black SE, Richard M, Defoy I, investigators Vs. Cognitive change in donepezil treated patients with vascular or mixed dementia. Can J Neurol Sci. 2013;40(4):564-571.
80. Xing C, Arai K, Lo EH, Hommel M. Pathophysiologic cascades in ischemic stroke. Int J Stroke. 2012;7(5):378-385.
81. Takano T, Tian G-F, Peng W, Lou N, Lovatt D, Hansen AJ, et al. Cortical spreading depression causes and coincides with tissue hypoxia. Nat Neurosci. 2007;10(6):754-762.
82. Li L, Lundkvist A, Andersson D, Wilhelmsson U, Nagai N, Pardo AC, et al. Protective role of reactive astrocytes in brain ischemia. J Cereb Blood Flow Metab. 2008;28(3):468-481.
83. Taylor RA, Sansing LH. Microglial responses after ischemic stroke and intracerebral hemorrhage. Clin Dev Immunol. 2013;2013(746068):1-10.
84. Huang L, Wu Z-B, Zhuge Q, Zheng W, Shao B, Wang B, et al. Glial scar formation occurs in the human brain after ischemic stroke. Int J Med Sci. 2014;11(4):344-348.
85. Turner RC, Dodson SC, Rosen CL, Huber JD. The science of cerebral ischemia and the quest for neuroprotection: navigating past failure to future success. J Neurosurg. 2013;118(5):1072-1085.
86. Lo EH, Dalkara T, Moskowitz MA. Mechanisms, challenges and opportunities in stroke. Nat Rev Neurosci. 2003;4(5):399-415.

87. del Zoppo GJ. Stroke and neurovascular protection. N Engl J Med. 2006;354(6):553-555.
88. Hawkins BT, Davis TP. The blood-brain barrier/neurovascular unit in health and disease. Pharmacol Rev. 2005;57(2):173-185.
89. Harder DR, Zhang C, Gebremedhin D. Astrocytes function in matching blood flow to metabolic activity. News Physiol Sci. 2002;17:27-31.
90. Ohtsuki S, Terasaki T. Contribution of carrier-mediated transport systems to the blood-brain barrier as a supporting and protecting interface for the brain; importance for CNS drug discovery and development. Pharm Res. 2007;24(9):1745-1758.
91. Persidsky Y, Ramirez SH, Haorah J, Kanmogne GD. Blood-brain barrier: structural components and function under physiologic and pathologic conditions. J Neuroimmune Pharmacol. 2006;1(3):223-236.
92. Zhang L, Zhang ZG, Chopp M. The neurovascular unit and combination treatment strategies for stroke. Trends Pharmacol Sci. 2012;33(8):415-422.
93. Xiong Y, Mahmood A, Chopp M. Angiogenesis, neurogenesis and brain recovery of function following injury. Curr Opin Investig Drugs. 2010;11(3):298-308.
94. Mann GE. Molecular mechanisms underlying neurovascular protection in stroke. J Physiol. 2011;589(17):4103-4104.
95. Broughton BRS, Reutens DC, Sobey CG. Apoptotic mechanisms after cerebral ischemia. Stroke. 2009;40(5):e331-e339.
96. Unal-Cevik I, Kilinç M, Can A, Gürsoy-Ozdemir Y, Dalkara T. Apoptotic and necrotic death mechanisms are concomitantly activated in the same cell after cerebral ischemia. Stroke. 2004;35(9):2189-2194.
97. Hou K, Xu D, Li F, Chen S, Li Y. The progress of neuronal autophagy in cerebral ischemia stroke: Mechanisms, roles and research methods. J Neurol Sci. 2019;400:72-82.
98. Wan J, Ren H, Wang J. Iron toxicity, lipid peroxidation and ferroptosis after intracerebral haemorrhage. Stroke Vasc Neurol. 2019;4(2):93-95.
99. Grupke S, Hall J, Dobbs M, Bix GJ, Fraser JF. Understanding history, and not repeating it. Neuroprotection for acute ischemic stroke: from review to preview. Clin Neurol Neurosurg. 2015;129:1-9.
100. Thored P, Arvidsson A, Cacci E, Ahlenius H, Kallur T, Darsalia V, et al. Persistent production of neurons from adult brain stem cells during recovery after stroke. Stem Cells. 2006;24(3):739-747.
101. Magnusson JP, Göritz C, Tatarishvili J, Dias DO, Smith EMK, Lindvall O, et al. A latent neurogenic program in astrocytes regulated by Notch signaling in the mouse. Science. 2014;346(6206):237-241.
102. Yamashita T, Ninomiya M, Hernández Acosta P, García-Verdugo JM, Sunabori T, Sakaguchi M, et al. Subventricular zone-derived neuroblasts migrate and differentiate into mature neurons in the post-stroke adult striatum. J Neurosci. 2006;26(24):6627-6636.
103. Jin K, Wang X, Xie L, Mao XO, Zhu W, Wang Y, et al. Evidence for stroke-induced neurogenesis in the human brain. Proc Natl Acad Sci U S A. 2006;103(35):13198-13202.
104. Arvidsson A, Collin T, Kirik D, Kokaia Z, Lindvall O. Neuronal replacement from endogenous precursors in the adult brain after stroke. Nat Med. 2002;8(9):963-970.
105. Brown LS, Foster CG, Courtney JM, King NE, Howells DW, Sutherland BA. Pericytes and Neurovascular Function in the Healthy and Diseased Brain. Frontiers in cellular neuroscience. 2019;13:282.
106. Compston A. From the archives. The cerebral arterial supply. By Charles E Beevor MD, FRCP. Brain 1908; 30: 403–25. Brain. 2013;136(Pt 2):362-367.
107. Liebeskind DS. Collateral circulation. Stroke. 2003;34(9):2279-2284.
108. Shuaib A, Butcher K, Mohammad AA, Saqqur M, Liebeskind DS. Collateral blood vessels in acute ischaemic stroke: a potential therapeutic target. Lancet Neurol. 2011;10(10):909-921.

109. Krupinski J, Issa R, Bujny T, Slevin M, Kumar P, Kumar S, et al. A putative role for platelet-derived growth factor in angiogenesis and neuroprotection after ischemic stroke in humans. Stroke. 1997;28(3):564-573.
110. Schaper W. Collateral circulation: past and present. Basic Res Cardiol. 2009;104(1):5-21.
111. Liebeskind DS, Tomsick TA, Foster LD, Yeatts SD, Carrozzella J, Demchuk AM, et al. Collaterals at angiography and outcomes in the Interventional Management of Stroke (IMS) III trial. Stroke. 2014;45(3):759-764.
112. Bang OY, Saver JL, Kim SJ, Kim G-M, Chung C-S, Ovbiagele B, et al. Collateral flow predicts response to endovascular therapy for acute ischemic stroke. Stroke. 2011;42(3):693-699.
113. Bang OY, Saver JL, Buck BH, Alger JR, Starkman S, Ovbiagele B, et al. Impact of collateral flow on tissue fate in acute ischaemic stroke. J Neurol Neurosurg Psychiatry. 2008;79(6):625-629.
114. Krupinski J, Kaluza J, Kumar P, Kumar S, Wang JM. Role of angiogenesis in patients with cerebral ischemic stroke. Stroke. 1994;25(9):1794-1798.
115. Arenillas JF, Sobrino T, Castillo J, Dávalos A. The role of angiogenesis in damage and recovery from ischemic stroke. Curr Treat Options Cardiovasc Med. 2007;9(3):205-212.
116. Hayashi T, Noshita N, Sugawara T, Chan PH. Temporal profile of angiogenesis and expression of related genes in the brain after ischemia. J Cereb Blood Flow Metab. 2003;23(2):166-180.
117. Akwii RG, Sajib MS, Zahra FT, Mikelis CM. Role of Angiopoietin-2 in Vascular Physiology and Pathophysiology. Cells. 2019;8((5) 471):1-19.
118. Geiseler SJ, Morland C. The Janus Face of VEGF in Stroke. Int J Mol Sci. 2018;19(5):1362.
119. Greenberg DA, Jin K. Vascular endothelial growth factors (VEGFs) and stroke. Cell Mol Life Sci. 2013;70(10):1753-1761.
120. Lapchak PA. Erythropoietin molecules to treat acute ischemic stroke: a translational dilemma! Expert Opin Investig Drugs. 2010;19(10):1179-1186.
121. Abbott NJ. Astrocyte-endothelial interactions and blood-brain barrier permeability. J Anat. 2002;200(6):629-638.
122. Zonta M, Angulo MC, Gobbo S, Rosengarten B, Hossmann K-A, Pozzan T, et al. Neuron-to-astrocyte signaling is central to the dynamic control of brain microcirculation. Nat Neurosci. 2003;6(1):43-50.
123. Takano T, Tian G-F, Peng W, Lou N, Libionka W, Han X, et al. Astrocyte-mediated control of cerebral blood flow. Nat Neurosci. 2006;9(2):260-267.
124. Iadecola C, Nedergaard M. Glial regulation of the cerebral microvasculature. Nat Neurosci. 2007;10(11):1369-1376.
125. Brown AM, Ransom BR. Astrocyte glycogen and brain energy metabolism. Glia. 2007;55(12):1263-1271.
126. Pekny M, Wilhelmsson U, Pekna M. The dual role of astrocyte activation and reactive gliosis. Neurosci Lett. 2014;565:30-38.
127. Pekny M, Nilsson M. Astrocyte activation and reactive gliosis. Glia. 2005;50(4):427-434.
128. Liu Z, Li Y, Cui Y, Roberts C, Lu M, Wilhelmsson U, et al. Beneficial effects of gfap/vimentin reactive astrocytes for axonal remodeling and motor behavioral recovery in mice after stroke. Glia. 2014;62(12):2022-2033.
129. Hayakawa K, Esposito E, Wang X, Terasaki Y, Liu Y, Xing C, et al. Transfer of mitochondria from astrocytes to neurons after stroke. Nature. 2016;535(7613):551-555.
130. McKeon RJ, Schreiber RC, Rudge JS, Silver J. Reduction of neurite outgrowth in a model of glial scarring following CNS injury is correlated with the expression of inhibitory molecules on reactive astrocytes. J Neurosci. 1991;11(11):3398-3411.
131. Smith GM, Strunz C. Growth factor and cytokine regulation of chondroitin sulfate proteoglycans by astrocytes. Glia. 2005;52(3):209-218.
132. Gris P, Tighe A, Levin D, Sharma R, Brown A. Transcriptional regulation of scar gene expression in primary astrocytes. Glia. 2007;55(11):1145-1155.

133. Iliff JJ, Wang M, Liao Y, Plogg BA, Peng W, Gundersen GA, et al. A paravascular pathway facilitates CSF flow through the brain parenchyma and the clearance of interstitial solutes, including amyloid β. Sci Transl Med. 2012;4(147):147ra111.
134. Gaberel T, Gakuba C, Goulay R, Martinez De Lizarrondo S, Hanouz J-L, Emery E, et al. Impaired glymphatic perfusion after strokes revealed by contrast-enhanced MRI: a new target for fibrinolysis? Stroke. 2014;45(10):3092-3096.
135. Jin R, Yang G, Li G. Inflammatory mechanisms in ischemic stroke: role of inflammatory cells. J Leukoc Biol. 2010;87(5):779-789.
136. Casano AM, Peri F. Microglia: multitasking specialists of the brain. Dev Cell. 2015;32(4):469-477.
137. Kettenmann H, Hanisch U-K, Noda M, Verkhratsky A. Physiology of microglia. Physiol Rev. 2011;91(2):461-553.
138. Wake H, Moorhouse AJ, Jinno S, Kohsaka S, Nabekura J. Resting microglia directly monitor the functional state of synapses in vivo and determine the fate of ischemic terminals. J Neurosci. 2009;29(13):3974-3980.
139. Kreutzberg GW. Microglia: a sensor for pathological events in the CNS. Trends Neurosci. 1996;19(8):312-318.
140. Nimmerjahn A, Kirchhoff F, Helmchen F. Resting microglial cells are highly dynamic surveillants of brain parenchyma in vivo. Science. 2005;308(5726):1314-1318.
141. Walker FR, Beynon SB, Jones KA, Zhao Z, Kongsui R, Cairns M, et al. Dynamic structural remodelling of microglia in health and disease: a review of the models, the signals and the mechanisms. Brain Behav Immun. 2014;37:1-14.
142. Thiel A, Radlinska BA, Paquette C, Sidel M, Soucy J-P, Schirrmacher R, et al. The temporal dynamics of poststroke neuroinflammation: a longitudinal diffusion tensor imaging-guided PET study with 11C-PK11195 in acute subcortical stroke. J Nucl Med. 2010;51(9):1404-1412.
143. Ito D, Tanaka K, Suzuki S, Dembo T, Fukuuchi Y. Enhanced expression of Iba1, ionized calcium-binding adapter molecule 1, after transient focal cerebral ischemia in rat brain. Stroke. 2001;32(5):1208-1215.
144. Morrison HW, Filosa JA. A quantitative spatiotemporal analysis of microglia morphology during ischemic stroke and reperfusion. J Neuroinflammation. 2013;10:4-4.
145. Rupalla K, Allegrini PR, Sauer D, Wiessner C. Time course of microglia activation and apoptosis in various brain regions after permanent focal cerebral ischemia in mice. Acta Neuropathol. 1998;96(2):172-178.
146. Colton CA. Heterogeneity of microglial activation in the innate immune response in the brain. J Neuroimmune Pharmacol. 2009;4(4):399-418.
147. Lalancette-Hébert M, Swarup V, Beaulieu JM, Bohacek I, Abdelhamid E, Weng YC, et al. Galectin-3 is required for resident microglia activation and proliferation in response to ischemic injury. J Neurosci. 2012;32(30):10383-10395.
148. Szalay G, Martinecz B, Lénárt N, Környei Z, Orsolits B, Judák L, et al. Microglia protect against brain injury and their selective elimination dysregulates neuronal network activity after stroke. Nat Commun. 2016;7(11499):1-13.
149. Jin W-N, Shi SX-Y, Li Z, Li M, Wood K, Gonzales RJ, et al. Depletion of microglia exacerbates postischemic inflammation and brain injury. J Cereb Blood Flow Metab. 2017;37(6):2224-2236.
150. Neher JJ, Emmrich JV, Fricker M, Mander PK, Théry C, Brown GC. Phagocytosis executes delayed neuronal death after focal brain ischemia. Proc Natl Acad Sci U S A. 2013;110(43):E4098-E4107.
151. Liu Z, Fan Y, Won SJ, Neumann M, Hu D, Zhou L, et al. Chronic treatment with minocycline preserves adult new neurons and reduces functional impairment after focal cerebral ischemia. Stroke. 2007;38(1):146-152.

152. Padma Srivastava MV, Bhasin A, Bhatia R, Garg A, Gaikwad S, Prasad K, et al. Efficacy of minocycline in acute ischemic stroke: a single-blinded, placebo-controlled trial. Neurol India. 2012;60(1):23-28.
153. Lampl Y, Boaz M, Gilad R, Lorberboym M, Dabby R, Rapoport A, et al. Minocycline treatment in acute stroke: an open-label, evaluator-blinded study. Neurology. 2007;69(14):1404-1410.
154. Malhotra K, Chang JJ, Khunger A, Blacker D, Switzer JA, Goyal N, et al. Minocycline for acute stroke treatment: a systematic review and meta-analysis of randomized clinical trials. J Neurol. 2018;265(8):1871-1879.
155. Koistinaho M, Malm TM, Kettunen MI, Goldsteins G, Starckx S, Kauppinen RA, et al. Minocycline protects against permanent cerebral ischemia in wild type but not in matrix metalloprotease-9-deficient mice. J Cereb Blood Flow Metab. 2005;25(4):460-467.
156. Park CH, Shin TK, Lee HY, Kim SJ, Lee WS. Matrix metalloproteinase inhibitors attenuate neuroinflammation following focal cerebral ischemia in mice. Korean J Physiol Pharmacol. 2011;15(2):115-122.
157. Kloppenburg M, Verweij CL, Miltenburg AM, Verhoeven AJ, Daha MR, Dijkmans BA, et al. The influence of tetracyclines on T cell activation. Clin Exp Immunol. 1995;102(3):635-641.
158. Kloppenburg M, Brinkman BM, de Rooij-Dijk HH, Miltenburg AM, Daha MR, Breedveld FC, et al. The tetracycline derivative minocycline differentially affects cytokine production by monocytes and T lymphocytes. Antimicrob Agents Chemother. 1996;40(4):934-940.
159. Brundula V, Rewcastle NB, Metz LM, Bernard CC, Yong VW. Targeting leukocyte MMPs and transmigration: minocycline as a potential therapy for multiple sclerosis. Brain. 2002;125(Pt 6):1297-1308.
160. Stirling DP, Khodarahmi K, Liu J, McPhail LT, McBride CB, Steeves JD, et al. Minocycline treatment reduces delayed oligodendrocyte death, attenuates axonal dieback, and improves functional outcome after spinal cord injury. J Neurosci. 2004;24(9):2182-2190.
161. Zhang J, Zhang Y, Xing S, Liang Z, Zeng J. Secondary neurodegeneration in remote regions after focal cerebral infarction: a new target for stroke management? Stroke. 2012;43(6):1700-1705.
162. Block F, Dihné M, Loos M. Inflammation in areas of remote changes following focal brain lesion. Prog Neurobiol. 2005;75(5):342-365.
163. Feeney DM, Baron JC. Diaschisis. Stroke. 1986;17(5):817-830.
164. Shan D-E. An explanation for putaminal CT, MR, and diffusion abnormalities secondary to nonketotic hyperglycemia. AJNR Am J Neuroradiol. 2005;26(1):194-195.
165. Ohara S, Kondo K, Kagoshima M, Yanagisawa N. Secondary degeneration of substantia nigra following massive basal ganglia infarction. Rinsho Shinkeigaku. 1989;29(11):1352-1356.
166. Kazui S, Kuriyama Y, Sawada T, Imakita S. Very early demonstration of secondary pyramidal tract degeneration by computed tomography. Stroke. 1994;25(11):2287-2289.
167. Tamura A, Tahira Y, Nagashima H, Kirino T, Gotoh O, Hojo S, et al. Thalamic atrophy following cerebral infarction in the territory of the middle cerebral artery. Stroke. 1991;22(5):615-618.
168. Duering M, Righart R, Csanadi E, Jouvent E, Hervé D, Chabriat H, et al. Incident subcortical infarcts induce focal thinning in connected cortical regions. Neurology. 2012;79(20):2025-2028.
169. Duering M, Righart R, Wollenweber FA, Zietemann V, Gesierich B, Dichgans M. Acute infarcts cause focal thinning in remote cortex via degeneration of connecting fiber tracts. Neurology. 2015;84(16):1685-1692.
170. Liang Z, Zeng J, Zhang C, Liu S, Ling X, Xu A, et al. Longitudinal investigations on the anterograde and retrograde degeneration in the pyramidal tract following pontine infarction with diffusion tensor imaging. Cerebrovasc Dis. 2008;25(3):209-216.
171. Nakane M, Tamura A, Sasaki Y, Teraoka A. MRI of secondary changes in the thalamus following a cerebral infarct. Neuroradiology. 2002;44(11):915-920.

172. Li C, Ling X, Liu S, Xu A, Zhang Y, Xing S, et al. Early detection of secondary damage in ipsilateral thalamus after acute infarction at unilateral corona radiata by diffusion tensor imaging and magnetic resonance spectroscopy. BMC Neurol. 2011;11(49):1-8.
173. Hervé D, Molko N, Pappata S, Buffon F, LeBihan D, Bousser MG, et al. Longitudinal thalamic diffusion changes after middle cerebral artery infarcts. J Neurol Neurosurg Psychiatry. 2005;76(2):200-205.
174. Jones KA, Zouikr I, Patience M, Clarkson AN, Isgaard J, Johnson SJ, et al. Chronic stress exacerbates neuronal loss associated with secondary neurodegeneration and suppresses microglial-like cells following focal motor cortex ischemia in the mouse. Brain Behav Immun. 2015;48:57-67.
175. Winter B, Brunecker P, Fiebach JB, Jungehulsing GJ, Kronenberg G, Endres M. Striatal Infarction Elicits Secondary Extrafocal MRI Changes in Ipsilateral Substantia Nigra. PLoS One. 2015;10(9):e0136483.
176. Prinz V, Hetzer A-M, Müller S, Balkaya M, Leithner C, Kronenberg G, et al. MRI heralds secondary nigral lesion after brain ischemia in mice: a secondary time window for neuroprotection. J Cereb Blood Flow Metab. 2015;35(12):1903-1909.
177. Baron J-C, Yamauchi H, Fujioka M, Endres M. Selective neuronal loss in ischemic stroke and cerebrovascular disease. J Cereb Blood Flow Metab. 2014;34(1):2-18.
178. Deschênes M, Veinante P, Zhang ZW. The organization of corticothalamic projections: reciprocity versus parity. Brain Res Brain Res Rev. 1998;28(3):286-308.
179. Guillery RW, Sherman SM. Branched thalamic afferents: what are the messages that they relay to the cortex? Brain Res Rev. 2011;66(1-2):205-219.
180. Behrens TEJ, Johansen-Berg H, Woolrich MW, Smith SM, Wheeler-Kingshott CAM, Boulby PA, et al. Non-invasive mapping of connections between human thalamus and cortex using diffusion imaging. Nat Neurosci. 2003;6(7):750-757.
181. Ohtomo G, Mano T, Seto A, Tsuji S. Degeneration of the Substantia Nigra Following Ipsilateral Striatal Infarction. Intern Med. 2018;57(5):767-768.
182. Schmitt AB, Brook GA, Buss A, Nacimiento W, Noth J, Kreutzberg GW. Dynamics of microglial activation in the spinal cord after cerebral infarction are revealed by expression of MHC class II antigen. Neuropathol Appl Neurobiol. 1998;24(3):167-176.
183. Nakane M, Teraoka A, Asato R, Tamura A. Degeneration of the ipsilateral substantia nigra following cerebral infarction in the striatum. Stroke. 1992;23(3):328-332.
184. Nishio K, Ihara M, Yamasaki N, Kalaria RN, Maki T, Fujita Y, et al. A mouse model characterizing features of vascular dementia with hippocampal atrophy. Stroke. 2010;41(6):1278-1284.
185. Baumgartner P, El Amki M, Bracko O, Luft AR, Wegener S. Sensorimotor stroke alters hippocampo-thalamic network activity. Sci Rep. 2018;8((1)15770):1-11.
186. Wang W, Redecker C, Bidmon H-J, Witte OW. Delayed neuronal death and damage of GDNF family receptors in CA1 following focal cerebral ischemia. Brain research. 2004;1023(1):92-101.
187. Akinyemi RO, Allan LM, Oakley A, Kalaria RN. Hippocampal Neurodegenerative Pathology in Post-stroke Dementia Compared to Other Dementias and Aging Controls. Front Neurosci. 2017;11(717):1-16.
188. Haque ME, Gabr RE, Hasan KM, George S, Arevalo OD, Zha A, et al. Ongoing Secondary Degeneration of the Limbic System in Patients With Ischemic Stroke: A Longitudinal MRI Study. Front Neurol. 2019;10(154):1-11.
189. Schaapsmeerders P, van Uden IWM, Tuladhar AM, Maaijwee NAM, van Dijk EJ, Rutten-Jacobs LCA, et al. Ipsilateral hippocampal atrophy is associated with long-term memory dysfunction after ischemic stroke in young adults. Hum Brain Mapp. 2015;36(7):2432-2442.
190. Buss A, Brook GA, Kakulas B, Martin D, Franzen R, Schoenen J, et al. Gradual loss of myelin and formation of an astrocytic scar during Wallerian degeneration in the human spinal cord. Brain. 2004;127(Pt 1):34-44.

191. Buss A, Pech K, Merkler D, Kakulas BA, Martin D, Schoenen J, et al. Sequential loss of myelin proteins during Wallerian degeneration in the human spinal cord. Brain. 2005;128(Pt 2):356-364.
192. Nishino H, Czurkó A, Fukuda A, Hashitani T, Hida H, Karadi Z, et al. Pathophysiological process after transient ischemia of the middle cerebral artery in the rat. Brain Res Bull. 1994;35(1):51-56.
193. Ross DT, Ebner FF. Thalamic retrograde degeneration following cortical injury: an excitotoxic process? Neuroscience. 1990;35(3):525-550.
194. Wei L, Ying D-J, Cui L, Langsdorf J, Yu SP. Necrosis, apoptosis and hybrid death in the cortex and thalamus after barrel cortex ischemia in rats. Brain research. 2004;1022(1-2):54-61.
195. Soriano MA, Ferrer I, Rodríguez-Farré E, Planas AM. Apoptosis and c-Jun in the thalamus of the rat following cortical infarction. Neuroreport. 1996;7(2):425-428.
196. Dihné M, Block F. Focal ischemia induces transient expression of IL-6 in the substantia nigra pars reticulata. Brain research. 2001;889(1-2):165-173.
197. Loos M, Dihné M, Block F. Tumor necrosis factor-alpha expression in areas of remote degeneration following middle cerebral artery occlusion of the rat. Neuroscience. 2003;122(2):373-380.
198. Dihné M, Grommes C, Lutzenburg M, Witte OW, Block F. Different mechanisms of secondary neuronal damage in thalamic nuclei after focal cerebral ischemia in rats. Stroke. 2002;33(12):3006-3011.
199. Ogawa T, Yoshida Y, Okudera T, Noguchi K, Kado H, Uemura K. Secondary thalamic degeneration after cerebral infarction in the middle cerebral artery distribution: evaluation with MR imaging. Radiology. 1997;204(1):255-262.
200. Pappata S, Levasseur M, Gunn RN, Myers R, Crouzel C, Syrota A, et al. Thalamic microglial activation in ischemic stroke detected in vivo by PET and [11C]PK1195. Neurology. 2000;55(7):1052-1054.
201. Gerhard A, Neumaier B, Elitok E, Glatting G, Ries V, Tomczak R, et al. In vivo imaging of activated microglia using [11C]PK11195 and positron emission tomography in patients after ischemic stroke. Neuroreport. 2000;11(13):2957-2960.
202. Morioka T, Kalehua AN, Streit WJ. Characterization of microglial reaction after middle cerebral artery occlusion in rat brain. J Comp Neurol. 1993;327(1):123-132.
203. Patience MJ, Zouikr I, Jones K, Clarkson AN, Isgaard J, Johnson SJ, et al. Photothrombotic stroke induces persistent ipsilateral and contralateral astrogliosis in key cognitive control nuclei. Neurochem Res. 2015;40(2):362-371.
204. Iizuka H, Sakatani K, Young W. Neural damage in the rat thalamus after cortical infarcts. Stroke. 1990;21(5):790-794.
205. Kluge MG, Abdolhoseini M, Zalewska K, Ong LK, Johnson SJ, Nilsson M, et al. Spatiotemporal analysis of impaired microglia process movement at sites of secondary neurodegeneration post-stroke. J Cereb Blood Flow Metab. 2019;39(12):2456-2470.
206. Kluge MG, Kracht L, Abdolhoseini M, Ong LK, Johnson SJ, Nilsson M, et al. Impaired microglia process dynamics post-stroke are specific to sites of secondary neurodegeneration. Glia. 2017;65(12):1885-1899.
207. Schroeter M, Zickler P, Denhardt DT, Hartung H-P, Jander S. Increased thalamic neurodegeneration following ischaemic cortical stroke in osteopontin-deficient mice. Brain. 2006;129(Pt 6):1426-1437.
208. Zuo X, Hou Q, Jin J, Zhan L, Li X, Sun W, et al. Inhibition of Cathepsin B Alleviates Secondary Degeneration in Ipsilateral Thalamus After Focal Cerebral Infarction in Adult Rats. J Neuropathol Exp Neurol. 2016;75(9):816-826.
209. Zhang Y, Xing S, Zhang J, Li J, Li C, Pei Z, et al. Reduction of β-amyloid deposits by γ-secretase inhibitor is associated with the attenuation of secondary damage in the ipsilateral thalamus and sensory functional improvement after focal cortical infarction in hypertensive rats. J Cereb Blood Flow Metab. 2011;31(2):572-579.

210. Zhang J, Zhang Y, Li J, Xing S, Li C, Li Y, et al. Autophagosomes accumulation is associated with β-amyloid deposits and secondary damage in the thalamus after focal cortical infarction in hypertensive rats. J Neurochem. 2012;120(4):564-573.
211. van Groen T, Puurunen K, Mäki H-M, Sivenius J, Jolkkonen J. Transformation of diffuse beta-amyloid precursor protein and beta-amyloid deposits to plaques in the thalamus after transient occlusion of the middle cerebral artery in rats. Stroke. 2005;36(7):1551-1556.
212. Haass C, Selkoe DJ. Soluble protein oligomers in neurodegeneration: lessons from the Alzheimer's amyloid beta-peptide. Nat Rev Mol Cell Biol. 2007;8(2):101-112.
213. Lesné S, Koh MT, Kotilinek L, Kayed R, Glabe CG, Yang A, et al. A specific amyloid-beta protein assembly in the brain impairs memory. Nature. 2006;440(7082):352-357.
214. Lesné SE, Sherman MA, Grant M, Kuskowski M, Schneider JA, Bennett DA, et al. Brain amyloid-β oligomers in ageing and Alzheimer's disease. Brain. 2013;136(Pt 5):1383-1398.
215. Giuffrida ML, Caraci F, De Bona P, Pappalardo G, Nicoletti F, Rizzarelli E, et al. The monomer state of beta-amyloid: where the Alzheimer's disease protein meets physiology. Rev Neurosci. 2010;21(2):83-93.
216. Pryor NE, Moss MA, Hestekin CN. Unraveling the early events of amyloid-β protein (Aβ) aggregation: techniques for the determination of Aβ aggregate size. Int J Mol Sci. 2012;13(3):3038-3072.
217. Walsh DM, Klyubin I, Fadeeva JV, Cullen WK, Anwyl R, Wolfe MS, et al. Naturally secreted oligomers of amyloid beta protein potently inhibit hippocampal long-term potentiation in vivo. Nature. 2002;416(6880):535-539.
218. Sheikh S, Safia, Haque E, Mir SS. Neurodegenerative Diseases: Multifactorial Conformational Diseases and Their Therapeutic Interventions. J Neurodegener Dis. 2013;2013(563481):1-9.
219. Nortley R, Korte N, Izquierdo P, Hirunpattarasilp C, Mishra A, Jaunmuktane Z, et al. Amyloid β oligomers constrict human capillaries in Alzheimer's disease via signaling to pericytes. Science. 2019;365(6450):1-13.
220. Mäkinen S, van Groen T, Clarke J, Thornell A, Corbett D, Hiltunen M, et al. Coaccumulation of calcium and beta-amyloid in the thalamus after transient middle cerebral artery occlusion in rats. J Cereb Blood Flow Metab. 2008;28(2):263-268.
221. Ong LK, Zhao Z, Kluge M, Walker FR, Nilsson M. Chronic stress exposure following photothrombotic stroke is associated with increased levels of Amyloid beta accumulation and altered oligomerisation at sites of thalamic secondary neurodegeneration in mice. J Cereb Blood Flow Metab. 2017;37(4):1338-1348.
222. Sarajärvi T, Lipsanen A, Mäkinen P, Peräniemi S, Soininen H, Haapasalo A, et al. Bepridil decreases Aβ and calcium levels in the thalamus after middle cerebral artery occlusion in rats. J Cell Mol Med. 2012;16(11):2754-2767.
223. Breydo L, Wu JW, Uversky VN. A-synuclein misfolding and Parkinson's disease. Biochim Biophys Acta. 2012;1822(2):261-285.
224. Jellinger KA. Potential role of α-synuclein in neurodegeneration: studies in a rat animal model. J Neurochem. 2012;122(4):659-660.
225. Unal-Cevik I, Gursoy-Ozdemir Y, Yemisci M, Lule S, Gurer G, Can A, et al. Alpha-synuclein aggregation induced by brief ischemia negatively impacts neuronal survival in vivo: a study in [A30P]alpha-synuclein transgenic mouse. J Cereb Blood Flow Metab. 2011;31(3):913-923.
226. Ingelsson M. Alpha-Synuclein Oligomers-Neurotoxic Molecules in Parkinson's Disease and Other Lewy Body Disorders. Front Neurosci. 2016;10(408):1-10.
227. Winner B, Jappelli R, Maji SK, Desplats PA, Boyer L, Aigner S, et al. In vivo demonstration that alpha-synuclein oligomers are toxic. Proc Natl Acad Sci U S A. 2011;108(10):4194-4199.
228. Yu S, Chan P. Role of α-synuclein in neurodegeneration: implications for the pathogenesis of Parkinson's disease. Essays Biochem. 2014;56:125-135.
229. Pacheco C, Aguayo LG, Opazo C. An extracellular mechanism that can explain the neurotoxic effects of α-synuclein aggregates in the brain. Front Physiol. 2012;3(297):1-10.

230. Kim T, Mehta SL, Kaimal B, Lyons K, Dempsey RJ, Vemuganti R. Poststroke Induction of α-Synuclein Mediates Ischemic Brain Damage. J Neurosci. 2016;36(26):7055-7065.
231. Braeuninger S, Kleinschnitz C. Rodent models of focal cerebral ischemia: procedural pitfalls and translational problems. Exp Transl Stroke Med. 2009;1(8):1-11.
232. Koizumi J-i, Yoshida Y, Nakazawa T, Ooneda G. Experimental studies of ischemic brain edema

1. A new experimental model of cerebral embolism in rats in which recirculation can be introduced in the ischemic area. Nosotchu. 1986;8(1):1-8.
233. Clark WM, Lessov NS, Dixon MP, Eckenstein F. Monofilament intraluminal middle cerebral artery occlusion in the mouse. Neurol Res. 1997;19(6):641-648.
234. Bogousslavsky J, Van Melle G, Regli F. The Lausanne Stroke Registry: analysis of 1,000 consecutive patients with first stroke. Stroke. 1988;19(9):1083-1092.
235. Durukan A, Tatlisumak T. Acute ischemic stroke: overview of major experimental rodent models, pathophysiology, and therapy of focal cerebral ischemia. Pharmacol Biochem Behav. 2007;87(1):179-197.
236. Kanemitsu H, Nakagomi T, Tamura A, Tsuchiya T, Kono G, Sano K. Differences in the extent of primary ischemic damage between middle cerebral artery coagulation and intraluminal occlusion models. J Cereb Blood Flow Metab. 2002;22(10):1196-1204.
237. Steele EC, Jr., Guo Q, Namura S. Filamentous middle cerebral artery occlusion causes ischemic damage to the retina in mice. Stroke. 2008;39(7):2099-2104.
238. Dittmar M, Spruss T, Schuierer G, Horn M. External carotid artery territory ischemia impairs outcome in the endovascular filament model of middle cerebral artery occlusion in rats. Stroke. 2003;34(9):2252-2257.
239. Overgaard K, Sereghy T, Boysen G, Pedersen H, Høyer S, Diemer NH. A rat model of reproducible cerebral infarction using thrombotic blood clot emboli. J Cereb Blood Flow Metab. 1992;12(3):484-490.
240. Sharkey J, Ritchie IM, Kelly PA. Perivascular microapplication of endothelin-1: a new model of focal cerebral ischaemia in the rat. J Cereb Blood Flow Metab. 1993;13(5):865-871.
241. Hughes PM, Anthony DC, Ruddin M, Botham MS, Rankine EL, Sablone M, et al. Focal lesions in the rat central nervous system induced by endothelin-1. J Neuropathol Exp Neurol. 2003;62(12):1276-1286.
242. Carmichael ST. Rodent models of focal stroke: size, mechanism, and purpose. NeuroRx. 2005;2(3):396-409.
243. Naidoo V, Naidoo S, Mahabeer R, Raidoo DM. Cellular distribution of the endothelin system in the human brain. J Chem Neuroanat. 2004;27(2):87-98.
244. Uzdensky AB. Photothrombotic Stroke as a Model of Ischemic Stroke. Transl Stroke Res. 2018;9(5):437-451.
245. Sommer CJ. Ischemic stroke: experimental models and reality. Acta Neuropathol. 2017;133(2):245-261.
246. Labat-gest V, Tomasi S. Photothrombotic ischemia: a minimally invasive and reproducible photochemical cortical lesion model for mouse stroke studies. J Vis Exp. 2013;76(50370):1-6.
247. Schroeter M, Jander S, Stoll G. Non-invasive induction of focal cerebral ischemia in mice by photothrombosis of cortical microvessels: characterization of inflammatory responses. J Neurosci Methods. 2002;117(1):43-49.
248. Corbett D, Carmichael ST, Murphy TH, Jones TA, Schwab ME, Jolkkonen J, et al. Enhancing the Alignment of the Preclinical and Clinical Stroke Recovery Research Pipeline: Consensus-Based Core Recommendations From the Stroke Recovery and Rehabilitation Roundtable Translational Working Group. Neurorehabil Neural Repair. 2017;31(8):699-707.
249. Zalewska K, Pietrogrande G, Ong LK, Abdolhoseini M, Kluge M, Johnson SJ, et al. Sustained administration of corticosterone at stress-like levels after stroke suppressed glial reactivity at sites of thalamic secondary neurodegeneration. Brain Behav Immun. 2018;69:210-222.

250. Lanens D, Spanoghe M, Van Audekerke J, Oksendal A, Van der Linden A, Dommisse R. Complementary use of T2-weighted and postcontrast T1- and T2*-weighted imaging to distinguish sites of reversible and irreversible brain damage in focal ischemic lesions in the rat brain. Magn Reson Imaging. 1995;13(2):185-192.
251. Bland ST, Schallert T, Strong R, Aronowski J, Grotta JC, Feeney DM. Early exclusive use of the affected forelimb after moderate transient focal ischemia in rats : functional and anatomic outcome. Stroke. 2000;31(5):1144-1152.
252. Schallert T. Behavioral tests for preclinical intervention assessment. NeuroRx. 2006;3(4):497-504.
253. Rogers DC, Campbell CA, Stretton JL, Mackay KB. Correlation between motor impairment and infarct volume after permanent and transient middle cerebral artery occlusion in the rat. Stroke. 1997;28(10):2060-2066.
254. Montoya CP, Campbell-Hope LJ, Pemberton KD, Dunnett SB. The "staircase test": a measure of independent forelimb reaching and grasping abilities in rats. J Neurosci Methods. 1991;36(2-3):219-228.
255. Baird AL, Meldrum A, Dunnett SB. The staircase test of skilled reaching in mice. Brain Res Bull. 2001;54(2):243-250.
256. Schallert T, Upchurch M, Lobaugh N, Farrar SB, Spirduso WW, Gilliam P, et al. Tactile extinction: distinguishing between sensorimotor and motor asymmetries in rats with unilateral nigrostriatal damage. Pharmacol Biochem Behav. 1982;16(3):455-462.
257. Rewell SSJ, Churilov L, Sidon TK, Aleksoska E, Cox SF, Macleod MR, et al. Evolution of ischemic damage and behavioural deficit over 6 months after MCAo in the rat: Selecting the optimal outcomes and statistical power for multi-centre preclinical trials. PLoS One. 2017;12((2)e0171688):1-19.
258. Modo M, Stroemer RP, Tang E, Veizovic T, Sowniski P, Hodges H. Neurological sequelae and long-term behavioural assessment of rats with transient middle cerebral artery occlusion. J Neurosci Methods. 2000;104(1):99-109.
259. Hamm RJ, Pike BR, O'Dell DM, Lyeth BG, Jenkins LW. The rotarod test: an evaluation of its effectiveness in assessing motor deficits following traumatic brain injury. J Neurotrauma. 1994;11(2):187-196.
260. Bouët V, Freret T, Toutain J, Divoux D, Boulouard M, Schumann-Bard P. Sensorimotor and cognitive deficits after transient middle cerebral artery occlusion in the mouse. Exp Neurol. 2007;203(2):555-567.
261. Allred RP, Jones TA. Maladaptive effects of learning with the less-affected forelimb after focal cortical infarcts in rats. Exp Neurol. 2008;210(1):172-181.
262. Gharbawie OA, Gonzalez CLR, Whishaw IQ. Skilled reaching impairments from the lateral frontal cortex component of middle cerebral artery stroke: a qualitative and quantitative comparison to focal motor cortex lesions in rats. Behav Brain Res. 2005;156(1):125-137.
263. Morris RG, Garrud P, Rawlins JN, O'Keefe J. Place navigation impaired in rats with hippocampal lesions. Nature. 1982;297(5868):681-683.
264. Yonemori F, Yamada H, Yamaguchi T, Uemura A, Tamura A. Spatial memory disturbance after focal cerebral ischemia in rats. J Cereb Blood Flow Metab. 1996;16(5):973-980.
265. Li W, Huang R, Shetty RA, Thangthaeng N, Liu R, Chen Z, et al. Transient focal cerebral ischemia induces long-term cognitive function deficit in an experimental ischemic stroke model. Neurobiol Dis. 2013;59:18-25.
266. Markgraf CG, Green EJ, Hurwitz BE, Morikawa E, Dietrich WD, McCabe PM, et al. Sensorimotor and cognitive consequences of middle cerebral artery occlusion in rats. Brain research. 1992;575(2):238-246.
267. Vorhees CV, Williams MT. Assessing spatial learning and memory in rodents. ILAR J. 2014;55(2):310-332.

268. Gionet TX, Thomas JD, Warner DS, Goodlett CR, Wasserman EA, West JR. Forebrain ischemia induces selective behavioral impairments associated with hippocampal injury in rats. Stroke. 1991;22(8):1040-1047.
269. Kiyota Y, Miyamoto M, Nagaoka A. Relationship between brain damage and memory impairment in rats exposed to transient forebrain ischemia. Brain research. 1991;538(2):295-302.
270. Bussey TJ, Holmes A, Lyon L, Mar AC, McAllister KAL, Nithianantharajah J, et al. New translational assays for preclinical modelling of cognition in schizophrenia: the touchscreen testing method for mice and rats. Neuropharmacology. 2012;62(3):1191-1203.
271. Horner AE, Heath CJ, Hvoslef-Eide M, Kent BA, Kim CH, Nilsson SRO, et al. The touchscreen operant platform for testing learning and memory in rats and mice. Nat Protoc. 2013;8(10):1961-1984.
272. del Zoppo GJ. Inflammation and the neurovascular unit in the setting of focal cerebral ischemia. Neuroscience. 2009;158(3):972-982.
273. Murphy TH, Corbett D. Plasticity during stroke recovery: from synapse to behaviour. Nat Rev Neurosci. 2009;10(12):861-872.
274. Hara Y. Brain plasticity and rehabilitation in stroke patients. J Nippon Med Sch. 2015;82(1):4-13.
275. Nudo RJ. Plasticity. NeuroRx. 2006;3(4):420-427.
276. Johansson BB. Brain plasticity and stroke rehabilitation. The Willis lecture. Stroke. 2000;31(1):223-230.
277. Frost SB, Barbay S, Friel KM, Plautz EJ, Nudo RJ. Reorganization of remote cortical regions after ischemic brain injury: a potential substrate for stroke recovery. J Neurophysiol. 2003;89(6):3205-3214.
278. Nudo RJ, Milliken GW. Reorganization of movement representations in primary motor cortex following focal ischemic infarcts in adult squirrel monkeys. J Neurophysiol. 1996;75(5):2144-2149.
279. Jin K, Sun Y, Xie L, Peel A, Mao XO, Batteur S, et al. Directed migration of neuronal precursors into the ischemic cerebral cortex and striatum. Mol Cell Neurosci. 2003;24(1):171-189.
280. Parent JM, Vexler ZS, Gong C, Derugin N, Ferriero DM. Rat forebrain neurogenesis and striatal neuron replacement after focal stroke. Ann Neurol. 2002;52(6):802-813.
281. Zhang RL, Zhang ZG, Zhang L, Chopp M. Proliferation and differentiation of progenitor cells in the cortex and the subventricular zone in the adult rat after focal cerebral ischemia. Neuroscience. 2001;105(1):33-41.
282. Kokaia Z, Thored P, Arvidsson A, Lindvall O. Regulation of stroke-induced neurogenesis in adult brain--recent scientific progress. Cereb Cortex. 2006;16 Suppl 1:i162-i167.
283. Zhang P-b, Liu Y, Li J, Kang Q-y, Tian Y-f, Chen X-l, et al. Ependymal/subventricular zone cells migrate to the peri-infarct region and differentiate into neurons and astrocytes after focal cerebral ischemia in adult rats. Di Yi Jun Yi Da Xue Xue Bao. 2005;25(10):1201-1206.
284. Kreuzberg M, Kanov E, Timofeev O, Schwaninger M, Monyer H, Khodosevich K. Increased subventricular zone-derived cortical neurogenesis after ischemic lesion. Exp Neurol. 2010;226(1):90-99.
285. Kuge A, Takemura S, Kokubo Y, Sato S, Goto K, Kayama T. Temporal profile of neurogenesis in the subventricular zone, dentate gyrus and cerebral cortex following transient focal cerebral ischemia. Neurol Res. 2009;31(9):969-976.
286. Ling L, Zeng J, Pei Z, Cheung RTF, Hou Q, Xing S, et al. Neurogenesis and angiogenesis within the ipsilateral thalamus with secondary damage after focal cortical infarction in hypertensive rats. J Cereb Blood Flow Metab. 2009;29(9):1538-1546.
287. Chen L, Wang X, Chen X, Xing S, Zhang J, Li J, et al. Tongxinluo attenuates neuronal loss and enhances neurogenesis and angiogenesis in the ipsilateral thalamus and improves neurological outcome after focal cortical infarction in hypertensive rats. Restor Neurol Neurosci. 2014;32(4):533-546.

288. Ruan L, Wang B, ZhuGe Q, Jin K. Coupling of neurogenesis and angiogenesis after ischemic stroke. Brain research. 2015;1623:166-173.
289. Manoonkitiwongsa PS, Jackson-Friedman C, McMillan PJ, Schultz RL, Lyden PD. Angiogenesis after stroke is correlated with increased numbers of macrophages: the clean-up hypothesis. J Cereb Blood Flow Metab. 2001;21(10):1223-1231.
290. Yu SW, Friedman B, Cheng Q, Lyden PD. Stroke-evoked angiogenesis results in a transient population of microvessels. J Cereb Blood Flow Metab. 2007;27(4):755-763.
291. Li Q, Ford MC, Lavik EB, Madri JA. Modeling the neurovascular niche: VEGF- and BDNF-mediated cross-talk between neural stem cells and endothelial cells: an in vitro study. J Neurosci Res. 2006;84(8):1656-1668.
292. Petraglia AL, Marky AH, Walker C, Thiyagarajan M, Zlokovic BV. Activated protein C is neuroprotective and mediates new blood vessel formation and neurogenesis after controlled cortical impact. Neurosurgery. 2010;66(1):165-172.
293. Clarkson AN, Overman JJ, Zhong S, Mueller R, Lynch G, Carmichael ST. AMPA receptor-induced local brain-derived neurotrophic factor signaling mediates motor recovery after stroke. J Neurosci. 2011;31(10):3766-3775.
294. Cramer SC. Repairing the human brain after stroke: I. Mechanisms of spontaneous recovery. Ann Neurol. 2008;63(3):272-287.
295. Cramer SC, Sur M, Dobkin BH, O'Brien C, Sanger TD, Trojanowski JQ, et al. Harnessing neuroplasticity for clinical applications. Brain. 2011;134(Pt 6):1591-1609.
296. Bernhardt J, Hayward KS, Kwakkel G, Ward NS, Wolf SL, Borschmann K, et al. Agreed definitions and a shared vision for new standards in stroke recovery research: The Stroke Recovery and Rehabilitation Roundtable taskforce. Int J Stroke. 2017;12(5):444-450.
297. Isaksson OG, Edén S, Jansson JO. Mode of action of pituitary growth hormone on target cells. Annu Rev Physiol. 1985;47:483-499.
298. Olarescu NC, Gunawardane K, Hansen TK, Møller N, Jørgensen JOL. Normal Physiology of Growth Hormone in Adults. In: Feingold KR, Anawalt B, Boyce A, Chrousos G, Dungan K, Grossman A, et al., editors. Endotext. South Dartmouth (MA): MDText.com, Inc.; 2000.
299. Nyberg F. Growth hormone in the brain: characteristics of specific brain targets for the hormone and their functional significance. Front Neuroendocrinol. 2000;21(4):330-348.
300. Aberg ND, Brywe KG, Isgaard J. Aspects of growth hormone and insulin-like growth factor-I related to neuroprotection, regeneration, and functional plasticity in the adult brain. ScientificWorldJournal. 2006;6:53-80.
301. Lobie PE, García-Aragón J, Lincoln DT, Barnard R, Wilcox JN, Waters MJ. Localization and ontogeny of growth hormone receptor gene expression in the central nervous system. Brain Res Dev Brain Res. 1993;74(2):225-233.
302. Lai Z, Emtner M, Roos P, Nyberg F. Characterization of putative growth hormone receptors in human choroid plexus. Brain Research. 1991;546(2):222-226.
303. Nyberg F, Burman P. Growth hormone and its receptors in the central nervous system--location and functional significance. Horm Res. 1996;45(1-2):18-22.
304. Aberg MAI, Aberg ND, Palmer TD, Alborn A-M, Carlsson-Skwirut C, Bang P, et al. IGF-I has a direct proliferative effect in adult hippocampal progenitor cells. Mol Cell Neurosci. 2003;24(1):23-40.
305. Werther GA, Abate M, Hogg A, Cheesman H, Oldfield B, Hards D, et al. Localization of insulin-like growth factor-I mRNA in rat brain by in situ hybridization--relationship to IGF-I receptors. Mol Endocrinol. 1990;4(5):773-778.
306. Chung YH, Shin CM, Joo KM, Kim MJ, Cha CI. Region-specific alterations in insulin-like growth factor receptor type I in the cerebral cortex and hippocampus of aged rats. Brain research. 2002;946(2):307-313.
307. Donahue CP, Jensen RV, Ochiishi T, Eisenstein I, Zhao M, Shors T, et al. Transcriptional profiling reveals regulated genes in the hippocampus during memory formation. Hippocampus. 2002;12(6):821-833.

308. Sun LY, Al-Regaiey K, Masternak MM, Wang J, Bartke A. Local expression of GH and IGF-1 in the hippocampus of GH-deficient long-lived mice. Neurobiol Aging. 2005;26(6):929-937.
309. Nyberg F, Hallberg M. Growth hormone and cognitive function. Nat Rev Endocrinol. 2013;9(6):357-365.
310. Falleti MG, Maruff P, Burman P, Harris A. The effects of growth hormone (GH) deficiency and GH replacement on cognitive performance in adults: a meta-analysis of the current literature. Psychoneuroendocrinology. 2006;31(6):681-691.
311. Deijen JB, de Boer H, van der Veen EA. Cognitive changes during growth hormone replacement in adult men. Psychoneuroendocrinology. 1998;23(1):45-55.
312. Schneider-Rivas S, Rivas-Arancibia S, Vázquez-Pereyra F, Vázquez-Sandoval R, Borgonio-Pérez G. Modulation of long-term memory and extinction responses induced by growth hormone (GH) and growth hormone releasing hormone (GHRH) in rats. Life Sci. 1995;56(22):PL433-PL441.
313. Drago F, Di Leo F, Ikonomou S, Anzallo C, Busà L, LoPresti L. Behavioral and endocrine effects of growth hormone administration in aged female rats. Psychoneuroendocrinology. 1996;21(4):401-410.
314. Stochholm K, Kiess W. Long-term safety of growth hormone-A combined registry analysis. Clin Endocrinol (Oxf). 2018;88(4):515-528.
315. Kgosidialwa O, Hakami O, Muhammad Zia-Ul-Hussnain H, Agha A. Growth Hormone Deficiency Following Traumatic Brain Injury. Int J Mol Sci. 2019;20(13):3323.
316. High WM, Jr., Briones-Galang M, Clark JA, Gilkison C, Mossberg KA, Zgaljardic DJ, et al. Effect of growth hormone replacement therapy on cognition after traumatic brain injury. J Neurotrauma. 2010;27(9):1565-1575.
317. Reimunde P, Quintana A, Castañón B, Casteleiro N, Vilarnovo Z, Otero A, et al. Effects of growth hormone (GH) replacement and cognitive rehabilitation in patients with cognitive disorders after traumatic brain injury. Brain Inj. 2011;25(1):65-73.
318. Moreau OK, Cortet-Rudelli C, Yollin E, Merlen E, Daveluy W, Rousseaux M. Growth hormone replacement therapy in patients with traumatic brain injury. J Neurotrauma. 2013;30(11):998-1006.
319. Gardner CJ, Mattsson AF, Daousi C, Korbonits M, Koltowska-Haggstrom M, Cuthbertson DJ. GH deficiency after traumatic brain injury: improvement in quality of life with GH therapy: analysis of the KIMS database. Eur J Endocrinol. 2015;172(4):371-381.
320. Zhang H, Han M, Zhang X, Sun X, Ling F. The effect and mechanism of growth hormone replacement on cognitive function in rats with traumatic brain injury. PLoS One. 2014;9((9)e108518):1-9.
321. Heredia M, Rodríguez N, Sánchez Robledo V, Criado JM, de la Fuente A, Devesa J, et al. Factors Involved in the Functional Motor Recovery of Rats with Cortical Ablation after GH and Rehabilitation Treatment: Cortical Cell Proliferation and Nestin and Actin Expression in the Striatum and Thalamus. Int J Mol Sci. 2019;20((22) 5770):1-21.
322. Heredia M, Palomero J, de la Fuente A, Criado JM, Yajeya J, Devesa J, et al. Motor Improvement of Skilled Forelimb Use Induced by Treatment with Growth Hormone and Rehabilitation Is Dependent on the Onset of the Treatment after Cortical Ablation. Neural Plast. 2018;2018(6125901):1-15.
323. Shin DH, Lee E, Kim J-W, Kwon B-S, Jung MK, Jee YH, et al. Protective effect of growth hormone on neuronal apoptosis after hypoxia-ischemia in the neonatal rat brain. Neurosci Lett. 2004;354(1):64-68.
324. Scheepens A, Sirimanne ES, Breier BH, Clark RG, Gluckman PD, Williams CE. Growth hormone as a neuronal rescue factor during recovery from CNS injury. Neuroscience. 2001;104(3):677-687.
325. Devesa P, Reimunde P, Gallego R, Devesa J, Arce VM. Growth hormone (GH) treatment may cooperate with locally-produced GH in increasing the proliferative response of hippocampal progenitors to kainate-induced injury. Brain Inj. 2011;25(5):503-510.

326. Le Grevès M, Zhou Q, Berg M, Le Grevès P, Fhölenhag K, Meyerson B, et al. Growth hormone replacement in hypophysectomized rats affects spatial performance and hippocampal levels of NMDA receptor subunit and PSD-95 gene transcript levels. Exp Brain Res. 2006;173(2):267-273.
327. Walser M, Hansén A, Svensson P-A, Jernås M, Oscarsson J, Isgaard J, et al. Peripheral administration of bovine GH regulates the expression of cerebrocortical beta-globin, GABAB receptor 1, and the Lissencephaly-1 protein (LIS-1) in adult hypophysectomized rats. Growth Horm IGF Res. 2011;21(1):16-24.
328. Lillicrap T, Garcia-Esperon C, Walker FR, Ong LK, Nilsson M, Spratt N, et al. Growth Hormone Deficiency Is Frequent After Recent Stroke. Front Neurol. 2018;9(713):1-4.
329. Boehncke S, Ackermann H, Badenhoop K, Sitzer M. Pituitary function and IGF-I levels following ischemic stroke. Cerebrovasc Dis. 2011;31(2):163-169.
330. Bondanelli M, Ambrosio MR, Carli A, Bergonzoni A, Bertocchi A, Zatelli MC, et al. Predictors of pituitary dysfunction in patients surviving ischemic stroke. J Clin Endocrinol Metab. 2010;95(10):4660-4668.
331. Kreber LA, Ashley MJ, Masel BE, Singh CK, Randle KD, Johnson C, et al. Prevalence of growth hormone deficiency in middle-age adults recovering from stroke. Brain Inj. 2020;34(2):276-280.
332. Song J, Park K, Lee H, Kim M. The effect of recombinant human growth hormone therapy in patients with completed stroke: a pilot trial. Ann Rehabil Med. 2012;36(4):447-457.
333. Jin G-H, Lee J-B. Effect of Recombinant Human Growth Hormone Add on Therapy on Acute Stroke Outcome. Brain Neurorehabil. 2018;11(1):1-9.
334. Ajo R, Cacicedo L, Navarro C, Sánchez-Franco F. Growth hormone action on proliferation and differentiation of cerebral cortical cells from fetal rat. Endocrinology. 2003;144(3):1086-1097.
335. Pathipati P, Surus A, Williams CE, Scheepens A. Delayed and chronic treatment with growth hormone after endothelin-induced stroke in the adult rat. Behav Brain Res. 2009;204(1):93-101.
336. Ong LK, Chow WZ, TeBay C, Kluge M, Pietrogrande G, Zalewska K, et al. Growth Hormone Improves Cognitive Function After Experimental Stroke. Stroke. 2018;49(5):1257-1266.
337. Sanchez-Bezanilla S, TeBay C, Nilsson M, Walker FR, Ong LK. Visual discrimination impairment after experimental stroke is associated with disturbances in the polarization of the astrocytic aquaporin-4 and increased accumulation of neurotoxic proteins. Exp Neurol. 2019;318:232-243.
338. Schaar KL, Brenneman MM, Savitz SI. Functional assessments in the rodent stroke model. Exp Transl Stroke Med. 2010;2(1):13-13.
339. Pietrogrande G, Zalewska K, Zhao Z, Johnson SJ, Nilsson M, Walker FR. Low Oxygen Post Conditioning as an Efficient Non-pharmacological Strategy to Promote Motor Function After Stroke. Transl Stroke Res. 2019;10(4):402-412.
340. Sanchez-Bezanilla S, Åberg ND, Crock P, Walker FR, Nilsson M, Isgaard J, et al. Growth Hormone Treatment Promotes Remote Hippocampal Plasticity after Experimental Cortical Stroke. International journal of molecular sciences. 2020;21(12).
341. Pietrogrande G, Zalewska K, Zhao Z, Abdolhoseini M, Chow WZ, Sanchez-Bezanilla S, et al. Low oxygen post conditioning prevents thalamic secondary neuronal loss caused by excitotoxicity after cortical stroke. Sci Rep. 2019;9(1):4841.
342. Kluge MG, Abdolhoseini M, Zalewska K, Ong LK, Johnson SJ, Nilsson M, et al. Spatiotemporal analysis of impaired microglia process movement at sites of secondary neurodegeneration post-stroke. J Cereb Blood Flow Metab. 2019;39(12):2456-2470.
343. Schaar KL, Brenneman MM, Savitz SI. Functional assessments in the rodent stroke model. Exp Transl Stroke Med. 2010;2((1)13):1-11.
344. Kwakkel G, Kollen B, Lindeman E. Understanding the pattern of functional recovery after stroke: facts and theories. Restor Neurol Neurosci. 2004;22(3-5):281-299.
345. Page SJ, Gater DR, Bach-Y-Rita P. Reconsidering the motor recovery plateau in stroke rehabilitation. Arch Phys Med Rehabil. 2004;85(8):1377-1381.

346. Kim CH, Heath CJ, Kent BA, Bussey TJ, Saksida LM. The role of the dorsal hippocampus in two versions of the touchscreen automated paired associates learning (PAL) task for mice. Psychopharmacology (Berl). 2015;232(21-22):3899-3910.
347. Barnett JH, Blackwell AD, Sahakian BJ, Robbins TW. The Paired Associates Learning (PAL) Test: 30 Years of CANTAB Translational Neuroscience from Laboratory to Bedside in Dementia Research. Curr Top Behav Neurosci. 2016;28:449-474.
348. Turner KM, Simpson CG, Burne THJ. BALB/c Mice Can Learn Touchscreen Visual Discrimination and Reversal Tasks Faster than C57BL/6 Mice. Front Behav Neurosci. 2017;11(16):1-10.
349. Morton AJ, Skillings E, Bussey TJ, Saksida LM. Measuring cognitive deficits in disabled mice using an automated interactive touchscreen system. Nat Methods. 2006;3((10)767):1.
350. Romberg C, Horner AE, Bussey TJ, Saksida LM. A touch screen-automated cognitive test battery reveals impaired attention, memory abnormalities, and increased response inhibition in the TgCRND8 mouse model of Alzheimer's disease. Neurobiol Aging. 2013;34(3):731-744.
351. Schaapsmeerders P, Maaijwee NAM, van Dijk EJ, Rutten-Jacobs LCA, Arntz RM, Schoonderwaldt HC, et al. Long-term cognitive impairment after first-ever ischemic stroke in young adults. Stroke. 2013;44(6):1621-1628.
352. Huang Y, Yang S, Jia J. Factors related to long-term post-stroke cognitive impairment in young adult ischemic stroke. Med Sci Monit. 2015;21:654-660.
353. Mellon L, Brewer L, Hall P, Horgan F, Williams D, Hickey A, et al. Cognitive impairment six months after ischaemic stroke: a profile from the ASPIRE-S study. BMC Neurol. 2015;15(31):1-9.
354. Anand KS, Dhikav V. Hippocampus in health and disease: An overview. Ann Indian Acad Neurol. 2012;15(4):239-246.
355. Lichtenwalner RJ, Parent JM. Adult neurogenesis and the ischemic forebrain. J Cereb Blood Flow Metab. 2006;26(1):1-20.
356. Yang Y, Kimura-Ohba S, Thompson J, Rosenberg GA. Rodent Models of Vascular Cognitive Impairment. Transl Stroke Res. 2016;7(5):407-414.
357. Chen J, Zhu RL, Nakayama M, Kawaguchi K, Jin K, Stetler RA, et al. Expression of the apoptosis-effector gene, Bax, is up-regulated in vulnerable hippocampal CA1 neurons following global ischemia. J Neurochem. 1996;67(1):64-71.
358. Stoica G, Lungu G, Bjorklund NL, Taglialatela G, Zhang X, Chiu V, et al. Potential role of α-synuclein in neurodegeneration: studies in a rat animal model. J Neurochem. 2012;122(4):812-822.
359. Zhang W, Wang T, Pei Z, Miller DS, Wu X, Block ML, et al. Aggregated alpha-synuclein activates microglia: a process leading to disease progression in Parkinson's disease. FASEB journal : official publication of the Federation of American Societies for Experimental Biology. 2005;19(6):533-542.
360. Danzer KM, Haasen D, Karow AR, Moussaud S, Habeck M, Giese A, et al. Different species of alpha-synuclein oligomers induce calcium influx and seeding. J Neurosci. 2007;27(34):9220-9232.
361. Tu J, Chen B, Yang L, Qi K, Lu J, Zhao D. Amyloid-β Activates Microglia and Regulates Protein Expression in a Manner Similar to Prions. Journal of molecular neuroscience : MN. 2015;56(2):509-518.
362. Mestre H, Hablitz LM, Xavier AL, Feng W, Zou W, Pu T, et al. Aquaporin-4-dependent glymphatic solute transport in the rodent brain. Elife. 2018;7(e40070):1-31.
363. Iliff JJ, Chen MJ, Plog BA, Zeppenfeld DM, Soltero M, Yang L, et al. Impairment of glymphatic pathway function promotes tau pathology after traumatic brain injury. J Neurosci. 2014;34(49):16180-16193.
364. Wang M, Iliff JJ, Liao Y, Chen MJ, Shinseki MS, Venkataraman A, et al. Cognitive deficits and delayed neuronal loss in a mouse model of multiple microinfarcts. J Neurosci. 2012;32(50):17948-17960.

365. Ren Z, Iliff JJ, Yang L, Yang J, Chen X, Chen MJ, et al. 'Hit & Run' model of closed-skull traumatic brain injury (TBI) reveals complex patterns of post-traumatic AQP4 dysregulation. J Cereb Blood Flow Metab. 2013;33(6):834-845.
366. Iadecola C. The pathobiology of vascular dementia. Neuron. 2013;80(4):844-866.
367. Smith EE, Greenberg SM. Beta-amyloid, blood vessels, and brain function. Stroke. 2009;40(7):2601-2606.
368. Clark TA, Sullender C, Kazmi SM, Speetles BL, Williamson MR, Palmberg DM, et al. Artery targeted photothrombosis widens the vascular penumbra, instigates peri-infarct neovascularization and models forelimb impairments. Sci Rep. 2019;9(1):2323.
369. Garcia-Alloza M, Gregory J, Kuchibhotla KV, Fine S, Wei Y, Ayata C, et al. Cerebrovascular lesions induce transient β-amyloid deposition. Brain. 2011;134(Pt 12):3697-3707.
370. Heredia M, Fuente A, Criado J, Yajeya J, Devesa J, Riolobos AS. Early growth hormone (GH) treatment promotes relevant motor functional improvement after severe frontal cortex lesion in adult rats. Behav Brain Res. 2013;247:48-58.
371. Jin K, Wang X, Xie L, Mao XO, Greenberg DA. Transgenic ablation of doublecortin-expressing cells suppresses adult neurogenesis and worsens stroke outcome in mice. Proc Natl Acad Sci U S A. 2010;107(17):7993-7998.
372. Sun F, Wang X, Mao X, Xie L, Jin K. Ablation of neurogenesis attenuates recovery of motor function after focal cerebral ischemia in middle-aged mice. PLoS One. 2012;7(10):e46326-e46326.
373. Lu W, Isozaki K, Roche KW, Nicoll RA. Synaptic targeting of AMPA receptors is regulated by a CaMKII site in the first intracellular loop of GluA1. Proc Natl Acad Sci U S A. 2010;107(51):22266-22271.
374. Ergul A, Alhusban A, Fagan SC. Angiogenesis: a harmonized target for recovery after stroke. Stroke. 2012;43(8):2270-2274.
375. Lissett CA, Shalet SM. Effects of growth hormone on bone and muscle. Growth Horm IGF Res. 2000;10 Suppl B:S95-101.
376. Boot AM, Engels MA, Boerma GJ, Krenning EP, De Muinck Keizer-Schrama SM. Changes in bone mineral density, body composition, and lipid metabolism during growth hormone (GH) treatment in children with GH deficiency. J Clin Endocrinol Metab. 1997;82(8):2423-2428.
377. Brigman JL, Feyder M, Saksida LM, Bussey TJ, Mishina M, Holmes A. Impaired discrimination learning in mice lacking the NMDA receptor NR2A subunit. Learn Mem. 2008;15(2):50-54.
378. Wilson EN, Abela AR, Do Carmo S, Allard S, Marks AR, Welikovitch LA, et al. Intraneuronal Amyloid Beta Accumulation Disrupts Hippocampal CRTC1-Dependent Gene Expression and Cognitive Function in a Rat Model of Alzheimer Disease. Cereb Cortex. 2017;27(2):1501-1511.
379. Horner AE, McLaughlin CL, Afinowi NO, Bussey TJ, Saksida LM, Komiyama NH, et al. Enhanced cognition and dysregulated hippocampal synaptic physiology in mice with a heterozygous deletion of PSD-95. Eur J Neurosci. 2018;47(2):164-176.
380. Johansson CB, Momma S, Clarke DL, Risling M, Lendahl U, Frisén J. Identification of a neural stem cell in the adult mammalian central nervous system. Cell. 1999;96(1):25-34.
381. David Aberg N, Lind J, Isgaard J, Georg Kuhn H. Peripheral growth hormone induces cell proliferation in the intact adult rat brain. Growth Horm IGF Res. 2010;20(3):264-269.
382. Aberg ND, Johansson I, Aberg MAI, Lind J, Johansson UE, Cooper-Kuhn CM, et al. Peripheral administration of GH induces cell proliferation in the brain of adult hypophysectomized rats. J Endocrinol. 2009;201(1):141-150.
383. Devesa P, Agasse F, Xapelli S, Almengló C, Devesa J, Malva JO, et al. Growth hormone pathways signaling for cell proliferation and survival in hippocampal neural precursors from postnatal mice. BMC Neurosci. 2014;15(100):1-12.
384. Carel JC, Butler G. Safety of recombinant human growth hormone. Endocrine development. 2010;18:40-54.

APPENDIX A: ADDITIONAL PUBLICATIONS

frontiers in Molecular Neuroscience

ORIGINAL RESEARCH
published: 30 July 2019
doi: 10.3389/fnmol.2019.00181

Can We Use 2,3,5-Triphenyltetrazolium Chloride-Stained Brain Slices for Other Purposes? The Application of Western Blotting

Sonia Sanchez-Bezanilla[1,2], Michael Nilsson[1,2,3,4,5], Frederick R. Walker[1,2,3,4] and Lin Kooi Ong[1,2,3,6]**

[1] School of Biomedical Sciences and Pharmacy and Priority Research Centre for Stroke and Brain Injury, The University of Newcastle, Callaghan, NSW, Australia, [2] Hunter Medical Research Institute, New Lambton Heights, NSW, Australia, [3] NHMRC Centre of Research Excellence in Stroke Rehabilitation and Brain Recovery, Heidelberg, VIC, Australia, [4] Centre for Rehab Innovations, The University of Newcastle, Callaghan, NSW, Australia, [5] Lee Kong Chian School of Medicine, Nanyang Technological University, Singapore, Singapore, [6] School of Pharmacy, Monash University Malaysia, Bandar Sunway, Malaysia

2,3,5-Triphenyltetrazolium chloride (TTC) staining is a commonly used method to determine the volume of the cerebral infarction in experimental stroke models. The TTC staining protocol is considered to interfere with downstream analyses, and it is unclear whether TTC-stained brain samples can be used for biochemistry analyses. However, there is evidence indicating that, with proper optimization and handling, TTC-stained brains may remain viable for protein analyses. In the present study, we aimed to rigorously assess whether TTC can reliably be used for western blotting of various markers. In this study, brain samples obtained from C57BL/6 male mice were treated with TTC (TTC+) or left untreated (TTC−) at 1 week after photothrombotic occlusion or sham surgery. Brain regions were dissected into infarct, thalamus, and hippocampus, and proteins were extracted by using radioimmunoprecipitation assay buffer. Protein levels of apoptosis, autophagy, neuronal, glial, vascular, and neurodegenerative-related markers were analyzed by western blotting. Our results showed that TTC+ brains display similar relative changes in most of the markers compared with TTC− brains. In addition, we validated that these analyses can be performed in the infarct as well as other brain regions such as the thalamus and hippocampus. Our findings demonstrate that TTC+ brains are reliable for protein analyses using western blotting. Widespread adoption of this approach will be key to lowering the number of animals used while maximizing data.

Keywords: stroke, 2,3,5-triphenyltetrazolium chloride, western blotting, infarct, thalamus, hippocampus

OPEN ACCESS

Edited by:
Robert J. Harvey,
University of the Sunshine Coast, Australia

Reviewed by:
Fabrizio Michetti,
Catholic University of the Sacred Heart, Italy
Shyam Gajavelli,
University of Miami, United States

****Correspondence:***
Sonia Sanchez-Bezanilla
sonia.sanchezbezanilla@uon.edu.au
Lin Kooi Ong
ong.linkooi@monash.edu

Received: *19 May 2019*
Accepted: *10 July 2019*
Published: *30 July 2019*

Citation:
Sanchez-Bezanilla S, Nilsson M, Walker FR and Ong LK (2019) Can We Use 2,3,5-Triphenyltetrazolium Chloride-Stained Brain Slices for Other Purposes? The Application of Western Blotting. Front. Mol. Neurosci. 12:181. doi: 10.3389/fnmol.2019.00181

INTRODUCTION

2,3,5-Triphenyltetrazolium chloride (TTC) is a marker of metabolic function and represents a reliable indicator of ischemic areas in experimental stroke models. TTC is a colorless water-soluble dye that is reduced by the mitochondrial enzyme succinate dehydrogenase of living cells into a water-insoluble, light sensitive compound (formazan) that turns healthy/normal tissue deep red.

In contrast, damaged/dead tissue remains white showing the absence of living cells, and thereby indicating the infarct region (Bederson et al., 1986; Li et al., 1997). TTC staining is a widely used technique in stroke and brain injury research because it is simple, cost effective, and offers a rapid visualization of infarct and penumbral areas (Benedek et al., 2006).

Currently, TTC is used as an immersion staining of fresh brain slices (Bederson et al., 1986) or by intracardiac injection (Sun et al., 2012). However, in the vast majority of studies, these TTC-stained brains are immediately discarded after infarct assessment as it is unclear whether the tissue is suitable for subsequent cellular and molecular analyses. Western blotting is a common method used to detect and analyze protein levels. This technique involves the separation of denatured proteins based on their molecular weight and visualization using antibodies specific to the target protein (Burnette, 1981; Liu et al., 2014). The simplicity and relevance of the method has led to its expansive application as a ubiquitous research tool in medical biochemistry.

TTC staining has been shown to be compatible for the analysis of some specific proteins. However, previous studies presented some limitations. A previous study by Sun et al. (2012) showed that *in vivo* TTC-labeling was compatible with immunofluorescence, mRNA, and protein analysis. However, this study only focused on apoptotic markers in penumbral tissue, and therefore it cannot be concluded that this technique can be used to study other markers and other brain regions. In addition, TTC was administered transcardially, which is highly toxic to the animals, instead of immersing the brain sections in a TTC-staining solution. Another study by Kramer et al. (2010) demonstrated that TTC processing *ex vivo* after middle cerebral artery occlusion in rats can be used for quantitative gene and protein expression analyses using RT-PCR and western blot. However, this study only analyzed the protein expression profile of the metalloprotease-disintegrin ADAM12 and the housekeeping protein β-actin. Additional work in this field has also demonstrated that TTC-stained brain sections can also be used for immunohistochemical quantification of Collagen IV and immunofluorescence analyses (Li L. et al., 2018; Li Z. et al., 2018).

Taken into account previous data, the main objective of the present study was to investigate whether TTC-treated tissues can be processed for downstream biochemical analyses, specifically by western blotting. We aimed to rigorously compare the protein expression profile of wide range of commonly used markers between TTC-treated (TTC+) and untreated (TTC−) brains across a number of different brain regions. We hypothesized that TTC treatment would not interfere with protein quantification in the regions studied.

MATERIALS AND METHODS

The data that support the findings for this study are available from the corresponding author on reasonable request.

Experimental Design

Animal research was undertaken in accordance with the ARRIVE guidelines (Animal Research: Reporting of *in vivo* Experiments). Experiments were approved by the University of Newcastle Animal Care and Ethics Committee (A-2013-340) and conducted in accordance with the New South Wales Animals Research Act and the Australian Code of Practice for the use of animals for scientific purposes. A total of 24 mice were randomly allocated to one of four groups: TTC− sham, TTC− stroke, TTC+ sham, and TTC+ stroke. At day 0, mice were subjected to photothrombotic occlusion or sham surgery. At day 7 post-stroke, mice were euthanized. Brains were collected and sliced using a matrix device into 2 mm coronal sections. One cohort (sham $n = 6$; stroke $n = 6$) was stained by TTC and the other cohort (sham $n = 6$; stroke $n = 6$) was not stained.

Sample Size Calculation

Sample size was estimated using G*Power 3.1 software. To determine the sample size required for this study, we used western blot data from our recent study (NeuN; sham = 1.00 ± 0.04 versus stroke = 0.65 ± 0.06; $n = 7$ per group). Allowing a type 1 error of 5%, $\alpha = 0.05$ with the power of 80%, $\beta = 0.2$ we calculated a sample size of six mice per group (Sanchez-Bezanilla et al., 2019).

Animals

C57BL/6 male mice (10 weeks old) were obtained from the Animal Services Unit at the University of Newcastle. Mice were maintained in a temperature (21°C ± 1) and humidity (~55%) controlled environment with food and water available *ad libitum*. Lighting was on a 12:12 h reverse light–dark cycle (lights on 19:00 h) with all procedures conducted in the dark phase. In all experiments, mice were acclimatized to the environment for a minimum of 7 days prior to the start of the experiment. Mice were housed between 2 and 4 per cage.

Photothrombotic Occlusion

Photothrombotic occlusion was performed as previously described (Ong et al., 2017c; Sanchez-Bezanilla et al., 2019). Briefly, mice were anesthetized by 2% isoflurane (Isothesia #029404, Henry Schein) during surgical procedures on a temperature controlled (37°C ± 1) stereotaxic frame. The skull was exposed by incision of the skin along the midline of the scalp. Rose Bengal (200 µl, 10 mg/ml solution in sterile saline, Sigma–Aldrich #330000, United States) was injected intraperitoneally. After 8 min, the skull was illuminated for 15 min by a 4.5 mm diameter cold light source (Zeiss KL2500LCD, Germany) positioned at 2.2 mm left lateral of bregma 0.0 mm, targeting the left motor and somatosensory cortices. For the sham group, the same surgical procedure was conducted except Rose Bengal was replaced with 200 µl of sterile saline (0.9% NaCl, Pfizer #SYM273384, Australia).

Brain Regions Preparation and Collection

At day 7, mice were deeply anesthetized via intraperitoneal injection of 200 µl of sodium pentobarbital (Lethabarb #3729556, Virbac, Australia). Mice were transcardially perfused with ice cold 0.9% NaCl (UNIVAR #AJA465-2.5KG) with 0.1%

diethylpyrocarbonate (Sigma–Aldrich #D5758, Australia) for 3 min. Brains were dissected and sliced using a matrix device (Zivic Instruments #5325, United States) into 2 mm coronal sections from the olfactory bulb to the cerebellum. For TTC+ brains (sham n = 6, stroke n = 6), sections were taken and incubated in 2% TTC (Sigma–Aldrich #T8877) in saline at 37°C for 10 min. TTC+ brain sections were captured with a digital camera (Sony HDR-PJ790) for infarct volume analyses. Infarct (identified as non-TTC-stained region in stroke mice and equivalent region in sham mice), thalamus (Bregma −1.0 to −2.2), and hippocampus (Bregma −1.5 to −2.5) areas were identified and dissected from the coronal sections and then frozen at −80°C. For TTC− brains (sham n = 6, stroke n = 6), same brain regions were dissected (infarct identified as part of the cortex that appeared to be occluded) and immediately frozen at −80°C (**Figure 1A**).

Infarct Volume Quantification

Contralateral and ipsilateral hemisphere and infarct areas were traced using ImageJ software. Infarct volume was corrected for edema using the formula: corrected infarct volume (mm^3) = infarct volume × (contralateral volume/ipsilateral volume). Edema was calculated by infarct volume minus corrected infarct volume (Murtha et al., 2016; **Figure 1B**).

Protein Extraction and Western Blotting

Western blot was performed as previously described with minor modification (Ong et al., 2017b, 2018). Infarct, thalamus, and hippocampus samples were sonicated using a UP50H microsonicator (Hielscher Ultrasonics GmbH, Germany) for 3 × 30 s pulses at 4°C in radioimmunoprecipitation assay (RIPA) buffer [25 mM Tris buffer pH 7.4, 150 mM NaCl, 0.5% sodium deoxycholate, 0.1% SDS, 1% Triton X-100, 1 protease inhibitor cocktail tablet (every 50 ml), 1× phosphatase inhibitor cocktail tablet (every 50 ml)]. Samples were centrifuged at 14,000 ×g for 20 min at 4°C. The supernatant fractions were collected. Protein concentrations were determined using a Pierce BCA protein assay kit (Thermo Fisher Scientific #23225, United States) according to the manufacturer's instructions. Each sample's final concentration was adjusted to 1.5 mg/ml and aliquoted. Samples were mixed with sample buffer (2% SDS, 10% glycerol, 1% dithiothreitol). Equal amounts of tissue protein samples were electrophoresed into Bio-Rad Criterion TGC stain-free 4–20% gels (Bio-Rad #5678095, Australia). To ensure that an equal amount of protein was loaded, one gel per region was scanned using ChemiDoc XRS+ system (Bio-Rad) before the transfer (**Supplementary Figure S1**). Gels were transferred to polyvinylidene difluoride membranes (Bio-Rad #1620177, Australia). PVDF membranes were washed three times in Tris-buffered saline with Tween (TBST) (150 mM NaCl, 10 mM Tris, 0.075% Tween-20, pH 7.5) and incubated in 5% skim milk powder in TBST for 1 h at room temperature. Membranes were incubated with primary antibodies (amyloid-β, α-synuclein, NeuN, glial fibrillary acidic protein (GFAP), ADLH1L1, PSD95, Tau5, P-Tau, P-Tau Ser396, synaptophysin, LC3, caspase-3, CD11b, VEGFA, Collagen IV, and CD31) overnight at 4°C and secondary antibody for 1 h at room temperature (see **Table 1** for antibodies details and concentration). In between each incubation step, membranes were washed three times in TBST. Membranes were visualized on an Amersham Imager 600 using Luminata Classico (Millipore #WBLUC0500, Australia) or Luminata Forte (Millipore #WBLUF0500, Australia) western blotting detection reagents. The density of the bands was measured using Amersham Imager 600 analysis software. The housekeeping protein β-actin was used as a loading control to normalize the levels of target protein. For representative images, two out of six bands per group were cropped from the raw blots and aligned together. The bands were then minimally

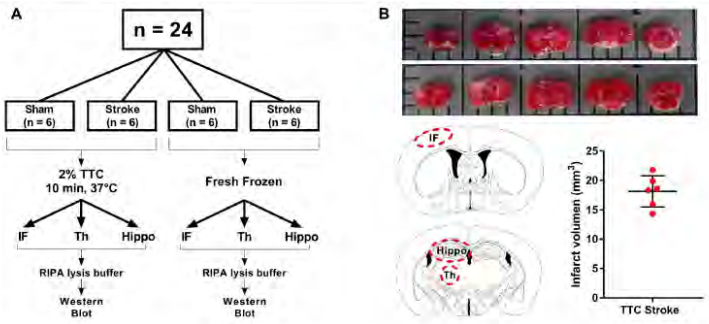

FIGURE 1 | Schematic illustration of the experimental design. **(A)** Mice were randomly allocated to sham or stroke group. At day 7 post-stroke mice were euthanized and brains were sliced into 2 mm thin sections using a matrix device. Brain samples were divided into two different groups. The brain slides from the first group (TTC+) were stained with 2% TTC at 37°C for 10 min, then further dissected into infarct (IF), thalamus (Th), and hippocampus (Hippo) and frozen at −80°C. The slices from the second group (TTC−) were dissected and immediately frozen at −80°C. **(B)** Top panel: images of TTC+ mouse brain slices after photothrombotic stroke. After the brain have been sliced, we placed the 2 mm section on a grid mat. Once we have taken a picture of one side (rostral, row 1) of the brain, we flipped the sections and take a picture of the other side (caudal, row 2). Bottom panel: schematic illustration showing the location of the examined regions (IF, Th, and Hippo) (left). Quantification of the IF volume in TTC+ stroke mice (right).

TABLE 1 | List of antibodies used for western blotting.

	Target	Description	Sources of antibodies	Dilution
Apoptosis and autophagy	Caspase-3	Caspase-3 is an intracellular proteases that mediates cell death and plays a critical role in apoptosis. Activation of caspase-3 requires proteolytic processing (Fernandes-Alnemri et al., 1994).	Sigma–Aldrich, anti-Caspase 3, #C8487-200UL	1:1000
	LC3	Light chain 3 (LC3) is an autophagy marker. Cleavage of LC3 yields the cytosolic LC3-I form. During autophagy, LC3-I is converted to LC3-II permitting LC3 to become associated with autophagic vesicles (Kabeya et al., 2000).	Sigma–Aldrich, anti-LC3, #L8918-200UL	1:1000
Neuronal	NeuN	Neuronal nuclei (NeuN) is a nuclear protein expressed in most post-mitotic neurons of the central and peripheral nervous systems (Mullen et al., 1992). Marker for mature neurons.	Cell Signaling, anti-NeuN (D3S31), #12943	1:2000
	Synaptophysin	Synaptophysin is an integral membrane protein of small synaptic vesicles in the brain (Wiedenmann et al., 1986).	Millipore, anti-Synaptophysin, #MAB329	1:10,000
	PSD95	Postsynaptic density protein 95 (PSD95) is a scaffolding protein involved in the assembly and function of the postsynaptic density complex (Chetkovich et al., 2002).	Cell Signaling, anti-Postsynaptic density protein 95, #2507	1:1000
Glial	GFAP	Glial fibrillary acidic protein (GFAP) forms intermediate filaments in astroglial cells and modulate their motility and shape. GFAP filaments are characteristic of differentiated and mature brain astrocytes (Eng et al., 2000).	Cell Signaling, anti-Glial Fibrillary Acidic Protein (GA5), #3670	1:5000
	ALDH1L1	10-Formyltetrahydrofolate dehydrogenase (ALDH1L1) is a multidomain protein that serves as a CNS astrocyte marker (Cahoy et al., 2008).	Millipore, anti-ALDH1L1 (N103/39), #MABN495	1:2000
	CD11b	Cluster of differentiation molecule 11b (CD11b) is a transmembrane protein expressed by neutrophils, monocytes, macrophages, and microglia (Solovjov et al., 2005).	Abcam, anti-CD11b, #ab75476	1:2000
Vascular	VEGFA	Growth factor active in angiogenesis, vasculogenesis, and endothelial cell growth. Induces endothelial cell proliferation, promotes cell migration, inhibits apoptosis, and induces permeabilization of blood vessels (Leung et al., 1989).	Abcam, anti-VEGFA #ab46154	1:1000
	CD31 (PECAM-1)	CD31 (Platelet Endothelial Cell Adhesion Molecule-1, PECAM-1) is a cell adhesion molecules expressed by circulating platelets, monocytes, neutrophils, some T cells, and makes up a large portion of endothelial cell intercellular junctions. Modulates cell adhesion, endothelial cell migration, and angiogenesis (Newman, 1997).	Cell Signaling, anti-CD31 (PECAM-1) (D8V9E) #77699 Sigma–Aldrich, anti-PECAM-1 #SAB4502167	1:1000 1:1000
	Collagen IV	Type IV collagen is the major structural component of basement membranes. Type IV collagen is a network-forming collagen that provides a molecular scaffold and interacts with cells, growth factors, and other basement membrane components such as laminin, nidogen, and perlecan (Kuhn, 1995).	Abcam, anti-Collagen IV #ab6586	1:1000
Neurodegeneration	Amyloid-β	Amyloid-β (Aβ) peptide produced through sequential proteolytic processing of amyloid precursor protein, and it is prone to aggregate in pathological conditions (Haass and Selkoe, 2007; Walsh and Selkoe, 2007).	Biolegend, anti-Amyloid-β (6E10), # SIG-39320	1:1000
	α-Synuclein	α-Synuclein (α-Syn) is expressed in brain, primarily in presynaptic nerve terminals. Although the exact function has not been determined, it has been linked to the prominent neurodegenerative disorders (Maroteaux et al., 1988; van der Putten et al., 2000).	BD Bioscience, anti-α-Synuclein, #610787	1:1000

(Continued)

TABLE 1 | Continued

	Target	Description	Sources of antibodies	Dilution
	Tau5	Tau5 detects total levels of Tau. Tau are a microtubule-associated proteins that bind to the tubulin subunits of microtubule structures, and promote and stabilize microtubule assembly (Avila et al., 2004; Johnson and Stoothoff, 2004).	Millipore, anti-Tau5, #MAB361	1:2000
	P-Tau (Ser400/ Thr403/Ser404)	Phospho-Tau (P-Tau) recognizes endogenous levels of tau protein when phosphorylated at Ser400 or Thr403 or Ser404. Studies have shown that tau phosphorylation at Ser404 destabilizes microtubules and that tau is hyperphosphorylated at Ser404 in Alzheimer's disease (Evans et al., 2000). Phosphorylation decreases the ability of tau to bind to microtubules, destabilizing the structure and driving it toward disassembly. Neurofibrillary tangles are a major hallmark of Alzheimer's disease; these tangles are composed of hyperphosphorylated tau (Johnson and Stoothoff, 2004).	Cell Signaling, anti-Phospo-Tau (Ser400/Thr403/Ser404), #11837	1:1000
	P-Tau (Ser396)	Phospho-Tau (Ser396) (P-Tau Ser396) detects endogenous levels of Tau only when phosphorylated at serine 396. Phosphorylation at Ser396 has shown to destabilize microtubules and contribute to different neurological disorders (Bramblett et al., 1993; Evans et al., 2000).	Cell Signaling, anti-Phospo-Tau (Ser396), #9632	1:1000
Housekeeping	β-Actin	β-Actin is a cytoskeletal housekeeping protein.	Sigma–Aldrich, monoclonal anti-β-actin-HRP antibody, A3854	1:50,000
Secondary	Rabbit IgG	Secondary antibody.	Bio-Rad, Anti-Rabbit-HRP antibody, #170-6515	1:7500
	Mouse IgG	Secondary antibody.	Bio-Rad, Anti-Mouse-HRP antibody, #170-6516	1:10,000

processed in term of brightness and contrast, and presented as the representative blots in the figures.

Statistics

All data were expressed as a fold increase of the mean ± SEM for each group relative to the mean of the TTC− sham group. These data were analyzed by using GraphPad Prism v7.02. Data from western blotting were analyzed using two-way analysis of variance (ANOVA) followed by Sidak's *post hoc* comparison. The significant differences shown on the graphs with asterisks (*) refer to the *post hoc* tests. All differences were considered to be significant at $p < 0.05$.

RESULTS

Apoptotic and Autophagy Markers

Protein levels of pro-caspase-3 and cleaved caspase-3 were significantly reduced in stroke mice compared to sham in the infarct area of both the TTC− (pro-caspase-3 $p = 0.0419$; cleaved caspase-3 $p = 0.0001$) and the TTC+ (pro-caspase-3 $p < 0.0001$; cleaved caspase-3 $p = 0.0432$) group. We found no significant differences in neither the thalamus nor hippocampus (**Figure 2A**). Quantification of LC3 showed a significant decrease in stroke mice compared to sham in the infarct of the TTC− (LC3I $p < 0.0001$; LC3II $p < 0.0001$) and TTC+ (LC3I $p < 0.0001$; LC3II $p < 0.0001$) group. Changes in the protein expression levels in the thalamus and hippocampus were not statistically significant between sham and stroke group (**Figure 2B**).

Neuronal Markers

Protein levels of NeuN were significantly reduced in stroke mice in the infarct and thalamus areas of both TTC− (NeuN infarct $p < 0.0001$, NeuN thalamus $p = 0.0021$) and TTC+ (NeuN infarct $p < 0.0001$; NeuN thalamus $p = 0.0086$) group. However, no significant differences were found in the hippocampus (**Figure 3A**). Protein levels of synaptophysin were significantly reduced in the infarct ($p = 0.0040$), thalamus ($p = 0.0019$), and hippocampus ($p = 0.0042$) of TTC− stroke. In the TTC+ group, synaptophysin was significantly reduced just in the hippocampus ($p < 0.0001$) (**Figure 3B**). We observed a significant decrease in PSD95 in the infarct area of TTC− ($p < 0.0001$) and TTC+ ($p < 0.0001$) brains. However, no significant changes were observed in the other regions (**Figure 3C**).

Glial Markers

Glial fibrillary acidic protein was significantly increased in all investigated regions in the TTC− stroke mice compared to sham (infarct $p = 0.0015$; thalamus $p < 0.0001$; hippocampus $p < 0.0001$). In the TTC+ stroke mice, GFAP was increased in the thalamus ($p = 0.0100$) and hippocampus ($p < 0.0001$)

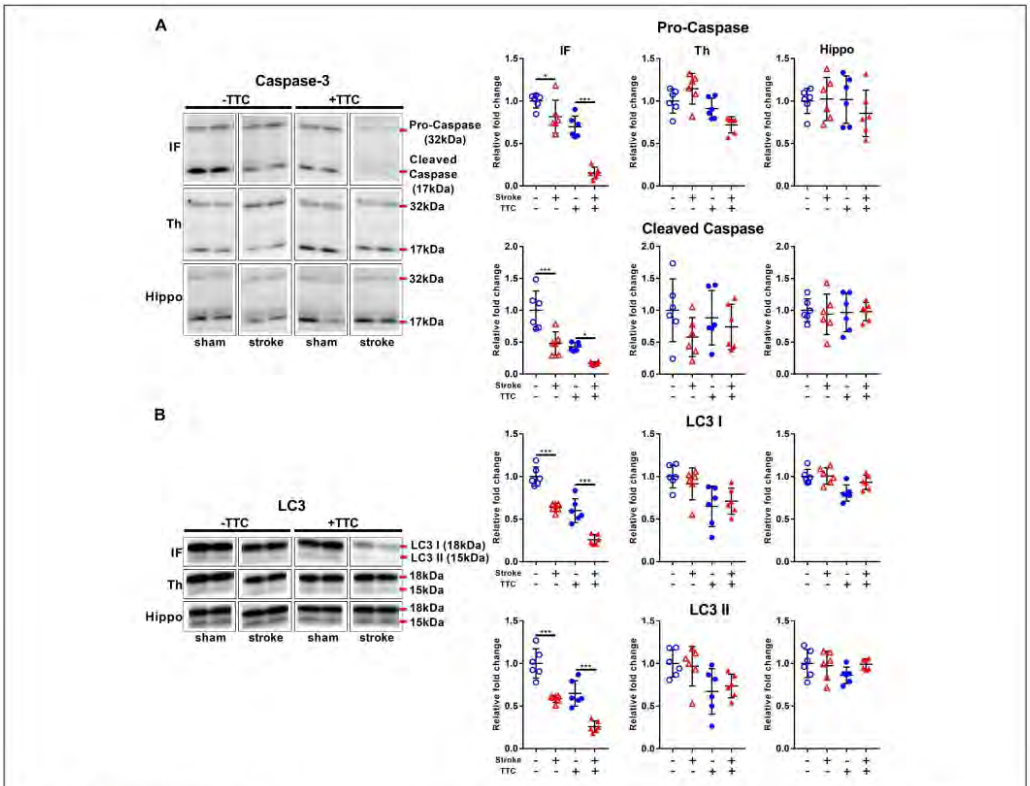

FIGURE 2 | Apoptotic and autophagy markers. Representative western blot and quantification of caspase-3 (pro-caspase and cleaved caspase) **(A)** and LC3 (LC3I and LC3II) **(B)** within the infarct (IF), thalamus (Th), and hippocampus (Hippo). Mean ± SEM (two-way ANOVA and Sidak's multiple comparisons). ○TTC− sham; △TTC− stroke; ●TTC+ sham; ▲TTC+ stroke. $^{*}p < 0.05$, $^{***}p < 0.001$.

(**Figure 4A**). In contrast, ALDH1L1 was significantly downregulated in the infarct area of both TTC− ($p < 0.0001$) and TTC+ ($p < 0.0001$) stroke mice (**Figure 4B**). No significant differences were found in other areas. CD11b showed increased protein levels in the infarct area of TTC− ($p = 0.0029$) and TTC+ ($p < 0.0001$) stroke mice (**Figure 4C**). CD11b was also increased in the thalamus of TTC− stroke mice ($p < 0.0001$). There were no significant differences in the hippocampus.

Vascular Markers

We analyzed the expression of Collagen IV, CD31, and VEGFA. VEGFA showed a significant decrease in the infarct area of TTC+ stroked mice. There were no differences in the thalamus or hippocampus (**Supplementary Figure S2**). However, we could not detect any bands for Collagen IV or CD31. This could be due to the protein extraction protocol was not suitable for these target proteins or the recommended conditions of the antibodies used were not optimized. It will be of considerable interest in future studies, using appropriate lysis buffer and protein extraction procedure as well as validated primary antibodies, to examine vascular markers in TTC-treated tissues.

Neurodegeneration-Related Markers

We analyzed the expression levels of three commonly investigated neurotoxic protein markers. First, we analyzed amyloid-β (Aβ) oligomerization after stroke. Specifically, we quantitated the pentamer (25 kDa), intermediate size oligomers (30 kDa), decamer (50 kDa), and dodecamer (55 kDa). We observed showed a significant increase of all Aβ oligomers studied in the infarct area of both TTC− (pentamer $p < 0.0001$; intermediate size oligomer $p < 0.0001$; decamer $p = 0.0175$; dodecamer $p = 0.0336$) and TTC+ (pentamer $p < 0.0001$; intermediate size oligomer $p = 0.0047$; decamer $p < 0.0001$; dodecamer $p < 0.0001$) stroke mice. In the thalamus, we observed a significant increase in the pentamer ($p = 0.0366$), intermediate size oligomers ($p = 0.0021$), and

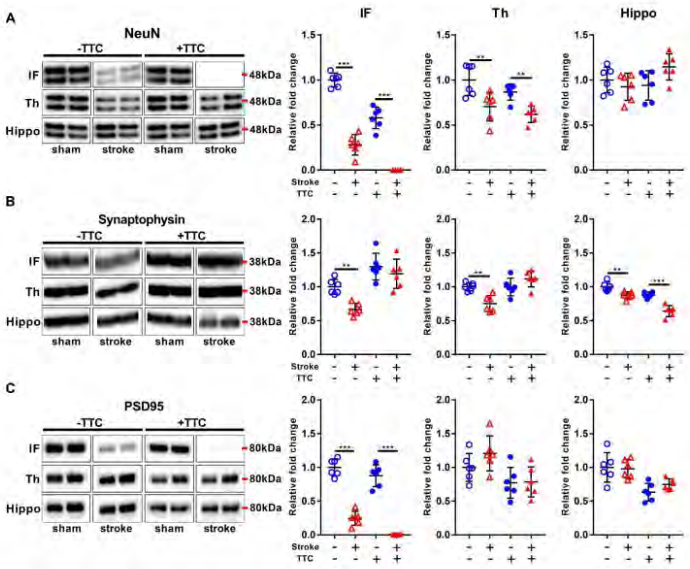

FIGURE 3 | Neuronal markers. Representative western blot and quantification of NeuN **(A)** Synaptophysin **(B)**, and PSD95 **(C)** within the infarct (IF), thalamus (Th), and hippocampus (Hippo). Mean ± SEM (two-way ANOVA and Sidak's multiple comparisons). ○TTC− sham; △TTC− stroke; ●TTC+ sham; ▲TTC+ stroke. $^{**}p < 0.01$, $^{***}p < 0.001$.

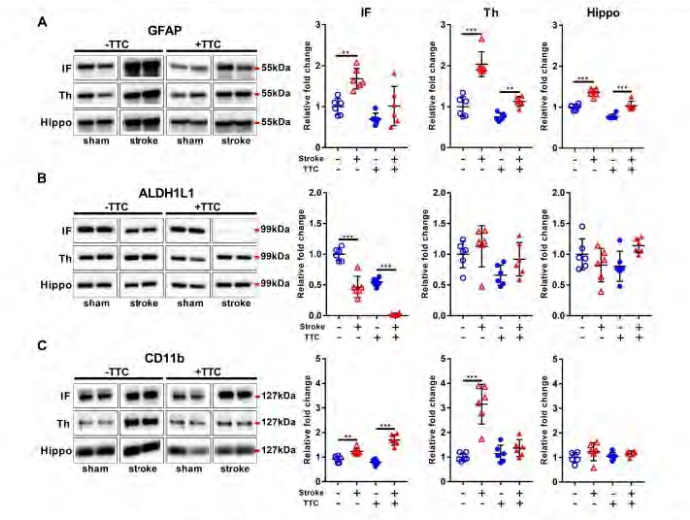

FIGURE 4 | Glial markers. Representative western blot and quantification of GFAP **(A)**, ALDH1L1 **(B)**, and CD11b **(C)** within the infarct (IF), thalamus (Th), and hippocampus (Hippo). Mean ± SEM (two-way ANOVA and Sidak's multiple comparisons). ○TTC− sham; △TTC− stroke; ●TTC+ sham; ▲TTC+ stroke. $^{**}p < 0.01$, $^{***}p < 0.001$.

decamer (p = 0.0022) in the TTC− stroke group. Protein levels in the TTC+ stroke group showed a trend toward an increase however was not statistically different to sham animals. Additionally, in the hippocampus we observed a significant increase in the pentamer in both TTC− (p = 0.0007) and TTC+ (p = 0.0009) group (**Figure 5**).

Secondly, we evaluated the monomer (14 kDa), dimer (28 kDa), and trimer (42 kDa) levels of α-Syn. In the infarct, we found a significant decrease of monomer levels, and a corresponding significant increase in α-Syn dimer and trimer levels in both TTC− (monomer $p < 0.0001$; dimer $p < 0.0001$; trimer $p < 0.0001$) and TTC+ (monomer $p < 0.0001$; dimer $p < 0.0001$; trimer $p < 0.0001$) group. In the thalamus, a significant reduction of monomer levels, and a corresponding significant increase in α-Syn trimer levels were observed in the TTC− group only (monomer p = 0.0026; dimer p = 0.0033; trimer p = 0.0011). The TTC+ group showed no significant differences in this region. In the hippocampus, we found no statistically significant changes in the monomer or trimer, but we observed a significant increase in the dimer levels in both groups (dimer TTC− $p < 0.0001$; dimer TTC+ p = 0.0378) (**Figure 6**).

Lastly, we evaluated protein levels of total Tau and two site-specific phosphorylated forms, which have been associated with the formation of neurofibrillary tangles in neurodegenerative diseases. The levels of total Tau, as evaluated by Tau5, were decreased in the infarct area of TTC− ($p < 0.0001$) and TTC+ ($p < 0.0001$) group. Thalamus and hippocampus showed no changes. We then assessed the levels of Phospho-Tau (Ser400/Thr403/Ser404) and Phospho-Tau Ser396 relative to the total Tau. Reduced P-Tau and P-Tau (Ser396) levels were observed in the infarct after stroke in both group (P-Tau TTC− $p < 0.0001$; P-Tau Ser396 TTC− p = 0.0203; P-Tau TTC+ $p < 0.0001$; P-Tau Ser396 TTC+ $p < 0.0001$). No significant differences were found in the thalamus and hippocampus (**Figure 7**).

DISCUSSION

In this study, we investigated whether TTC+ tissues can be processed for downstream biochemical analyses, specifically by western blotting. Our results suggest that brain samples that are processed by TTC staining can be routinely used for protein analyses. Overall, the hippocampus shows same relative changes between TTC− and TTC+ group for all the markers studied, whereas thalamus and infarct differ in a couple of makers (summary of the results **Supplementary Figure S3**). This study demonstrates and further supports the usage of TTC staining for downstream protein analysis.

Previous studies have demonstrated that TTC+ stroke brains can be used for histology, gene, and protein expression analyses (Kramer et al., 2010; Sun et al., 2012; Li L. et al., 2018; Li Z. et al., 2018). Taking all these studies together suggest that TTC-stained tissue can be used for biochemical analyses without restrictions. However, there are a few limitations regarding

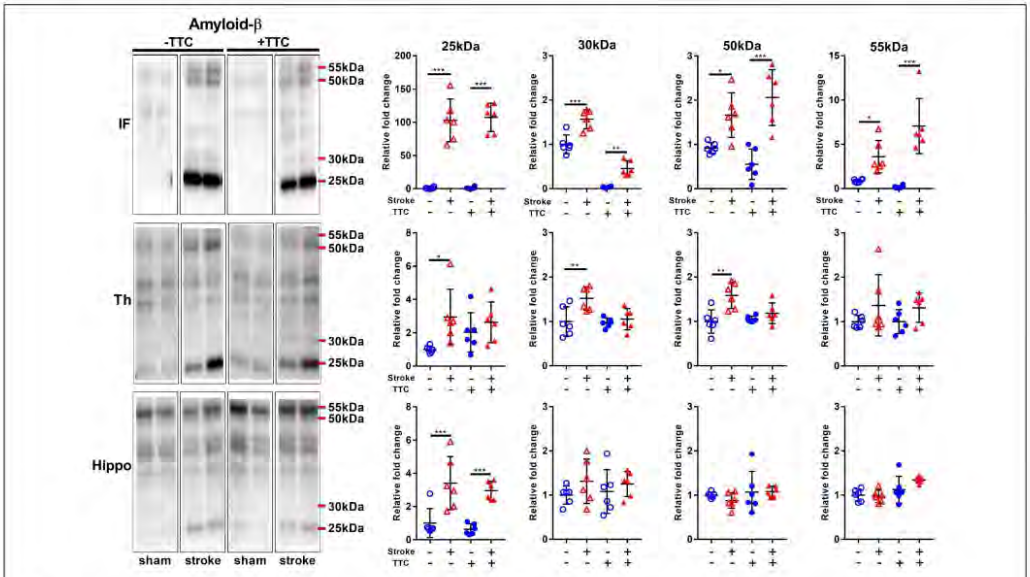

FIGURE 5 | Representative western blot and quantification of amyloid-β expression profile within the infarct (IF), thalamus (Th), and hippocampus (Hippo). Our analyses focused on different molecular weight oligomers (25, 30, 50, and 55 kDa). Mean ± SEM (two-way ANOVA and Sidak's multiple comparisons). ○TTC− sham; △TTC− stroke; ●TTC+ sham; ▲TTC+ stroke. *$p < 0.05$, **$p < 0.01$, ***$p < 0.001$.

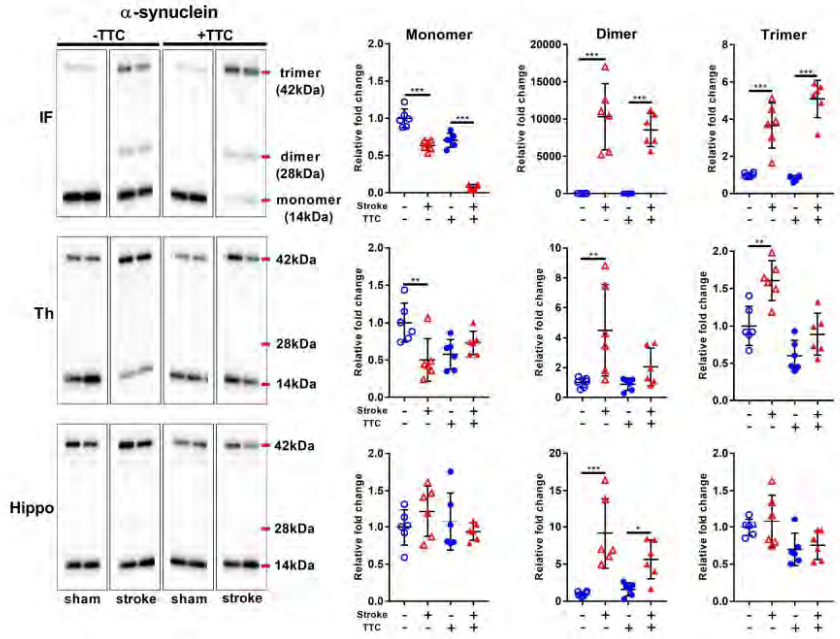

FIGURE 6 | Representative western blot and quantification of α-synuclein expression profile within the infarct (IF), thalamus (Th), and hippocampus (Hippo). Our analysis focused on the monomer (14 kDa), dimer (28 kDa), and trimer (42 kDa). Mean ± SEM (two-way ANOVA and Sidak's multiple comparisons). ○TTC− sham; △TTC− stroke; ●TTC+ sham; ▲TTC+ Stroke. $^{*}p < 0.05$, $^{**}p < 0.01$, $^{***}p < 0.001$.

the protein expression analyses that we wanted to address in our study. Firstly, previous studies have just focused on a limited number of markers, mainly apoptotic markers and housekeeping proteins (Kramer et al., 2010; Sun et al., 2012; Mohammad-Gharibani et al., 2014; Gharibani et al., 2015; She et al., 2018) and therefore it cannot be definitely asserted that other proteins can also be studied after TTC treatment. Secondly, other studies did not study the effects of TTC on protein modification such as phosphorylation and aggregation. Finally, the penumbra and surrounding areas have been the primary focus; however, there may be different reactions to TTC in other brain regions. Therefore, here we analyzed a total of 16 markers, which include apoptotic, autophagy, neuronal, glial, vascular, and neurodegeneration-related markers. In addition, we analyzed the changes in the primary infarct area and in regions that have been previously linked with secondary neurodegeneration processes (thalamus and hippocampus) (Xie et al., 2011; Ong et al., 2017a; Baumgartner et al., 2018; Sanchez-Bezanilla et al., 2019).

We observed that in the infarct region all the markers with the exception of synaptophysin, VEGFA, and GFAP presented the same relative changes in the TTC− and TTC+ group. In the thalamus, TTC-stained and non-stained tissue showed similar relative changes in 9 out of 13 markers studied. Aβ, α-Syn, CD11b, and synaptophysin were the only markers that exhibited different results when comparing TTC+ and TTC− in the thalamus. In the hippocampus, all the markers showed the same changes in both group. The discrepancies observed in the infarct region can be explained by the procedure used to define the area considered infarct. While in the TTC+ group the infarct area is clearly delineated as the colorless area, in the TTC− group is not easy to visually determine the infarct area. Therefore, surrounding tissue could have been potentially collected as part of the infarct in the TTC− group. Further, the differences observed in some of the markers studied could be related to the TTC staining protocol. Firstly, proteolysis may occur for some proteins when the brain sections are incubated at 37°C for 10 min. Secondly, the formazan pigment (deep red color) may interfere with the protein estimation using the BCA colorimetric protein assay. Interestingly, we observed that Tau5, P-Tau (Ser400/Thr403/Ser404), and P-Tau (S396) showed the same relative changes in all the areas, suggesting that TTC staining does not present a major interference with protein phosphorylation. We also observed that TTC does not interfere with protein aggregation processes in the infarct and

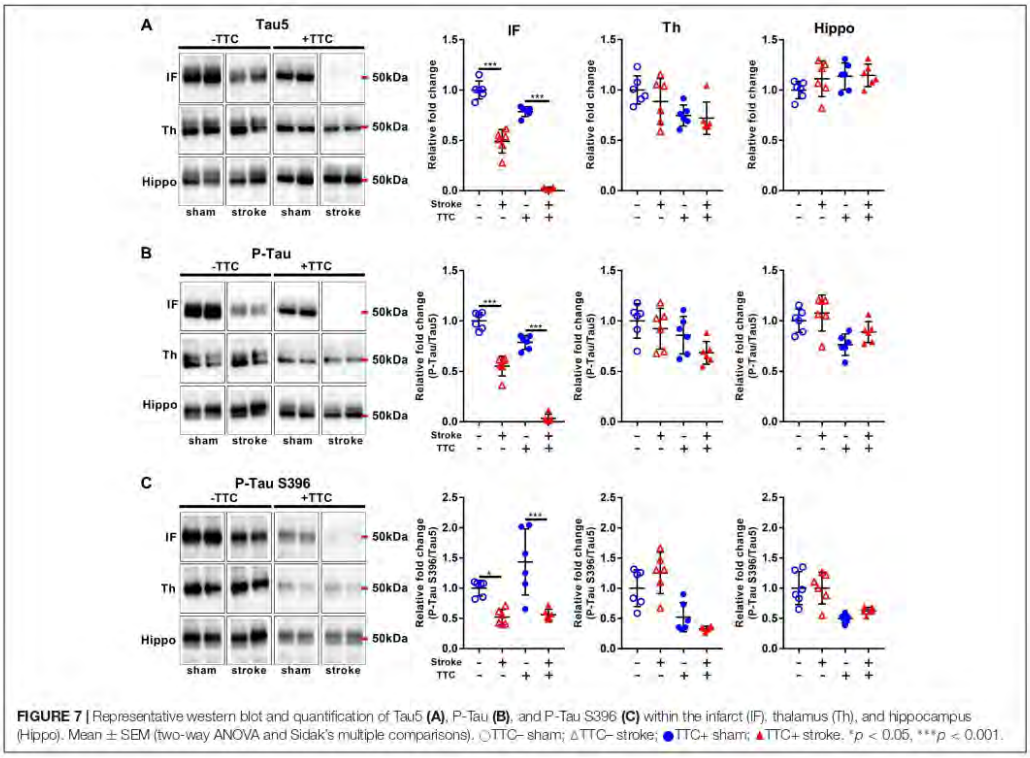

FIGURE 7 | Representative western blot and quantification of Tau5 **(A)**, P-Tau **(B)**, and P-Tau S396 **(C)** within the infarct (IF), thalamus (Th), and hippocampus (Hippo). Mean ± SEM (two-way ANOVA and Sidak's multiple comparisons). ○TTC– sham; △TTC– stroke; ●TTC+ sham; ▲TTC+ stroke. $^{*}p < 0.05$, $^{***}p < 0.001$.

hippocampus as both Aβ and α-Syn presented the same relative changes. From these results, we can conclude that brain sections that are processed by TTC staining are viable for western blotting. While the usage of western blotting following TTC staining can produce high-throughput qualitative and semi-quantitative data for a variety of protein markers, the end-user should optimize the protocols and conditions accordingly.

In this study, we provide a useful procedure to repurpose brain sections after they have been treated with TTC staining, which brings multiple advantages. Firstly, TTC staining is a simple, rapid, and inexpensive method that allows to delineate the size of the cerebral infarct area and distinguish from the penumbra and intact tissue. Therefore, we can precisely select the area of the brain that it is more suited for protein expression analyses. Furthermore, we can select brains with the same infarct size and reduce the experimental variability. This procedure can also be used to investigate protein modification such as protein phosphorylation and aggregation. Another important benefit of this approach is that it permits a reduction in the number of animals required for investigation as the same brains can be used for infarct quantification and protein quantification. Specifically, we demonstrated that we could use western blotting for the simultaneous assessment of a large number of different markers as well as protein phosphorylation and aggregation after brains have been treated with TTC. In conclusion, our study demonstrates that TTC brains should not be discarded as they can be used for further protein analyses of a wide variety of commonly used markers.

DATA AVAILABILITY

The datasets generated for this study are available on request to the corresponding author.

ETHICS STATEMENT

The animal study was reviewed and approved by the University of Newcastle Animal Care and Ethics Committee (A-2013-340).

AUTHOR CONTRIBUTIONS

SS-B and LKO designed the research, performed the experiments, and prepared the first draft of the manuscript.

FRW and MN supervised the study. SS-B and LKO analyzed the data and interpreted the results. All authors reviewed and contributed to the final version of the manuscript.

FUNDING

This study was supported by the Hunter Medical Research Institute (HMRI 896), Faculty of Health and Medicine Pilot Grant, the Priority Research Centre for Stroke and Brain Injury Research Support Grant, the Mary Costello Alzheimer's Pilot Grant, and The University of Newcastle, Australia. LKO and SS-B also acknowledge the support from the Research Advantage for ECR Higher Degree by Research (HDR) Scholarship and Greaves Family Postgraduate Scholarships in Medical Research (HMRI 1054).

ACKNOWLEDGMENTS

We would like to acknowledge the insights and comments provided by Rebecca Hood on early versions of the manuscript.

SUPPLEMENTARY MATERIAL

The Supplementary Material for this article can be found online at: https://www.frontiersin.org/articles/10.3389/fnmol.2019.00181/full#supplementary-material

REFERENCES

Avila, J., Lucas, J. J., Perez, M., and Hernandez, F. (2004). Role of tau protein in both physiological and pathological conditions. *Physiol. Rev.* 84, 361–384. doi: 10.1152/physrev.00024.2003

Baumgartner, P., El Amki, M., Bracko, O., Luft, A. R., and Wegener, S. (2018). Sensorimotor stroke alters hippocampo-thalamic network activity. *Sci. Rep.* 8:15770. doi: 10.1038/s41598-018-34002-9

Bederson, J. B., Pitts, L. H., Germano, S. M., Nishimura, M. C., Davis, R. L., and Bartkowski, H. M. (1986). Evaluation of 2,3,5-triphenyltetrazolium chloride as a stain for detection and quantification of experimental cerebral infarction in rats. *Stroke* 17, 1304–1308.

Benedek, A., Moricz, K., Juranyi, Z., Gigler, G., Levay, G., Harsing, L. G. Jr., et al. (2006). Use of TTC staining for the evaluation of tissue injury in the early phases of reperfusion after focal cerebral ischemia in rats. *Brain Res.* 1116, 159–165. doi: 10.1016/j.brainres.2006.07.123

Bramblett, G. T., Goedert, M., Jakes, R., Merrick, S. E., Trojanowski, J. Q., and Lee, V. M. (1993). Abnormal tau phosphorylation at Ser396 in Alzheimer's disease recapitulates development and contributes to reduced microtubule binding. *Neuron* 10, 1089–1099.

Burnette, W. N. (1981). "Western blotting": electrophoretic transfer of proteins from sodium dodecyl sulfate–polyacrylamide gels to unmodified nitrocellulose and radiographic detection with antibody and radioiodinated protein A. *Anal. Biochem.* 112, 195–203.

Cahoy, J. D., Emery, B., Kaushal, A., Foo, L. C., Zamanian, J. L., Christopherson, K. S., et al. (2008). A transcriptome database for astrocytes, neurons, and oligodendrocytes: a new resource for understanding brain development and function. *J. Neurosci.* 28, 264–278. doi: 10.1523/jneurosci.4178-07.2008

Chetkovich, D. M., Bunn, R. C., Kuo, S. H., Kawasaki, Y., Kohwi, M., and Bredt, D. S. (2002). Postsynaptic targeting of alternative postsynaptic density-95 isoforms by distinct mechanisms. *J. Neurosci.* 22, 6415–6425.

Eng, L. F., Ghirnikar, R. S., and Lee, Y. L. (2000). Glial fibrillary acidic protein: GFAP-thirty-one years (1969-2000). *Neurochem. Res.* 25, 1439–1451.

Evans, D. B., Rank, K. B., Bhattacharya, K., Thomsen, D. R., Gurney, M. E., and Sharma, S. K. (2000). Tau phosphorylation at serine 396 and serine 404 by human recombinant tau protein kinase II inhibits tau's ability to promote microtubule assembly. *J. Biol. Chem.* 275, 24977–24983. doi: 10.1074/jbc.M000808200

Fernandes-Alnemri, T., Litwack, G., and Alnemri, E. S. (1994). CPP32, a novel human apoptotic protein with homology to caenorhabditis elegans cell death protein Ced-3 and mammalian interleukin-1 beta-converting enzyme. *J. Biol. Chem.* 269, 30761–30764.

Gharibani, P., Modi, J., Menzie, J., Alexandrescu, A., Ma, Z., Tao, R., et al. (2015). Comparison between single and combined post-treatment with S-Methyl-N,N-diethylthiolcarbamate sulfoxide and taurine following transient focal cerebral ischemia in rat brain. *Neuroscience* 300, 460–473. doi: 10.1016/j.neuroscience.2015.05.042

Haass, C., and Selkoe, D. J. (2007). Soluble protein oligomers in neurodegeneration: lessons from the Alzheimer's amyloid beta-peptide. *Nat. Rev. Mol. Cell Biol.* 8, 101–112.

Johnson, G. V., and Stoothoff, W. H. (2004). Tau phosphorylation in neuronal cell function and dysfunction. *J. Cell Sci.* 117, 5721–5729. doi: 10.1242/jcs.01558

Kabeya, Y., Mizushima, N., Ueno, T., Yamamoto, A., Kirisako, T., Noda, T., et al. (2000). LC3, a mammalian homologue of yeast Apg8p, is localized in autophagosome membranes after processing. *EMBO J.* 19, 5720–5728. doi: 10.1093/emboj/19.21.5720

Kramer, M., Dang, J., Baertling, F., Denecke, B., Clarner, T., Kirsch, C., et al. (2010). TTC staining of damaged brain areas after MCA occlusion in the rat does not constrict quantitative gene and protein analyses. *J. Neurosci. Methods* 187, 84–89. doi: 10.1016/j.jneumeth.2009.12.020

Kuhn, K. (1995). Basement membrane (type IV) collagen. *Mat. Bio.* 14, 439–445.

Leung, D. W., Cachianes, G., Kuang, W. J., Goeddel, D. V., and Ferrara, N. (1989). Vascular endothelial growth factor is a secreted angiogenic mitogen. *Science* 246, 1306–1309. doi: 10.1126/science.2479986

Li, F., Irie, K., Anwer, M. S., and Fisher, M. (1997). Delayed triphenyltetrazolium chloride staining remains useful for evaluating cerebral infarct volume in a rat stroke model. *J. Cereb. Blood Flow Metab.* 17, 1132–1135. doi: 10.1097/00004647-199710000-00016

Li, L., Yu, Q., and Liang, W. (2018). Use of 2,3,5-triphenyltetrazolium chloride-stained brain tissues for immunofluorescence analyses after focal cerebral ischemia in rats. *Pathol. Res. Pract.* 214, 174–179. doi: 10.1016/j.prp.2017.11.016

Li, Z., Bishop, N., Chan, S. L., and Cipolla, M. J. (2018). Effect of TTC treatment on immunohistochemical quantification of collagen iv in rat brains after stroke. *Transl. Stroke Res.* 9, 499–505. doi: 10.1007/s12975-017-0604-9

Liu, Z. Q., Mahmood, T., and Yang, P. C. (2014). Western blot: technique, theory and trouble shooting. *North Am. J. Med Sci.* 6:160. doi: 10.4103/1947-2714.128482

Maroteaux, L., Campanelli, J. T., and Scheller, R. H. (1988). Synuclein: a neuron-specific protein localized to the nucleus and presynaptic nerve terminal. *J. Neurosci.* 8, 2804–2815.

Mohammad-Gharibani, P., Modi, J., Menzie, J., Genova, R., Ma, Z., Tao, R., et al. (2014). Mode of action of S-methyl-N, N-diethylthiocarbamate sulfoxide (DETC-MeSO) as a novel therapy for stroke in a rat model. *Mol. Neurobiol.* 50, 655–672. doi: 10.1007/s12035-014-8658-0

Mullen, R. J., Buck, C. R., and Smith, A. M. (1992). NeuN, a neuronal specific nuclear protein in vertebrates. *Development* 116, 201–211.

Murtha, L. A., Beard, D. J., Bourke, J. T., Pepperall, D., McLeod, D. D., and Spratt, N. J. (2016). Intracranial pressure elevation 24 h after ischemic stroke in aged rats is prevented by early, short hypothermia treatment. *Front. Aging Neurosci.* 8:124. doi: 10.3389/fnagi.2016.00124

Newman, P. J. (1997). The biology of PECAM-1. *J. Clin. Invest.* 99, 3–8. doi: 10.1172/jci119129

Ong, L. K., Chow, W. Z., TeBay, C., Kluge, M., Pietrogrande, G., Zalewska, K., et al. (2018). Growth hormone improves cognitive function after experimental stroke. *Stroke* 49, 1257–1266. doi: 10.1161/strokeaha.117.020557

Ong, L. K., Walker, F. R., and Nilsson, M. (2017a). Is stroke a neurodegenerative condition? a critical review of secondary neurodegeneration and amyloid-beta accumulation after stroke. *AIMS Med. Sci.* 4, 1–16. doi: 10.3934/medsci.2017.1.1

Ong, L. K., Zhao, Z., Kluge, M., TeBay, C., Zalewska, K., Dickson, P. W., et al. (2017b). Reconsidering the role of glial cells in chronic stress-induced dopaminergic neurons loss within the substantia nigra? Friend or foe? *Brain Behav. Immun.* 60, 117–125. doi: 10.1016/j.bbi.2016.10.001

Ong, L. K., Zhao, Z., Kluge, M., Walker, F. R., and Nilsson, M. (2017c). Chronic stress exposure following photothrombotic stroke is associated with increased levels of amyloid beta accumulation and altered oligomerisation at sites of thalamic secondary neurodegeneration in mice. *J. Cereb. Blood Flow Metab.* 37, 1338–1348. doi: 10.1177/0271678x16654920

Sanchez-Bezanilla, S., TeBay, C., Nilsson, M., Walker, F. R., and Ong, L. K. (2019). Visual discrimination impairment after experimental stroke is associated with disturbances in the polarization of the astrocytic aquaporin-4 and increased accumulation of neurotoxic proteins. *Exp. Neurol.* 318, 232–243. doi: 10.1016/j.expneurol.2019.05.001

She, D. T., Wong, L. J., Baik, S. H., and Arumugam, T. V. (2018). SIRT2 inhibition confers neuroprotection by downregulation of foxo3a and mapk signaling pathways in ischemic stroke. *Mol. Neurobiol.* 55, 9188–9203. doi: 10.1007/s12035-018-1058-0

Solovjov, D. A., Pluskota, E., and Plow, E. F. (2005). Distinct roles for the alpha and beta subunits in the functions of integrin alphaMbeta2. *J. Biol. Chem.* 280, 1336–1345. doi: 10.1074/jbc.M406968200

Sun, Y. Y., Yang, D., and Kuan, C. Y. (2012). Mannitol-facilitated perfusion staining with 2,3,5-triphenyltetrazolium chloride (TTC) for detection of experimental cerebral infarction and biochemical analysis. *J. Neurosci. Methods* 203, 122–129. doi: 10.1016/j.jneumeth.2011.09.029

van der Putten, H., Wiederhold, K. H., Probst, A., Barbieri, S., Mistl, C., Danner, S., et al. (2000). Neuropathology in mice expressing human alpha-synuclein. *J. Neurosci.* 20, 6021–6029.

Walsh, D. M., and Selkoe, D. J. (2007). A beta oligomers - a decade of discovery. *J. Neurochem.* 101, 1172–1184. doi: 10.1111/j.1471-4159.2006.04426.x

Wiedenmann, B., Franke, W. W., Kuhn, C., Moll, R., and Gould, V. E. (1986). Synaptophysin: a marker protein for neuroendocrine cells and neoplasms. *Proc. Natl. Acad. Sci. U. S. A.* 83, 3500–3504. doi: 10.1073/pnas.83.10.3500

Xie, M., Yi, C., Luo, X., Xu, S., Yu, Z., Tang, Y., et al. (2011). Glial gap junctional communication involvement in hippocampal damage after middle cerebral artery occlusion. *Ann. Neurol.* 70, 121–132. doi: 10.1002/ana.22386

Conflict of Interest Statement: The authors declare that the research was conducted in the absence of any commercial or financial relationships that could be construed as a potential conflict of interest.

Supplementary material

Supplementary Figure S1

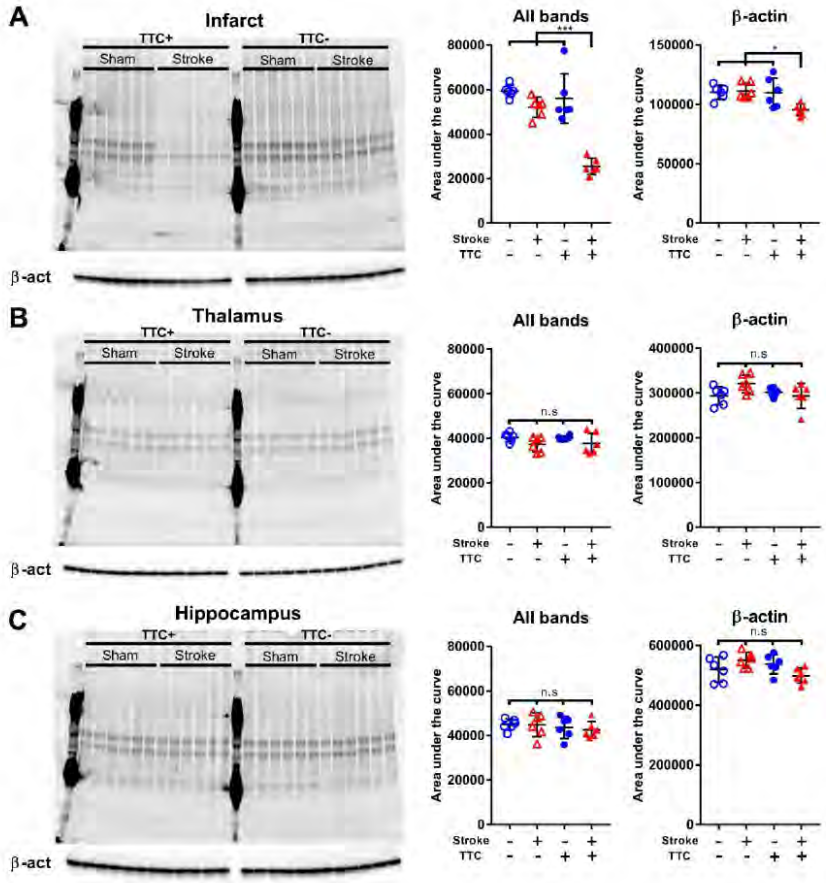

Supplementary Figure S1. Images of the total amount of proteins loaded in the gels and β-actin (β-act) representative gels. To ensure that equal amount of protein was loaded, one gel per region was scanned using ChemiDoc XRS+ system before the transfer. The housekeeping protein β-actin was also used as a loading control to normalised the levels of protein detected. (A) Stroke brains treated with TTC (TTC+) present a significantly lower amount of total protein as well as less β-actin in the infarct area. This might explained due to the lack of living tissue in the infarct area of TTC+ stroke group. In the TTC- stroke group surrounding tissue could have been potentially collected together with the infarct, increasing the amount of total protein. We could not observed any significant differences in the total protein loaded or β-actin levels in the thalamus (B) or hippocampus (C). Mean ± SEM (two-way ANOVA and Sidak's multiple comparisons). ○TTC- Sham; △TTC- Stroke; ●TTC+ Sham; ▲TTC+ Stroke. * $p < 0.05$, *** $p < 0.001$, n.s = not significant

Supplementary Figure S2

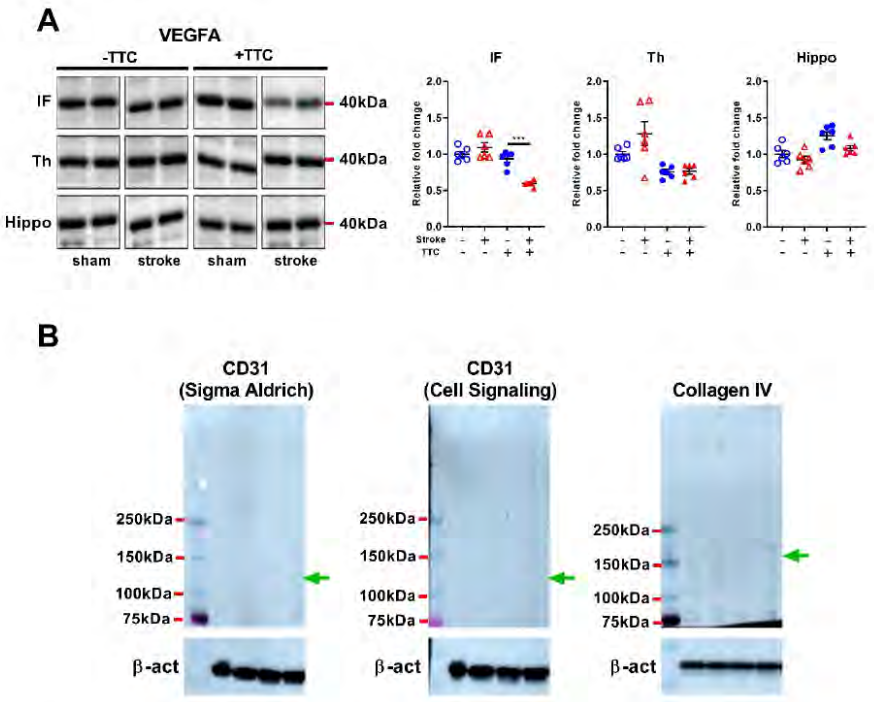

Supplementary Figure S2. Vascular markers. **(A)** Representative western blot and quantification of VEGFA within the infarct (IF), thalamus (Th) and hippocampus (Hippo). **(B)** Western blot of CD31 (expected molecular weight: 130kDa) and collagen IV (expected molecular weight: 160-190kDa). No bands could be detected. The loading controls were performed by the analysis of β-actin (β-act). Green arrows show expected molecular weight. Mean ± SEM (two-way ANOVA and Sidak's multiple comparisons). ○TTC- Sham; △TTC- Stroke; ●TTC+ Sham; ▲TTC+ Stroke. *** $p < 0.001$.

Supplementary Figure S3

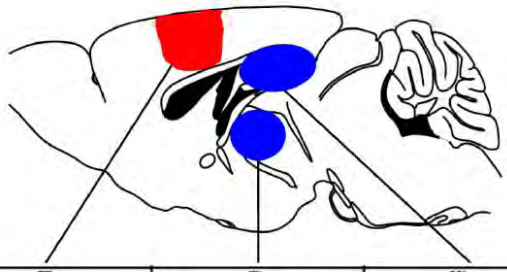

	IF		Th		Hippo	
	TTC-	TTC+	TTC-	TTC+	TTC-	TTC+
Pro-Caspase	↓0.8	↓0.2	–	–	–	–
Cleaved Caspase	↓0.4	↓0.6	–	–	–	–
LC3I	↓0.6	↓0.4	–	–	–	–
LC3II	↓0.6	↓0.4	–	–	–	–
NeuN	↓0.3	↓0.005	↓0.7	↓0.8	–	–
Synaptophysin	↓0.6	–	↓0.75	–	↓0.8	↓0.7
PSD95	↓0.2	↓0.008	–	–	–	–
GFAP	↑1.7	–	↑2	↑1.5	↑1.4	↑1.3
ALDH1L1	↓0.5	↓0.03	–	–	–	–
CD11b	↑1.2	↑2.15	↑3.15	–	–	–
Aβ - 25kDa	↑102	↑93	↑2.73	–	↑3.4	↑4.7
Aβ - 30kDa	↑1.5	↑12	↑1.5	–	–	–
Aβ - 50kDa	↑1.5	↑3.7	↑1.6	–	–	–
Aβ - 55kDa	↑3.4	↑40	–	–	–	–
α-Syn - Monomer	↓0.6	↓0.1	↓0.5	–	–	–
α-Syn - Dimer	↑10300	↑3336	↑4.5	–	↑9.2	↑3.5
α-Syn - Trimer	↑3.7	↑6.2	↑1.6	–	–	–
Tau5	↓0.5	↓0.03	–	–	–	–
P-Tau	↓0.5	↓0.04	–	–	–	–
P-Tau S396	↓0.5	↓0.16	–	–	–	–
VEGFA	–	↓0.6	–	–	–	–

Supplementary Figure S3. A summary of the changes observed in the infarct (IF), thalamus (Th) and hippocampus (Hippo) evoked by stroke when brains are TTC-stained (TTC+) and non-TTC-stained (TTC-). All changes are presented as fold change of stroke group relative to sham. Decreases in protein expression in stroke mice relative to sham are shown by downward arrows and increases by upward arrows. No changes are indicated by a horizontal dash.

APPENDIX B: COPYRIGHT PERMISSIONS

Copyright Permissions

I, Sonia Sanchez Bezanilla, warrant that I have obtained, permission from the copyright owners to use any third party copyright material reproduced in the thesis and those of my own published work in which the copyright is held by another party.

As an author, copyright permission is not required for the right to include a publication in a thesis or dissertation from the following publications and publishers: Experimental Neurology (Elsevier), International journal of Molecular Science (MDPI) and Frontiers in Molecular Neuroscience (Frontiers).

WOLTERS KLUWER HEALTH, INC. LICENSE
TERMS AND CONDITIONS

Feb 17, 2020

This Agreement between Lot 1, Kookaburra Cct ("You") and Wolters Kluwer Health, Inc. ("Wolters Kluwer Health, Inc.") consists of your license details and the terms and conditions provided by Wolters Kluwer Health, Inc. and Copyright Clearance Center.

License Number	4771640075637
License date	Feb 17, 2020
Licensed Content Publisher	Wolters Kluwer Health, Inc.
Licensed Content Publication	Stroke
Licensed Content Title	New Directions in Treatments Targeting Stroke Recovery
Licensed Content Author	David J. Lin, Seth P. Finklestein, Steven C. Cramer
Licensed Content Date	Nov 9, 2018
Licensed Content Volume	49
Licensed Content Issue	12
Type of Use	Dissertation/Thesis
Requestor type	University/College
Sponsorship	No Sponsorship
Format	Electronic
Will this be posted on a password protected website?	Yes
Portion	Figures/tables/illustrations
Number of figures/tables/illustrations	1
Author of this Wolters Kluwer article	No
Will you be translating?	No
Intend to modify/adapt the content	No
Title	Exploring functional outcomes after stroke and underlying mechanisms
Institution name	University of Newcastle
Expected presentation date	Oct 2020
Portions	figure 1
Requestor Location	Lot 1, Kookaburra Cct Lot 1, Kookaburra Cct New Lambton Heights, New South Wales 2305 Australia Attn: Lot 1, Kookaburra Cct
Total	0.00 USD
Terms and Conditions	

Wolters Kluwer Health Inc. Terms and Conditions

1. **Duration of License:** Permission is granted for a one time use only. Rights herein do not apply to future reproductions, editions, revisions, or other derivative works. This permission shall be effective as of the date of execution by the parties for the maximum period of 12 months and should be renewed after the term expires.
    i. When content is to be republished in a book or journal the validity of this agreement should be the life of the book edition or journal issue.
    ii. When content is licensed for use on a website, internet, intranet, or any publicly accessible site (not including a journal or book), you agree to remove the material from such site after 12 months, or request to renew your permission license
2. **Credit Line:** A credit line must be prominently placed and include: For book content: the author(s), title of book, edition, copyright holder, year of publication; For journal

content: the author(s), titles of article, title of journal, volume number, issue number, inclusive pages and website URL to the journal page. If a journal is published by a learned society the credit line must include the details of that society.

3. **Warranties:** The requestor warrants that the material shall not be used in any manner which may be considered derogatory to the title, content, authors of the material, or to Wolters Kluwer Health, Inc.
4. **Indemnity:** You hereby indemnify and hold harmless Wolters Kluwer Health, Inc. and its respective officers, directors, employees and agents, from and against any and all claims, costs, proceeding or demands arising out of your unauthorized use of the Licensed Material.
5. **Geographical Scope:** Permission granted is non-exclusive and is valid throughout the world in the English language and the languages specified in the license.
6. **Copy of Content:** Wolters Kluwer Health, Inc. cannot supply the requestor with the original artwork, high-resolution images, electronic files or a clean copy of content.
7. **Validity:** Permission is valid if the borrowed material is original to a Wolters Kluwer Health, Inc. imprint (J.B.Lippincott, Lippincott-Raven Publishers, Williams & Wilkins, Lea & Febiger, Harwal, Rapid Science, Little Brown & Company, Harper & Row Medical, American Journal of Nursing Co, and Urban & Schwarzenberg - English Language, Raven Press, Paul Hoeber, Springhouse, Ovid), and the Anatomical Chart Company
8. **Third Party Material:** This permission does not apply to content that is credited to publications other than Wolters Kluwer Health, Inc. or its Societies. For images credited to non-Wolters Kluwer Health, Inc. books or journals, you must obtain permission from the source referenced in the figure or table legend or credit line before making any use of the image(s), table(s) or other content.
9. **Adaptations:** Adaptations are protected by copyright. For images that have been adapted, permission must be sought from the rightsholder of the original material and the rightsholder of the adapted material.
10. **Modifications:** Wolters Kluwer Health, Inc. material is not permitted to be modified or adapted without written approval from Wolters Kluwer Health, Inc. (with the exception of text size or color. The adaptation should be credited as follows: Adapted with permission from Wolters Kluwer Health, Inc. [the author(s), title of book edition, copyright holder, year of publication] or [the author(s), titles of article, title of journal, volume number, issue number, inclusive pages and website URL to the journal page].
11. **Full Text Articles:** Republication of full articles in English is prohibited.
12. **Branding and Marketing:** No drug name, trade name, drug logo, or trade logo can be included on the same page as material borrowed from *Diseases of the Colon & Rectum, Plastic Reconstructive Surgery, Obstetrics & Gynecology (The Green Journal), Critical Care Medicine, Pediatric Critical Care Medicine, the American Heart Association publications and the American Academy of Neurology publications.*
13. **Open Access:** Unless you are publishing content under the same Creative Commons license, the following statement must be added when reprinting material in Open Access journals: "The Creative Commons license does not apply to this content. Use of the material in any format is prohibited without written permission from the publisher, Wolters Kluwer Health, Inc. Please contact permissions@lww.com for further information."
14. **Translations:** The following disclaimer must appear on all translated copies: Wolters Kluwer Health, Inc. and its Societies take no responsibility for the accuracy of the translation from the published English original and are not liable for any errors which may occur.
15. **Published Ahead of Print (PAP):** Articles in the PAP stage of publication can be cited using the online publication date and the unique DOI number.
    i. Disclaimer: Articles appearing in the PAP section have been peer-reviewed and accepted for publication in the relevant journal and posted online before print publication. Articles appearing as PAP may contain statements, opinions, and information that have errors in facts, figures, or interpretation. Any final changes in manuscripts will be made at the time of print publication and will be reflected in the final electronic version of the issue. Accordingly, Wolters Kluwer Health, Inc., the editors, authors and their respective employees are not responsible or liable for the use of any such inaccurate or misleading data, opinion or information contained in the articles in this section.
16. **Termination of Contract:** Wolters Kluwer Health, Inc. must be notified within 90 days of the original license date if you opt not to use the requested material.
17. **Waived Permission Fee:** Permission fees that have been waived are not subject to future waivers, including similar requests or renewing a license.
18. **Contingent on payment:** You may exercise these rights licensed immediately upon issuance of the license, however until full payment is received either by the publisher or our authorized vendor, this license is not valid. If full payment is not received on a timely basis, then any license preliminarily granted shall be deemed automatically revoked and shall be void as if never granted. Further, in the event that you breach any of these terms and conditions or any of Wolters Kluwer Health, Inc.'s other billing and payment terms and conditions, the license is automatically revoked and shall be void as if never granted. Use of materials as described in a revoked license, as well as any use of the materials beyond the scope of an unrevoked license, may constitute copyright infringement and publisher reserves the right to take any and all action to protect its copyright in the materials.
19. **STM Signatories Only:** Any permission granted for a particular edition will apply to subsequent editions and for editions in other languages, provided such editions are for the work as a whole in situ and do not involve the separate exploitation of the permitted illustrations or excerpts. Please view: STM Permissions Guidelines
20. **Warranties and Obligations:** LICENSOR further represents and warrants that, to the best of its knowledge and belief, LICENSEE's contemplated use of the Content as represented to LICENSOR does not infringe any valid rights to any third party.
21. **Breach:** If LICENSEE fails to comply with any provisions of this agreement, LICENSOR may serve written notice of breach of LICENSEE and, unless such breach is fully cured within fifteen (15) days from the receipt of notice by LICENSEE, LICENSOR may thereupon, at its option, serve notice of cancellation on LICENSEE whereupon this Agreement shall immediately terminate.
22. **Assignment:** License conveyed hereunder by the LICENSOR shall not be assigned or granted in any manner conveyed to any third party by the LICENSEE without the consent in writing to the LICENSOR.
23. **Governing Law:** The laws of The State of New York shall govern interpretation of this Agreement and all rights and liabilities arising hereunder.
24. **Unlawful:** If any provision of this Agreement shall be found unlawful or otherwise legally unenforceable, all other conditions and provisions of this Agreement shall remain in full force and effect.

For Copyright Clearance Center / RightsLink Only:

1. **Service Description for Content Services:** Subject to these terms of use, any terms set forth on the particular order, and payment of the applicable fee, you may make the following uses of the ordered materials:
    i. **Content Rental:** You may access and view a single electronic copy of the materials ordered for the time period designated at the time the order is placed. Access to the materials will be provided through a dedicated content viewer or other portal, and access will be discontinued upon expiration of the designated time period. An order for Content Rental does not include any rights to print, download, save, create additional copies, to distribute or to reuse in any way the full text or parts of the materials.
    ii. **Content Purchase:** You may access and download a single electronic copy of the materials ordered. Copies will be provided by email or by such other means as publisher may make available from time to time. An order for Content Purchase does not include any rights to create additional copies or to distribute copies of the materials.

Other Terms and Conditions:

v1.18

Figure 3.

WOLTERS KLUWER HEALTH, INC. LICENSE
TERMS AND CONDITIONS

Feb 17, 2020

This Agreement between Lot 1, Kookaburra Cct ("You") and Wolters Kluwer Health, Inc. ("Wolters Kluwer Health, Inc.") consists of your license details and the terms and conditions provided by Wolters Kluwer Health, Inc. and Copyright Clearance Center.

License Number	4771631259322
License date	Feb 17, 2020
Licensed Content Publisher	Wolters Kluwer Health, Inc.
Licensed Content Publication	Stroke
Licensed Content Title	Secondary Neurodegeneration in Remote Regions After Focal Cerebral Infarction
Licensed Content Author	Jian Zhang, Yusheng Zhang, Shihui Xing, et al
Licensed Content Date	Apr 5, 2012
Licensed Content Volume	43
Licensed Content Issue	6
Type of Use	Dissertation/Thesis
Requestor type	University/College
Sponsorship	No Sponsorship
Format	Electronic
Will this be posted on a password protected website?	Yes
Portion	Figures/tables/illustrations
Number of figures/tables/illustrations	2
Author of this Wolters Kluwer article	No
Will you be translating?	No
Intend to modify/adapt the content	No
Title	Exploring functional outcomes after stroke and underlying mechanisms
Institution name	University of Newcastle
Expected presentation date	Oct 2020
Portions	Figure 1 and 2
Requestor Location	Lot 1, Kookaburra Cct Lot 1, Kookaburra Cct New Lambton Heights, New South Wales 2305 Australia Attn: Lot 1, Kookaburra Cct
Total	0.00 AUD
Terms and Conditions	

Wolters Kluwer Health Inc. Terms and Conditions

1. **Duration of License:** Permission is granted for a one time use only. Rights herein do not apply to future reproductions, editions, revisions, or other derivative works. This permission shall be effective as of the date of execution by the parties for the maximum period of 12 months and should be renewed after the term expires.
    i. When content is to be republished in a book or journal the validity of this agreement should be the life of the book edition or journal issue.
    ii. When content is licensed for use on a website, internet, intranet, or any publicly accessible site (not including a journal or book), you agree to remove the material from such site after 12 months, or request to renew your permission license

2. **Credit Line:** A credit line must be prominently placed and include: For book content: the author(s), title of book, edition, copyright holder, year of publication; For journal content: the author(s), titles of article, title of journal, volume number, issue number, inclusive pages and website URL to the journal page; If a journal is published by a learned society the credit line must include the details of that society.
3. **Warranties:** The requestor warrants that the material shall not be used in any manner which may be considered derogatory to the title, content, authors of the material, or to Wolters Kluwer Health, Inc.
4. **Indemnity:** You hereby indemnify and hold harmless Wolters Kluwer Health, Inc. and its respective officers, directors, employees and agents, from and against any and all claims, costs, proceeding or demands arising out of your unauthorized use of the Licensed Material.
5. **Geographical Scope:** Permission granted is non-exclusive and is valid throughout the world in the English language and the languages specified in the license.
6. **Copy of Content:** Wolters Kluwer Health, Inc. cannot supply the requestor with the original artwork, high-resolution images, electronic files or a clean copy of content.
7. **Validity:** Permission is valid if the borrowed material is original to a Wolters Kluwer Health, Inc. imprint (J.B. Lippincott, Lippincott-Raven Publishers, Williams & Wilkins, Lea & Febiger, Harwal, Rapid Science, Little Brown & Company, Harper & Row Medical, American Journal of Nursing Co, and Urban & Schwarzenberg - English Language, Raven Press, Paul Hoeber, Springhouse, Ovid), and the Anatomical Chart Company.
8. **Third Party Material:** This permission does not apply to content that is credited to publications other than Wolters Kluwer Health, Inc. or its Societies. For images credited to non-Wolters Kluwer Health, Inc. books or journals, you must obtain permission from the source referenced in the figure or table legend or credit line before making any use of the image(s), table(s) or other content.
9. **Adaptations:** Adaptations are protected by copyright. For images that have been adapted, permission must be sought from the rightsholder of the original material and the rightsholder of the adapted material.
10. **Modifications:** Wolters Kluwer Health, Inc. material is not permitted to be modified or adapted without written approval from Wolters Kluwer Health, Inc. with the exception of text size or color. The adaptation should be credited as follows: Adapted with permission from Wolters Kluwer Health, Inc. : [the author(s), title of book, edition, copyright holder, year of publication] or [the author(s), titles of article, title of journal, volume number, issue number, inclusive pages and website URL to the journal page].
11. **Full Text Articles:** Republication of full articles in English is prohibited.
12. **Branding and Marketing:** No drug name, trade name, drug logo, or trade logo can be included on the same page as material borrowed from *Diseases of the Colon & Rectum, Plastic Reconstructive Surgery, Obstetrics & Gynecology (The Green Journal), Critical Care Medicine, Pediatric Critical Care Medicine, the American Heart Association publications and the American Academy of Neurology publications.*
13. **Open Access:** Unless you are publishing content under the same Creative Commons license, the following statement must be added when reprinting material in Open Access journals. "The Creative Commons license does not apply to this content. Use of the material in any format is prohibited without written permission from the publisher, Wolters Kluwer Health, Inc. Please contact permissions@lww.com for further information."
14. **Translations:** The following disclaimer must appear on all translated copies: Wolters Kluwer Health, Inc. and its Societies take no responsibility for the accuracy of the translation from the published English original and are not liable for any errors which may occur.
15. **Published Ahead of Print (PAP):** Articles in the PAP stage of publication can be cited using the online publication date and the unique DOI number.
    i. Disclaimer: Articles appearing in the PAP section have been peer-reviewed and accepted for publication in the relevant journal and posted online before print publication. Articles appearing as PAP may contain statements, opinions, and information that have errors in facts, figures, or interpretation. Any final changes in manuscripts will be made at the time of print publication and will be reflected in the final electronic version of the issue. Accordingly, Wolters Kluwer Health, Inc., the editors, authors and their respective employees are not responsible or liable for the use of any such inaccurate or misleading data, opinion or information contained in the articles in this section.
16. **Termination of Contract:** Wolters Kluwer Health, Inc. must be notified within 90 days of the original license date if you opt not to use the requested material.
17. **Waived Permission Fee:** Permission fees that have been waived are not subject to future waivers, including similar requests or renewing a license.
18. **Contingent on payment:** You may exercise these rights licensed immediately upon issuance of the license, however until full payment is received either by the publisher or our authorized vendor, this license is not valid. If full payment is not received on a timely basis, then any license preliminarily granted shall be deemed automatically revoked and shall be void as if never granted. Further, in the event that you breach any of these terms and conditions or any of Wolters Kluwer Health, Inc.'s other billing and payment terms and conditions, the license is automatically revoked and shall be void as if never granted. Use of materials as described in a revoked license, as well as any use of the materials beyond the scope of an unrevoked license, may constitute copyright infringement and publisher reserves the right to take any and all action to protect its copyright in the materials.
19. **STM Signatories Only:** Any permission granted for a particular edition will apply to subsequent editions and for editions in other languages, provided such editions are for the work as a whole in situ and do not involve the separate exploitation of the permitted illustrations or excerpts. Please view: STM Permissions Guidelines
20. **Warranties and Obligations:** LICENSOR further represents and warrants that, to the best of its knowledge and belief, LICENSEE's contemplated use of the Content as represented to LICENSOR does not infringe any valid rights to any third party.
21. **Breach:** If LICENSEE fails to comply with any provisions of this agreement, LICENSOR may serve written notice of breach of LICENSEE and, unless such breach is fully cured within fifteen (15) days from the receipt of notice by LICENSEE, LICENSOR may thereupon, at its option, serve notice of cancellation on LICENSEE whereupon this Agreement shall immediately terminate.
22. **Assignment:** License conveyed hereunder by the LICENSOR shall not be assigned or granted in any manner conveyed to any third party by the LICENSEE without the consent in writing to the LICENSOR.
23. **Governing Law:** The laws of The State of New York shall govern interpretation of this Agreement and all rights and liabilities arising hereunder.
24. **Unlawful:** If any provision of this Agreement shall be found unlawful or otherwise legally unenforceable, all other conditions and provisions of this Agreement shall remain in full force and effect.

For Copyright Clearance Center / RightsLink Only:

1. **Service Description for Content Services:** Subject to these terms of use, any terms set forth on the particular order, and payment of the applicable fee, you may make the following uses of the ordered materials:
    i. **Content Rental:** You may access and view a single electronic copy of the materials ordered for the time period designated at the time the order is placed. Access to the materials will be provided through a dedicated content viewer or other portal, and access will be discontinued upon expiration of the designated time period. An order for Content Rental does not include any rights to print, download, save, create additional copies, to distribute or to reuse in any way the full text or parts of the materials.
    ii. **Content Purchase:** You may access and download a single electronic copy of the materials ordered. Copies will be provided by email or by such other means as publisher may make available from time to time. An order for Content Purchase does not include any rights to create additional copies or to distribute copies of the materials.

Other Terms and Conditions:

v1.18

Questions? customercare@copyright.com or +1-855-239-3415 (toll free in the US) or +1-978-646-2777.

Agreed Definitions and a Shared Vision for New Standards in Stroke Recovery Research: The Stroke Recovery and Rehabilitation Roundtable Taskforce

Author: Julie Bernhardt, Kathryn S. Hayward, Gert Kwakkel, et al
Publication: Neurorehabilitation and Neural Repair
Publisher: SAGE Publications
Date: 09/01/2017

Gratis Reuse

Permission is granted at no cost for use of content in a Master's Thesis and/or Doctoral Dissertation. If you intend to distribute or sell your Master's Thesis/Doctoral Dissertation to the general public through print or website publication, please return to the previous page and select 'Republish in a Book/Journal' or 'Post on intranet/password-protected website' to complete your request.

BACK CLOSE WINDOW